Molecular Pharmacology of the electron transport chain of *Mycobacterium tuberculosis*

Thesis submitted in accordance with the requirements of the University of Liverpool for the degree of Doctor of Philosophy

by

Teresa Sofia Rito

November 2012

Declaration

I confirm that the work submitted in this thesis is my own and that appropriate credit has been given where reference has been made to the work of others.

This copy has been supplied on the understanding that it is copyright material and that no quotation from this thesis may be published without proper acknowledgment.

The material contained in this thesis has not been presented, either wholly or in part for any other degree or other qualification.

The research work was carried out in the Liverpool School of Tropical Medicine, United Kingdom.

.....

Teresa Sofia Rito

Acknowledgments

I would like to express by words my gratitude to all of those who helped me throughout the completion of this work.

I would like to thank Professor Stephen Ward since he was with me since the beginning. He was always helpful. He is extremely kind and quite an example of scientific merit. Also my sincere gratitude goes to Doctor Giancarlo Biagini, for always dealing with me very gently. He helped me (re)gaining motivation and led me to an exciting turn and finally to the conclusion of this PhD.

I would like to thank Doctor Henry Mwandumba, Professor Alister Craig and Professor Peter Winstanley for choosing me in the interview for this position. I found it a precious experience.

A special thanks to all my colleagues from the Molecular and Biochemical Parasitology group and also to Doctor Stephen Gordon and for the members of the Clinical Pulmonary group, in particular to Doctors Helen Tolmie, Duncan Fullerton and Derek Sloan.

Thanks to Doctor Gavin Laing, for all the help and for managing so well the TB lab. For precious help, expertise and patience, I would like to thank Doctor Ashley Warman. Many thanks to Angela Travis and Mary Creegan for their precious help submitting this thesis.

My special gratitude goes to my fellow Portuguese friends in the group, Susana and Tiago. They gave me strength and their words were encouraging and sweet during my last times in Liverpool. Thank you very much for that. I will never forget it. Also, to Upali and Doss, my sincere thanks for all their cheering, nice mood and unforgettable talks. We are such different people and even when we were just complaining about small things, it was really nice!

A very special thanks to my current boss Doctor Luísa Pereira, for all the advice and for giving me time and allowing me to complete this PhD during my working hours. I would like to thank Professor Martin Richards and his family for helping me throughout my times in the UK.

I would like to thanks my lovely parents, my brother José and his family, for not forgetting me in all the important dates when I was away and for always making me feel welcomed and missed!

And for being able to stand me, taking care of me and still love me throughout all this process, a very special thanks to Pedro. He knows that without him nothing makes really sense. Finally, thank you Ana. Despite all the sleepless nights you helped me a lot, just because you exist. Love you both.

Abstract

Mycobacterium tuberculosis, the slow-growing bacteria responsible for the disease tuberculosis (TB) was thought to be effectively controlled in the developed world by antibiotics, discovered by the middle of the twentieth century and integrating a revolutionary treatment called DOTS where patients are closely monitored by health professionals that assure the completion of the long and demanding treatment.

Unfortunately, in poverty-stricken countries the disease never stopped being a plague and jointly with AIDS, decimated populations. The emergence of drug resistance draws even more attention to this disease which is considered a global epidemic and is responsible for one third of the World's population being latently infected.

The need for new drugs able to shorten the length of the treatment, compatible with antiviral medication, effective against resistant Mtb strains and able to kill the latent form of the organism is now well recognised.

The electron transport chain (ETC) of *M. tuberculosis* is a validated target for drug research due to its essentiality in the respiratory process. In mycobacterial membranes, type II NADH: menaquinone oxidoreductase (Ndh-2) is predicted to be an essential enzyme that catalyses the initial step in the respiratory chain. Phenothiazines target this type II NADH: menaquinone oxidoreductase and are already recognised as a new class of anti-tubercular compounds with potential inhibitory effects against latent mycobacteria, specifically inhibiting *ndh* activity.

In this thesis the hypoxic Wayne model and a simple colorimetric experiment, the microplate alamarBlue® assay (MABA) were used to test

known electron transport chain inhibitors and phenothiazines, for their antitubercular activities. Throughout this thesis, different Mtb culture models were tried and optimised and finding the ideal conditions that could mimic the scenario of mycobacterial infection is one of the major challenges when working with this highly pathogenic organism. *M. smegmatis* was initially tested as an alternative, non-pathogenic model in humans for Mtb, but despite being useful for biochemical studies, results need to be treated cautiously due to significant differences between the electron transport chains of *M. smegmatis* and Mtb. For this reason, the model proved to be poor and drug susceptibility tests were performed only in Mtb. Phenothiazines were confirmed as effective against Mtb using different models, the results obtained being particularly interesting in anaerobic conditions. However, it is possible that not all phenothiazines have the same mode of action.

Additionally, an attempt was made to study in detail the protein encoded by the *ndhA* gene, a homologue of the *ndh* gene. This gene was cloned and transformed, however expression of *ndhA* proved challenging. A phylogenetic analysis of all hypothetical *ndh* homologues in Actinomycetales (the group that includes mycobacteria) was conducted. The analyses suggest that *ndh* and *ndhA* share a recent common ancestor. The *ndh* and *ndhA* genes, as well as the two hypothetical homologues display similar rates of non-synonymous to synonymous mutations. Suggesting they have been under strict purifying selection pressure which can be interpreted as meaning that they have been functional and important genes during the evolution of this organism.

Contents

List of figures

List of tables

Abbreviations and acronyms

°C	Degrees Celsius
A, C, G, T	Nucleotides adenine, cytosine, guanine and timine
aa	Amino-acids
ACDP	Advisory Committee on Dangerous Pathogens
ACP	Acyl carrier protein
AIDS	Acquired Immune Deficiency Syndrome
ATP	Adenosine triphosphate
BCG	Bacillus Calmette-Guérin
BLAST	Basic local alignment search tool
bp	Base pairs
BSA	Bovine serum albumin
CFU	Colony forming units
cm	Centimetre
CoA	Coenzyme A
CPZ	Chlorpromazine
cyt	Cytochrome
ddH_2O	Double distilled water
dH_2O	Deionised water
DMF	dimethylformamide
DMSO	Dimethyl sulfoxide
dN	Non-synonymous mutations
DNA	Deoxyribonucleic acid
DosR	Dormancy survival regulon
DOTS	Directly observed treatment, short-course
dS	Synonymous mutations
EDTA	Ethylenediaminetetraacetic acid
EHR	Enduring hypoxic response
EMB	Ethambutol
ETC	Electron transport chain
FAS	Fatty acid synthase
FIC	Fractional inhibitory concentration
G	Gauge
g	Grams

g	Relative centrifugal force
HIV	Human Immunodeficiency Virus
HTS	High-throughput screening
IC	Inhibitory concentration
IC_{50}	Half maximal inhibitory concentration
IC_{90}	90% inhibitory concentration
INH	Isoniazid
IPTG	Isopropyl β-d-1-thiogalactopyranoside
Ka	Non-synonymous mutations
KS	Synonymous mutations
L	Litre
LB	Luria-Bertani
LORA	Low-Oxygen-Recovery assay
LRT	Likelihood ratio test
LSTM	Liverpool School of Tropical Medicine
MABA	Microplate alamarBlue® assay
MCMC	Markov chain Monte Carlo
MDR-TB	Multi-drug resistant TB
mg	Milligram
MGIT	*Mycobacterium* Growth Indicator Tube method
MIC	Minimal inhibitory concentration
ml	Millilitres
mm	Millimetre
mM	Milimolar
Mtb	*Mycobacterium tuberculosis*
MTT	3-(4,5-dimethylthiazol-2-yl)-2,5-diphenyl tetrazolium bromide
NAD	Nicotinamide adenine dinucleotide
NCBI	National centre for biotechnology information
Ndh-2	Type II NADH menaquinone dehydrogenase
nm	Nanometres
NRA	Nitrate reductase assay
NRP-1/NRP-2	Non-replicating phases 1 and 2
OADC	Oleic acid, albumin, dextrose and catalase supplement
OD	Optical density
OD_{600}	Optical density measured at a wavelength of 600nm
PAS	Para-aminosalicylic acid

PBS	Phosphate buffered saline
PCR	Polymerase chain reaction
PE	Novel glycine-alanine rich protein
PPE	Novel glycine-asparagine-rich protein
psi	Pressure unit
PTFE	Polytetrafluoroethylene
PZA	Pyrazinamide
Q-cycle	Quinone cycle
RMP	Rifampicin
RNA	Ribonucleic acid
rpm	Revolutions *per* minute
RT-qPCR	Quantitative real time polymerase chain reaction
SDS	Sodium dodecyl sulphate
SE	Standard error
SOC	Super optimal broth with glucose
SSR	Mononucleotide simple sequences repeat
TB	Tuberculosis
TBE	Tris-borate-EDTA
TCA	Tricarboxylic acid
TEM	Transmission electron microscopy
THZ	Thioridazine
Tm	Melting temperature
TSB	Tryptic soy broth
TST	Tuberculin skin testing
UV	Ultraviolet light
v/v	Volume concentration
VIS	Visible light
w/v	Mass concentration
WGND	Working group of new drugs, Stop TB partnership
WHO	World Health Organization
XDR-TB	Extensively drug resistant TB
µl	Microlitres
µm	Micrometre
µM	Micromolar

Chapter 1. General introduction

Tuberculosis (TB) is caused by the slow growing organism *Mycobacterium tuberculosis* (Mtb). Despite numerous efforts to control this human pathogen, TB remains the deadliest bacterial disease worldwide and it is recognised as one of the three greatest maladies of the developing countries, alongside malaria and the acquired immune deficiency syndrome (AIDS) (WHO 2009).

Anti-TB treatment is prolonged and demanding and it is not always strictly followed by the patient which leads to the emergence of drug resistant strains (Johnson et al. 2006). Multiple-drug resistant TB (MDR-TB) occurs when there is resistance to the two most effective first line TB drugs: rifampicin and isoniazid, while extensively drug resistant TB (XDR-TB) occurs when the bacteria are also resistant to one of the three classes of second-line drugs. Currently, there is no effective treatment against XDR-TB so it remains virtually without a cure (Gillespie 2002).

In the last few decades mainly due to co-infection with Human Immunodeficiency Virus (HIV) and the worrying appearance of resistant strains, it became obvious the need for the development of new treatments against TB. These new therapies should be able to target not only the growing bacteria responsible for the active disease, but also the sub-populations of resistant, slow-growing and persistent organisms that are responsible for the recalcitrance of the disease .

However, the organisms to kill are bacteria. Bacteria have great plasticity of behaviour, and this is one of the reasons why numerous compounds that were successfully tested *in vitro* failed to present positive results *in vivo*. Mycobacteria have various strategies to overcome adverse conditions, and this allows them to adapt and survive inside a hostile

host. Also worth pointing out is the inefficacy of the current models used to mimic the complexity of the host environment during infection.

Despite all the interest in mycobacteria, these organisms and some of their basic behaviour and processes, remain unknown. A good understanding of the biology of mycobacteria is the first milestone in the journey towards an effective cure.

1.1. TB throughout history

Tuberculosis was a well-known disease in the nineteenth century and it was often associated with a romantic notion since many young artists died from it, like the English poet John Keats or the Scottish novelist Robert Louis Stevenson. TB affected everyone, from every social class, regardless of age or gender. People affected with TB, often called consumption, would become pale, lethargic, with a persistent cough, associated with blood in the later stages of the disease. The principle measure to fight TB was to isolate people in sanatoriums, preferably in cold areas and avoid contact with them, since it was known very early on that the disease affected the lungs and was highly contagious.

In 1882, Robert Koch discovered a staining technique capable of seeing Mtb but it was only 62 years later that the first active drug against TB appeared and revolutionized the treatments against the disease. Streptomycin was the first chemotherapeutic agent used against TB and it rendered the surgical procedures used at the time, obsolete and unnecessary. In the second half of the twentieth century, other drugs were discovered (e.g.: isoniazid, rifampicin, ethambutol and pyrazinamide) and the complete elimination of the disease was thought to be an achievable goal. Unfortunately, there were areas where TB cure was never on the horizon, namely the poor populations of Africa, where TB remained the

number one cause of death among infectious diseases especially among HIV carriers (Granich et al. 2010).

In developed countries, TB cases decreased exponentially after the appearance of the new and effective antibiotics mentioned above (Zhang 2005). In the 1980s the disease was pretty much limited to communities of immigrants, drug users and the homeless, however TB was still a major cause of death in third world countries, associated with famine and poor health and unhygienic conditions (WHO 2009). The scientific incentives for the study of Mtb were recognised but the wakeup call happened towards the end of the twentieth century when multidrug-resistant TB emerged (Gillespie 2002).

With the appearance of new multi-drug resistant phenotypes of the bacteria that cannot be cured with current first line chemotherapies, new strategies were adopted, namely the use of second line drugs, but in extreme cases, the patient benefits from the surgical removal of parts of the affected lungs (Takeda et al. 2005). This physically removes agglomerates of bacteria and increases the exposure of the remaining bacteria to drugs and to the host immune response.

In 1993, WHO (World Health Organisation) finally recognized TB as a global health emergency.

1.2. Impact of TB globally: facts and numbers

WHO declared TB as an epidemic in 1997. According to their last estimates, over 9 million people worldwide fall ill with TB every year (WHO 2009). Its effects are particularly devastating in developing countries, where poor health conditions and difficulties with access to basic medical care and medicines are major problems for the populations. It is estimated that 86% of TB cases are located in Africa and South-East

Asia (WHO 2009), with South America and Northern Asia as additional areas of high prevalence of TB. A map showing the worldwide distribution of new TB cases per 100,000 individuals is displayed in Fig. 1.1.

An estimated 15% of the population infected with TB (1.4 million people) are co-infected with HIV and each year the mortality rate ascends to more than 1.3 million deaths (WHO 2011).

To add to these scary figures, there were an estimated 0.5 million cases of multi-drug resistant TB (MDR-TB) in 2007 (WHO 2009). In MDR-TB the patient shows resistance to the two most effective first line drugs against TB: rifampicin and isoniazid, rendering the currently used treatment ineffective (Sharma and Mohan 2006).

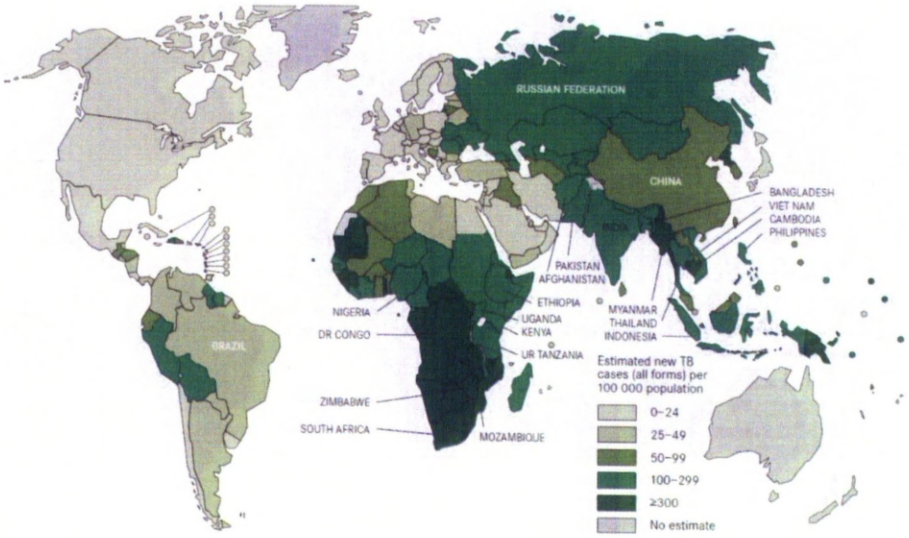

Fig. 1.1.: Worldwide distribution of new TB cases per 100,000 people in 2010, according to WHO report, 2011 (WHO 2011).

1.3. *Mycobacterium tuberculosis*: biology of infection

Mtb usually enters the body through an aerosol route, when an actively infected individual coughs or sneezes, spreading small droplets that reach the new host's respiratory routes. A scheme of the Mtb cycle is shown in Fig. 1.2.

In the normal phagocytic process bacteria that enter the host are internalised inside macrophages in a membrane-bound organelle called the phagosome. The phagosome will undergo a maturation process along the endocytic pathway leading to fusion with late endosomes and finally lysosomes, forming the phagolysosome where the ingested bacilli are degraded. Pathogenic mycobacteria survive inside the host macrophage by blocking the normal maturation of the phagosome (Vergne et al. 2004). At this point, either they establish an episode of active disease, or the host immune system is able to induce a localized immune response, with recruitment of specific effector cells that results in the containment of the pathogen in granulomas. At this point, the latent-TB carrier is not contagious. Despite the fact that the Mtb bacilli are obligate aerobes, they are capable of surviving for long periods of time, even decades in microaerophilic or even anaerobic environments as long as they have time to adapt to these extreme conditions, entering a non-replicating state or latent form of the disease (Glickman and Jacobs Jr. 2001; Russell 2001).

The risk of reactivation of the infection remains since the Mtb are not dead but only lying dormant, consequently a change in the immune system conditions of the host (e.g. as a result of HIV infection) may result in disease reactivation. When left untreated, due to bacteria multiplication, the lung tissue is destroyed and severe cough with bloody sputum and chest pain appear. At this point the TB carrier is highly contagious, allowing the cycle to re-start.

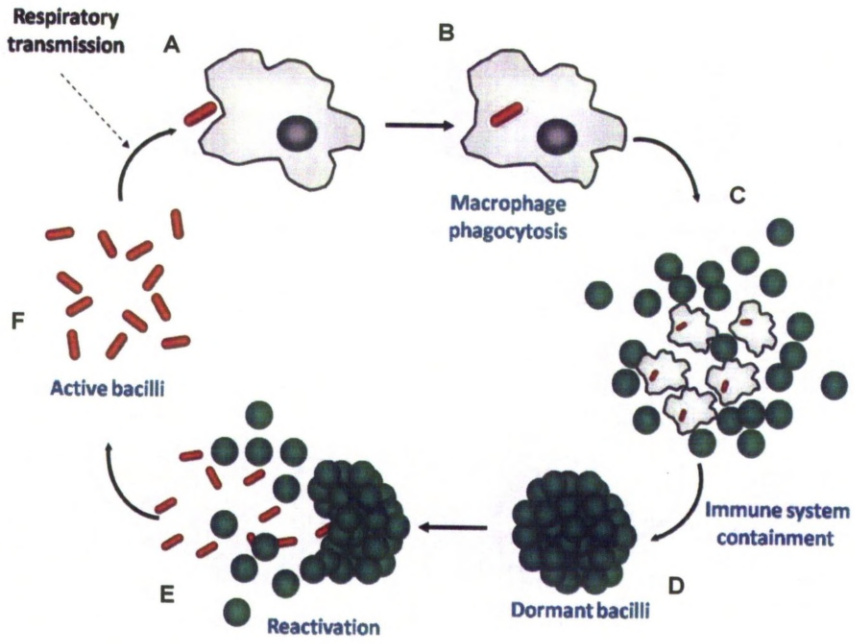

Fig. 1.2.: Life cycle of *Mycobacterium tuberculosis* inside the human host: (A) The bacilli enter the human body through a respiratory route, through a cough or sneeze from an actively infected individual; (B) in the lung the bacteria are phagocysed by macrophages and (C) eventually contained inside granulomas; (D) at this point the host is considered to have latent TB; (E) however the bacteria are not dead and they remain capable of reactivating the infection if at some point there is a breach in the immune system of the individual; (F) re-initiating the cycle as active bacilli.

1.4. The granuloma

The characteristics of granuloma formation are still largely unknown, despite efforts to recreate models of *in vitro* granulomas and *in vivo* dissections. The use of animal models is often questioned due to the fact that they are not truly representative of the human scenario. It is known that granuloma formation occurs in the early stages of an infection episode, trying to ensure pathogen containment (Ulrichs and Kaufmann 2006). The granuloma is described as having a central core of necrotic tissue that will be the source of nutrients to the contained mycobacteria and that augments along time, surrounded by dense layers of immune system cells, like macrophages and specialised leukocytes, epithelioid

cells, dendritic cells, large multinucleated cells (Langhans giant cells) and lymphocytes. The development of the granulomas and recruitment of cells to control the invader organisms is due to the presence of cytokines and chemokines produced by local tissue cells and leucocytes (Ulrichs and Kaufmann 2006; Gupta et al. 2012). During latency, the granulomatous tissue will become fibrotic and will calcify, creating nodular lesions visible under X-ray, providing evidence of latent TB (Ehlers 2009).

According to Peyron and collaborators, the highly pathogenic mycobacteria stimulate the formation of foamy macrophages. These cells are granuloma-specific and have a high lipid content, that may be used as a nutritive reservoir for long-term persistence (Peyron et al. 2008).

Via and colleagues studied granulomas in various animal models, using pimonidazole (a hypoxyprobe which is an imaging agent indicative of hypoxic conditions) as well as metronidazole (a drug only effective against anaerobes) in order to better understand the nature of granulomas in these animals. In guinea pigs, rabbits and nonhuman primates caseous (necrotic) lesions are hypoxic, while solid cellular lesions have a reduced oxygen tension. In mice, despite being less oxygenated, TB lesions are not hypoxic. Metronidazole showed a profound effect on rabbits but proved ineffective when used in mice (Via et al. 2008), suggesting that mice are not a good model for the study of granulomas.

However, some research groups propose that the Mtb bacilli containment in granulomas can be replicated *in vitro*. Puissegur and colleagues developed a model to obtain mycobacteria-induced or mycobacterial antigen-induced granulomas. When peripheral blood mononuclear cells were isolated from a human blood sample from a Bacillus Calmette-Guérin (BCG)-vaccinated non-infected individual and then exposed to mycobacterial antigen-coated beads, or live-mycobacteria, they produced

a cellular aggregation response, similar to the granuloma, with progressive recruitment and differentiation of cells (Puissegur et al. 2004).

1.5. Pathogenic mycobacteria: reasons for success

There are a number of reasons why Mtb bacteria are as successful pathogens as they are. Some of the more obvious are the unique composition of its cell wall, its modular electron transport chain (ETC), and its capacity to persist through decades, remaining viable and able to resume growth as soon as a breach in the immune system of the host occurs (Bentrup and Russell 2001; Dick 2001; Wayne and . 2001).

1.5.1. The unique cell wall of Mtb

The mycobacterial cell wall is tripartite unlike other eubacteria and it consists of a membrane of trehalose dimycolates and glycopeptidolipids, also called mobile layer and then by three other covalently attached layers: a peptidoglycan layer, a layer of hydrophilic arabinogalactan and then a unique hydrophobic layer of mycolic acids. Mycolic acids are long chain branched β hydroxyl fatty acids (Fig. 1.3.). These layers constitute a barrier for both hydrophobic and hydrophilic compounds and as a consequence of this lipid- and glucolipid-rich membrane, the outer surface of the organism is extremely hydrophobic (Glickman and Jacobs Jr. 2001; Nguyen and Pieters 2009; Niederweis et al. 2010).

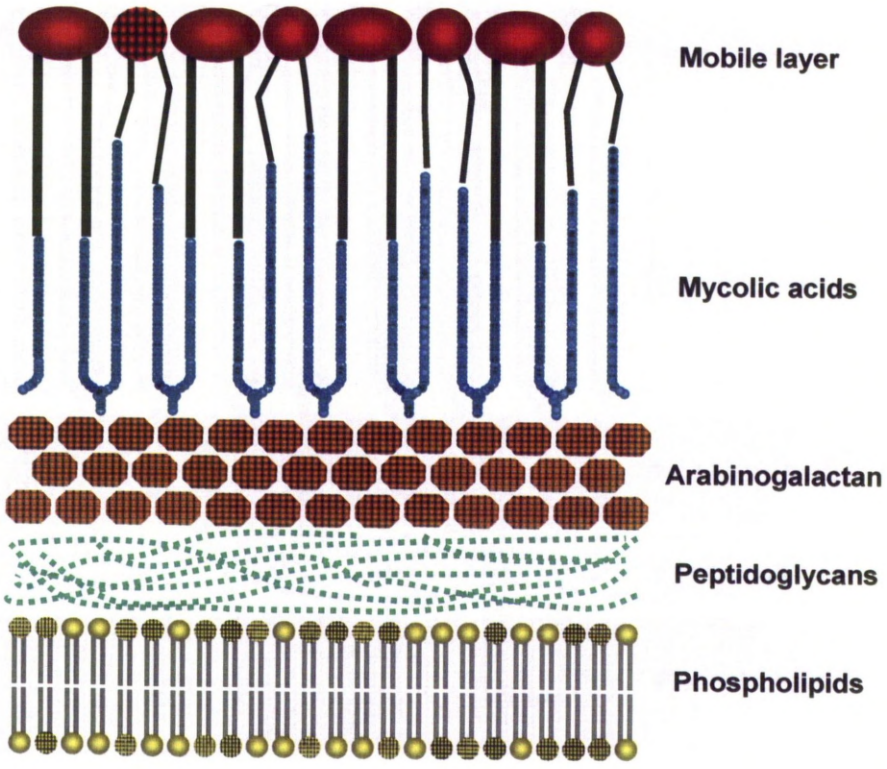

Fig. 1.3.: Schematic representation of the cell wall of *Mycobacterium tuberculosis*.

1.6. Latency of Mtb

Mtb has the capacity to remain alive in the human host, without displaying symptoms of a primary active infection and with virulence mechanisms intact, enabling the organism, at some point during the host lifetime to reactivate and cause active disease in the host.

This phenomenon, where Mtb remain in a dormant state, is called latency. During this period, despite not showing clinical signs of infection, the individual infected will have strong immune response against Mtb antigens, detected through tuberculin skin testing (TST) (Ehlers 2009). Unfortunately this test is far from adequate due to the fact that it gives a high rate of false positives. The premise is that a person that was previously exposed to Mtb will have a strong reaction against

Mtb proteins of tuberculin. But often the immune response is the result of a contact with Mtb proteins through vaccination or non-pathogenic mycobacteria, and are not indicative of the person being latently infected (Glickman and Jacobs Jr. 2001; Zumla et al. 2011) .

The reactivation of these dormant bacilli can occur at any time, even decades after the primary infection took place. Usually it occurs due to impairment of the immune system either caused by age, chronic illness or acquired immunodeficiency (Leung 1999). It is also not always easy to distinguish if an active TB infection in later life is due to reactivation or to a new episode of infection (Zumla et al. 2011). Verver and collaborators use bacterial DNA fingerprinting in order to identify if a subsequent infection was a reinfection or a new episode of TB infection (Verver et al. 2005). This characterisation is only possible if a study was performed during the first episode of infection, which is unlikely in a normal clinical scenario.

1.6.1. Non-, slow- or continuous- replication of Mtb during its latent state

Despite various *in vivo* and *in vitro* attempts to fully characterise the state of Mtb during latency, this issue is still controversial. There are two current hypotheses. The first hypothesis proposes that Mtb carry on living through decades, in a near-static state of non-replication or very slow replication that allows them to evade the host immune system and become insensitive to antibiotics (Ehlers 2009). The other hypothesis defends a dynamic state of continuous replication of the latent organisms being contained by the immune system. In both states the host and the bacteria live for decades in a precarious equilibrium which if disturbed,

leads to reactivation of infection and active disease (Ehlers 2009)(Gomez and McKinney 2004).

Yang and colleagues, in an attempt to further classify the existence or not of replication during latency, used genomics and molecular epidemiology data, to study patients that after more than three decades of an initial episode of TB, showed signs of disease reactivation (Yang et al. 2011). They ruled out the possibility of individuals being infected by new strains of Mtb. Their research supports a scenario where Mtb does not replicate during latency. These inferences were obtained by comparing the frequency of insertion and deletions in 14 selected sets of mononucleotide simple sequence repeats (SSRs or microsatellites) in samples of Mtb from the initial infection with samples 30 years older, and finding no significant differences in their genomic profiles. However, the study has some limitations, namely the small number of cases studied, the very limited portion of the genome analysed and the fact that mutation rates of the SSRs in Mtb are unknown. In order to accept or refute their conclusion one would need to properly assess the mutation rate of the SSRs during normal replication by continuous culturing of the bacteria (Yang et al. 2011).

Gill and colleagues favour the second hypothesis, where Mtb bacilli are constantly replicating in the human host. In order to monitor Mtb replication, they used Mtb transformed with the plasmid pBP10 during mice infection. This plasmid is unstable and it is known that not all cells after replication will carry this plasmid. They used a mathematical model to assess bacterial growth, assuming a constant decay along time of the presence of the plasmid in each generation, independent of the replication rate of the cells. The loss of plasmid during chronic infection pointed to bacterial replication during this period, in contrast to what is commonly assumed in latency (Gill et al. 2009). Another argument in the defence of this continuous replication during latency is the fact that isoniazid, if

given as a 9-month course of therapy is able to achieve complete sterilisation, avoiding TB reactivation. As this drug targets mycolic acid biosynthesis, to have an effect, it requires active replication. Hence if isoniazid is able to completely sterilize the host from bacteria, that suggests that at least part of the Mtb latent population is replicating (Ehlers 2009). The most recent research seems to support this idea (Zumla et al. 2011).

1.6.2. Models used in the study of Mtb latency

In order to study latency and the adaptive processes of Mtb that allow it to become latent and in a state of almost non-proliferation, two of the most utilised models are the Cornell mouse model, a drug induced model, and the Wayne hypoxia model. They are just two examples of how in the laboratory, it is possible to grow dormant Mtb populations, modulating some conditions that are known to reduce Mtb metabolism and induce the latent state. Considering that the focus of this thesis is in the ETC and metabolism, only a description of the main patterns of expression of genes involved in ETC and metabolism will be presented.

1.6.2.1. The Cornell model

The Cornell mouse model is an alternative dormancy model, first described in the 1950s by McCune, McDermott and colleagues at the Cornell University. According to this model, Mtb infected mice are treated with isoniazid and pyrazinamide for 12 weeks, before treatment is stopped. The mice do not present any evidence of active TB disease and no Mtb bacilli can be cultured from mouse spleens (McCune et al. 1956). After 12 weeks of not being treated with any antibiotic, one third of the mice have active and drug-sensitive Mtb. Therefore, these 12 weeks

between disappearance and then reappearance of the infection are considered the latent period of the disease (Fig. 1.4.) (McCune and Tompsett 1956; Parrish et al. 1998). For this evidence of a period of Mtb "disappearance" with a "resuscitation" afterwards, the Cornell model is sometimes pointed out as the most convincing evidence of Mtb dormancy (Zhang 2004). Scanga and collaborators suggested some pertinent variations in the original Cornell mouse model, namely they suggested the antibiotic regimen should start 4 weeks after the initial infection and not immediately after Mtb incubation (Scanga et al. 1999). This is due to the fact that the original Cornell model did not take into account the role of the immune system in the establishment of the latent infection and Scanga and colleagues tried to address this in their study.

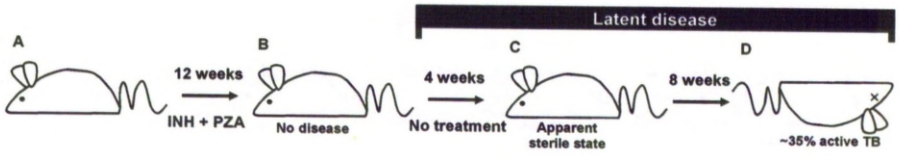

Fig. 1.4.: Schematic representation of the Cornell mouse model of dormancy. (A) A population of mice was infected with Mtb; (B) after a 12 weeks treatment with isoniazid (INH) and pyrazinamide (PZA), mice did not present any evidence of TB; (C) after no treatment for 4 weeks, mice remained healthy; (D) after 8 more weeks without treatment, 35% of the mice population was infected with active TB, i.e. by the end of 12 weeks of latent disease, reactivation occurred and the mice showed signs of active disease. Adapted from Parrish et al. 1998.

1.6.2.2. The Wayne model

In order to induce dormancy using this model, bacteria are submitted to a slow shift from aerobic to anaerobic conditions. The Mtb bacilli are grown in liquid media being constantly stirred in sealed tubes, with a precise proportion between air and liquid, with no disturbance on the surface of the liquid, leading to a gradual depletion of oxygen, occurring from the bottom of the vial to the top in a very progressive and controlled

manner. Instead of dying, similar to what happens when there is an abrupt change of aeration in a culture, the bacilli are able to adapt successfully, entering a 2-phase state called non-replicating persistence (NRP) (Wayne 1994; Wayne and Hayes 1996; Boshoff and Barry III 2005).

During the non-replicating phases of NRP-1 and NRP-2, there is no increase in the number of viable mycobacteria. During NRP-1, when oxygen saturation is approximately 1%, there is still a small increase in the turbidity of the culture, due to cell enlargement, however the number of viable bacteria and DNA synthesis are stationary (Wayne and Sohaskey 2001). Finally during NRP-2, when the oxygen saturation reaches 0.06%, the culture shifts to complete anaerobic conditions, a complete shutdown, or at least a significant reduction of metabolism occurs and morphological changes of bacteria also cease (Wayne and Hayes 1996; Wayne and Sohaskey 2001).

It is known that Mtb have their growth arrested at the same stage (phenomenon called synchronisation) (Wayne 1994). The shift from being active to the latent state of Mtb in terms of genetic expression profiles indicates the up-regulation of nitrate reductase and glycine dehydrogenase (Muttucumaru et al. 2004). Nitrate reductase is linked to nitrate reduction ensuring that the intake of energy during NRP and glycine dehydrogenase is linked to reductive amination of glyoxylate to glycine that leads to the oxidation of NADH, meaning a regeneration of NAD^+ under hypoxia (Wayne and Sohaskey 2001).

The bacilli remain able to resume growth (Wayne 1994). In terms of drug susceptibility, dormant bacilli exhibit increased tolerance, but are nevertheless still susceptible to rifampicin and isoniazid and they become susceptible to metronidazole. This fact serves as evidence for the relevance of hypoxia in the phenomenon of latency, since metronidazole is only active against anaerobic or microaerophilic bacteria (Wayne and

Hayes 1996).

In terms of patterns of gene expression, NRP stage 1 and NRP stage 2 present different gene expression profiles (reviewed in detail by Muttucumaru et al. 2004). Many important regulatory genes are induced in both stages, namely *acr*, a gene encoding a heat-shock protein (α-crystallin) and the DosR regulon (see Section 1.16.). The activity of the enzymes isocitrate lyase, glycine dehydrogenase and nitrate reductase (encoded by *narX* and the *narGHJI* regulon) increase during the NRP-2 stage of hypoxia (Sherman et al. 2001; Muttucumaru et al. 2004).

1.6.2.3. Other models used to recreate the dormancy phenomenon

Due to the recognition of the importance of the dormancy phenomenon in the pathology of TB disease, efforts were made in order to replicate this state *in vitro*. Besides the Wayne model of hypoxia, which is one of the best characterized models, and the Cornell mouse model, other attempts were made in order to induce the latent state of Mtb. Mtb bacilli were submitted to conditions that appear to be present in the macrophage, phagosome or granuloma environment or tuberculous lesions (Wayne and Sohaskey 2001), and some of those models are described in the sections below.

1.6.2.3.1. The nutrition starvation model

This model is based on evidence that points to the existence of severe limitations in terms of nutrients in TB lesions. Loebel and collaborators created this model in the 1930s (Loebel et al. 1933) which consists of the transfer of Mtb bacteria, after being grown in a typical nutrient rich media, to a phosphate buffered saline (PBS) solution, where the bacteria are forced to starve, but with no limitations on the degree of aeration. It

was observed that bacilli remain viable but with impaired growth and a diminished respiratory rate. The bacteria also display tolerance to isoniazid, rifampicin and metronidazole (Betts et al. 2002; Gengenbacher et al. 2010).

In terms of patterns of gene expression, there is a general down-regulation of metabolic genes, apart from the enzyme isocitrate lyase (encoded by *icl*) (Betts et al. 2002). Regarding genes involved in the respiratory process, microarray analyses show a down-regulation of the genes involved in aerobic respiration (Teh et al. 2007). Type I NADH dehydrogenase (encoded by the genes *nuoA-M*) is the primary electron donor to the aerobic ETC, which catalyses the oxidation of NADH to NAD^+ and leads to production of ATP, is down-regulated. However, alanine dehydrogenase (gene *ald*) is up-regulated suggesting a role for this enzyme in replenishing the NAD^+ pool converting pyruvate to alanine (Betts et al. 2002; The et al. 2007). Also of note is the down-regulation of genes *atpA-H* that encode the ATP synthase complex and the significant up-regulation of *pdhABC* genes that encode the pyruvate dehydrogenase enzyme complex that converts pyruvate to acetyl coenzyme A (CoA) and CO_2 and the up-regulation of *frdA* that encodes fumarate reductase which is important in anaerobic respiration (Betts et al. 2002).

Gengenbacher and colleagues, comparing the oxygen deprived bacilli from the Wayne model, and the starved ones from Loebel, concluded that in terms of intracellular levels of ATP, the Loebel bacilli are less sensitive to ATP depletion, meaning that their metabolism is even more reduced than the dormant Wayne model bacilli, but both need F_0F_1 ATP synthase to maintain viability (Gengenbacher et al. 2010).

1.6.2.3.2. Phosphate depletion

Rifat and colleagues mimicked the macrophage restrictive environment, limiting the phosphate in an Mtb culture. As a consequence, the bacilli presented restricted growth, morphological alterations such as bacterial elongation and altered acid fast characteristics, and exhibited phenotypic tolerance to isoniazid. Suggesting that phosphate starvation leads to a stress response similar to the one that occurs in dormancy (Rifat et al. 2009).

1.6.2.3.3. The prolonged stationary-phase model

A number of groups have highlighted the similarities between persistence and bacteria continuously maintained in stationary phase (Hampshire et al. 2004; Voskuil et al. 2004). According to this model, after the exponential phase where the medium is depleted of nutrients and saturated with waste products and cell debris that result from cell metabolism and death, a percentage of bacteria survive by entering a non-replicating state. In this model the bacteria are maintained in a continuously monitored chemostat (Hampshire et al. 2004)

In terms of expression of genes involved in metabolism in this aerobic nutrient-depletion adaptation model, the more significantly up-regulated genes are the ones involved in fatty acid degradation and in the glyoxylate shunt (this is indicative of the shift between carbohydrate sources of energy to fatty acids) and anaerobic respiration. There are similarities between this model and the nutrition starvation model. In terms of metabolism, the pattern of gene expression is similar, apart from isocitrate lyase which is up-regulated in this model contrary to what occurs in the nutrition starvation model (Betts et al. 2002). Perhaps the cause is that in the nutrition starvation model, the bacteria are

immediately starved, not allowing for the gradual adaptation to starvation that occurs in this model (Hampshire et al. 2004).

1.6.2.3.4. The multiple-stress model

Recently, Deb and colleagues suggested a multiple-stress model for inducing dormancy in Mtb. According to this model, the bacteria are submitted to a combination of stresses (namely, low oxygen, high CO_2, low nutrient and acidic pH) as an alternative to the previous models where only a single factor of stress was induced. The reasoning for this model proposal is that in the human host, the bacteria are likely to be submitted to various stresses that limit their growth, so it is more realistic to induce dormancy by submitting the bacteria to more than one single stress factor. Applying this combination of stresses, a representative dormant state may be induced, where the bacteria stop replicating and acquire phenotypic antibiotic tolerance (Deb et al. 2009).

The advantage of these models is that since they generate bacilli that meet all the criteria of dormancy, they can be used in high-throughput screening for drugs targeting the persistent organisms.

1.6.3. Other mycobacteria and the dormancy phenomenon

There are a number of studies proving that *M. bovis* BCG (an attenuated strain of *M. bovis* used as a live vaccine) is capable of a similar dormancy response when induced by oxygen deprivation to the one manifested by Mtb (Lim et al. 1999; Boon et al. 2001; Boon and Dick 2002).

M. bovis bacilli, submitted to the gradual depletion of oxygen enter the states of non-replicating persistence, with consequential induction of glycine dehydrogenase and induction of an α-crystallin-like small heat

shock protein (whose up-regulation correlates with cell wall thickening of the bacilli). Apart from these two molecular markers, the bacilli acquired sensitivity to metronidazole (Lim et al. 1999).

Despite some studies defending the use of fast-growing, non-pathogenic strains, namely *M. smegmatis* to successfully recreate the phenomenon of persistence, the use of these models remain questionable since the results obtained with these models can differ from the ones obtained using slow growing pathogenic mycobacterial strains (Hutter and Dick 1998).

1.7. The difficulties of studying *M. tuberculosis*

There are a number of reasons why Mtb research for new effective treatment against TB is complex.

The use of appropriate models remains controversial. The animal models are not representative. The pathology of the human disease is not similar to the one presented in animals, such as rodents, mainly due to the fact that TB does not occur naturally in them. The disease exception is the use of nonhuman primates, such as *Macaca fascicularis*, commonly called cynomolgus macaques, that when infected with Mtb develop signs of TB disease, similar to the human species, namely presenting signs of granulomatous pathology (Lin et al. 2009).

In an attempt to study some of the most used animal models, namely mouse, guinea pig, rabbit and nonhuman primate and the conditions inside their granulomas, Via and colleagues used three major strategies in order to verify the existence of complete hypoxia inside these structures. They used a hypoxia marker called pimonidazole hydrochloride (hypoxyprobe), that forms adducts in hypoxic areas, that can be detected by immuno-histochemical staining. They measured the oxygen tension of the rabbit granulomas directly, using a surgical method and they also

tested the drug metronidazole, in both rabbit and mice. This drug is known to be active only against bacteria kept in anaerobiosis. The conclusions pointed to the existence of truly hypoxic granulomas in guinea pigs, rabbits, and nonhuman primates. In the case of mice, their granulomas are not hypoxic (Via et al. 2008) and they do not become necrotic or calcified (Cosma et al. 2003). This conclusion was corroborated by further studies (Klinkenberg et al. 2008). Also, the disease does not evolve as per the human form; the bacterial burden can become extremely high and without being cleared at all (Cosma et al. 2003) with the bacilli found mainly intracellularly (Hoff et al. 2011). A summary table of Mtb infection outcome characteristics in four different animal models is displayed in Table 1.1.

Table 1.1.: Comparison of different animal models used to study Mtb and their limitations. Adapted from Rustad et al. 2009; Chao and Rubin 2010.

Model	Primary infection	Caseating and hypoxic granulomas	Latent infection	Reactivation
Mouse	Yes	No	No true latent state	No
Guinea Pig	Yes	Yes	No true latent stage	No
Rabbit	No	Yes	Not demonstrated	Requires immune system repression
Monkey	Yes	Yes	Yes	Yes

The use of laboratory adapted strains of Mtb is also controversial due to the fact that the nutritive media used for the growth of the strains does not represent the human host environment. Clinical Mtb strains are heterogeneous and present differences in immunogenicity and pathogenicity (Dormans et al. 2004). There are also important differences at the level of whole genomes between clinical strains and laboratory

adapted Mtb strains (Fleischmann et al. 2002). Another difficulty in studying Mtb in the lab environment is that in order to mimic the persistent phenotype, Mtb cells would be submitted to severe levels of stress and competition, where the bacilli will replicate and accumulate mutations at a much higher rate than in a normal infection episode (Gomez and McKinney 2004). Efforts are also aimed at the development of a new anti-TB vaccine. BCG, the current anti-TB vaccine, administered in children has variable efficacy, with reported success rates between 0 and 80% (Brandt et al. 2002). These different responses are attributed to different host susceptibilities and exposure to environmental mycobacteria, as well as loss in efficacy of BCG along the years (Brewer 2000; Brandt et al. 2002). The development of a new vaccine, able to induce immunity in infants but also that could be administered at any time of life, inducing a total control and clearance of the infection, with an effect against latent forms of the disease (Castañón-Arreola and López-Vidal 2004) is currently underway, but there are paradoxical ideas supporting vaccination (Parida and Kaufmann 2010).

There are strong beliefs that since the human body does not present a natural immunity when re-infected with mycobacteria, it may not be capable of establishing an effective immune response even when previously stimulated by vaccination (Barry 2001). One of the most difficult challenges in overcoming TB is the unpredictability, complexity and limited knowledge of the disease. TB is not easily categorised since it presents a whole spectrum of disease states, from complete sterilised scars, permanent disease, re-infections that occur decades after the first contact with the pathogen, immediate hyper-sensitivity to the bacilli, slowly developing disease or complete asymptomatic responses (Dheda et al. 2010; Achkar and Jenny-Avital 2011).

In the search for new anti-TB drugs, efforts are often concentrated on the identification of Mtb essential genes or Mtb virulence genes. The

reduced genome of *Mycobacterium leprae*, exclusively adapted to grow on a human host, contrasting with the biggest genome of environmental non-pathogenic species as *M. smegmatis* suggests that many genes are possibly redundant and all those retained in *Mycobacterium leprae* are essential (Gómez-Valero et al. 2007). Another way of identifying essential genes is by causing random mutations in the mycobacterial genome and to observe how these mutations impair Mtb survival in different environmental settings (Sassetti et al. 2003; Sassetti and Rubin 2003).

1.8. The current therapy: limitations

The first-line drug regimen currently in place is called DOTS (directly observed treatment, short-course) and it involves the direct monitoring of the patient by trained health-care professionals, to ensure that the regimen is strictly followed. In order to avoid the emergence of resistance and to assure complete sterilisation, it involves an initial phase of two months with a combination of the four first line drugs (isoniazid, rifampicin, ethambutol and pyrazinamide), followed by a second phase with four months duration of therapy with isoniazid and rifampicin alone (Bayer and Wilkinson 1995; Zhang 2005). The need for combinations of drugs is due, not only to the synergistic reaction of these drugs but also in an attempt to minimise the occurrence of resistance (Michel et al. 2008).

DOTS is an extremely demanding therapeutic option and can result in patient non-compliance. As soon as they start feeling better, they may abandon the treatment. Not only patient non-compliance but also wrong dosage and prescription of DOTS, as well as individual characteristics can lead to treatment failure (Gillespie 2002; Johnson et al. 2006).

The reason why DOTS duration cannot be shortened is often attributed to persistent organisms that exhibit phenotypic tolerance and evade the

effect of antibiotics, due to their inactivity, since antibiotics usually target actively growing bacteria. These phenotypically tolerant organisms are in the stationary phase and are dormant bacteria(Zhang 2005), that have a reduced metabolism, but they are sensitive to the treatments since they do not have any genetic mutation and they are occasionally dividing, meaning that the prolonged exposure to DOTS will kill them (Mitchison and Coates 2004).

A more detailed characterisation of the drugs of the DOTS regimen is given below.

1.8.1. Isoniazid

Isoniazid (INH) (Fig. 1.5.) was discovered in 1952 by three different drug companies: Hoffman LaRoche, E. R. Squibb & Sons and Bayer, and it remains an important anti-TB drug, due to the fact that it is highly potent, well tolerated by the patient and inexpensive (Zhang 2005). Despite its importance, its mechanisms of action are not yet completely understood. There are still contradictory ideas in the field and new hypotheses of how INH works are regularly proposed in the literature.

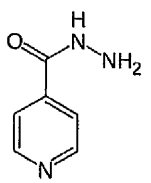

Fig. 1.5.: Structure of isoniazid, $C_6H_7N_3O$.

INH is a pro-drug and it requires activation by Mtb catalase-peroxidase, encoded by the gene *katG*. This enzyme generates reactive oxygen species and reactive oxygen radicals toxic to Mtb. INH inhibits the

synthesis of mycolic acids, important constituents of the cell wall of Mtb, inhibiting specifically the enoyl acyl carrier protein (ACP) reductase, encoded by *InhA* (Lei et al. 2000; Zhang 2005). In 1998 Mdludi and colleagues published a highly-cited study, and at the time highly controversial, attributing the inhibitory effect of isoniazid to be directed against the Mtb ketoacyl ACP synthase (Mdluli et al. 1998). The authors were criticised for over-simplifying a very complex process.

Resistance to the drug is caused either by mutations in *KatG*, the gene that encodes catalase-peroxidase which is involved in the activation of INH; mutations in the promoter regions of *InhA* (INH target) (Zhang 2005; Handbook of anti-tuberculosis agents 2008; Zhang and Yew 2009) or by mutations in *ndh* that alters the NADH/NAD ratios along the electron transport chain. High levels of NADH either competitively inhibits the binding between the drug and the enzyme encoded by *InhA* or the activation of INH by the enzyme encoded by *KatG* (Miesel et al. 1998; Lee et al. 2001; Vilchèze et al. 2005).

The success of INH is due to its specificity against TB and to the fact that it is cheap. However its side effects may include hepatitis and peripheral neuropathy (Thompson 1978).

1.8.2. Rifampicin

Rifampicin (RMP) (Fig. 1.6.) acts by binding and inhibiting DNA-dependent RNA polymerase in prokaryotic cells, i.e. inhibiting transcription. Resistance is caused by mutations in the *rpoB* gene that encodes the β-subunit of RNA polymerase. Rifampicin is active against on-growing organisms and also against non-multipliers and it is due to its action that chemotherapy against TB does not have an even longer duration (Zhang 2005; Zhang and Yew 2009). Prolonged use of

rifampicin for at least 6 months and a careful identification of an optimum dosage is recommended for better outcomes, in terms of decreasing the risk of drug resistance and relapse rates (Menzies et al. 2009).

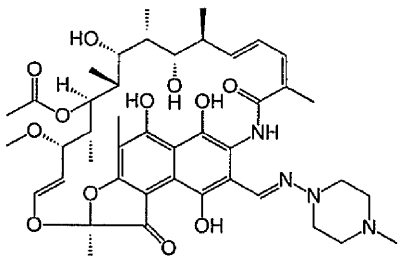

Fig. 1.6.: Structure of rifampicin, $C_{43}H_{58}N_4O_{12}$.

1.8.3. Ethambutol

Ethambutol (EMB) (Fig. 1.7.) was discovered in 1956 by the Lederle Research Laboratories, after knowing that polyamines and diamines were active against Mtb (Thomas et al. 1961; Zhang 2005).

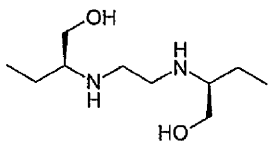

Fig. 1.7.: Structure of ethambutol, $C_{10}H_{24}N_2O_2$.

EMB hampers the synthesis of arabinogalactan, a polymer of the Mtb cell wall, hence the specificity of EMB to mycobacterial cells. Resistance emerges due to mutations in *embCAB* operon, especially *embB*, the gene that encodes the enzyme involved in the synthesis of arabinogalactan (Zhang 2005; Handbook of anti-tuberculosis agents 2008; Zhang and Yew 2009). However, there are EMB-resistant Mtb strains that do not

present mutations in *embB*, suggesting other determinants for resistance (Sreevatsan et al. 1997; Zhang and Yew 2009).

1.8.4. Pyrazinamide

Pyrazinamide (PZA) (Fig. 1.8.) was discovered in 1952 by the Lederle Research Laboratories, that based their studies in the same fact that led to the discovery of INH, the fact that nicotinamide had an inhibitory effect against Mtb (Malone et al. 1952; Zhang 2005). Nicotinamide is a structural analogue of PZA.

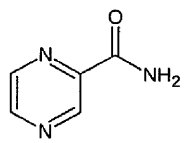

Fig. 1.8.: Structure of pyrazinamide, $C_5H_5N_3O$.

PZA is a pro-drug that requires the activation by the enzyme PZase/nicotinamidase, encoded by the Mtb *pncA* gene, which converts it to its active form, pyrazinoic acid. One of the theories currently proposed for its mode of action is that PZA enters the mycobacterial cell, where it is converted to pyrazinoic acid, which leaves the cell. If the extracellular pH is acidic, protonated pyrazinoic acid will be formed and will re-enter the cell (Zimic et al. 2012), causing cellular damage, due to the defective efflux in Mtb. Hence PZA interferes with membrane energy metabolism (Zhang and Mitchison 2003; Zhang 2005; Handbook of anti-tuberculosis agents 2008). PZA is more active in anaerobic or microaerophilic conditions. In these conditions, the energy production by Mtb is reduced and PZA disrupts the already low energy cell metabolism (Zhang and Mitchison 2003; Wade and Zhang 2004). This drug is inactive at neutral

pH so it is only active in acidic conditions and at low cell densities. This effect is important since after the initial infection, Mtb organisms are phagocysed and contained in acidic compartments inside the host macrophages (Salfinger and Heifets 1988).

The specific target of PZA was proposed to be FAS-I (fatty acid synthase I), although fatty acid synthesis either *in vivo* or *in vitro* is not inhibited by pyrazinoic acid suggesting that PZA has non-specific mechanisms of cell death (Boshoff et al. 2002).

Resistance to pyrazinamide is mainly due to mutations in the *pncA* Mtb gene (Zhang 2005; Handbook of anti-tuberculosis agents 2008; Zhang and Yew 2009).

1.8.5. Streptomycin

Streptomycin (Fig. 1.9.) was discovered in 1944 by Schatz and Waksman and it was the first effective drug against Mtb, representing the beginning of modern Mtb chemotherapy. It is an aminoglycoside antibiotic that inhibits bacterial protein synthesis. Resistance to this drug is associated with mutations in the genes that encode the small ribosomal subunit, namely *rpsL* and *rrs* (Zhang 2005; Handbook of anti-tuberculosis agents 2008).

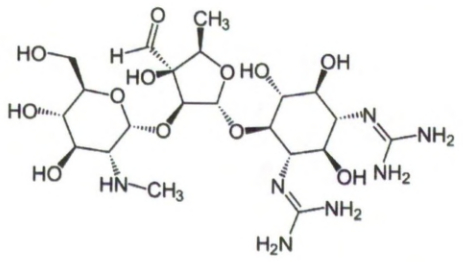

Fig. 1.9.: Structure of streptomycin, $C_{21}H_{39}N_7O_{12}$.

1.9. Other anti-mycobacterial agents

Despite being considered one of the deadliest diseases of the 20th century, due to the introduction in the 1960s of rifampicin and ethambutol tuberculosis was considered for many years an easily controlled disease. This scenario changed due to the emergence of hyper-virulent and drug resistant strains and co-infection with HIV. So, when the regular regimen is not effective, due to resistance or unwanted side effects of the first line drugs, there are a number of second line drugs that can be used (capreomycin, cycloserine, streptomycin, clarithromycin and ciprofloxacin) (Mukherjee et al. 2004). These second line drugs are less effective, have less tolerable side effects and their costs are higher.

Many anti-TB drugs were discovered between 1950 and 1960 from the screening of antibiotics isolated from soil microbes that proved to have an effect against Mtb. That was the case of the second line anti-TB drugs such as cycloserine, kanamycin, amikacin, viomycin, capreomycin, rifamycins and rifampin. In the 1980s quinolone drugs were discovered (Zhang 2005).

1.9.1. Metronidazole, a drug against anaerobic bacteria

Metronidazole (Fig. 1.10.) is classified as a nitroimidazole, and it is a drug known to act against anaerobic or microaerophilic bacteria, hence its possible importance against latent Mtb. Metronidazole damages the pathogen DNA but it does not have an effect against active on-growing Mtb (Sacchettini et al. 2008). Metronidazole is often used as a control in the anaerobic TB studies since it is known to be active against dormant bacteria and it serves as an indicator of positive drug activity in anaerobic conditions. Also it does not have an antagonistic effect when used in conjunction with the first line anti-TB drugs (Wayne and Sramek 1994).

Metronidazole shows low or no activity against the persistent bacilli in the Cornell mouse model, probably due to the non-establishment of complete hypoxia in this infection scenario (Dhillon et al. 1998).

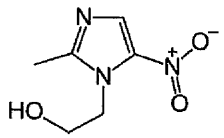

Fig. 1.10.: Structure of metronidazole, $C_6H_9N_3O_3$.

A study sponsored by NIAID, the National Institute for Allergy and Infectious Diseases (www.niaid.nih.gov) is currently testing the effect of adding metronidazole to the treatment against multi-drug resistant TB, in patients from Masan, South Korea.

1.10. Resistance to antimycobacterial drugs

It was the discovery and development in the 1940s of effective anti-bacterial drugs that led to an astonishing reduction in the mortality caused by bacterial infections. However, in parallel with these effective treatments against the pathogenic organisms, bacteria successfully developed their own strategies to counteract the effect of the drugs and this resulted in the emergence of resistant strains. Therefore, it is due to this phenomenon of resistance that TB, which was once controlled by a therapeutic regimen, is now one of the deadliest infections worldwide, with strains that are resistant to conventional forms of therapy (Gillespie 2002; Mitchison 2005; WHO 2010).

The main cause for the emergence of resistant strains is the non-compliance of patients to an extremely demanding and prolonged therapeutic regimen often associated with lack of access to essential medical care (Gillespie 2002), this is called secondary resistance, also

called acquired resistance. Apart from patient non-compliance, also to blame in the emergence of drug resistant Mtb strains are inaccurate prescribing patterns, often with a wrong selection of drugs as well as an incorrect dosage and treatment duration (Sharma and Mohan 2006).

TB primary resistance occurs when the person is infected with an already drug-resistant strain of Mtb. Drug resistance mutations occur either in the genes that encode the target or in the genes that encode the drug activator (Sacchettini et al. 2008).

For a long period there was very little interest from pharmaceuticals companies in investing resources into research for new anti-TB drugs. However, in the past few years the pressing need for novel compounds was finally recognised, due to the fact that the current therapy is ineffective against resistant strains and persistent organisms (Russell et al. 2010). All this led to considerable efforts that are now in place aimed at creating new and more effective ways of treatment (Gillespie 2002).

The dates of discovery of the current available anti-TB therapy are represented in Fig. 1.11. The time line shows the rise in resistant strains of TB as well as co-infection with HIV that represent the main worries for the TB eradication efforts.

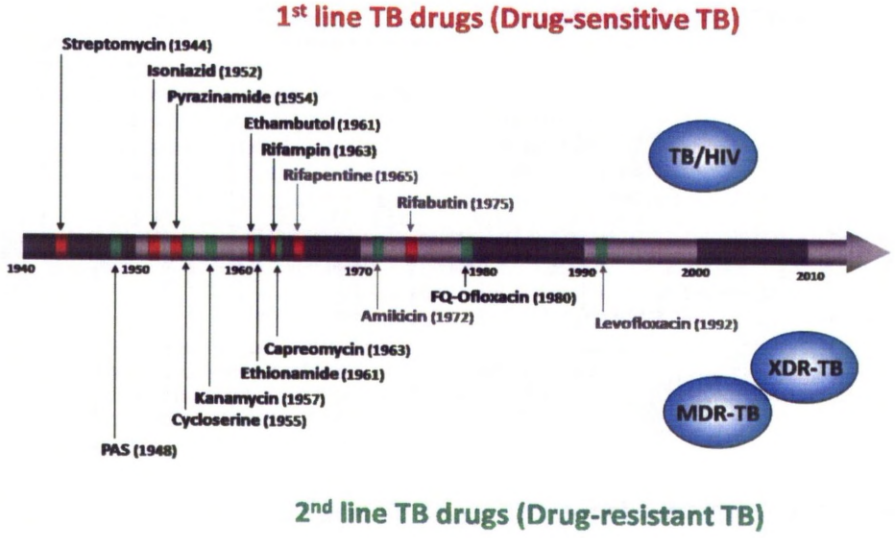

Fig. 1.11.: Time line of the discovery of the first and second line anti-TB drugs. Also represented is the emergence around the year 2000 of TB/HIV co-infection, multiple-drug resistant TB (MDR-TB) and extensively drug resistant TB (XDR-TB). Scheme adapted from TB Alliance Organization. In the figure, PAS represents para-aminosalicylic acid and FQ represents fluoroquinolone.

Multiple-drug resistant TB (MDR-TB) is defined as resistance to the two most effective first line TB drugs: rifampicin and isoniazid, while extensively drug resistant TB (XDR-TB) occurs when bacteria are also resistant to one of the three classes of second-line drugs, namely aminoglycosides, such as amikacin or kanamycin, cyclic polypeptides such as capreomycin and fluoroquinolones such as ciprofloxacin or levofloxacin (Barry III and Blanchard 2010). These resistant phenotypes are acquired by a sequence of cumulative mutations in the genes involved in individual drug resistance (Zhang and Yew 2009). A summary of the mechanisms of resistance involved in each of the first and second line drugs is displayed in Table 1.2.

Table 1.2.: Summary table of drugs currently used against TB and their mechanisms of resistance. Cells in white represent first line drugs and cells in grey represent second line drugs. Adapted from Sacchettini et al. 2008; Zhang and Yew 2009.

Drug	Mechanism of action	Target	Gene involved in resistance	Gene product	Effect on
Isoniazid	Inhibits mycolic acid synthesis	Primary: InhA Secondary: KasA and DfrA	*katG* *inhA*	Catalase-peroxidase Enoyl ACP reductase	Replicating bacilli
Rifampicin	Inhibits RNA synthesis	RNA polymerase β-subunit	*rpoB*	β-subunit of RNA polymerase	Replicating and non-replicating bacilli
Ethambutol	Inhibits arabinogalactan synthesis	EmbB	*embB*	Arabinosyl transferase	Replicating bacilli
Pyrazinamide	Depletes membrane energy	(FAS-I)	*pncA*	Nicotinamidase/pyrazinamidase	Persister bacilli
Streptomycin	Inhibits protein synthesis	30S ribosomal unit	*rpsL* *rrs* *gidB*	S12 ribosomal protein 16S rRNA rRNA methyltransferase	Replicating bacilli
Amikacin/Kanamycin	Inhibits protein synthesis	Ribosomes	*rrs*	16S rRNA	Replicating bacilli
Capreomycin	Inhibits protein synthesis	Methylated nucleotides in ribosomal subunits	*tlyA* *rrs*	2'-O-methyltransferase 16S rRNA	No conclusive data
Fluoroquinolones	Inhibition DNA gyrase	DNA gyrase	*gyrA* *gyrB*	DNA gyrase subunit A DNA gyrase subunit B	No conclusive data
Ethionamide	Inhibits mycolic acid synthesis	InhA	*ethA* *inhA*	Flavin monooxygenase Enoyl ACP reductase	Replicating bacilli
Para-aminosalicylic acid	Inhibits folate metabolism	Dihydropteroate synthase?	*inhA* *thyA*	Enoyl ACP reductase Thymidylate synthase	No conclusive data
Cycloserine	Inhibits peptidoglycan synthesis	Alanine racemase D-alanine-D-alanine ligase	*alr* *ddl*	Alanine racemase D-alanyl-alanine synthetase A	No conclusive data

The WHO report of 2010 summarizes the latest estimates of the global epidemic of MDR-TB and XDR-TB and it includes an assessment of the progress that countries from all over the world are making in terms of diagnosis and treatment of these cases (WHO 2010). A map showing the worldwide distribution of XDR-TB cases is displayed in Fig. 1.12. A large part of Africa does not have reported XDR-TB cases but this is believed to be due to laboratory limitations in diagnosis (WHO 2010).

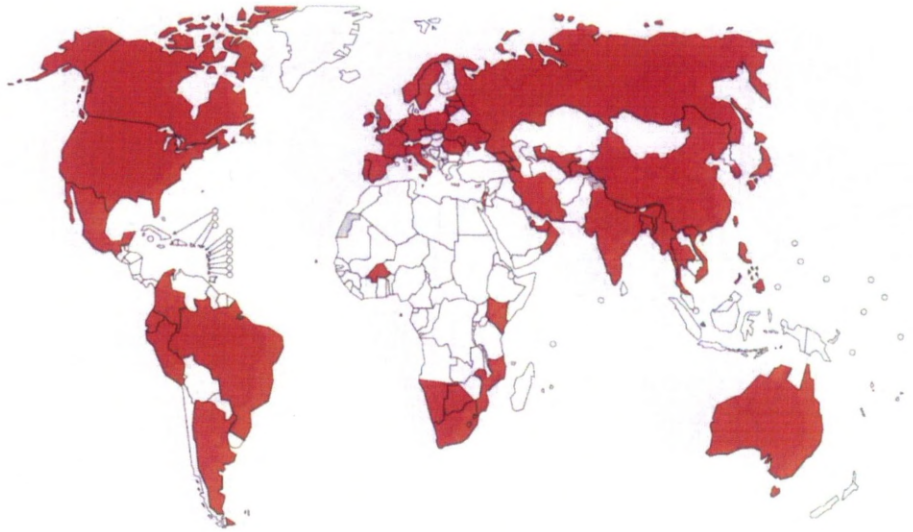

Fig. 1.12.: Worldwide distribution of countries reporting at least one case of XDR-TB (in red), according to WHO report, 2010 (WHO 2010).

1.10.1. Treatment of drug resistant TB

WHO published a guideline with recommendations for the treatment of drug resistant TB (WHO 2011). The success of the treatment depends on the early identification of the drug-resistance involved and in the establishment of a treatment focused on the particular individual and his background (Johnston et al. 2009).

WHO recommendations are that in the intensive phase of the treatment, a regimen of at least four drugs should be implemented: a parenteral agent should be used (either kanamycin, amikacin or capreomycin, but often the first due to its lower cost), a fluoroquinolone, an oral bacteriostatic drug (either ethionamide or prothionamide) and pyrazinamide whose inclusion may represent a slight improvement in the outcome of the treatment (WHO 2011).

The duration of the MDR-TB treatment can last from 8 to 20 months, with increased risks of adverse reactions after 12 months (WHO 2011).

1.10.2. The future of anti-TB therapy

With the appearance of XDR Mtb strains by the end of the twentieth century that are virtually impossible to kill by the current chemotherapy, the need for new bactericidal compounds became urgent.

There are a number of ideal characteristics that a drug should have in order to improve the outcome of anti-TB therapy. Namely, the inhibitory compound should have great effectiveness, in order to reduce the duration of treatment and avoid patient noncompliance; should be active against drug-resistant strains of Mtb including the organisms in the latent state and it should be compatible with the current DOTS drugs (Cole and Alzari 2007).

Another feature to take into account is the affordability of new anti-TB compounds, since the new successful drugs need to be introduced into resource-poor countries so costs cannot be ignored (Dye and Floyd 2006; Young 2009).

1.10.2.1. Organisations involved in the fight against TB

There are several worldwide associations that are placing an effort in the development of new drug therapies.

The Stop TB partnership was founded in 2001 with the objective of eliminating TB from the list of public health dangers and ultimately to eradicate TB worldwide. It comprises an international network containing public and private sectors (http://www.stoptb.org/). One of the seven Working Groups of the partnership, the Working Group on New Drugs (WGND) aims to accelerate the discovery, development and implementation of new drugs that are both effective and affordable in the fight against TB. The WGND is to act as a platform of communication and collaboration between the different partners involved.

The TB Alliance, the Global Alliance for TB Drug Development (www.tballiance.org) is another worldwide partnership, whose mission is to discover and develop better, faster acting and affordable drugs to fight tuberculosis.

Another relevant association in the fight against TB is the Bill & Melinda Gates foundation (www.gatesfoundation.org/tuberculosis). They focus their investments in innovation, aiming to find new drugs, diagnostics or a vaccine effective against TB and the accessibility and affordability of these new solutions across the World. They raise public awareness and advocate for funding.

1.10.2.2. Anti-TB drugs in the pipeline

In 2010 Barry and Blanchard reviewed the state of the art of compounds that were going into phase I and II clinical trials. These included the diarylquinoline R207910, the nitroimidazoles PA-824 and OPC67683, the diamine SQ109, the β-lactams clavulanate and carbapenems and

oxazolidinones linezolid and PNU-100480 (Barry III and Blanchard 2010).

Some promising drugs have already moved to the final step, phase III, of clinical trials, which includes testing in more than 900 TB patients (http://www.newtbdrugs.org/pipeline.php). Gatifloxacin and moxifloxacin are fluoroquinolones and they have already shown great potential in decreasing the duration time of TB treatment.

The fluoroquinolones moxifloxacin (Fig. 1.13.B) and gatifloxacin (Fig. 1.13A) also have an effect in many other infections, namely respiratory infections, such as pneumonia and hospital acquired infections caused by *Staphylococcus aureus* (Sacchettini et al. 2008). These two compounds have the highest *in vitro* activity against Mtb, but there are concerns regarding the emergence of resistant strains, since *gyrA* mutations are common (Rivers and Mancera 2008).

Fluoroquinolones interact with DNA gyrase and topoisomerase IV stopping the process of transcription, repair and replication of DNA, leading to the blocking of bacterial reproduction (Nguyen and Pieters 2009). Rifapentine (Fig. 1.13.C) is a rifamycin. Rifapentine has some advantages compared to its analogue, rifampicin, specifically its serum half-life which is much longer than rifampicin hence requires less frequent dosing (Sacchettini et al. 2008).

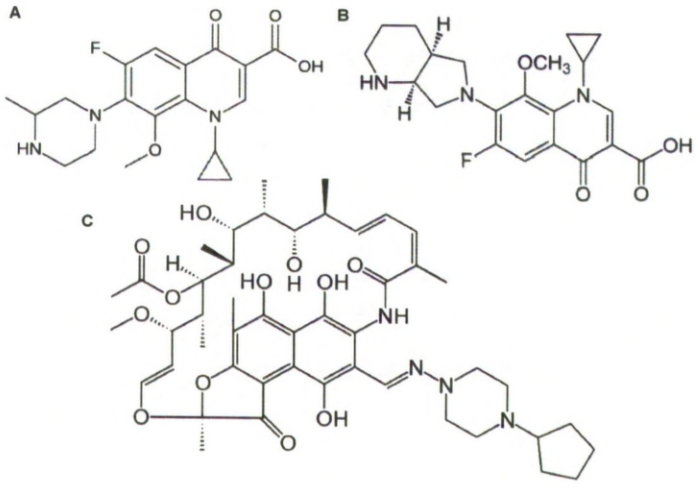

Fig. 1.13.: Structure of (A) gatifloxacin, $C_{19}H_{22}FN_3O_4$, (B) moxifloxacin, $C_{21}H_{24}FN_3O_4$ and (C) rifapentine, $C_{47}H_{64}N_4O_{12}$.

1.11. High-throughput screening

High throughput screening is pivotal in the discovery of new drugs. Using informatics resources, a large amount of information can be compiled and analysed. This may include characterization of genes, structures of compounds, data generated *in silico* and cross-checking with the literature, which generates a large number of informatic hits. These hits may identify compounds with the desirable pharmacokinetic features. This high throughput screening allows the testing of a large number of these compounds (Sacchettini et al. 2008). Ananthan and colleagues described the testing of 3200 representative compounds from a set of 13440 on Mtb H37Rv (Ananthan et al. 2009).

Inglese and colleagues proposed a series of directives to optimise and standardize the experiments and presentation of results in order to create comparable databases as well as to establish a quality control measure for the biochemical assays (Inglese et al. 2007; Inglese et al. 2007).

The Tuberculosis Antimicrobial Acquisition and Coordinating Facility (TAACF) was established in 1994 by the USA National Institute of Allergy and Infectious Diseases with the purpose of concentrating commercial, academic and government efforts worldwide in identifying new anti-TB compounds and in their evaluation *in vivo* and *in vitro*. The TAACF experience ended in March 2010 but the outcome of their screening activities resulted in several promising anti-TB agents (http://www.taacf.org/).

1.12. Persister organisms

The existence of persistent organism, able to evade not only the defences of the host immune system but also antibiotics used in anti-TB treatment, was always neglected. However, nowadays their importance and their role in chronic infections are finally recognised. They impair drug effectiveness and extend the duration of treatment (Mitchison and Coates 2004).

Persister cells are a very small fraction of cells of antibiotic sensitive strains of Mtb that despite being genotypically drug sensitive, are able to evade its effects (as well as the immune system of the host) due to phenotypic tolerance (Balaban et al. 2004). Despite not having genetic modifications, they present a distinct genetic expression profile: they have an impaired growth rate, and they divide very slowly compared to the remaining cells in the population (Mitchison and Coates 2004; Coates and Hu 2008). Despite this slow metabolism, persisters are dividing because INH and RMP, that exclusively target actively growing organisms, still have a bactericidal effect against these persisters, if taken over a long period (Mitchison and Coates 2004).

According to Mitchison and Coates, the heterogeneity in the growth of sub-populations inside the human host is the most important reason for

slow Mtb sterilization. This fact is corroborated by an initial rapid clearance of active Mtb at the beginning of treatment, followed by this killing rate becoming increasingly slower as time goes by, which corresponds to the killing of the very slow growth persister organisms (Mitchison and Coates 2004).

The distinction between persister cells and mutants is depicted in Fig. 1.14.. The latter ones have genetic alterations that confer drug resistance and these alteration will be vertically transmitted to their descendants, originating a drug resistant population (Fauvart et al. 2011).

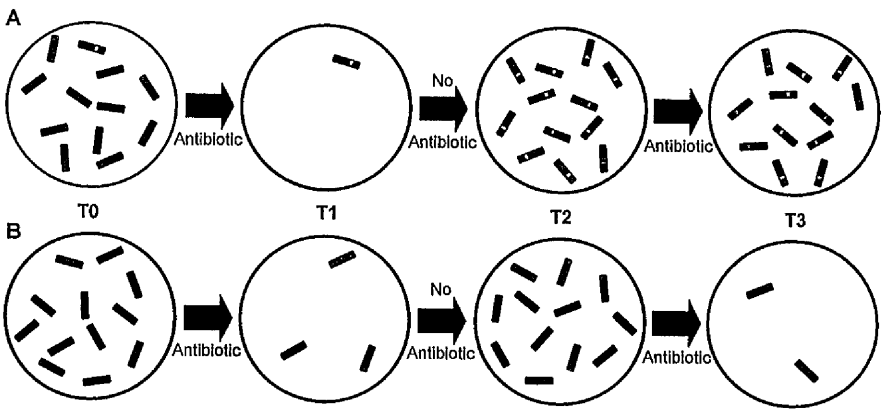

Fig. 1.14.: Difference between antibiotic resistance (A) and persistence (B). Population A is composed of drug-sensitive bacteria (blue bacilli) and a mutant resistant cell (blue bacilli with red dot). After antibiotic treatment, sensitive bacteria are killed and only the mutants survive, originating a population of resistant cells. If at T3 the cells were treated again with the same antibiotic, it will have no effect since they are resistant. Population B is composed of cells with no genetic alteration but this population contains a small percentage of persister cells that survive antibiotic treatment and are able to resume growth originating a drug-sensitive population that would be equally reduced if treated with the same antibiotic. Adapted from Fauvart et al. 2011.

It should also be pointed out that persister and non-multiplier organisms are two different things. Non-multipliers are all the dormant populations of bacteria that grow slowly and that include organisms in stationary phase, non-dividing or slow-dividers. Persisters are regularly referred to

as a well-defined sub-population of these non-multiplying bacteria, extremely antibiotic resistant, with a different gene profile (Coates and Hu 2008).

1.13. The Genomic Era in the study of Mtb

The complete sequencing of the Mtb H37Rv genome was published in 1998 by Cole and collaborators (Cole et al. 1998).

TubercuList (http://tuberculist.epfl.ch/) is a publicly available database with the genome details of Mtb, created by the Institute Pasteur and it is a valuable genetic research tool. Detailed genetic information about the Mtb genome can be easily assessed and in this way a better understanding of the protein coding genes and genetic pathways of Mtb gained, allowing comparisons between pathogenic and non-pathogenic organisms which helps to clarify the mechanisms of virulence and drug resistance of Mtb.

The mapping of different strains of Mtb genomes is an on-going process, and is being constantly updated with further annotations. At present the Mtb H37Rv complete genome, as available in NCBI (http://www.ncbi.nlm.nih.gov/genome?Db=genome&Cmd=ShowDetailView&TermToSearch=135) has a length of 4,411,532 nucleotides sequenced and a GC content of 65%. Usually this GC content confers high stability of the DNA (G and C connect by 3 hydrogen bounds to the opposite DNA strand while A and T connect by two hydrogen bounds) and it is also characteristic of Gram positive Actinobacteria. 90% of the Mtb H37Rv genome is functional with a total of 4047 genes detected of which 3988 are protein coding genes.

In the Mtb genome there are more than 250 genes coding for enzymes involved in fatty acid metabolism. Approximately 9% of the genome

encodes glycine-rich proteins, the PE (novel glycine-alanine rich protein) and PPE (novel glycine-asparagine-rich protein) that could correspond to a source of antigenic variation, representing a pathogenic advantage (Domenech et al. 2001).

With the advent of complete genomes of Mtb, it became possible to develop microarrays that would target the complete transcriptome of the bacteria. This allowed researchers to develop probes (oligonucleotides) that are complementary to every single gene (in the case of whole genome microarrays) or of a specific set of genes of interest, and to study the patterns of gene expression under particular conditions (Debouck and Goodfellow 1999). Microarray results usually need further validation by other methods, typically quantitative real time PCR (RT-qPCR) whose data confirm the pattern of expression of a very limited number of genes (Butcher 2004).

Sassetti and colleagues analysed the complete Mtb genome and using transposon site hybridization (TraSH), identified 614 genes that were not mutating in growing bacteria which means that they are probably essential genes for the survival of the organism (Sassetti et al. 2003). Using the same methodology, Sassetti and Rubin, instead of just culturing Mtb *in vitro*, used the bacteria to infect mice and determined the Mtb genes that were essential to mycobacteria survival *in vivo* during infection. They were able to identify 194 genes (Sassetti and Rubin 2003).

Nowadays bioinformatics tools can be useful to identify new drug targets. Murphy and Brown compiled results from genome-wide DNA microarray experiments that determined gene expression patterns in the latent state of Mtb and combined them with gene essentiality data. This analysis allowed them to identify potential new drug targets for new therapeutic treatments (Murphy and Brown 2007). Also mathematical

models allowed the study of the gene expression profiles of Mtb during latency using monitored experiments over time (Magombedze and Mulder 2012).

1.14. Peculiarities of *M. tuberculosis* metabolism

As reviewed in (Niederweis 2008), the main sources of energy necessary for Mtb to survive are carbohydrates or alternatively fatty acids. There is some evidence that points to the switch from carbohydrates to fatty acid metabolism during the passage from the acute to the chronic phase of Mtb infection (Boshoff and Barry III 2005; Muñoz-Elías and McKinney 2005). Titgemeyer and colleagues identified only 5 putative carbohydrate transporters in pathogenic Mtb. Despite glycerol being the standard carbon source for Mtb growth, they did not identify any uptake system for it. This carbohydrate is directly diffused through the lipid membranes of the bacilli (Titgemeyer et al. 2007).

During infection Mtb switches its carbon sources of glycerol and glucose to fatty acids. A large portion of the Mtb genome refers to genes for lipid synthesis and degradation, biochemical activation and oxidation of fatty acids (Cole et al. 1998; Boshoff and Barry III 2005). During infection, the genes associated with fatty acid metabolism are up-regulated (Sassetti and Rubin 2003).

The fatty acid degradation involves the tricarboxylic acid (TCA) cycle and glyoxylate shunt (Fig. 1.15.). Isocitrate is converted to succinate and glyoxylate, by the enzyme isocitrate lyase encoded by two homologous genes (*icl1* and *icl2*) (Cox and Cook 2007), and to α-ketoglutarate by isocitrate dehydrogenase in the TCA cycle. Deletion of both copies of the *icl* gene, which encode isocitrate lyases 1 and 2 of the glyoxylate cycle completely impaired the *in vitro* bacterial growth on fatty acids but had little effect on the use of carbohydrates by the bacteria. *In vivo*, bacteria

lacking *icl1* and *icl2* do not grow in mice and are rapidly eliminated, so this supports the idea that fatty acid metabolism is pivotal during infection and the glyoxylate cycle could be a good target for drug development (McKinney et al. 2000; Muñoz-Elías and McKinney 2005). However, recognising the importance of fatty acid metabolism does not exclude the possibility of a parallel uptake of carbohydrates from the human host.

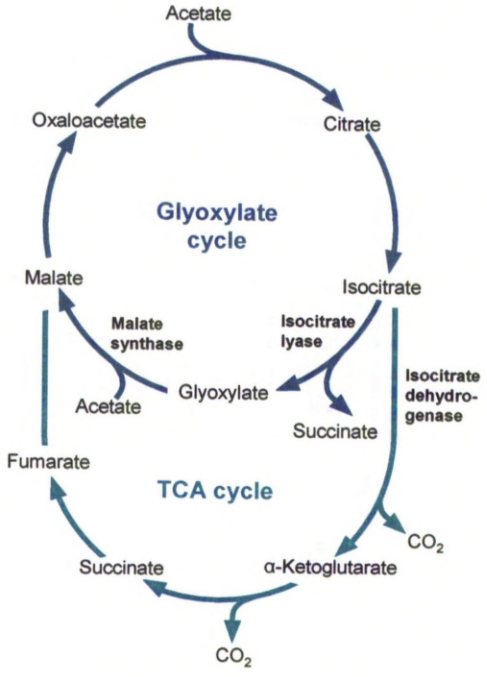

Fig. 1.15.: Schematic representation of the glyoxylate shunt pathway. In the glyoxylate cycle, isocitrate is converted to succinate and glyoxylate, by the enzyme isocitrate lyase. In the tricarboxylic acid (TCA) cycle, isocitrate dehydrogenase converts isocitrate to α-ketoglutarate. Adapted from Russell 2001.

1.15. Electron transport chain

The electron transport chain (ETC) is a modular complex of enzymes within the bacterial membrane that is able to create a proton gradient across this membrane with the purpose of generating ATP. This ETC is considered to have two different sides: a menaquinone-reducing part,

where a series of enzymes transfer electrons to menaquinone, reducing it to menaquinol; and a second part, the menaquinol-oxidizing part, where enzymes accept electrons from the reduced quinol, oxidizing it back to the quinone form and subsequently passing them to terminal electron acceptors (Kana et al. 2009).

The first part includes the NADH: menaquinone oxidoreductases: one type I NADH dehydrogenase and two type II NADH dehydrogenases; a succinate: menaquinone oxidoreductase and flavoproteins that pass electrons to the quinone pool. In terms of the menaquinol-oxidizing part of the ETC, there is one electron acceptor which receives electrons directly from the menaquinol pool: the cytochrome *bd* oxidase, and an aa_3-type cytochrome *c* oxidase that receives electrons from a menaquinol: cytochrome *c* oxidoreductase (the *bc1* complex). Finally, a multi-subunit ATP-synthase, generates ATP using the proton gradient created across the cytoplasmic membrane (Rao et al. 2001).

Hypoxia leads to a down-regulation of genes associated with aerobic respiration and an up-regulation to genes involved in fumarate and nitrate reduction (involving a fumarate and a nitrate reductase) and microaerophilic respiration. So there is a clear distinction between the ETC under normal aerobic conditions, where the energy production is at its maximum and the conditions that exist when the organism is submitted to an environment of very limited oxygen or completely depleted of oxygen (Boshoff and Barry III 2005).

A general scheme of ETC is shown in Fig. 1.16. but a much more detailed biochemical overview of the ETC processes and constituents can be found in Yagi and Matsuno-Yagi 2003, Brandt 2006 and Hosler et al. 2006.

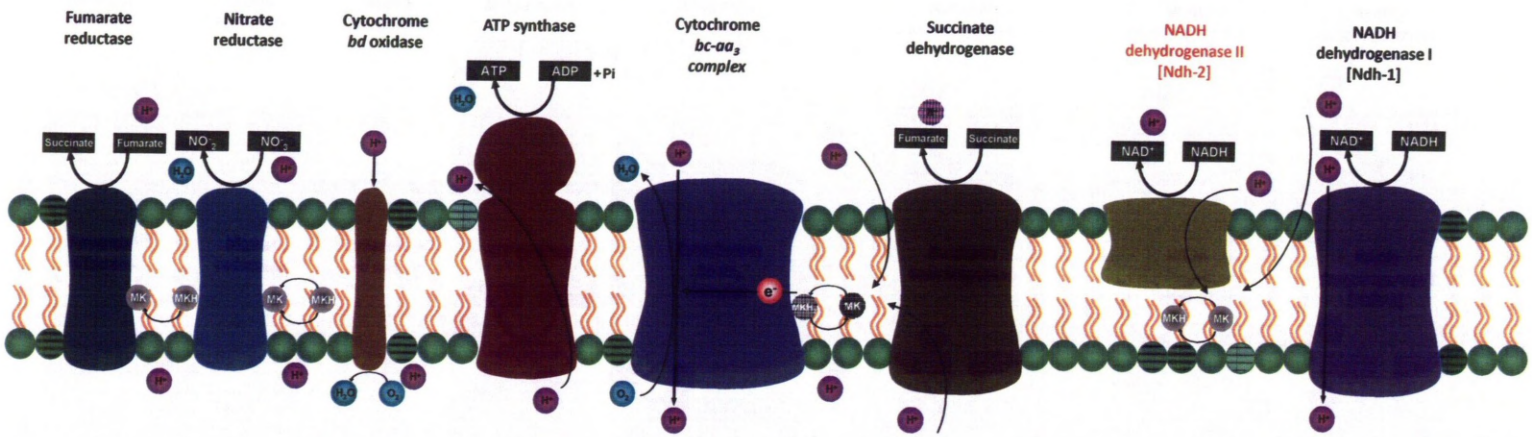

Fig. 1.16.: Schematic representation of the electron transport chain of Mtb. Adapted from Boshoff and Barry III 2005; Kana et al. 2009. Menaquinone (MK) is reduced by either NADH dehydrogenases or via succinate dehydrogenase, and oxidised by the cytochrome *bc-aa*$_3$ complex or by the cytochrome *bd* (according to aeration conditions). Nitrate reductase, in the presence of nitrate can also generate the protonmotive force. The electron transport chain couples with ATP synthase that produces ATP through oxidative phosphorylation.

1.15.1. Electron donors

1.15.1.1. The three NADH: menaquinone oxidoreductases

The 14 subunits of the Type I NADH: menaquinone oxidoreductase (Ndh-1) are encoded by the genes *nuoABCDEFGHIJKLMN*, each one with similarities to homologous proteins in the mammalian mitochondrion (Yagi et al. 2001). In mitochondria, this enzyme (Complex I) is composed of 46 subunits, but it is quite similar to its bacterial homologue, in terms of sensitivity to the drugs rotenone and piericidin A (Yagi and Matsuno-Yagi 2003).

Type II NADH: menaquinone oxidoreductases are encoded by the gene *ndh* and its homologue *ndhA*. The type II NADH dehydrogenase (Ndh-2) single-subunit enzyme catalyses the transfer of electrons from NAD(P)H to the quinone pool without pumping protons across the membrane (Yagi and Matsuno-Yagi 2003). It is essential during hypoxia since it has a pivotal role in maintaining the NADH/NAD^+ ratios within the Mtb cell (Vilchèze et al. 2005). Drug inhibition of the enzyme has been shown to lead to the non-replenishing of the NAD^+ pool and consequent interruption of the electron transport cycle and cell death (Rao et al. 2001; Kerscher et al. 2007).

Type I NADH dehydrogenase is not essential for mycobacterial growth in low oxygen conditions, therefore during hypoxia, Mtb is solely dependent on Ndh-2 (Rao et al. 2001). Contrary to type I NADH dehydrogenase, Ndh-2 does not have a human equivalent which makes it an even more desirable drug target (Weinstein et al. 2005). Ndh-2 is often the only type of NADH dehydrogenase present in many living prokaryotes (Melo et al. 2004).

1.15.1.2. The succinate: menaquinone oxidoreductase

Mtb succinate: menaquinone oxidoreductase is a flavoprotein encoded by the genes *sdhABCD* and it is composed of two hydrophilic subunits and two hydrophobic subunits and it is an integral part of the tricarboxylic acid (TCA) cycle. The two hydrophilic subunits, encoded by the genes *sdhAB* accommodate a substrate binding site, FAD, and three iron-sulfur clusters (Bott and Niebisch 2003; Kana et al. 2009). The two hydrophobic subunits, encoded by *sdhCD*, contain two *b*-type hemes and a quinone binding site. This enzyme does not pump protons and it is very similar to fumarate reductase (see section 1.15.4.2). The enzymes differ in that they catalyse the same reaction but in different directions. Succinate reductase reduces quinone and catalyses the oxidation of succinate to fumarate. Fumarate reductase catalyses the oxidation of quinol and concomitant reduction of fumarate to succinate (Bott and Niebisch 2003; Kana et al. 2009).

1.15.1.3. Other electron donors

In its genome Mtb has other genes including dehydrogenases, namely L-lactase, glycerol-3-phosphate, malate and proline, but their functions are unknown (Kana et al. 2009).

1.15.2. Quinones in *M. tuberculosis*

Quinones are lipid-soluble molecules that transport electrons between the protein complexes in the electron transport chain. They transfer electrons between hydrogenases and cytochromes, functioning as reversible redox components of the electron transport chain (Farrand and Taber 1974). Quinones are an essential part in the respiratory chain (Brandt and Trumpower 1994). Ubiquinone is the quinone present in mammalian cells

and most Gram positive and anaerobic bacteria contain menaquinone and/or demethylmenaquinones as their main quinone (Fig. 1.17.) (Bentley and Meganathan 1982). Mycobacteria have menaquinone, which has a lower redox potential than ubiquinone, meaning that it has less tendency to accept electrons and being reduced (Kana et al. 2009). In bacteria containing both ubiquinones and menaquinones, each quinone may have a specific and distinct electron-carrying role (Bentley and Meganathan 1982), although mycobacteria do not possess this plasticity.

The quinone structure consists of an isoprenoid unit which is hydrophobic and which allows the quinones to be soluble in the interior of membranes, where they can move freely (Roehm 2001), transferring electrons between the membrane-bound proteins.

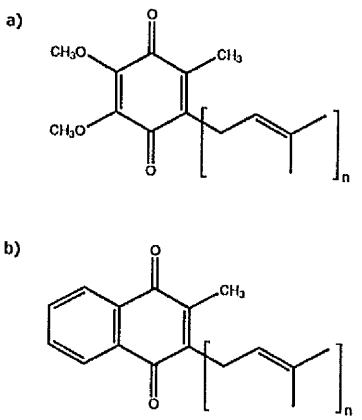

Fig. 1.17.: Structures of (a) ubiquinone and (b) menaquinone

The biosynthesis of menaquinone has been studied in *E. coli*. In this organism, chorismate is converted into menaquinone by seven enzymes, encoded by the genes *menA* to *menG* (Hiratsuka et al. 2008). The biosynthesis of menaquinone in mycobacteria is schematized in Fig. 1.18. and it diverges from the ubiquinone biosynthesis pathway at the first step, with the conversion of chorismate to isochorismate. The bacterial

enzymes of this pathway, such as MenB, are potential targets for anti-TB drugs since they do not have human homologues (Truglio et al. 2003).

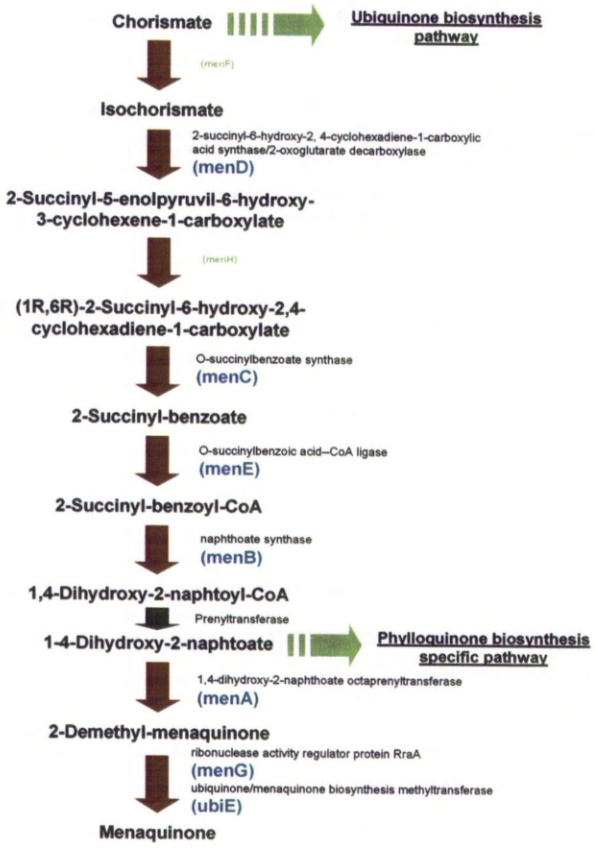

Fig. 1.18.: Menaquinone biosynthesis pathway in mycobacteria, showing enzymes and intermediate products involved in the biosynthesis of chorismate to menaquinone. Green arrows refer to points where the pathway diverges into the production of ubiquinone and phylloquinone (neither present in mycobacteria). Light green letter genes (*menF* and *menH*) are present in other bacterial pathways but have not been identified in either *Corynebacterium* or *Mycobacterium* genus.

Mtb uses demethylmenaquinone-9 (DMK-9) as a lipid soluble electron/proton carrier in the quinone pool, encoded by *menABCDEG* (Teh et al. 2007). However, accordingly to Weinstein and colleagues, this carrier is demethylmenaquinone-8 (DMK-8) (Weinstein et al. 2005).

Genomic data support the notion that Mtb uses only menaquinone in the electron transport chain, since the Mtb genome contains homologues of most of the *E. coli men* genes, while homologues of the key ubiquinone biosynthesis genes are not present (Cole et al. 1998).

1.15.3. Electron acceptors

1.15.3.1. The menaquinol: cytochrome *c* oxidoreductase (bc_1 complex)

The menaquinol: cytochrome *c* oxidoreductase or bc_1 complex cytochrome *c*, is encoded by the *qcrCAB* operon. It is composed of cytochrome *b* and cytochrome *cc*. This enzyme transfers electrons from menaquinol to electron acceptors like cytochrome *c* and translocates protons across the membrane, in what is called the quinone cycle mechanism (Crofts 2004). The Mtb bc_1 complex is associated with the aa_3-type cytochrome *c* oxidase forming a bc_1-aa_3 super-complex, transferring electrons to this terminal oxidase (Kana et al. 2009). The disruption of this super-complex is not lethal in *M. smegmatis*, but it is lethal in Mtb (Matsoso et al. 2005).

1.15.3.2. The two terminal oxidases

The cytochrome *bd* oxidase is encoded by *cydABCD* and contains two structural subunits, encoded by *cydA* and *cydB* and three heme groups (two *b*-type hemes and one heme *d*). The genes *cydC* and *cydD* encode a probable ATP-binding cassette (ABC)-type transporter (Cole et al. 1998). This enzyme catalyses the oxidation of menaquinol and it has high affinity for oxygen, hence its important role when bacteria are submitted to low oxygen conditions (Kana et al. 2009).

In the other branch of the respiratory chain cytochrome *c* is fused to a third subunit of the bc_1 complex, forming a super-complex terminating in an aa_3-type cytochrome *c* oxidase, encoded by the cluster of genes *ctaBCDEF* (see section 1.15.3.1.) (Weinstein et al. 2005).

1.15.4. The anaerobic respiratory enzymes of the ETC

The ETC of Mtb contains enzymes that are able to catalyse the oxidation of menaquinol and transfer electrons to a final acceptor that is nitrate rather than oxygen. They are denominated denitrification enzymes. The final electron acceptor can also be nitrite or fumarate, thus Mtb has a nitrite reductase, encoded by *nirBD*, and a fumarate reductase, encoded by *frdABCD* that could be used for anaerobic fumarate respiration (Sohaskey ; Sohaskey 2008).

1.15.4.1. Nitrate reductase

In the absence of oxygen, Mtb is capable of using nitrate as an alternative electron acceptor. The enzyme nitrate reductase, encoded by *narGHJI*, oxidises menaquinol and reduces nitrate to nitrite (Sohaskey 2005). In parallel with the over-expression of this cluster of genes, there is also an up-regulation of the *nark2-narX* operon, which encode the transporter NarK2 (nitrite-efflux system), and the inactive nitrate reductase NarX (Shi et al. 2005). With hypoxia, the reduction of nitrate to nitrite provides energy while bacteria adapt to anaerobiosis. There is evidence that nitrate respiration plays a role in persistence of Mtb in macrophages (Boshoff and Barry III 2005).

The expression of the operon *narGHJI* is not induced by hypoxia. It is *nark2*, the nitrate transporter, that is induced by the regulator DosR and

so it is responsible for the up-regulation of nitrate reductase activity seen in non-replicating cultures (Park et al. 2003). Oxygen inhibits nitrate reduction and *narK2*, while hypoxia results in an inactive cytochrome oxidase and the increase of reduced components of the ETC, that may serve as a signal for *narK2* activity (Sohaskey 2005).

1.15.4.2. Fumarate reductase

Fumarate reductase is encoded by *frdABCD* and it is structurally composed of 4 subunits, two hydrophilic subunits (encoded by *frdAB* containing one FAD and three iron-sulfur clusters) and two membrane anchor subunits (encoded by *frdCD* containing one heme *b*). Fumarate reductase is used as a terminal oxidase in some bacteria and parasites for fumarate respiration, but its role in Mtb is not yet clear (Watanabe et al. 2011). It is probable that this enzyme is involved in the persistence phenomenon (Tian et al. 2005). This enzyme is similar to succinate and catalyses a similar reaction, but in the opposite direction (see section 1.15.1.2.) (Kana et al. 2009).

1.15.4.3. Nitrite reductase

Nitrite reductase is a flavoprotein, encoded by *nirBD,* whose function in Mtb growth is unclear (Kana et al. 2009).

Fumarate, nitrite and nitrate reductase are less efficient in terms of energy output (Stouthamer et al. 1982). They do not use oxygen as the ultimate electron acceptor, resulting in a small ATP production and once again supporting the idea of low energy requirement during hypoxia (Boshoff and Barry III 2005).

1.15.5. F_1F_0-ATP synthase

F_1F_0-ATP synthase is encoded by the *atpABCDEFGH* gene cluster and is responsible for the production of ATP by oxidative phosphorylation in aerobic conditions. It works as an ATPase, pumping protons through the membrane in anaerobic conditions (Tran and Cook 2005). The *atpD* gene that encodes the β-subunit of F_1F_0-ATP synthase is an essential gene for Mtb (Sassetti et al. 2003; Tran and Cook 2005). Under hypoxia, the energy requirements are less, due to reduced metabolism, hence F_1F_0-ATP synthase is under-expressed (Berney and Cook 2010), but it remains essential (Rao et al. 2001).

1.15.6. Important drugs that target Mtb ETC

The drugs diarylquinolines and phenothiazines have in common the fact that both target oxidative phosphorylation in mycobacteria (Hurdle et al. 2011). Phenothiazines target the initial step of the Mtb ETC, inhibiting type II NADH: menaquinone oxidoreductase and diarylquinolines are a class of drugs that target the subunit *c*, encoded by the gene *atpE* of the F_1F_0-ATP synthase enzyme in order to kill Mtb (Koul et al. 2007). As well as killing actively growing bacilli, diarylquinolines may have an even more active effect against dormant bacteria (Koul et al. 2008). This is indicative of the fact that since ATP synthase is under-expressed during latency, dormant bacteria still need residual activity of ATP synthase to survive and are more sensitive to alterations in ATP levels, than actively growing Mtb bacilli (Rao et al. 2001; Koul et al. 2008)

1.16. DosR regulon

The electron transport chain is a dynamic modular complex that is capable of adjusting to environmental conditions, namely the availability of oxygen and nitric oxide (Brandt 2006). The changes in the respiratory chain of Mtb are often controlled by transcriptional regulators, such as the DosR regulon, that are known to change gene expression levels, in response to aerobic or anaerobic conditions (Boon and Dick 2002).

DosR is a two-component signalling system that is required for the Mtb response to hypoxia (Voskuil et al. 2004). Many of the genes up-regulated during hypoxia require DosR for their induction (Park et al. 2003; Roberts et al. 2004; Voskuil et al. 2004). Boon and Dick named Rv3133c gene as *dosR* (dormancy survival regulator) (Boon and Dick 2002).

Apart from oxygen deprivation, which is typical of latency, nitric oxide (the product of activated macrophages *in vivo*) also modulates the expression of DosR (Voskuil et al. 2003; Kendall et al. 2004). DosR is often referred to as conferring a selective advantage in anaerobic conditions during infection (Reed et al. 2007).

Kendall and colleagues in an attempt to identify other stresses capable of up-regulating DosR regulon, observed that this regulon is induced in standing cultures, due to the settling of bacteria and the probable oxygen gradient and stress induced in the settled bacteria (Kendall et al. 2004).

Kumar and colleagues described in detail the two sensor kinase regulon, called DosS and DosT, controlled by the transcription factor DosR. They claimed that DosS is the redox sensor while DosT is an hypoxia sensor and carbon monoxide also induces the expression of the Mtb Dos regulon (Kumar et al. 2007), reinforcing the idea that the expression of DosR is mediated by environmental factors. More recently, Rustad and colleagues investigated the role of the 48-gene regulon in the hypoxic response.

They argued that DosR regulon induction is transient and later a set of 230 genes of an enduring hypoxic response (EHR) are induced (Rustad et al. 2008). EHR is independent of DosR since it occurs in a DosR mutant. The hypothesis proposed is that DosR may regulate the initial response *in vitro* and *in vivo* mice infections, but then to establish persistence and virulence, this regulon is dispensable. It is proposed that EHR is more stable and extensive than DosR response, being induced for a longer period (Rustad et al. 2008). This remains debatable.

In order to assess the role of this regulon in antibacterial drug tolerance, Bartek and colleagues, constructed a DosR mutant and showed that despite being needed for long-term survival in dormancy, this regulon is not required for *in vivo* or *in vitro* phenotypic drug tolerance (Bartek et al. 2009).

In terms of genes induced by the DosR regulator, DosS/T and DosR regulate the expression of almost 50 genes (Kumar et al. 2007; Rustad et al. 2008), the majority of them still of unknown function. Within those that are already characterised, several are involved in adaptations to anaerobic conditions, namely the up-regulation of *narX* (nitrate reductase) and *narK2* (nitrate transporter) and the repression of Type I menaquinone oxidoreductase (Ndh-1); the up-regulation of *fdxA* (ferredoxin), *acr* (α-crystallin protein) and *nrdZ* (dNTPs microaerophilic synthesis) and *tgs1* (triglyceride synthase) and others (Park et al. 2003; Rustad et al. 2008). Given its functional significance, DosR is often suggested as a possible drug target (Zhang 2005; Chao and Rubin 2010).

In 2004, Boshoff and colleagues using microarray profiling were able to characterise different patterns of gene expression, with the view to highlighting possible targets for better drug development. Organisms were submitted to different conditions of aeration and nutrition in the presence of nitric oxide or drugs. By analysing more than 400 different

profiles of gene expression under these conditions, the authors identified 150 clusters of co-regulated genes (Boshoff et al. 2004).

In terms of the respiratory chain, the study from Boshoff and colleagues recognised the importance of the phenothiazines in inhibiting oxygen consumption and in inhibiting two quinone reductases (type II NADH: menaquinone dehydrogenase and succinate dehydrogenase), which are associated with a rapid drop of ATP levels (Boshoff et al. 2004).

1.17. Phenothiazines

Phenothiazines (Fig. 1.19.) were never considered as potential anti-tubercular drugs, despite some anecdotal recognition of anti-TB effects observed in mental patients being treated with phenothiazines due to their psychiatric maladies (Amaral et al. 2004). Also, chronic administration of these tricyclic compounds is associated with severe side effects, making their use prohibitive to cure a long-lasting infection like TB that needs prolonged treatments (Amaral et al. 2001).

Chlorpromazine (CPZ) is a clear example that exhibits these two setbacks. It was the first compound of the phenothiazine class that was used in the 1950s in the psychiatric field and this period corresponds to the golden era of the discovery of antitubercular agents, so it was never considered as an anti-TB drug. Also early on, it was known that the prolonged used of this drug was associated with severe side effects, namely acute and chronic liver damage, cholestatic disease, agrunalocytosis and retinopathy, making its use prohibitive (Amaral et al. 2001; Amaral et al. 2004).

Nowadays due to the emergence of resistance and the inefficacies of the current agents, scientific research aims to find new solutions or to (re)discover alternative and more effective anti-TB treatments. This led to

the consideration of already discovered compounds that show anti-microbial activity, despite having some contraindications. In this context, phenothiazines re-emerged as potential anti-TB agents (Amaral and Kristiansen 2000; Amaral et al. 2004; Amaral et al. 2008).

Early studies showed phenothiazines as having promising anti-tuberculosis effects. One of the problems associated with phenothiazines used against TB were the non-achievable clinical doses of the drug needed to inhibit Mtb growth. However, studies showed that human macrophages concentrate phenothiazines increasing its concentration in the pulmonary tissue to 10-100 times its plasma concentration, killing the phagocysed mycobacteria, suggesting that the drug appears to be more effective *in vivo* than *in vitro* (Amaral et al. 2001; Amaral et al. 2004; Sacchettini et al. 2008).

Phenothiazines are responsible for enhancing the anti-tubercular effect of some of the drugs currently used for first-line anti-TB treatment, namely rifampicin and streptomycin (Amaral et al. 2008). Interestingly, phenothiazine treatment proved to be equally effective in normal or drug-resistant Mtb strains (Amaral et al. 2001; Viveiros and Amaral 2001; Amaral et al. 2008). For these reasons, Amaral and colleagues are amongst the advocates of the use of phenothiazines as adjuvants to four- or five-drug regimens against TB, defending the idea that the synergistic interaction between the agents will diminish the phenothiazine-associated severe side effects, since it will allow lower dosages of the drugs to be used, which may produce relatively milder side effects. Phenothiazines do not enhance the effect of isoniazid (Viveiros and Amaral 2001).

Experimental evidence demonstrates the complete inhibition of mycobacterial growth by trifluoperazine and suggests its use or similar calmodulin antagonists as anti-tubercular drugs (Amaral et al. 2004). They inhibit the transport of calcium by binding to the calcium-binding

protein calmodulin or calmodulin-type proteins (Ratnakar and Murthy 1992; Amaral et al. 2004) and they also inhibit the K^+ transport from external to internal cellular compartments and between intracellular compartments (Amaral et al. 2007), compromising membrane integrity.

Phenothiazines are potent inhibitors of type II NADH menaquinone dehydrogenase (Ndh-2) as well as succinate dehydrogenase. These drugs are able to block the NADH-dependent O_2 consumption by the Mtb membrane, altering NADH/NAD and menaquinone/menaquinol ratios, altering cellular respiration and cell metabolism (Yano et al. 2006; Sacchettini et al. 2008; Dutta et al. 2010).

Thioridazine is the more promising phenothiazine in the TB research field. It can be used as a multi-target inhibitor (Dutta et al. 2010). It has broad-spectrum antibacterial activity against Mtb and it appears to be equally active against persistent organisms (Amaral et al. 1996; Amaral et al. 2010). Dutta and colleagues found that thioridazine treatment caused damage to the Mtb envelope and altered its energy metabolism. Using transmission electron microscopy (TEM) they demonstrated that thioridazine caused changes in the envelope morphology of tested cells, that increased with the exposure time to the drug (Dutta et al. 2010). Thioridazine enhanced the activity of rifampicin and streptomycin against TB, suggesting the potential for dosing reduction of these antibiotics (Amaral et al. 2001; Viveiros and Amaral 2001), and it proves to be extremely and equally potent against growing and resistant Mtb using a murine model (Soolingen et al. 2010).

In terms of side effects, cardio-toxicity is a concern with phenothiazines. This was verified during *in vivo* on studies with animals treated for a prolonged time and with high dosages of thioridazine, but no similar effects were observed in humans treated with low dosages. In terms of its psychiatric use, thioridazine proved over the years not to have the severe

side effects associated with chlorpromazine so is considered a mild phenothiazine with only drowsiness associated with its use (Amaral et al. 2001; Thanacoody 2007).

There are publications that report much more serious and frequent side effects, which are mediated as consequences of strong alpha-blocking activity (Handbook of anti-tuberculosis agents 2008). Due to the recognition of the potential of phenothiazines against Mtb, new phenothiazine derivatives are being biosynthesized, in an attempt to enhance their potency and selectivity (Bate et al. 2007; Madrid et al. 2007; Martins et al. 2007).

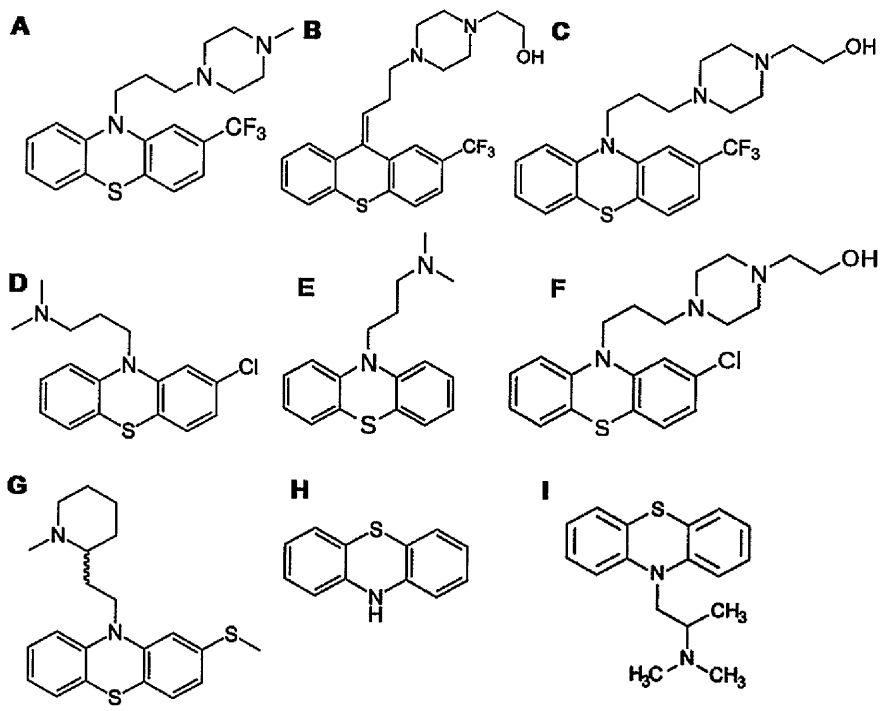

Fig. 1.19.: Chemical structure of different compounds that belong to the class of phenothiazines. (A) Trifluoperazine, $C_{21}H_{24}F_3N_3S$; (B) flupenthixol, $C_{23}H_{25}F_3N_2OS$; (C) fluphenazine, $C_{22}H_{26}F_3N_3OS$; (D) chlorpromazine, $C_{17}H_{19}ClN_2S$; (E) promazine, $C_{17}H_{20}N_2S$; (F) perphenazine, $C_{21}H_{26}ClN_3OS$; (G) thioridazine, $C_{21}H_{26}N_2S_2$; (H) phenothiazine, $C_{12}H_9NS$ and (I) promethazine, $C_{17}H_{20}N_2S$.

1.18. Aims of the thesis

This thesis has four different objectives that interconnect in order to augment the knowledge of the ETC of Mtb. The main focus is in the importance of mycobacterial ETC components in persistence, namely the type II NADH: menaquinone oxidoreductase (Ndh-2) and in the confirmation of this enzyme as a potential drug target.

The main objectives are:

1. To validate the use of *M. smegmatis* as a non-pathogenic model for the detailed study of the biochemical respiratory phenomenon of mycobacteria. If *M. smegmatis* proves to be a good model it would enable objectives two and three to be more easily achieved since no containment level III would be required.

2. To set up and validate the Wayne model of hypoxia for the study of dormancy in mycobacteria. This consists of the use of different models of cell culture in order to replicate the *in vivo* conditions faced in the host by the bacteria and to establish a quantitative and reliable measure of the susceptibility of Mtb to different compounds. Drugs tested against Mtb were either the currently used therapy that worked as a validation for the method or compounds specifically targeting the ETC, namely the phenothiazines. Phenothiazines are inhibitors of the ETC enzyme Type II NADH: menaquinone oxidoreductase, encoded by the gene *ndh*.

3. To investigate the gene *ndhA*, homologue of *ndh* that encodes Ndh-2, and to investigate its functionality in the bacteria with the view to understanding if the presence of this *ndh* homologue confers some kind of evolutionary advantage to the Mtb organism. The gene was cloned, expressed and its activity and functionality were studied.

4. To contextualize under an evolutionary perspective the *ndh* genes present in Mtb within the overall Actinomycetales group that includes

mycobacteria. The available genomes of this group were scrutinized for hypothetical *ndh* homologues and phylogenetic relationships analysed.

These aims together contribute to the overall goal of the work presented in this thesis; the identification and theoretical and experimental validation of an enzyme of the Mtb ETC as potential drug target.

Chapter 2. *Mycobacterium smegmatis*, a non-pathogenic model for the study of *M. tuberculosis*

2.1. Introduction

The complete genome of the *M. smegmatis* has been available at NCBI since 2006 (NC_008596) and this rapid-growing, saprophytic organism has been used as a model for the study of Mtb virulence and regulatory pathways at least for the last two decades (Waagmeester et al. 2005).

The major advantage of using *M. smegmatis* as a model organism for the study of Mtb is the fact that it is not pathogenic for humans and therefore it does not require containment level III facilities. The use of *M. smegmatis* in an initial phase of this study allowed the employment of all the resources of the general lab and made it possible to initiate the mycobacterial study while the category III areas were still being commissioned.

2.1.1. The ETC of *M. smegmatis*

Analysis of the *M. smegmatis* genome and spectroscopic studies led to the conclusion that in terms of enzymes oxidizing menaquinol, this organism possesses a cytochrome bc_1 complex that is a cytochrome *bcc* associated with an aa_3-type cytochrome *c* oxidase and its second terminal oxidase is a cytochrome *bd* oxidase (Kana et al. 2001; Nantapong et al. 2005; Megehee et al. 2006; Megehee and Lundrigan 2007).

The branch constituted by the super-complex bc_1-aa_3 establishes a functional association (Megehee and Lundrigan 2007), where the cytochrome accepts electrons from a Rieske Fe-S cluster and passes them

to the quinol cytochrome *c* reductase (Kana et al. 2001). This is particularly important for the growth of *M. smegmatis* in aerobic conditions. Mutants with this pathway disrupted survive using the alternative, less energy efficient pathway, through the branch of the ETC terminating in cytochrome *bd* oxidase that is highly over-expressed (Matsoso et al. 2005). Although growth is impaired, this branch is particularly important for the organism's survival in environments with limited oxygen or when the other branch of the chain is impaired (Kana et al. 2001; Matsoso et al. 2005). Under these conditions of low oxygen, the *cydAB* gene expression increases and *d*-heme expression increases (Matsoso et al. 2005). Cytochrome *bd* does not pump protons through the membrane but it oxidizes menaquinol and has a very high affinity for oxygen (Megehee et al. 2006).

2.1.2. The use of *M. smegmatis* as a model to study Mtb

In the last few years, the use of *M. smegmatis* as a model to study Mtb has been challenged by some researchers. The arguments are that *M. smegmatis* is a saprophyte, fast growing and non-pathogenic organism. It has a higher resistance to high salt concentrations and exhibits remarkable differences in terms of oxidative stress response, virulence and drug susceptibility (Bloch 1977; Gray et al. 1982; Horsburgh Jr. 1996). Barry claims that the differences between Mtb and *M. smegmatis* are much more complex than just virulence and rate of growth (Barry III 2001).

M. smegmatis proved to be more resistant to acidic pH than slow growing mycobacteria. Optimal growth of *M. smegmatis* occurs over a wide pH range (pH 5.0 to 7.4), and partial growth can be observed at a pH as low as 4.6. Even acid tolerance can be conferred to the bacilli if *M. smegmatis*

is previously exposed to a lower pH (e.g. pH 5.0) before being placed in a normally deadly pH of 3.0 (Rao et al. 2001).

Titgemeyer and colleagues studied in detail the mechanisms of carbon uptake systems of *M. smegmatis* and Mtb which are particularly different. The plasticity of *M. smegmatis* and adaptation capabilities were notorious due to the fact that it has 28 different transporters of carbohydrates so it is able to grow using a great variety of sugars as energy sources, while Mtb is poorly equipped with only 5 (Titgemeyer et al. 2007). The porins in the *M. smegmatis* membrane, which increase the permeability of the bacilli represent a highly efficient nutrient exchange mechanism but limit the intracellular persistence of *M. smegmatis* (Sharbati-Tehrani et al. 2005).

Smeulders and collaborators used *M. smegmatis* as a model for the study of persistence under nutrition starvation and they concluded that bacilli were able to survive 650 days without carbon, nitrogen and phosphorus. Their results were contrary to the idea of *M. smegmatis* entering a dormant state, since during the apparent latency cells remained growing and dividing reinforcing the idea that *M. smegmatis* did not enter a true quiescent state. This study showed that the majority of the starved *M. smegmatis* population remains active, with a slower metabolism. However this study did not rule out the possibility of the existence of a very small sub-population of truly dormant bacilli (Smeulders et al. 1999).

Some researchers argue that *M. smegmatis* is able to exhibit dormancy behaviour induced by hypoxia, similar to Mtb (Dick et al. 1998; Anuchin et al. 2009). They argue that submitting *M. smegmatis* to a gradual depletion of oxygen, instead of a sudden shift, leads to the survival of the bacteria, in a state of persistence. Under these conditions, the bacteria show sensitivity to metronidazole, resistance to antibiotics and synchronization of growth if reactivation occurs (Dick et al. 1998). These are typical hallmarks of latent Mtb but it is known that *M. smegmatis*

lacks two typical genes directly related to dormancy in Mtb, the sigma factor *sigF* (DeMaio et al. 1996) and alpha-crystallin (Yuan et al. 1996). The up-regulation of alanine dehydrogenase was also reported in this "dormant" state of *M. smegmatis*, compared to cultures grown under no oxygen limitation (Hutter and Dick 1998), suggesting that this enzyme plays a role in dormancy. The oxidation of NADH in parallel with alanine generation maintains an NAD^+ pool in conditions of limited oxygen (Hutter and Dick 1998). Glycine dehydrogenase activity that increased in the case of latent Mtb (Wayne and Hayes 1996) was not reported in *M. smegmatis*.

Despite this controversy and non-acceptance by some researchers of *M. smegmatis* as a reliable model of Mtb study, this organism remains a widely used model for the study of its pathogenic relative Mtb, mainly due to the fact that it does not require level III containment. It serves as a useful tool to study Mtb but the results need further validation and must be interpreted with caution. The diarylquinoline TMC-207, an important anti-TB drug currently in the pipeline which inhibits Mtb ATP synthesis, was discovered using whole-cell screening against *M. smegmatis* (Andries et al. 2005). However, Altaf and colleagues argue that 50% of active anti-TB compounds would not be identified as active in a screening using *M. smegmatis* due to the differences between organisms mentioned above (Altaf et al. 2010).

2.2. Methods

2.2.1. General considerations

Unless otherwise stated, all chemicals used were purchased from Sigma (Sigma-Aldrich, UK).

All cell culture work was carried out using standard aseptic techniques

inside a Class II laminar flow cabinet.

Nutrient broths were prepared by diluting media powder in ddH_2O according to manufacturer's instructions and autoclaved for 10min at 121°C.

Sterile, disposable plasticware was utilised throughout.

2.2.2. *M. smegmatis* strain and growth media

M. smegmatis strain mc^2155 was grown in tryptic soy broth (TSB) (Fluka, UK), supplemented with 0.1% (v/v) Tween® 80. Depending on the experiment performed it was also grown in Middlebrook 7H9 broth (BD Diagnostic, UK) enriched with 0.2% (v/v) of glycerol, 0.2% (v/v) glucose or 0.2% (v/v) succinate and 0.05% (v/v) Tween® 80.

2.2.2.1. Monitoring *M. smegmatis* growth

In order to assess the state of growth of cultures, optical density was monitored at 600 nm (OD_{600}) using a Genesys 10UV Spectrophotometer (Thermo Scientific, UK).

To establish the zero point of the growth curve, the absorbance of 800 µl of sterile broth contained in a disposable cuvette (VWR International) was recorded. To monitor growth of inoculated flasks, aliquots of culture were removed at regular intervals and OD_{600} recorded. When stationary phase (i.e. no further appreciable change in the turbidity of the culture) had been reached, plots of time *versus* OD_{600} were generated to visualise the *M. smegmatis* growth curve.

2.2.2.2. Storage of *M. smegmatis* stocks

Cells to be frozen were grown until mid-log phase, (i.e. OD_{600} 0.6-0.9). An equal volume of storage medium was added to the cells prior to storage at -80°C. The storage medium consisted of 3 g TSB powder, 20 ml 100% glycerol and 80 ml distilled water (ddH_2O), autoclaved and stored at -4°C for up to 6 months.

2.2.2.3. *M. smegmatis* growth conditions

M. smegmatis was submitted to different oxygen conditions and nutrient availability during growth. 5 ml of TSB supplemented with 0.1% (v/v) Tween® 80 was inoculated with 50 µl of *M. smegmatis* from a frozen stock and incubated overnight at 37°C in an Innova 4230 orbital shaking incubator (New Brunswick Scientific, USA) set to 200 rpm.

Assuring the same provenance of bacteria in the different conditions of this study, the suspension was then sub-cultured according to the methods stated below.

2.2.2.3.1. Aerobic growth of *M. smegmatis*

For aerobic growth, an inoculum of 200 µl was added to 200 ml TSB in a 500 ml Erlenmeyer flask (with a total capacity of 600 ml). To avoid culture contamination and permit maximal aeration, sterile tin foil was used to cover the culture flask opening. Cultures were incubated at 37°C and shaken at 200 rpm in an Innova 4230 orbital shaking incubator to allow rapid diffusion of oxygen between the headspace and the culture. At 4-5 hours intervals the OD_{600} of the culture was measured as previously described (Section 2.2.2.1.).

2.2.2.3.2. Anaerobic growth of *M. smegmatis*

To create a micro-aerophilic environment *M. smegmatis* was cultured in a 500 ml Erlenmeyer flasks (600 ml of total capacity) containing 400 ml of TSB. In order to obtain persistent *M. smegmatis* bacilli in *in vitro* culture the hypoxia model proposed by Wayne and colleagues was used (Wayne and Hayes 1996). As such, a headspace (air): culture media ratio of 0.5 (i.e. 200 ml air: 400 ml media) was used throughout.

400 ml of TSB was inoculated with 400 µl of *M. smegmatis* culture and a rubber skirted stopper (VWR International) was used to limit oxygen supply to the culture. To ensure anaerobic conditions the opening was further sealed with Parafilm (Pechiney Plastic Packaging Company, USA). The culture was incubated at 37°C and gently stirred on a magnetic stirrer, using a 50 mm stirring bar. At 4-5 hours intervals, and ensuring sterile conditions, the rubber stopper was pierced using a 40 mm, 20 G needle (BD Diagnostic, UK) to remove and transfer an aliquot of bacterial culture to a disposable cuvette. The OD_{600} was measured as previously described (Section 2.2.2.1.) and a curve of time *versus* the optical density plotted.

2.2.2.3.3. Nutrient-starved *M. smegmatis* culture

To achieve nutrient-starvation conditions, after inoculating 200 ml of TSB with 200 µl of *M. smegmatis* culture, cells were allowed to grow for 24 h or until $OD_{600} = 1.0$. During this period, the cultures were shaken at 200 rpm in an Innova 4230 orbital shaking incubator, at 37°C with unlimited oxygen supply.

Cells were then harvested by centrifugation at 3000 *g* for 5 min, washed twice using sterile phosphate buffered saline (PBS) pH 7.4 and re-

suspended in 200 ml sterile PBS pH 7.4. Cultures were returned to the incubator and grown under the conditions described above.

OD_{600} measurements were taken at 4-5 hours intervals until the turbidity of the culture stabilized (Section 2.2.2.1.) in order to plot a growth curve of time *versus* optical density.

2.2.2.3.4. Validation of viability of the organisms

At the end of the experiments and to verify that the turbidity observed in the cultures was the result of viable organisms in those different culture media, and not produced by cell debris or dead organisms that only grew in the first stages of the experiments, 200 µl of each *M. smegmatis* culture were incubated in aerobic conditions according to Section 2.2.2.3.1, for 24 h. The growth was then monitored in order to confirm viability of the samples (see Section 2.2.2.1).

2.2.2.4. Preparation of membranes of *M. smegmatis* for spectral analysis and protein quantification

The preparation of *M. smegmatis* membranes was based in the protocol by Fisher et al. 2009. The *M. smegmatis* cells were grown until mid-log phase (OD_{600} = 0.6-0.9) at 37°C with continuous shaking at 200 rpm in an Innova 4230 orbital shaking incubator. Cells were harvested by centrifugation at 4000 *g* for 20 minutes. The supernatant was discarded and the resultant pellet resuspended in 50 mM potassium phosphate buffer pH 7.4 (60 ml of buffer were added for every 1 L of cell culture) and centrifuged again at 4000 *g* for 20 minutes. Once again the supernatant was discarded and the pellet re-suspended in the same buffer (20 ml of buffer were added for every 1 L of cell culture). Cells were

maintained on ice for 30 minutes following the addition of hen-egg lysozyme to a final concentration of 0.2 $mg \cdot ml^{-1}$.

A One Shot cell disruptor (Constant Systems Ltd, UK) was used to break the cells. Cells were maintained on ice to avoid denaturation of proteins due to generation of heat and submitted to 1 shot at 30,000psi. An anti-foam cup was used in order to minimise foam production during the process and 6 ml of cell culture were used per shot. The high pressure forces the sample through a small fixed orifice in the cup to cause cell disruption.

The suspension was centrifuged at 10,000 *g* for 30 minutes at 4°C before the supernatant was collected and centrifuged at 39,000 rpm for 1 hour. The resultant pellet was homogenized in 2 ml of 50 mM potassium phosphate buffer, 2 mM ethylenediaminetetraacetic acid (EDTA) pH 7.4 containing 20% (v/v) glycerol. The isolated membrane preparation was stored at -80°C until required.

2.2.2.5. Microplate Bradford assay method for protein quantification of *M. smegmatis* membranes

The total amount of protein in the crude membrane preparations was determined by the Bradford assay using bovine serum albumin (BSA) as the standard. The assay was performed in sterile 96-well microtitre flat bottom plates (NUNC, UK). A 1 $mg \cdot ml^{-1}$ stock solution of BSA was serially diluted in ddH_2O into three columns of the plate. The dilutions were prepared in triplicate. 20 µl of each *M. smegmatis* membrane preparation were plated and 200 µl of Bradford Dye reagent (Bio-Rad, UK) was added to each of the wells and mixed thoroughly. Following incubation at room temperature for 10 minutes a photometric reading of the plate was made at 575 nm using a Varioskan plate reader (Thermo

Electron Corporation, UK). A calibration curve was generated for the protein standards (concentration of BSA was plotted *versus* absorbance) and this curve was used to determine the protein concentration in sample wells.

2.2.2.6. Spectral analysis of *M. smegmatis* membrane cytochromes

Spectra were recorded at room temperature using a Cary-UV 4000 UV-VIS spectrophotometer (Varian, UK). Aliquots of the membrane preparation (typically 1-2 µl) were mixed with 700 µl of 50 mM potassium phosphate, 2 mM EDTA, pH 7.4. Oxidised membrane spectra were recorded following the addition of a single crystal of potassium ferricyanide ($K_3Fe(CN)_6$) whilst a few grains of sodium dithionite were added to generate the reduced spectra. Five spectra were recorded for each oxidation state and averages calculated prior to creating a difference spectrum by subtracting the average oxidised spectrum from the average reduced spectrum. To ensure complete oxidation/reduction of samples spectra were re-recorded following further addition of sodium dithionite/potassium cyanide. If no further spectral changes were observed complete oxidation/reduction was assumed.

2.2.3. Testing drug toxicity against *M. smegmatis* using the microplate alamarBlue® assay (MABA)

MABA is used for measuring cell proliferation and viability by monitoring the oxidation-reduction state of the environment of cellular growth. AlamarBlue® (AbD Serotec, UK) is a soluble, non-toxic oxidation-reduction (redox) dye stable in culture medium. It incorporates an oxidation-reduction indicator that changes colour in response to the

chemical reduction of the medium, i.e. the dye changes from blue to pink upon reduction due to cell growth..

The drugs to test were solubilised either in ethanol or distilled H_2O, according to Table 2.1. 10mM stock solutions were sterilised through a 0.22μm pore filter and stored at -20°C.

1 in 3 serial dilutions of the initial 10mM stocks were prepared using TSB supplemented with 0.1% (v/v) Tween® 80. For each compound eight serial dilutions were made. All dilutions were prepared at double the required final well concentration to allow for further dilution in the test wells with TSB.

Table 2.1.: Details of compounds tested against *M. smegmatis* strain mc²155 using an *in vitro* microplate alamarBlue® assay (MABA). The table presents the name, molecular weight and solvents used to dilute each respective drug used in the MABA bioassay.

Compound	Molecular Weight	Solvent
Ethambutol dihydrochloride	277.23	dH_2O
Isoniazid	137.14	dH_2O
Pyrazinamide	123.11	dH_2O
Rifampicin	822.94	Ethanol
Streptomycin sulphate salt	728.69	dH_2O

MABA was performed in sterile 96-well microtitre flat bottom plates (NUNC, UK). 50μl of broth were plated in row C (2 to 11) and in columns 6 and 11 (D, E and F). 50μl of each pre-prepared drug dilution were added into columns 2, 3, 4, 5, 7, 8, 9 and 10. The concentration of drug decreased from left to right, Column 2 containing the highest drug concentration and column 10 the lowest drug concentration. Finally, 50μl of *M. smegmatis* inoculum was added in rows D, E and F (2 to 11).

Wells in columns 6 and 11 (D, E, F) were free-drug controls containing

50µl of broth and 50µl of bacteria inoculum. Wells in row C (2 to 11) were *M. smegmatis*-free wells, acting as blanks containing 50µl of broth and 50µl of the respective drug dilution. The other wells were test wells with bacteria and varying concentrations of the test compounds (See Fig. 2.1, for plate format).

After 16 hours incubation at 37°C, 20µl of alamarBlue® were added per well and the plates were returned to the incubator. After 4 hours, plates were read using an Opsys MR™ Microplate Reader (Dynex Technologies, USA) at an absorbance of 570nm.

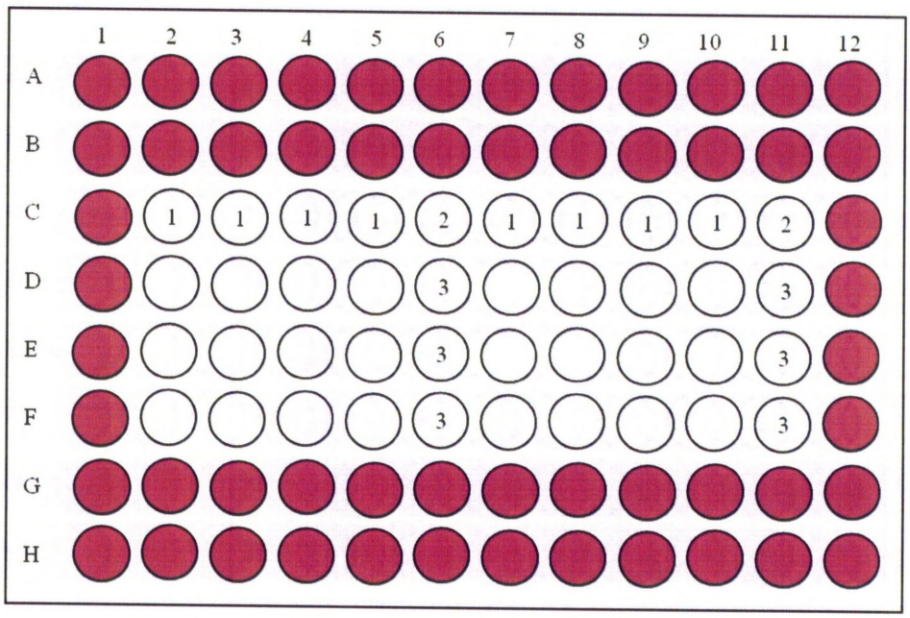

Fig. 2.1.: Representative 96 well microplate format for screening drug susceptibility of *M. smegmatis* to various compounds using MABA. ● represents blank wells, ① corresponds to wells containing 50µl broth and 50µl drug dilution, ② contained 100µl of broth, ③ were wells containing 50µl broth and 50µl *M. smegmatis* inoculums and ○ were wells containing 50µl drug dilutions and 50µl of *M. smegmatis* cells.

2.2.4. Data analysis

Graphs were generated plotting the concentration of drug against the percentage of growth of the bacteria in the test wells. The bioassay was normalised for the 100% growth in the control wells (drug-free wells), with *M. smegmatis* grown without inhibitor. All the test wells were compared to this value in order to obtain a percentage of growth.

The IC_{50} (half maximal inhibitory concentration) refers to the concentration of drug which causes 50% inhibition of growth. The IC_{90} (90% inhibitory concentration) refers to the concentration of drug which causes inhibition of 90% of microbial growth. All the ICs are presented in μM with their respective standard deviations (SD).

A data report was generated using the Revelation QuickLink™ 1.0 software (Dynex Technologies, USA), from the data obtained with the plate reader. A concentration *versus* response graph was plotted using GraphPad Prism version 5.00 for Windows (GraphPad Software, USA). The software allowed the inference of both IC_{50} and IC_{90} from a generated log-concentration response sigmoid curve that was constrained between 0 and 100%. Results were given as the mean of two independent experiments.

2.3. Results

The aim of this chapter was to classify the effectiveness of *M. smegmatis* as an Mtb model and if successful to employ this model for further work in this thesis. The focus was to look at its electron transport chain and patterns of growth. If *M. smegmatis* presents similarities with Mtb, this organism could be used to test potential inhibitors to Mtb, without requiring Containment Level 3 facilities.

M. smegmatis bacilli grown from the same batch were submitted to different growth conditions and their growth monitored, as a turbidity change of the liquid media, in an optical density meter.

As expected, *M. smegmatis* grows optimally in conditions of unlimited aeration. There is an initial lag phase with a slow increase of the number of bacteria, shown by an increase in OD_{600} that lasts 10 to 14 hours. This was followed by a phase of exponential growth. When the medium is saturated, with cell debris and products of cell metabolism, at around 40 hours after the start of the experiment the curve reaches a plateau (stationary phase), were the number of bacteria remains constant (Fig. 2.2.- red line).

Submitting the cultures to anaerobiosis created an environment with severe hypoxia resulted in limited growth of the cultures. The cultures never grew exponentially and reached a plateau at 8-fold lower than in the aerobic cultures 24 hours after the beginning of the experiment (Fig. 2.2.- blue line *vs* red line).

In the case where an initial culture of *M. smegmatis* with an OD_{600} of 1 was cultured in a minimal medium without any source of nutrients, there was an abrupt decrease in the number of organisms, followed by a small increase in numbers which was not sustained. The culture reached a plateau 10 hours after the beginning of the experiment (Fig. 2.2.- green line).

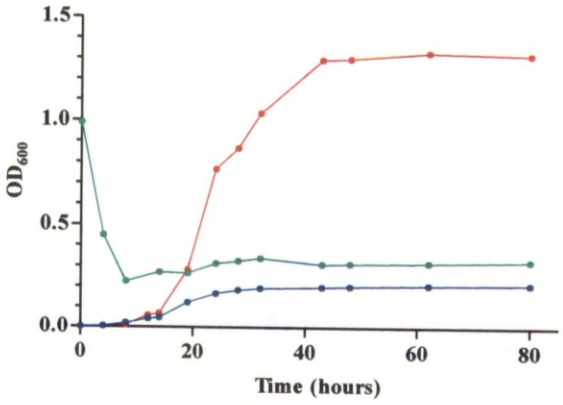

Fig. 2.2.: Growth curves of *Mycobacterium smegmatis* cultures under different conditions. (_, red line) corresponds to cultures grown under conditions of unlimited oxygen supply, (_, blue line) represents the cultures grown under limited aeration conditions and in (_, green line) the bacterial cells were deprived of a carbon source of energy. The experiment was monitored over 80 hours. The data shown are the averages from two independent experiments performed in duplicate.

In order to assess any quantitative differences between the proteins expressed in the membranes of the organisms grown under distinct conditions, the total amount of proteins in the crude membranes of *M. smegmatis* preparations grown in aerobiosis and anaerobiosis were determined by the Bradford assay. A calibration curve was generated for protein standards and this curve was used to determine the protein concentration in test samples (Fig. 2.3.).

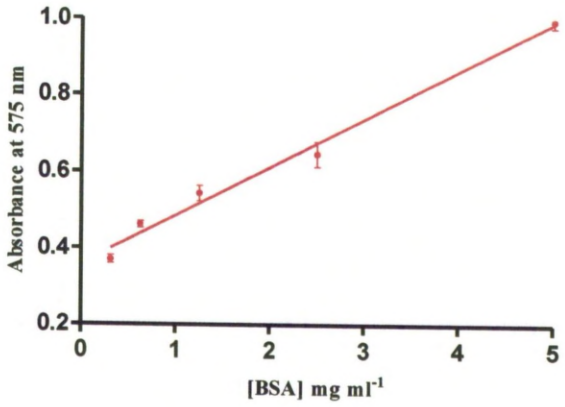

Fig. 2.3.: Linear correlation between the absorbance at 575nm and the concentration of protein. BSA was used as the standard. The graph represents the range when the relation between the concentration of BSA and the respective absorbance showed linearity. The obtained linear relationship infers that concentration of protein ($mg \cdot ml^{-1}$)=[Absorbance at 575nm - (0.3586 ± 0.02124)] / 0.1266 ± 0.008229), r^2=0.9875. Results were based on 4 independent replicates.

The total amount of protein was higher in the cultures grown under severe hypoxia, compared to the ones submitted to unlimited aeration, unfortunately, as there were no discrimination of the kind of proteins no conclusions can be drawn about what causes this phenomenon (Table 2.2.). Also, considering the uncertainty of the results, this difference is most certainly non-significant. The 95% confidence intervals are large and they overlap at about 85% of their range.

Table 2.2.: Total protein concentration of the prepared membrane fractions, using BSA as the protein standard based on two independent replicates. Values between brackets indicate the 95% confidence interval.

Growth conditions	Protein concentration (mg/ml)
Aerobic culture	0.716 [0.515; 0.945]
Anaerobic culture	0.780 [0.575; 1.014]

Spectral analyses were performed on the *M. smegmatis* membranes in order to investigate the peak profiles of the cytochromes under different growth conditions (Fig. 2.4.). Based on previously defined cytochrome profiles (Vrij et al. 1987), it is assumed that a peak at 552nm corresponds to cytochrome *c*, a peak at 563nm relates to cytochrome *b* and a peak at 600nm belongs to cytochrome *a*. A peak at 630nm corresponds to cytochrome *bd*. A peak around 530nm shows a summation of all the hemes of the cytochromes present.

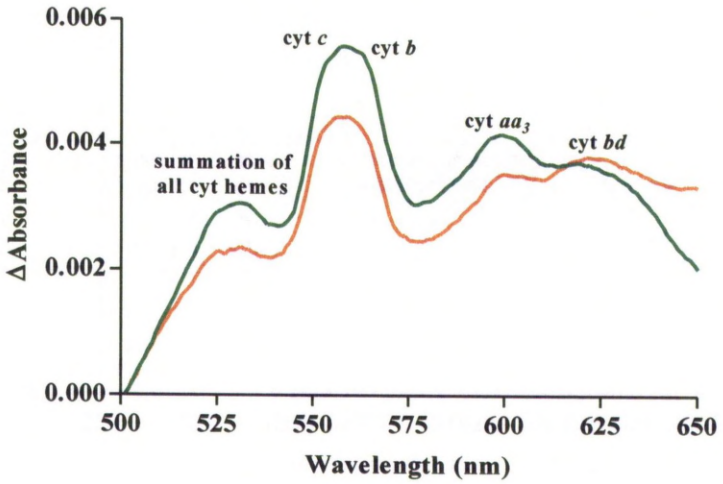

1

Fig. 2.4.: Reduced minus oxidised spectra of *Mycobacterium smegmatis* membranes grown under (_, green line) aerobic and (_, orange line) anaerobic conditions.

To further characterise the spectra, ratios were calculated in order to quantify the differences between the cytochromes in the membranes when grown under conditions of different aeration and nutrition (Table 2.3.).

The use of ratios was required since the values of absorbance variation obtained in each spectrum are not normalised and interest focuses on the relative peaks within each run. Thus, the peak height of a given cytochrome is divided by the peak height of a second cytochrome from

the same spectrum. Comparing different spectra it is possible to evaluate if a given cytochrome is preferred in relation to another, depending on the growth conditions.

Table 2.3.: Ratios between the different signals corresponding to the different cytochromes present in the *Mycobacterium smegmatis* membranes from cultures grown under different conditions. Ratios were calculated from difference spectra peaks.

Growth conditions	Cyt *c*:*b*	Cyt *c*:*aa*$_3$	Cyt *c*:*bd*	Cyt *b*:*aa*$_3$	Cyt *b*:*bd*	Cyt *aa*$_3$:*bd*
Early aerobic	1.04	1.76	8.5	1.69	8.17	4.83
Late aerobic	1.11	2.49	3.46	2.25	3.13	1.39
Hypoxia	1.01	4.03	2.69	4.00	2.67	0.67
Starvation	1.00	1.64	1.76	1.64	1.76	1.07

The ratios for cytochromes *b*, *c* and *aa*$_3$ in relation to cytochrome *bd* are substantially higher in early aerobiosis, with late aerobiosis having the second highest value. The ratio between *b* and *aa*$_3$ is higher in hypoxia and it is also higher between *c* and *aa*$_3$. The ratio between *c* and *b* is very similar between the four growth conditions and always approximately 1.

The following graphs (Fig. 2.5., A-H)) are the spectral analyses of the membranes obtained from *M. smegmatis* cultured under different conditions. They show some of the variability that can exist between spectra, although there are some trends, described below.

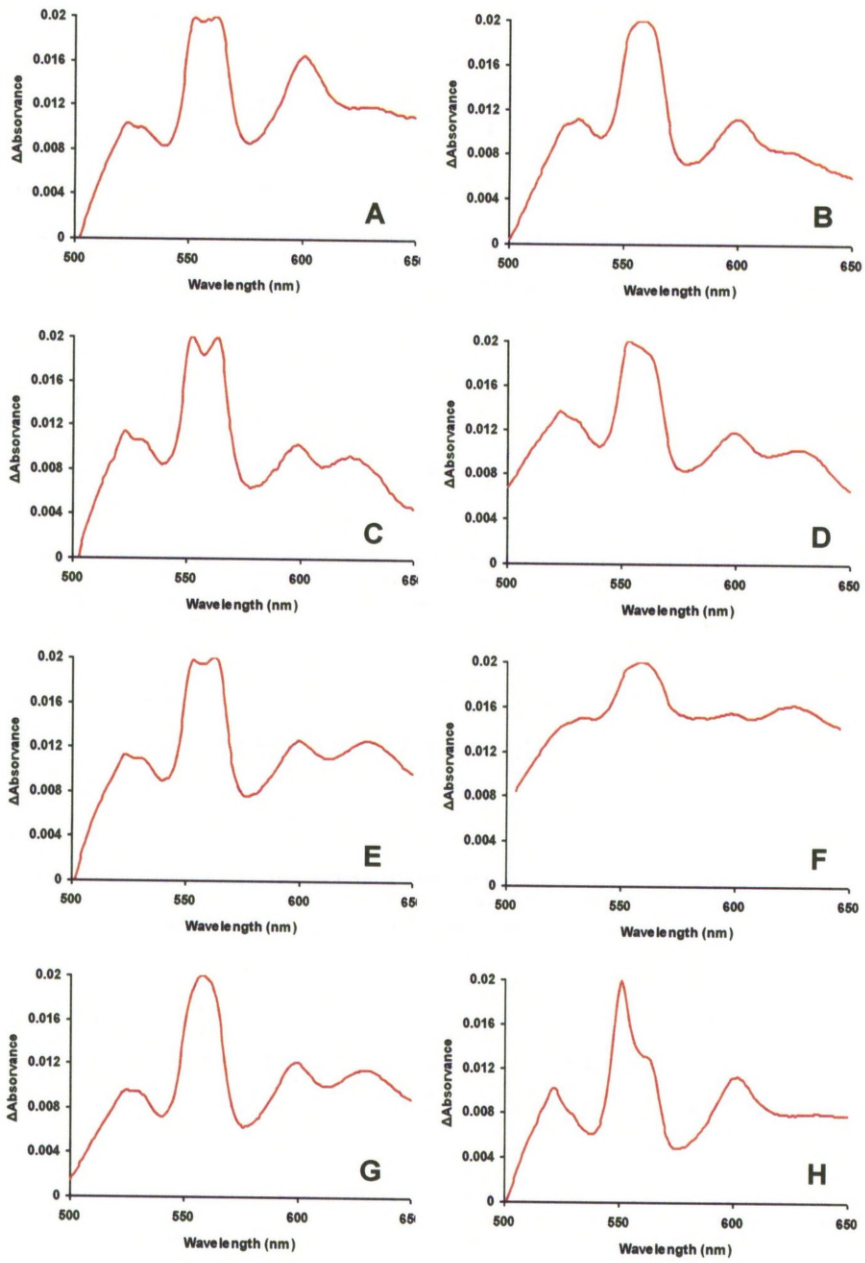

Fig. 2.5.: UV-visible difference spectra of membrane fractions isolated from *Mycobacterium smegmatis* grown under different conditions. Difference spectra were generated by subtracting potassium ferricyanide-oxidised spectra from sodium dithionite-reduced spectra: A-B correspond to cultures in an initial phase of growth under aerobic conditions; C-D correspond to cultures with 40h growth under aerobic conditions; E-F correspond to cells that were grown under severe hypoxia; G cells were submitted to nutrient starvation; H cells grew with unlimited oxygen but the carbon source was succinate instead of glycerol.

Cytochrome aa_3 is the preferred cytochrome when the cultures are grown aerobically, with a small peak related to cytochrome *bd*, at 630nm (Fig. 2.5., A-B). After 40 hours of aerobic growth, the spectra show the probable oxygen limitation in the culture medium due to high density of individuals which resulted in a higher peak at 630nm that corresponds to cytochrome *bd* (Fig. 2.5., C-D).

Cytochrome *b* (at 563nm) and *c* (at 552nm) can exhibit two different peaks (as in Fig. 2.5., C) but they can also appear as one single peak (as in Fig. 2.5., G). Usually the membranes have similar quantities of these two cytochromes, although when the carbon source of the cells was succinate, instead of glycerol, an apparent reduction of cytochrome *b* occurred, compared to cytochrome *c* (Fig. 2.5., H). There is an increase in cytochrome *bd* (at 630nm) when in conditions of anaerobiosis and a less pronounced increase of this cytochrome in conditions of late aerobiosis (Fig. 2.5., E-F), consistent with the table of ratios (Table 2.3.).

In the case of nutrient starvation (Fig. 2.5., G), despite no oxygen limitation, the pattern of cytochromes is similar to the one presented in anaerobiosis or late aerobiosis, this reflecting the high amount of stress and low metabolism of the analysed cultures (as observed through their limited growth).

Drug susceptibility tests were performed in the *M. smegmatis* organisms. The current DOTS chemotherapeutic agents were tested against this non-pathogenic organism. The results are shown in Table 2.4. and the respective IC_{50} curves are displayed in Fig. 2.6. to 2.10. Only streptomycin and rifampicin were effective against *M. smegmatis*, enabling an IC_{50} calculation (Fig. 2.6. and Fig. 2.8.). Ethambutol (Fig. 2.7.) and isoniazid (Fig. 2.9.) had some inhibitory effect at the highest concentration tested (100μM), meaning that the IC_{50} would be greater than 100 μM and could not be calculated.

Table 2.4.: Bactericidal IC_{50} and IC_{90} values of the inhibitor compounds tested against *M. smegmatis*. The results are presented with the respective standard errors and were obtained by calculating an average of two independent replicate experiments.

Drug tested	IC_{50} (μM)	SE (μM)	IC_{90} (μM)	SE (μM)
Streptomycin	0.98	0.226	25.56	13.497
Ethambutol	>100	-	>100	-
Rifampicin	4.35	0.751	92.08	63.405
Isoniazid	>100	-	>100	-
Pyrazinamide	>100	-	>100	-

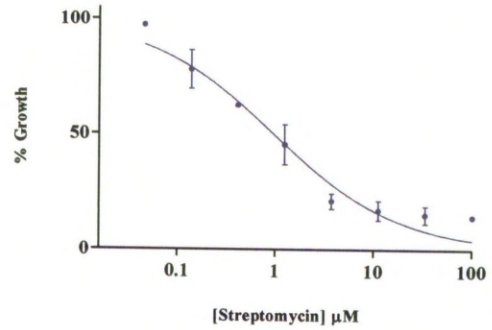

Fig. 2.6.: Curve of *M. smegmatis* growth inhibition when exposed to different concentrations of streptomycin. Percentages of growth were estimated assuming that 100% growth occurred in the absence of the inhibitor. Error bars were calculated from two independent experiments.

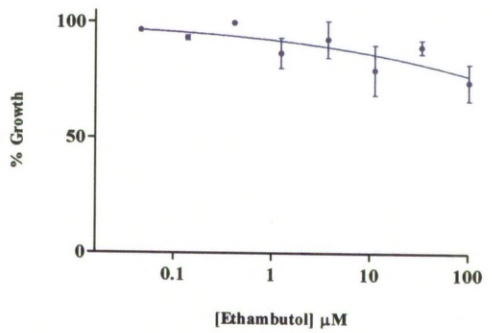

Fig. 2.7.: Curve of *M. smegmatis* growth inhibition when exposed to different concentrations of ethambutol. Percentages of growth were estimated assuming that 100% growth occurred in the absence of the inhibitor. Error bars were calculated from two independent experiments.

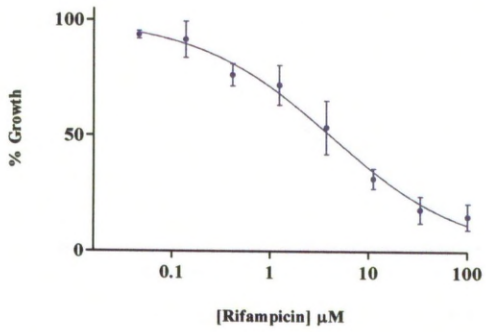

Fig. 2.8.: Curve of *M. smegmatis* growth inhibition when exposed to different concentrations of rifampicin. Percentages of growth were estimated assuming that 100% growth occurred in the absence of the inhibitor. Error bars were calculated from two independent experiments.

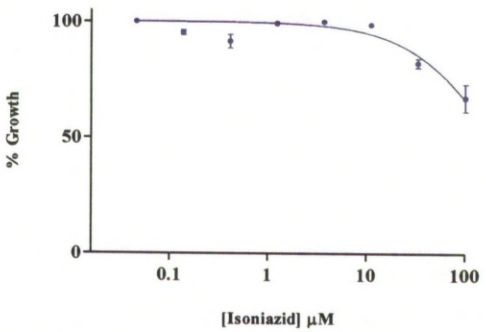

Fig. 2.9.: Curve of *M. smegmatis* growth inhibition when exposed to different concentrations of isoniazid. Percentages of growth were estimated assuming that 100% growth occurred in the absence of the inhibitor. Error bars were calculated from two independent experiments.

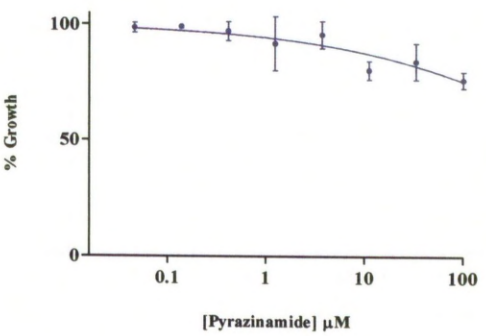

Fig. 2.10.: Curve of *M. smegmatis* growth inhibition when exposed to different concentrations of pyrazinamide. Percentages of growth were estimated assuming that 100% growth occurred in the absence of the inhibitor. Error bars were calculated from two independent experiments.

2.4. Discussion

The motivation for the use of the *M. smegmatis* membranes in this study was due to the fact that they could serve as models for the cytochromes present in the mycobacteria membranes and the handling of this organism does not involve the safety restrictions that severely limit the Mtb study. During the beginning of this work, the containment level III facilities at the Liverpool School of Tropical Medicine (LSTM) were still being commissioned and this impaired the work with *Mycobacterium tuberculosis*. In this context, the use of *M. smegmatis* also allowed establishing microbiology techniques that would be required for the study of Mtb.

The major disadvantage of using *M. smegmatis* is related to the fact that there are differences in its ETC compared with Mtb ETC, namely the existence of a second cytochrome *bd* and the presence of a super complex cytochrome *bcc* in the non-pathogenic organism (Kana et al. 2001), need to be taken into account if drugs against Mtb ETC were tested against *M. smegmatis*.

The spectral analysis of *M. smegmatis* showed that cytochrome expression in the *M. smegmatis* membranes is dependent on growth conditions and submitting the bacteria to different models of growth correlates directly with the spectra displayed. Mycobacterial electron transport chain is branched, meaning that the flow of electrons after menaquinone oxidation will occur either through the branch with a terminal cytochrome bc_1-aa_3 oxidase or through the branch terminating in the alternative cytochrome *bd* oxidase.

Cytochrome aa_3 is mainly associated with aerobic growth (Matsoso et al. 2005). The ratios between cytochrome *b* and aa_3, and between *c* and aa_3 are substantially higher in hypoxia, reflecting the lower expression of the denominator cytochrome aa_3 in the absence of oxygen. The ratio between

cytochrome aa_3 and *bd* is lower in hypoxia and it is much higher in early aerobiosis (Table 2.3.). These results are in agreement with previous work from Matsoso et al. 2005 and Kana et al. 2001, that reported an association between cytochrome aa_3 and growth under aerobic conditions.

On the other hand, cytochrome *bd* is mainly associated with hypoxia. The ratios between *c*, *b* or aa_3 and *bd* are consistently higher in early aerobiosis, they decrease in late aerobiosis were there is already some oxygen limitation due to the overgrowth of the organisms and they are lower in hypoxia (Table 2.3.). These results are consistent with the literature (Kana et al. 2001) that reports the association between cytochrome *bd* and anaerobiosis or low oxygen conditions.

Under unlimited aeration, where oxygen acts as the final electron acceptor, cytochrome *c* (including aa_3-type cytochrome *c*) is the main cytochrome utilized, with the less energy efficient cytochrome *bd* being under-expressed (Kana et al. 2001; Niebisch and Bott 2003). This was what was observed analysing the data regarding early aerobiosis, where cultures are growing without any stress (related to oxygen limitation or media nutrients limitation). Thus the ratios where cytochrome *bd* is the denominator are higher due to the lower expression of *bd* (Table 2.3.).

In the case of *M. smegmatis* grown under nutrient starvation, the results presented do not show a clear trend towards any of the two pathways, meaning no cytochrome is preferred. Berney and Cook determined that in starvation conditions, both cytochrome aa_3 and *bd* are under-expressed (Berney and Cook 2010). The data presented here (Fig. 2.5, G) do not allow inferences as to whether the cytochromes aa_3 and *bd* are being under-expressed, but are in agreement with the work of Berney and Cook since no preference in expression of these two cytochromes was observed.

A similar spectral analysis was performed with *M. smegmatis* by Kana and colleagues (Kana et al. 2001) and later on, the same principles (Weinstein et al. 2005) and whose conclusions are coincident with the data presented here.

Once the containment level III facilities became available, a similar spectral analysis work was considered. However, to study Mtb membranes in the spectrophotometer located in the general lab the cells would need to be previously killed, potentially damaging the proteins to be monitored. A possible way of doing it would be as Weinstein and colleagues by exposing Mtb to gamma radiation (Weinstein et al. 2005), something that could not be done due to technical difficulties. An attempt was made trying to kill Mtb using different concentrations of paraformaldehyde, but paraformaldehyde altered irreversibly the obtained spectra.

Drug susceptibility tests were performed on *M. smegmatis* using the five first line drugs currently used against TB: streptomycin, ethambutol, rifampicin, isoniazid and pyrazinamide using the MABA assay.

Some of these drugs are specific against all mycobacteria so a comparable result between Mtb and *M. smegmatis* could be expected. However, *M. smegmatis* shows much lower sensitivity to the drugs than Mtb (Collins and Franzblau 1997), a statement that can be supported by the IC_{50} values obtained against Mtb in Chapter 3.

Altaf and colleagues assessed the efficacy of *M. smegmatis* as an *in vitro* model for the detection of possible inhibitory compounds against Mtb. Screening with a library of anti-mycobacterial compounds demonstrated that half of the compounds that were detected as active against Mtb were not detected using *M. smegmatis* (Altaf et al. 2010).

These arguments question the use of *M. smegmatis* as a model for Mtb drug susceptibility testing. However the obtained results also differ from other published studies using the same strain of *M. smegmatis*. While there are not many published IC_{50} results to compare with the ones obtained (Table 2.4.), they have been compiled in Table 2.5.

Table 2.5.: IC_{50} values of compounds tested against *M. smegmatis* mc^2 155 with their respective standard errors.

Compound	IC_{50} (μM)	SE (μM)	References
Ethambutol	3.66	0.10	(Miller et al. 2009)
Rifampicin	4.36	0.49	(Miller et al. 2009)
Streptomycin	0.50	0.09	(Miller et al. 2009)
Isoniazid	7.80	0.60	(Delaine et al. 2010)

Although the assay could have been further replicated and optimized, by then the containment level III laboratories were already available at LSTM, *M. smegmatis* was abandoned and the assay was carried out with just Mtb.

However, it is unlikely that the discrepancies between the published results and the ones obtained in this study are only due to assay limitations, since for two of the compounds (streptomycin and rifampicin) the results obtained are very similar to the ones in the literature (Miller et al. 2009). For ethambutol and isoniazid, the results obtained here (Fig. 2.6. and 2.9.) suggest that *M. smegmatis* could be highly tolerant to these compounds, while the published *M. smegmatis* drug susceptibility profile suggest drug sensitivity with both IC_{50} values less than 10 μM (Table 2.5.). The most probable explanation is that the culture of *M. smegmatis* could be composed of some highly tolerant

individuals to both ethambutol and isoniazid. The existence of sub-populations of bacilli that display different susceptibility to drugs in M. smegmatis cultures is known (Islam et al. 2012). In Mtb simultaneous resistance to these two compounds is often reported (Parsons et al. 2005).

In this chapter, a spectroscopic characterization of cytochrome components of *M. smegmatis* was successfully established. The next step would be to test ETC inhibitors against the crude membranes, in order to compare the alterations in the spectra, as done in Kana et al. 2001 and Weinstein et al. 2005. The analyses of the spectra using different inhibitors could show differences in relation to the expected cytochrome patterns, which would be indicative of the target and mode of action of the inhibitors under different growth conditions (Weinstein et al. 2005).

In summary, these data indicate that *M. smegmatis* is a convenient model to study the effect of inhibitors on ETC components due to the ease in which difference spectra can be obtained. However, the significant difference in the sensitivity of *M. smegmatis* to first line drugs renders this model unsuitable for whole-cell sensitivity testing in either replicating or slow-growing models.

Chapter 3. Drug susceptibility of *Mycobacterium tuberculosis*, using the MABA

3.1. Introduction

In this section, different compounds currently used in TB treatment and some promising new drug candidates, specifically targeting the ETC, namely phenothiazines will be tested, using the Microplate AlamarBlue® assay (MABA). As outlined in the general introduction, inhibitors of the mycobacterial electron transport chain could be a promising new class of anti-tuberculosis drugs.

3.1.1. Brief description of different drug susceptibility tests used for *M. tuberculosis*

One of the biggest problems in terms of the study of Mtb is the lack of truly standardised procedures and the lack of directives as to how to present data (Simons and Soolingen 2011). Even when similar methodologies are used, the results are not always comparable.

Below is a brief overview of the most common used methods to study Mtb drug susceptibility. Throughout the work presented in this thesis, the MABA assay was used.

3.1.1.1. Microdilution and proportion methods

The microdilution and proportion methods serve as the basic reference for all the current susceptibility tests (Canetti et al. 1963). They consist of incubating either in liquid (microdilution) or solid (proportion) media, a constant volume of Mtb inoculum, with different concentrations of a

compound to test. At the time necessary to quantify visible bacterial growth, a comparison is made between bacterial number in the presence of different concentrations of drug and the controls (where bacteria grow in identical medium without addition of the inhibitory compound). This assessment of the numbers is made directly, either by colony counting (in the case of solid media growth) or by simple fluorimetric absorbance measurements.

The advantages of the use of these methods are that they are reliable, they allow multiple-drug testing at different concentrations and they can be used with a variety of conditions. The disadvantages are the long duration of the experimentation required to assess visible growth in Mtb cultures. In addition, the number of plates needed to generate conclusions and to perform drug combination testing is prohibitive (Wallace Jr. et al. 1986).

3.1.1.2. Microplate AlamarBlue® assay (MABA)

AlamarBlue®, the commercial name for resazurin is a soluble, non-toxic, blue and non-fluorescent dye that is reduced to resorufin turning pink and fluorescent. Cell growth leads to the reduction of growth medium and this colour change can be assessed by direct visualisation or using fluorometer or spectrophotometer readers (O'Brien et al. 2000). MABA is a simple, rapid and reliable method. A number of studies confirm the efficacy of this method over the ones obtained using proportion methods (Yajko et al. 1995; Collins and Franzblau 1997; Franzblau et al. 1998; Palomino and Portaels 1999). MABA can be used not only to test drugs against mycobacteria grown in a nutrient medium, but can also assess the effects of these drugs in mycobacteria-infected cells (Hartkoorn et al. 2007). As it is fairly inexpensive and does not need complex detector devices, it can be performed in developing countries (Franzblau et al. 1998).

A major criticism of the method is that data generated from it are often irreproducible (Leonard et al. 2008). The assay results need to be carefully analysed and extensively repeated in order to obtain valid conclusions.

3.1.1.3. 3-(4,5-dimethylthiazol-2-yl)-2,5-diphenyl tetrazolium bromide (MTT) assay

The MTT assay is a low-cost method used to check cytotoxicity. MTT is a yellow tetrazolium salt that is converted into blue formazan by succinate dehydrogenase of a live cell (Mossman 1983; Abate et al. 2004). The assumption made is that the quantity of formazan is directly proportional to the number of living cells in the media. The formazan precipitate is then dissolved by the detergent sodium dodecyl sulphate (SDS) and the absorbance is read in a fluorimetric detector. The advantages of this colorimetric method are its simplicity and affordability to be used for routine cytotoxicity diagnosis in resource-limited countries. MTT is particularly useful as a diagnostic tool for detection of Mtb and even subpopulations of resistant strains. It can be used as a simple assay to evaluate the activity of antimicrobial compounds. However, it is difficult to standardise the method for all drugs. For example, isoniazid is known to interfere with the normal reduction of MTT, resulting in misleading results (Abate et al. 1998).

3.1.1.4. BACTEC radiometric method

The BACTEC radiometric method was introduced in 1977 and revolutionised the conventional methods of Mtb detection (Roberts et al. 1983). The average detection time for Mtb positive cultures was reduced from 25-30 days to 4-10 days.

The BACTEC tubes contain Middlebrook 7H12 broth containing a ^{14}C-radio-labeled substrate, palmitate. The viable bacteria use this carbon source, releasing $^{14}CO_2$ that is detected by an ionic sensor of the BACTEC instrument (Roberts et al. 1983). Drug susceptibility testing can be done comparing the radioactive counts in the test tubes with the ones in control tubes with no added drugs.

The major benefit of the use of this radiometric method is that it reduces the duration of the experiment. Compared to the conventional plating methods, besides being rapid, this method is easily standardized and it is reproducible between different research groups. It can also be easily adapted to study latent Mtb (Kharatmal et al. 2009).The major disadvantage of BACTEC is the fact that the researcher will be dealing with radioactivity with all the handling and radioisotope disposal charges that it carries (Collins and Franzblau 1997).

3.1.1.5. Nitrate reductase assay

The nitrate reductase assay (NRA) uses the ability of live Mtb to reduce nitrate to nitrite. The Mtb cells are incubated in a medium with potassium nitrate (KNO_3) and the drugs to test (Angeby et al. 2002; Lemus et al. 2006). After incubation the presence of nitrite can be detected when there was growth of the colonies, using a mixture of 50% concentrated hydrochloric acid, 0.2% sulphanilamide and 0.1% *n*-(1-naphtyl)ethylenediamide dihydrochloride, due to colour change of the media. This method is inexpensive and it allows faster results than the direct visualization of growing colonies. However, nitrite can be further reduced to nitrite oxide, and this compound is not detected in the NRA, causing false negative results (Angeby et al. 2002).

3.1.1.6. Low-Oxygen-Recovery assay

The Low-Oxygen-Recovery assay (LORA) is used in studies of drug tolerance using bacilli in the non-replicating persistent state (Cho et al. 2007). The cells are cultured for extended periods of time under controlled conditions of limited aeration and then allowed to "recover" for 28 hours under aerobic conditions, before being either counted by direct plate counting or the absorbance of the culture suspensions assessed using a spectrophotometer (Cho et al. 2007). The aerobic recovery time is determined by the amount of time necessary to detect growth in drug-free control cultures.

3.1.1.7. MB/BacT

The MB/BacT method was developed by Organon Teknica corp. and it is considered accurate, rapid and does not require the use of radioactivity. MB/BacT bottles contain a non-selective growth media and after incubation with Mtb, the CO_2 released by growing bacteria is detected through a colorimetric sensor. The MB/BacT detection system recognises positive growth when there is a change in this colorimetric indicator (Piersimoni et al. 2001).

The method is fully automated, reducing the need for constant monitoring and making it ideal to process a large amount of cases (Díaz-Infantes et al. 2000). It allows the study of drug susceptible Mtb but also resistant Mtb (Díaz-Infantes et al. 2000; Piersimoni et al. 2006). Despite being a rapid and easy method, MB/BacT requires heavy investments in equipment and running costs (Mueller et al. 2008).

3.1.1.8. Mycobacterium Growth Indicator Tube method (MGIT)

The MGIT is a rapid and non-radiometric system of culture, detection and recovery of Mtb and in parallel with MB/BacT system, represented a step forward in the isolation of mycobacteria from clinical samples. The MGIT consists of a tube filled with an enriched media with a fluorescent indicator at the bottom. This indicator is quenched in the presence of the medium with oxygen. By using a transluminator with UV light, the tubes that have viable organisms can be identified due to the consumption of oxygen by live organisms, allowing the fluorescence to be detected. Drug susceptibility testing can be performed comparing the fluorescence in the test tubes with the fluorescence of control tubes with no added drugs (Walters and Hanna 1996).

3.2. Methods

3.2.1. General considerations regarding Mtb culturing

Mtb is classed as hazard group 3 by the Advisory Committee on Dangerous Pathogens (ACDP) and therefore all work involving manipulation of specimens and culture material was carried out within a Nuaire Labguard Class II biological safety cabinet (Nuaire, USA) within a Containment Level 3 laboratory.

All media and reagents were sterilised by autoclaving or filtration through a 0.22μm pore syringe filter (Gelman Sciences, UK).

Inside the incubator and during transport from the incubator to the safety cabinet, Mtb cultures were safely contained inside a Bio Transport™ Carrier box (Nalgene®, USA).

5% (v/v) Surfanios (Anios lab, France) was used throughout as disinfectant due to its superior ability to sterilise mycobacteria. All waste

generated was autoclaved and liquid waste was immersed in a solution of 5% (v/v) of Surfanios prior to being autoclaved.

Some of the standard procedures used throughout the lab work involving Mtb were adapted from a compilation of Mtb protocols (Parish and Stoker 2001).

3.2.2. Mtb strain and growth media

Mtb strain H37Rv (ATCC#25618) was grown in Middlebrook 7H9 Broth (BD Diagnostic, UK) enriched with 0.2% (v/v) glycerol, 0.05% (v/v) Tween® 80 and 10% (v/v) OADC, in Middlebrook 7H11 Agar plates supplemented with 0.2% (v/v) glycerol and 10% (v/v) OADC and Löwenstein-Jensen slopes (BD Diagnostic, UK) depending on the experiment. OADC is an enrichment supplement composed of oleic acid, albumin, dextrose and catalase, which are essential for mycobacterial growth.

3.2.3. Storage of Mtb stocks

The continuous sub-culture of Mtb in solid or liquid medium was avoided since during prolonged *in vitro* culture mutations occur frequently (David 1970). In addition cultures were kept as a backup measure in the case of contamination of the initial stock. The storage medium consisted of 0.47g Middlebrook 7H9 Broth powder supplemented with 10ml OADC, 20ml glycerol and 70ml ddH_2O. This solution was sterilized through a 0.22μm pore filter and stored at 4°C for up to 4 months.

The Mtb suspension to be frozen was grown until it reached the turbidity of a McFarland standard number 2, that corresponds to 6×10^8 CFU/ml

(see Section 3.2.5.). 250µl aliquots of cell culture were added to an equal volume of storage medium and stored immediately at -20°C.

3.2.4. Culturing Mtb from frozen stocks

A vial containing 500µl of frozen Mtb was retrieved from the -20°C freezer, and allowed to defrost at room temperature. 50µl of the Mtb stock was inoculated directly into 10ml of Middlebrook 7H9 Broth and incubated at 37°C in a 5% CO_2 HERACell 150 CO_2 incubator (Thermo Scientific, UK).

From the same vial, a pre-warmed Löwenstein-Jensen slope was inoculated using a 10µl disposable loop (NUNC, UK).

After 2-3 weeks growth, using a 10µl disposable loop an isolated Mtb colony was transferred from the slope to a 50ml Falcon tube containing 10ml of Middlebrook 7H9 Broth. The culture was vortexed and subsequently incubated for a minimum of 2 weeks before use. Slopes were incubated for up to 4 months, functioning as a cell reservoir and the visual verification that cell stocks were not contaminated.

Any cells remaining in the defrosted vial were not returned to storage but were instead discarded in 5% (v/v) Surfanios.

3.2.5. Quantification of viable Mtb in liquid culture using McFarland Equivalence Turbidity Standards

The McFarland standards are commercially available from Pro-Lab (Pro-Lab Diagnostics, UK). Standards can be prepared using different combinations of barium chloride ($BaCl_2$) and sulphuric acid (H_2SO_4) but a mixture of water and latex beads which is commercially available is

more stable and reliable (Zamora and Pérez-Gracia 2012). When the turbidity of an unknown sample is adjusted to match the turbidity of the McFarland standard, it produces predictable bacterial counts (McFarland 1907).

The number of bacteria in a suspension was estimated from the standard curve obtained from a plot of the OD_{600} of the McFarland standard against the number of bacteria equivalent to that standard.

3.2.6. Confirmation of the number of viable Mtb by colony counting

To confirm the validity of the McFarland Equivalence Turbidity Standards as a method to assess bacterial numbers, direct counting of visible colonies in Petri dishes was performed.

An 800µl aliquot of Mtb culture was placed in a disposable cuvette and the OD_{600} measured and recorded as previously described (Section 2.2.2.1.). A second aliquot of 200µl from the same culture was placed in a sterile Eppendorf and serially diluted with sterile 10mM PBS, pH 7.2 in a range between 1 to 10^3 and 1 to 10^9. The dilutions were thoroughly mixed by vortexing to ensure homogeneity, followed by the spread of 100µl of each of these cultures onto Petri dishes containing 20ml of Middlebrook 7H10 Agar, supplemented with 10% (v/v) OADC, 0.05% (v/v) and 0.2% (v/v) glycerol.

Plates were bagged, boxed and incubated at 37°C, 5% CO_2 for 3 weeks, until visible colonies appeared. Plates presenting 50-100 organisms were selected and counted.

The number of bacteria in the original sample corresponds to the number of bacteria counted in the plate multiplied by the dilution factor used. Finally, this value was compared to the number of bacteria predicted

using the McFarland spectrophotometer procedure described above (see Section 3.2.5.) to confirm the validity of the assay.

3.2.7. Mtb growth curves and generation time

In order to plot growth curves for Mtb cultures, the culture turbidity was monitored twice weekly at 600nm using a WPA CO 8000 Biowave cell density meter (Biochrom, UK).

The generation time, defined as the time for Mtb cells to double in number, was assessed by plotting a curve of time *versus* calculated colony forming units (CFU), obtained from the OD_{600} of the culture (see Section 3.2.5.). CFU were expressed as the number of viable cells/ml.

3.2.7.1. pH dependent growth of Mtb

In order to identify the optimal pH for the growth of Mtb and to characterise Mtb growth under different pH ranges, the growth medium (Middlebrook 7H9 Broth enriched with 0.2% (v/v) glycerol, 0.05% (v/v) Tween® 80 and 10% (v/v) OADC) was modified, adding KOH and KCl to adjust the solution to a range of pH: 4.5; 5.6; 6.5; 7.4 and 8.3.

Mtb curves were plotted against time, according to section 3.2.7..

3.2.8. Sterilisation of Mtb cells

To ensure the safety of the assays performed and that the sterilisation methods used to kill Mtb were effective, cultures were diluted to a McFarland standard number 1 (see Section 3.2.5.) in Middlebrook 7H9 Broth and incubated with 100µl paraformaldehyde at 8 different

concentrations (0%, 0.01%, 0.05%, 0.1%, 0.5%, 1%, 5%, and 10% (v/v) paraformaldehyde diluted in ddH_2O). After 2h incubation at 37°C 100µl of the cell suspension were plated on Middlebrook 7H11 Agar plates. The plates were incubated for 4 weeks at 37°C before scoring the colony growth as culture positive or negative.

3.2.9. Mtb growth conditions

Assuring the same provenance of bacteria, a 2 week culture of Mtb at OD_{600}~0.9 was selected and used throughout this experiment, being sub-cultured according to one of the methods stated in Section 3.2.9.1-4, depending on the endpoint being investigated.

3.2.9.1. Preparation of Mtb aerobic cultures

50µl of Mtb inoculum were transferred to a 50ml Falcon tube containing 10ml of Middlebrook 7H9 sterile Broth, supplemented with 0.2% (v/v) glycerol, 0.05% (v/v) Tween® 80 and 10% (v/v) OADC. The culture was vortexed and incubated for a minimum of 2 weeks at 37°C in a 5% CO_2 incubator before use. The turbidity of the culture was monitored until it stabilized (see Section 3.2.7.) and discarded when 3 months old.

3.2.9.2. Hypoxia model of growth: cultures grown in limited oxygen conditions

The model used for Mtb growth was an adaptation of the Wayne model of growth (Wayne and Hayes 1996).

For growth under limited aeration which results in the creation of a microaerophilic environment, 375µl of the log-exponential phase Mtb

were cultured in 50ml Falcon tubes containing 37.5ml of Middlebrook 7H9 Broth. Each tube contained a Polytetrafluoroethylene-coated (PTFE-coated) magnetic stirring bar (VWR International, UK) with 8 × 5mm dimensions that were autoclaved before use.

Two 50ml flasks were used to monitor the growth of the culture. Rubber skirted stoppers (VWR International, UK) were used to limit oxygen supply to the cultures. To ensure anaerobic conditions the opening was further sealed with Parafilm® (Pechiney Plastic Packaging Company, USA). At selected times, the syringe was inserted into the sealed flasks through the rubber stopper and an aliquot of culture was collected and its turbidity determined in the portable WPA CO 8000 Biowave cell density meter (Biochrom, UK).

Thereafter, 20µl of this suspension were diluted $1:1\times10^5$ and $1:1\times10^7$ in sterile broth and inoculated in Löwenstein-Jensen slopes to assess the time when the number of viable bacteria stabilised.

In one 50ml flask, a stock sterile solution of methylene blue (500µg/ml solubilised in ddH_2O) was added to a final concentration of 1.5µg/ml. The reduction-associated decolourization of this dye was used as a visual indicator of oxygen depletion (Wayne and Hayes 1996). Cultures were incubated in a 5% CO_2 incubator at 37°C, stirring at 160rpm on a Biostir 4 magnetic stirrer (Wheaton Industries Inc, USA).

3.2.9.3. Preparation of Mtb cultures grown in fatty acid rich media

50µl of Mtb inoculum were transferred to a 50ml Falcon tube containing 10ml of fatty acid rich media.

The preparation of the fatty acid rich medium was adapted from Schnappinger and colleagues (Schnappinger et al. 2003) and consisted of minimal media supplemented with a saturated fatty acid. Media was

prepared by adding 0.5g asparagine, 1g KH_2PO_4, 2.5g Na_2PO_4, 10mg $MgSO_4 \cdot 7H_2O$, 50mg ferric ammonium citrate, 0.5mg $CaCl_2$, 0.1mg $ZnSO_4$ and 0.5ml Tween® 80. 0.2% (w/v) sodium palmitate was dissolved in ddH_2O at 50°C and added to the media at a final concentration of 0.05mM. The final volume was adjusted to 1 litre using ddH_2O. The solution was filtered through a 0.22μm pore syringe filter and the pH adjusted to 6.6.

The culture was mixed by vortexing and incubated at 37°C in a 5% CO_2 incubator. The turbidity of the culture was monitored up to 3 months and after this time, the culture was discarded.

3.2.9.4. Preparation of Mtb cultures grown under nutrient starvation

50μl of Mtb inoculum were transferred to a 50ml Falcon tube containing 10ml of sterile PBS pH 6.5. The culture was vortexed and incubated at 37°C in a 5% CO_2 incubator for 3 months. The preparation of Mtb starved cultures was based on the method described by Betts et al. 2002.

3.2.10. *In vitro* Mtb drug sensitivity assays using the microplate alamarBlue® assay (MABA)

The MABA involved the addition of alamarBlue® solution to a 96-well microplate containing varying concentrations of test compounds and cultures of Mtb, strain H37Rv. After the incubation period the growth of Mtb was observed as a change in the colouration of the alamarBlue® solution. The methodology was previously described for *M. smegmatis* in Section 2.2.3 but it is described here in more detail with reference to Mtb.

The setting of the plate (see Section 3.2.10.4. and Fig. 3.1.) included drug-free controls, representing the undisturbed growth of the Mtb cells.

The control wells will have 100% growth and all the test wells were compared to this value in order to obtain a percentage of growth.

The setting of the plate also included Mtb-free controls which allowed the correction of the final results, subtracting the absorbance of the background (drug, media, alamarBlue® and paraformaldehyde) against the test wells, in order to obtain just the absorbance related to the Mtb growth.

3.2.10.1. Determination of the optimum cell density for the sensitivity of the assay

To identify the optimal cell concentration to use for the determination of the IC_{50} values, cells were serially diluted in complete nutrient broth and incubated overnight at 37°C with 20µl alamarBlue®. The reaction was terminated by addition of 100µl of 10% (v/v) paraformaldehyde to every well followed by an incubation period of 2h. The sterilised plates were read using a plate reader at 570nm. The concentration of cells was plotted *versus* the absorbance signal to identify the range of optimal cell density to use in the assay, corresponding to the linearity of the correlation.

3.2.10.2. Preparation of Mtb inoculums used in MABA

A constant bacterial density was used throughout all experiments. An Mtb culture, either grown under aerobic or anaerobic conditions (as described in Section 3.2.9.1. and 3.2.9.2.), was diluted to the turbidity of a McFarland Standard number 1 (i.e. corresponding to a bacterial concentration of 3×10^8 CFU/ml). This solution was further diluted 1:30, to obtain a final concentration of 1×10^7 CFU/ml. Dilutions were made using complete Middlebrook 7H9 Broth.

3.2.10.3. Preparation of drug dilutions used in MABA

All compounds tested were dissolved either in DMSO, ethanol, methanol, or ddH_2O (Table 3.1.). DMSO, ethanol and methanol were of analytical grade (≥99.5% purity), were not further diluted and are commercially available (Sigma, USA). 10mM stock solutions were prepared and sterilised through a 0.22μm pore filter and stored at -20°C.

1 in 3 serial dilutions of the initial 10mM stocks were prepared using Middlebrook 7H9 Broth enriched with 0.2% (v/v) glycerol, 0.05% (v/v) Tween® 80 and 10% (v/v) OADC. For each compound eight serial dilutions were made. All dilutions were freshly prepared at double the required final well concentration to allow for further dilution in the test wells with Middlebrook 7H9 Broth and to ensure compound degradation was not a factor affecting data.

Table 3.1.: Details of compounds tested against Mtb strain H37Rv using an *in vitro* microplate alamarBlue® assay (MABA). The table presents the name, molecular weight and solvents used to dissolve each drug used in the MABA bioassay.

Compound	Molecular Weight	Solvent
Chlorpromazine hydrochloride	355.33	DMSO
cis-(z)-Flupenthixol dihydrochloride	507.44	DMSO
Ethambutol dihydrochloride	277.23	dH_2O
Fluphenazine dihydrochloride	510.44	DMSO
Isoniazid	137.14	dH_2O
Metronidazole	171.15	DMSO
Perphenazine	403.97	DMSO
Phenothiazine	199.27	DMSO
Promazine hydrochloride	320.88	DMSO
Promethazine hydrochloride	320.88	DMSO
Pyrazinamide	123.11	dH_2O
Rifampicin	822.94	Ethanol
Streptomycin sulphate salt	728.69	dH_2O
Thioridazine hydrochloride	407.04	Methanol
Trifluoperazine dihydrochloride	480.42	Methanol

3.2.10.4. Preparation of the 96-well microplate for the Mtb MABA

The assay was performed in sterile 96-well microtitre flat bottom plates (NUNC, UK). 200µl of ddH_2O were added to the wells at the perimeter of the microplate in order to minimize evaporation of medium in test wells during incubation (see Fig. 3.1. for plate format).

50µl of broth were plated in row C (columns 2 to 11) and in columns 6 and 11 (rows D, E and F). 50µl of each pre-prepared drug dilution were added into columns 2, 3, 4, 5, 7, 8, 9 and 10. The concentration of drug decreased from left to right, with column 2 containing the highest drug concentration and column 10 the lowest drug concentration. Finally, 50µl of Mtb inoculum was added in rows D, E and F (2 to 11).

Wells in columns 6 and 11 (rows D, E and F) were free-drug controls containing 50µl of broth and 50µl of bacteria inoculum. Wells in row C (2 to 11) were Mtb -free wells, acting as blanks containing 50µl of broth and 50µl of the respective drug dilution. The other wells were test wells with bacteria and varying concentrations of the test compounds.

Each plate was then bagged, placed inside a sealed protective box and transferred to a 5% CO_2 incubator.

3.2.10.5. Addition of alamarBlue® to MABA

After 7 days incubation at 37°C, 20µl of alamarBlue® was added to each well and the plates returned to the incubator.

After 24h, plates were sterilised by adding 100µl of 10% (v/v) paraformaldehyde to each well. The solution of 10% (v/v) was freshly prepared on the day of the experiment, from a commercially available 37% (v/v) stock solution from Sigma. 27ml of the stock solution were

diluted in 73ml ddH_2O) and filtered through a 0.22µm pore filter to eliminate particles that could affect the photometric reading of the plate.

After a minimum of 2h, plates were wiped thoroughly with 5% (v/v) Surfanios and read using an Opsys MR™ Microplate Reader (Dynex Technologies, USA) at an absorbance of 570nm.

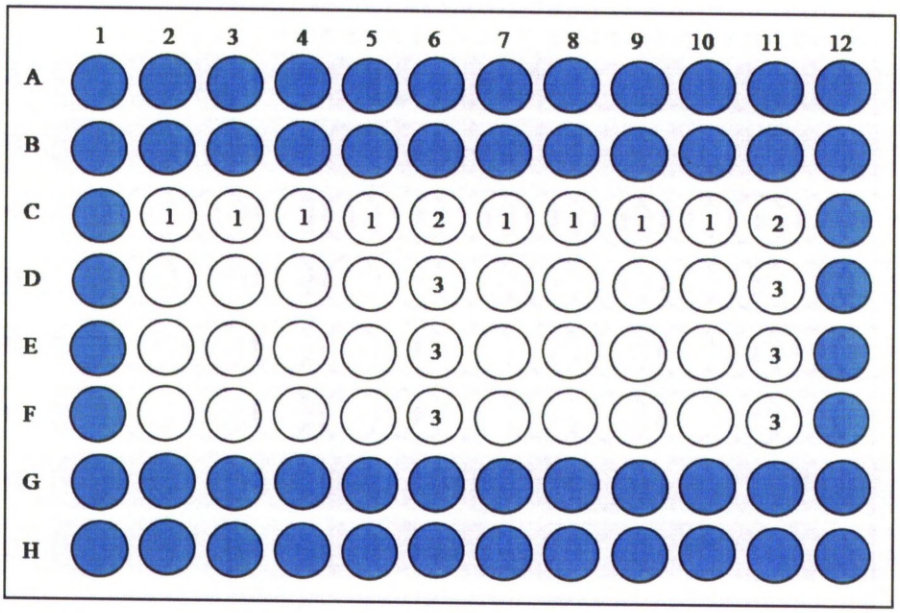

Fig. 3.1.: Representative 96 well microplate format for screening drug susceptibility of Mtb to various compounds using MABA. ● represents wells containing 200µl of ddH_2O, ① corresponds to wells containing 50µl broth and 50µl drug dilution, ② contained 100µl of broth, ③ were wells containing 50µl broth and 50µl Mtb inoculums and ○ were wells containing 50µl drug dilutions and 50µl of Mtb cells.

3.2.10.6. Time-dependent effects of test compounds on Mtb growth

In order to assess if the exposure time to the drug affected its ability to inhibit the growth of Mtb, the bioassay included some modifications. Here, three 96-well plates were set up. After the usual 7 days of incubation, alamarBlue® was added to each well of one of the plates and the plate returned to the incubator and the assay processed as described in Section 3.2.10.5. To the second of the plates, alamarBlue® was added

after 14 days of incubation and to the third plate, alamarBlue® was added after 21 days of incubation with the test compounds.

3.2.10.7. Modification of MABA in order to test the susceptibility of Mtb growing under micro-aerophillic conditions

In order to test the drug susceptibility of Mtb grown under micro-aerophillic conditions, the bioassay used included some modifications. The format of the 96-well plate was maintained, but after plate preparation, it was placed inside an anaerobic bag with an Aerocult IS sachet (Merck, Germany) that was humidified with 8ml ddH2O in order to produce the necessary anaerobic environment. The bag, part of the Aerocult IS kit was sealed with a thermal sealer and incubated in a 5% CO_2 incubator at 37°C.

After 7 days, the plate was removed from the anaerobic conditions and placed inside a zipped bag and returned to the incubator.

After further 7 days incubation, the assay was terminated as described in Section 3.2.10.5.

3.2.10.8. Data analysis of drug susceptibility testing

The results of drug susceptibility testing were presented in terms of the efficacy of each drug in inhibiting the growth of Mtb.

Graphs were generated plotting the concentration of drug against the percentage of growth of the bacteria in the test wells. This percentage was calculated assuming 100% growth in control wells without any inhibitor.

The IC_{50} (half maximal inhibitory concentration) refers to the concentration of drug which causes 50% inhibition of growth. The IC_{90} (90% inhibitory concentration) refers to the concentration of drug which causes inhibition of 90% of microbial growth.

A data report was generated using the Revelation QuickLink™ 1.0 software (Dynex Technologies, USA), from the data obtained with the plate reader. A dose *versus* response graph was plotted using GraphPad Prism version 5.00 for Windows (GraphPad Software, USA), with the respective number of replicates. The software allowed the inference of both IC_{50} and IC_{90} from a generated log-dose response sigmoid curve that was constrained between 0 and 100% and the standard errors associated with this inference.

3.2.11. Drug combination assay

In order to assess the effect of some of the drugs used in combination, a modification of the method of Berenbaum (Berenbaum 1978) was used.

The IC_{50} values of each drug to be tested in combination were determined alone and these values were used to prepare two individual working drug solutions with a concentration sixteen times the IC_{50} of the drug being tested.

Thereafter, these prepared drug solutions were combined in fixed ratio combinations of 10:0, 9:1, 7:3, 5:5, 3:7, 1:9 and 0:10. Each combination was then serially diluted 8 times before being tested against Mtb as described above.

With the data from the plate reader the IC_{50} for each drug combination was determined and used to calculate the 50% fractional inhibitory

concentration (FIC) for each compound, at each of the ratios, according to the formulae below.

$FIC_{drug\ A}$ = (IC_{50} of drug A in combination/IC_{50} of drug A alone)

$FIC_{drug\ B}$ = (IC_{50} of drug B in combination/IC_{50} of drug B alone)

Using these interaction coefficients it was possible to draw an isobologram of $FIC_{drug\ A}$ *versus* $FIC_{drug\ B}$ (Fig. 3.2.).

The sum of $FIC_{drug\ A}$ and $FIC_{drug\ B}$ determines whether the combined bacteriostatic effect of the two drugs tested was synergistic, additive or antagonistic. When the sum equals 1.0 the isobologram represents an additive effect, when the sum is less than 1.0 the isobologram represents a trend toward a synergistic effect and when the sum is higher than 1.0 it represents a trend towards an antagonistic effect (Fig. 3.2.).

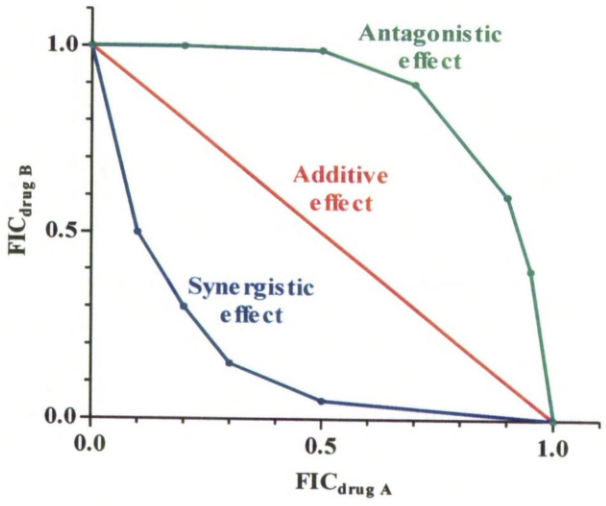

Fig. 3.2.: Classical isobologram and chemical interaction between compounds A and B. Adapted from Tallarida 2006.

3.2.12. Specimen collection and preparation of slides for Mtb staining

Mtb strain H37Rv grown under unlimited aeration or microaerophillic conditions (Section 3.2.9.1. and 3.2.9.2.) were harvested by centrifugation at 3000*g* for 10 minutes. The supernatant was discarded and the pellet resuspended in sterile PBS, pH 7.4. Thin and uniform smears were prepared on clean black oval slides with CELL-BOND coating (Alpha-Tec systems, USA) using 10µl of the resuspended cells. Slides were fixed by heating at 65-70°C for 10 minutes on a heat block placed inside an appropriate biological safety cabinet. Slides were allowed to cool before being transferred to a staining rack.

3.2.12.1. Dyes and reagents used for staining Mtb

Auramine phenol and potassium permanganate are commercially available from ProLab (Pro-Lab Diagnostics, USA) and were prepared according to the manufacturer instructions. Briefly, the reagents were diluted 1 in 10 in ddH2O and stored at room temperature in the dark.

Nile Red was dissolved in absolute ethanol to create a stock concentration of 0.5mg/ml. It was stored at -20°C and further diluted 1:50 in ethanol to obtain a working solution of 0.1µg/ml as required.

Differentiator solution consisted of 1% (v/v) hydrochloric acid and 75% (v/v) absolute ethanol in ddH2O.

3.2.12.2. Staining procedure

For auramine phenol staining of Mtb, slides were flooded with the fluorescent stain, left to stand for 10 minutes and then rinsed with ddH_2O. Slides were then flooded with differentiator solution (1% hydrochloric acid: methanol: dH_2O) for 10 minutes, rinsed a second time with ddH_2O,

flooded with 0.1% (w/v) potassium permanganate for 45 seconds and finally rinsed again with ddH_2O before being air dried.

The Nile Red staining method included an extra step compared to the Auramine phenol method. Briefly, slides were flooded with auramine phenol and left to stand for 10 minutes before the stain was rinsed with ddH_2O. Slides were then flooded with differentiator solution for 10 minutes, rinsed with $ddH_2O$and flooded with freshly prepared Nile Red solution for 10 minutes. The slides were then rinsed with ddH_2O, flooded with 0.1% (w/v) potassium permanganate for 45 seconds and rinsed again with ddH_2O before being air dried.

Air dried slides were mounted in 100µl of sterile PBS, a coverslip was placed on top of the smears and the slides sealed using nail polish. Slides were kept in darkness and examined immediately by fluorescence oil immersion microscopy using a wide blue (> 525 nm) long-pass filter at an amplification of 100x. Images were captured using a camera fitted to the fluorescence microscope.

3.3. Results

3.3.1. Patterns of Mtb growth when submitted to different conditions

Mtb bacilli grown from the same batch were submitted to different growth conditions and their growth monitored by a change in turbidity of the liquid media, in an optical density meter.

As expected, Mtb grows optimally in conditions of unlimited aeration (Fig. 3.3.- blue line). Around day 5, there is exponential growth of bacteria. Around day 23 there is a stabilisation of the numbers, the bacteria reach a stationary phase.

Submitting the cultures to severe hypoxia, mimicking the environment that exists inside the granuloma involves the gradual depletion of oxygen from the culture. The bacteria present a distinctive three-stage optical curve of growth (Fig. 3.3.- red line). In Fig. 3.4. this curve is presented in detail. For the first 8-9 days, there is sufficient oxygen in the media to support exponential growth. Then for 10-11 days there is a shift into microaerobic NRP-1 stage, where there is a continuous slow rise in OD due to cell enlargement, but not cell number (this was expected and confirmed by plating Mtb at day 15, 18 and 20 and obtaining a similar number of bacteria despite the increase in OD) (Wayne and Sohaskey 2001). From day 20 the bacteria shift to NRP-2, the culture becomes anaerobic and there is no further cell enlargement (Fig. 3.4.). This curve pattern is characteristic of the slow stirring model of Mtb hypoxic growth (Wayne and Sohaskey 2001). Cell enlargement of Mtb cells grown anaerobically is shown in Fig. 3.58.B and Fig. 3.59.A-D.

The cells grown in a fatty acid rich media had a small exponential growth phase followed by the stabilisation of the number of mycobacteria (Fig. 3.3.- green line). *Mycobacterium* has fatty acid as its major nutrient source of energy inside granulomas *in vivo*, so instead of glucose and glycerol they use exclusively fatty acids as carbon sources of energy (McKinney et al. 2000; Schnappinger et al. 2003; Niederweis 2008). Mtb cells were able to subsist in the fatty acid rich medium but their growth was very limited.

The cells grown in a minimal medium (Fig. 3.3.- pink line), without carbon sources of energy showed very limited growth.

To confirm that viable bacteria remained in all the differently grown batches, bacteria were subcultured in Löwenstein-Jensen slopes and their viability confirmed visually after 3 weeks.

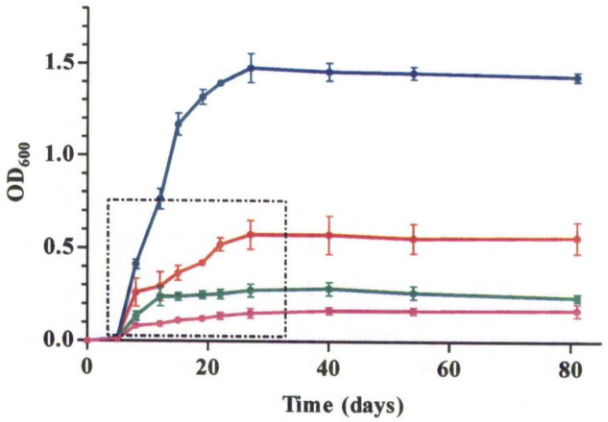

Fig. 3.3.: Typical growth curves of Mtb cultures grown under different conditions. (▬, blue line) corresponds to cultures grown under conditions of unlimited oxygen supply, (▬, red line) represents the cultures grown under limited aeration conditions, in (▬, green line) the bacterial cells were grown in a fatty acid rich media and in (▬, pink line) the cells were deprived of a carbon source of energy. The data shown are the averages and standard deviations of 6 replicates. Cross-section indicates the anaerobic growth region to be analysed in detail in Fig. 3.4..

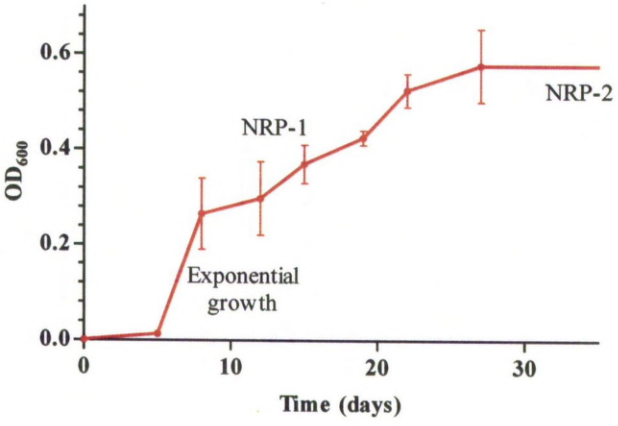

Fig. 3.4.: Detail of the growth curve of Mtb grown anaerobically, red line from Fig. 3.3.. There was a gradual depletion of oxygen from the culture and the bacteria present a distinctive three-stage optical curve of growth. An initial exponential growth phase followed by two phases of non-replicative persistence (NRP), where there is no increase in the numbers of bacteria, just a small increase in the optical densities and then the stabilisation of the numbers. The data shown are the averages and standard deviations of 6 replicates.

3.3.1.1. pH dependence of growth of Mtb

In terms of acidity/alkalinity of the medium, Mtb bacilli grow optimally at a strict pH range. The ideal pH is 6.5. (Fig. 3.5.- green line) if the pH was a little higher (pH7.4) the growth is impaired but possible (Fig. 3.5.- pink line). At alkaline pH of 8.3 (Fig. 3.5.- black line) or acidic pH of 4.5 (Fig. 3.5.- red line) or 5.6 (Fig. 3.5.- blue line), the growth is reduced to a minimum.

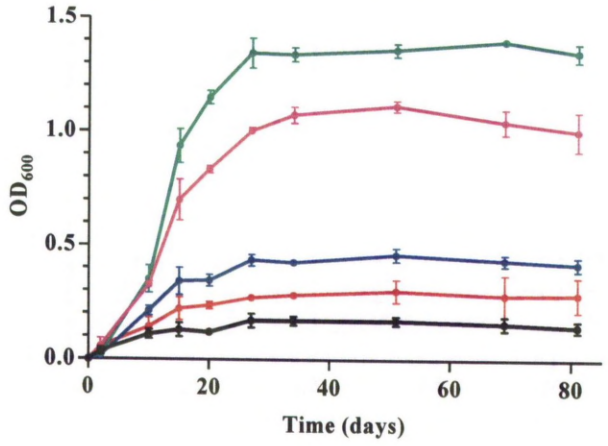

Fig. 3.5.: Typical growth curves of Mtb cultures grown under different pH conditions. (▁, red line) corresponds to cultures grown at the acidic pH of 4.5, (▁, blue line) represents the cultures grown at pH 5.6, in (▁, green line) the pH was 6.5 and this correspond to the pH of Middlebrook broth, in (▁, pink line) the cultures were grown at pH 7.4 and (▁, black line) represents the cultures grown at alkaline pH of 8.3. The data shown are the averages and standard deviations of 6 replicates.

3.3.2. Quantification of bacterial numbers and sterilisation of Mtb

In order to quantify the number of bacteria in a suspension and to standardize the quantity of bacteria used *per* experiment, McFarland standards were used. Fig. 3.6. shows the standard curve of Mtb using the McFarland standards, which allows for the estimation of the number of bacteria in a given bacterial suspension.

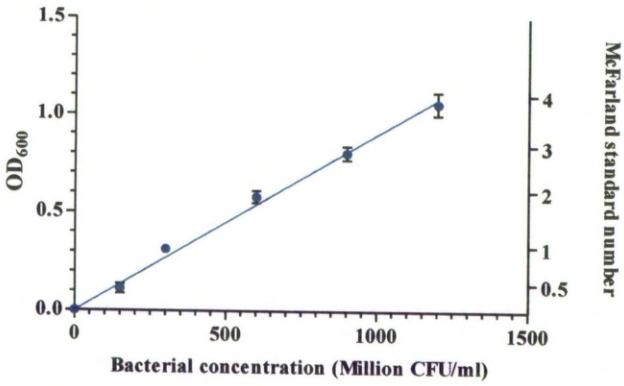

Fig. 3.6.: Linear correlation between the OD_{600} and the bacterial concentration of a sample. The right side Y-axis indicates the number of the McFarland standard used to obtain this calibration curve. The obtained linear relation was bacterial concentration (MCFU/ml) = OD_{600} /(0.0009410 ± 0.00001962). Each datapoint was obtained from three different bacterial suspensions.

To assess the bactericidal power of the decontamination agent, paraformaldehyde, a simple assay was performed and Fig. 3.7. shows the data obtained. Paraformaldehyde caused a concentration dependent decrease in the viability of Mtb, with 1% (v/v) causing total loss of viability.

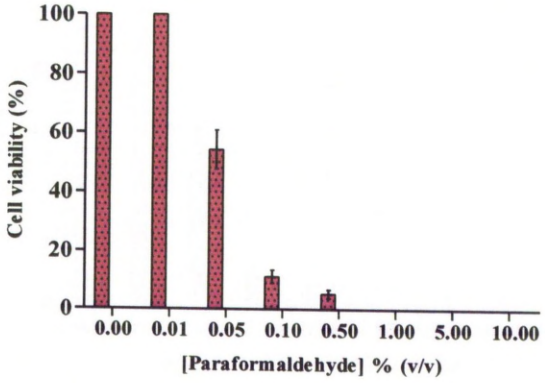

Fig. 3.7.: *M. tuberculosis* strain H37Rv viability after 2h exposure to different concentrations of paraformaldehyde.

3.3.3. Drug testing of various compounds against Mtb under no aeration limitations

The following graphs display the results obtained for the drug susceptibility tests of various compounds tested under unlimited aeration. In the first five assays (Fig. 3.8. to 3.12.), Mtb were grown in the presence of the first line anti-TB agents: streptomycin (Fig. 3.8.), ethambutol (Fig. 3.9.), rifampicin (Fig. 3.10.), isoniazid (Fig. 3.11.) and pyrazinamide (Fig. 3.12.).

The first line anti-TB agents were all effective against Mtb strain H37Rv, apart from pyrazinamide that did not have any effect on Mtb growth. Pyrazinamide is reported to be effective only in acidic pH, being completely inactive at a neutral pH (Zhang and Mitchison 2003). Due to severe limitations in culture growth when submitted to acidic pH conditions, the assay could not be adapted to test pyrazinamide.

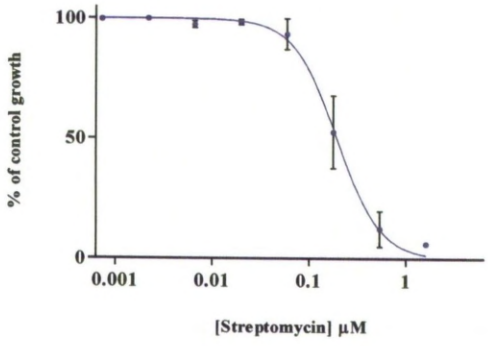

Fig. 3.8.: Curve of the Mtb inhibition of growth when exposed to different concentrations of streptomycin. The percentages of growth were estimated assuming that 100% growth occurred in the absence of the inhibitor.

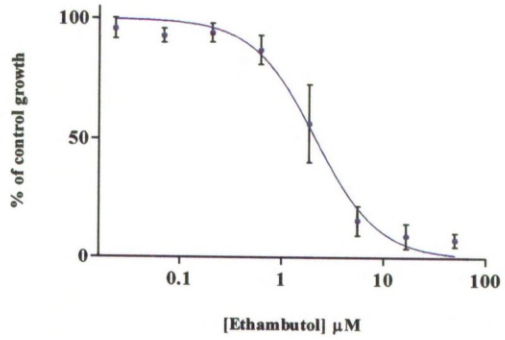

Fig. 3.9.: Curve of the Mtb inhibition of growth when exposed to different concentrations of ethambutol. The percentages of growth were estimated assuming that 100% growth occurred in the absence of the inhibitor.

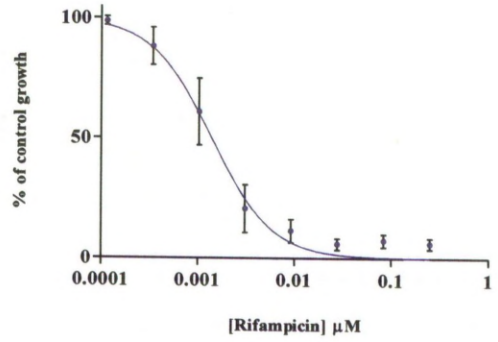

Fig. 3.10.: Curve of the Mtb inhibition of growth when exposed to different concentrations of rifampicin. The percentages of growth were estimated assuming that 100% growth occurred in the absence of the inhibitor.

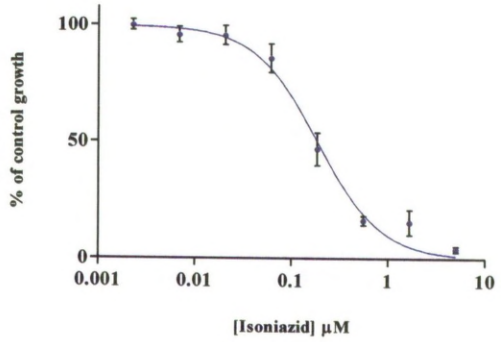

Fig. 3.11.: Curve of the Mtb inhibition of growth when exposed to different concentrations of isoniazid. The percentages of growth were estimated assuming that 100% growth occurred in the absence of the inhibitor.

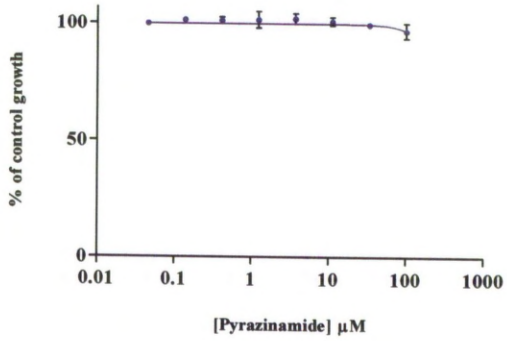

Fig. 3.12.: Curve of the Mtb inhibition of growth when exposed to different concentrations of pyrazinamide. The percentages of growth were estimated assuming that 100% growth occurred in the absence of the inhibitor.

Metronidazole (Fig. 3.13.) did not have a significant inhibitory effect against aerobic Mtb showing just a small decrease in mycobacterial growth when submitted to high concentrations of the drug.

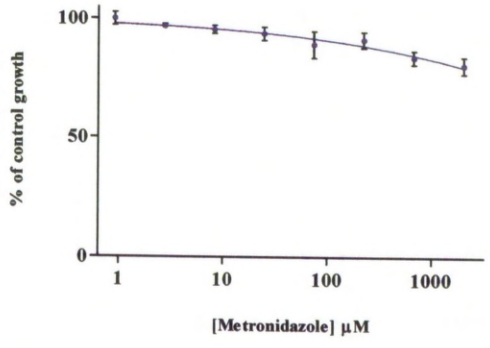

Fig. 3.13.: Curve of the Mtb inhibition of growth when exposed to different concentrations of metronidazole. The percentages of growth were estimated assuming that 100% growth occurred in the absence of the inhibitor.

The following graphs (Fig. 3.14. to 3.22.) show the inhibitory effects of nine phenothiazine compounds tested against aerobic Mtb H37Rv. All the compounds had an inhibitory effect against Mtb and an order of potency

can be established: trifluoperazine (Fig. 3.15.) > thioridazine (Fig. 3.14.) > flupenthixol (Fig. 3.21.) > fluphenazine (Fig. 3.20.) > perphenazine (Fig. 3.19.) > chlorpromazine (Fig. 3.22.) > promethazine (Fig. 3.17.) > promazine (Fig. 3.16.) > phenothiazine (Fig. 3.18.). Phenothiazine was the only agent that did not present an IC_{50} for the studied concentrations.

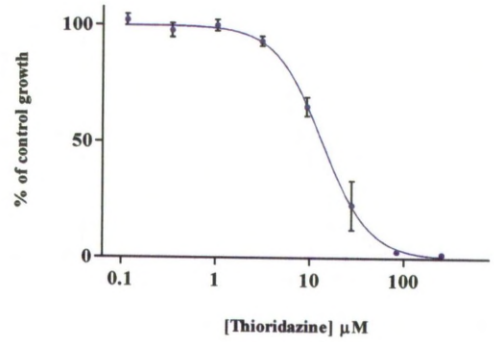

Fig. 3.14.: Curve of the Mtb inhibition of growth when exposed to different concentrations of thioridazine. The percentages of growth were estimated assuming that 100% growth occurred in the absence of the inhibitor.

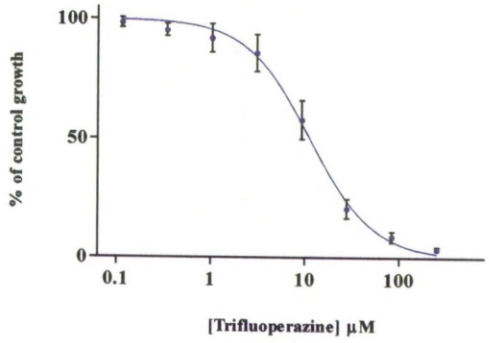

Fig. 3.15.: Curve of the Mtb inhibition of growth when exposed to different concentrations of trifluoperazine. The percentages of growth were estimated assuming that 100% growth occurred in the absence of the inhibitor.

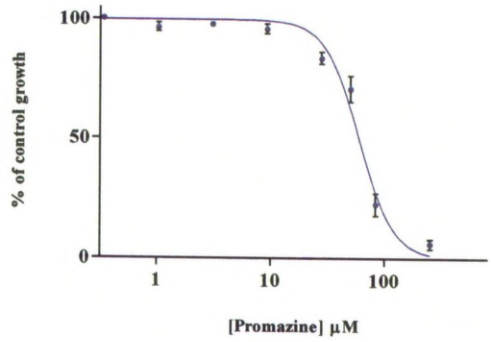

Fig. 3.16.: Curve of the Mtb inhibition of growth when exposed to different concentrations of promazine. The percentages of growth were estimated assuming that 100% growth occurred in the absence of the inhibitor.

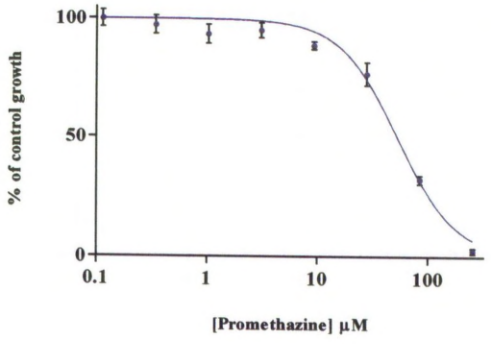

Fig. 3.17.: Curve of the Mtb inhibition of growth when exposed to different concentrations of promethazine. The percentages of growth were estimated assuming that 100% growth occurred in the absence of the inhibitor.

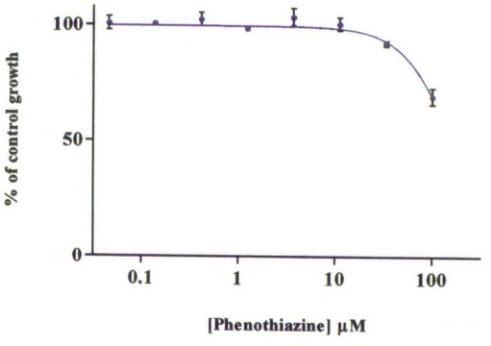

Fig. 3.18.: Curve of the Mtb inhibition of growth when exposed to different concentrations of phenothiazine. The percentages of growth were estimated assuming that 100% growth occurred in the absence of the inhibitor.

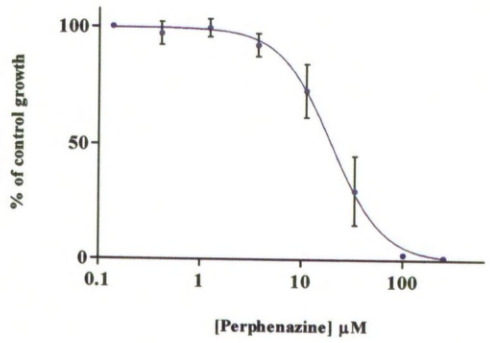

Fig. 3.19.: Curve of the Mtb inhibition of growth when exposed to different concentrations of perphenazine. The percentages of growth were estimated assuming that 100% growth occurred in the absence of the inhibitor.

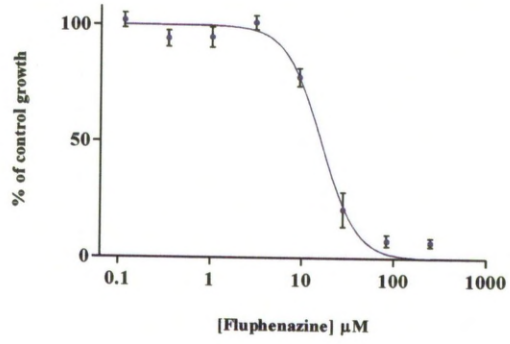

Fig. 3.20.: Curve of the Mtb inhibition of growth when exposed to different concentrations of fluphenazine. The percentages of growth were estimated assuming that 100% growth occurred in the absence of the inhibitor.

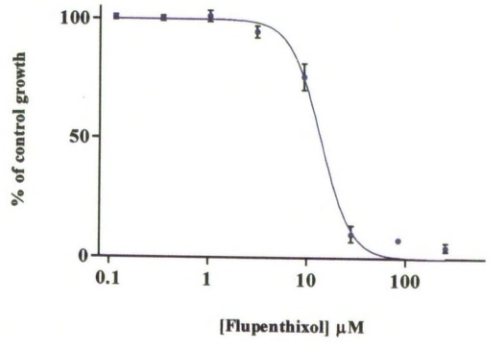

Fig. 3.21.: Curve of the Mtb inhibition of growth when exposed to different concentrations of flupenthixol. The percentages of growth were estimated assuming that 100% growth occurred in the absence of the inhibitor.

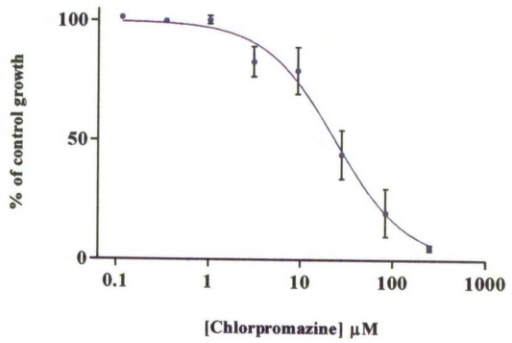

Fig. 3.22.: Curve of the Mtb inhibition of growth when exposed to different concentrations of chlorpromazine. The percentages of growth were estimated assuming that 100% growth occurred in the absence of the inhibitor.

Mefloquine (Fig. 3.23.) is a synthetic analogue of quinine, a drug used in malaria treatment that had previously been reported as having a strong inhibitory effect against Mtb (Mao et al. 2007).

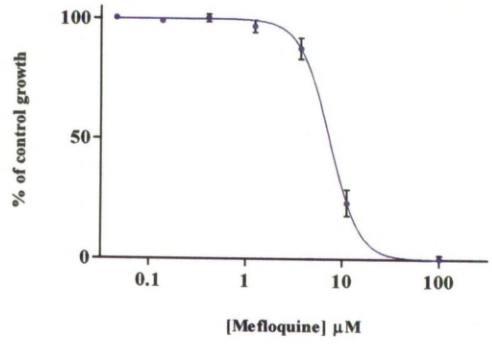

Fig. 3.23.: Curve of the Mtb inhibition of growth when exposed to different concentrations of mefloquine. The percentages of growth were estimated assuming that 100% growth occurred in the absence of the inhibitor.

Piericidin A (Fig. 3.24.) is a specific inhibitor of complex I NADH dehydrogenase and despite the fact that it does not present a clinically relevant IC_{50}, was able to completely inhibit the growth of Mtb at concentrations higher than 1000μM.

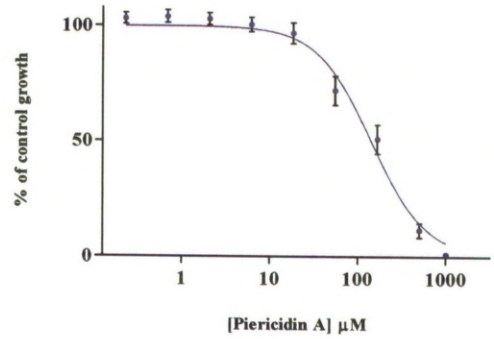

Fig. 3.24.: Curve of the Mtb inhibition of growth when exposed to different concentrations of piericidin A. The percentages of growth were estimated assuming that 100% growth occurred in the absence of the inhibitor.

Atovaquone (Fig. 3.25.), a ubiquinone analogue that blocks mitochondrial electron transport (Srivastava et al. 1997) does not inhibit significantly Mtb H37Rv growth. This is the expected result considering that menaquinone is the electron acceptor of Mtb, and not ubiquinone.

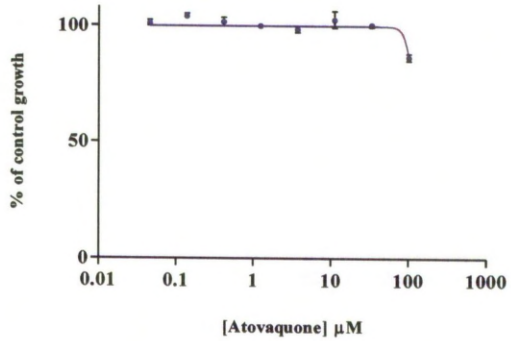

Fig. 3.25.: Curve of the Mtb inhibition of growth when exposed to different concentrations of atovaquone. The percentages of growth were estimated assuming that 100% growth occurred in the absence of the inhibitor.

Rotenone (Fig. 3.26.), which inhibits the oxidation of NADH to NAD does not have a significant effect against Mtb H37Rv, since Mtb possess Ndh-2, an alternative NADH dehydrogenase insensitive to rotenone (Yagi and Matsuno-Yagi 2003).

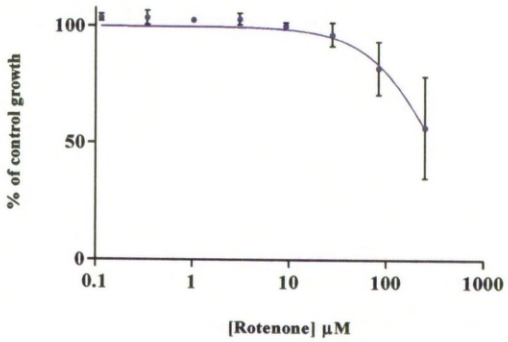

Fig. 3.26.: Curve of the Mtb inhibition of growth when exposed to different concentrations of rotenone. The percentages of growth were estimated assuming that 100% growth occurred in the absence of the inhibitor.

1-hydroxy-2-dodecyl-4(1*H*)quinolone (HDQ) (Fig. 3.27.), a quinolone-like compound that has high affinity for alternative NADH dehydrogenases, did not have a significant effect against aerobic Mtb H37Rv (Saleh et al. 2007) probably due to the existence of type I NADH dehydrogenases able to donate electrons to the ETC.

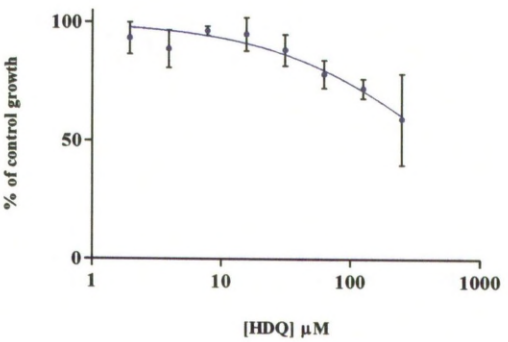

Fig. 3.27.: Curve of the Mtb inhibition of growth when exposed to different concentrations of 1-hydroxy-2-dodecyl-4(1*H*)quinolone (HDQ). The percentages of growth were estimated assuming that 100% growth occurred in the absence of the inhibitor.

Table 3.2. displays the IC_{50} and IC_{90} values and the respective standard errors of the compounds tested against Mtb under conditions of unlimited aeration. The number of replicates used in that determination is also indicated. The variation in the level of replication for each drug tested is explained by quality control performed on the results of the assays and not by an initial different number of replications of the procedure. Plates presenting anomalous or missing reads for a given test wells were entirely rejected. These IC_{50} and IC_{90} values are the summing up of the graphs described above (Fig. 3.8. to Fig. 3.27.).

Table 3.2.: Summary table of the IC_{50} and IC_{90} values of the inhibitor compounds tested against Mtb strain H37Rv using a MABA assay. The results are presented with the respective standard errors. n indicates the number of replicates.

Compound tested	IC_{50} (µM)	SE (µM)	IC_{90} (µM)	SE (µM)	n
Streptomycin	**0.19**	0.020	**0.59**	0.146	4
Ethambutol	**2.16**	0.330	**10.33**	3.564	6
Rifampicin	**1.38×10^{-3}**	2.069×10^{-4}	**6.70×10^{-3}**	2.192×10^{-3}	7
Isoniazid	**0.19**	0.019	**0.97**	0.213	7
Metronidazole	**>2000**	-	**>2000**	-	5
Thioridazine	**13.43**	1.078	**47.37**	8.245	5
Trifluoperazine	**11.23**	1.208	**61.40**	14.430	7
Promazine	**59.45**	2.331	**126.90**	11.820	4
Promethazine	**52.16**	3.841	**194.90**	30.840	4
Phenothiazine	**>100**	-	**>100**	-	4
Perphenazine	**19.85**	2.453	**71.22**	18.540	4
Fluphenazine	**15.99**	1.214	**42.04**	6.168	5
Flupenthixol	**13.64**	0.711	**29.35**	3.173	4
Chlorpromazine	**23.83**	3.554	**166.70**	55.200	4
Mefloquine	**7.31**	0.340	**15.71**	1.158	8
Piericidin A	**141.20**	12.560	**670.30**	125.300	4
Atovaquone	**>100**	-	**>100**	-	3
Rotenone	**>100**	-	**>100**	-	4
HDQ	**>100**	-	**>100**	-	3

3.3.4. Drug testing of thioridazine and trifluoperazine when used in combination with 4 DOTS drugs under no aeration limitations

The following graphs (Fig. 3.28.A - O) present the results obtained upon testing two compounds in combination against Mtb in aerobic conditions. Two of the more effective phenothiazines (thioridazine and trifluoperazine) were tested in combination with four of the current anti-TB compounds (ethambutol, isoniazid, rifampicin and streptomycin).

The isobologram representing the combination of thioridazine and trifluoperazine (Fig. 3.28.-A) shows a curve significantly concave, with FIC values less than 1.0 suggesting a synergistic effect between these two compounds (Berenbaum 1978; Tallarida 2006). A synergistic effect means that both drugs used in combination will have a stronger effect than when used separately.

Streptomycin, when used in combination with trifluoperazine (Fig. 3.28.-B) or thioridazine (Fig. 3.8.-C) shows a slight subadditivity effect and the same happens with rifampicin when used in combination with trifluoperazine (Fig. 3.8.-D), thioridazine (Fig. 3.8.-E) or streptomycin (Fig. 3.8.-F). The isoboles remain close to the additive line meaning that the slight antagonistic effect is not significant according to the convention of Berenbaum (Berenbaum 1978).

The isobolograms representing the combination of isoniazid and trifluoperazine (Fig. 3.28.-G) or thioridazine (Fig. 3.28.-H) show convexity with FIC values higher than 2, indicating antagonism (Tallarida 2006). An antagonistic effect means that both drugs used in combination will be less effective than when used separately.

The effect of isoniazid against Mtb H37Rv when used in combination with streptomycin (Fig. 3.28.-I) or rifampicin (Fig. 3.28.-J) is additive.

Ethambutol when titrated against trifluoperazine (Fig. 3.28.-K) or thioridazine (Fig. 3.28.-L) showed slightly more convexity than either streptomycin or rifampicin when tested in combination with the phenothiazines, suggesting a subadditivity effect. The same occurs when ethambutol is tested in combination with rifampicin (Fig. 3.28.-N) or isoniazid (Fig. 3.28.-O). A completely additive effect was obtained when ethambutol was tested in combination with streptomycin (Fig. 3.28.-M).

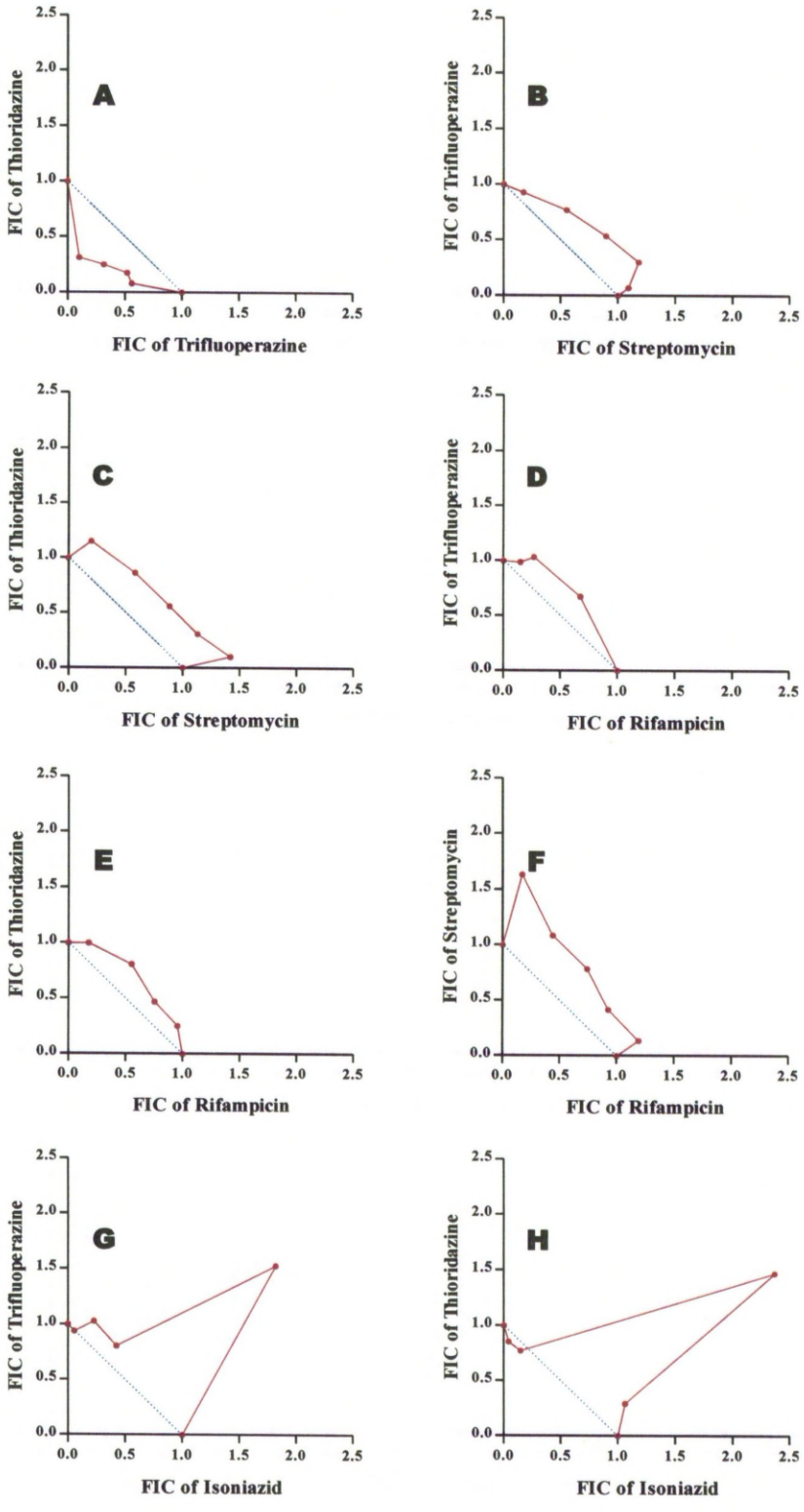
A
FIC of Thioridazine
FIC of Trifluoperazine
B
FIC of Trifluoperazine
FIC of Streptomycin
C
FIC of Thioridazine
FIC of Streptomycin
D
FIC of Trifluoperazine
FIC of Rifampicin
E
FIC of Thioridazine
FIC of Rifampicin
F
FIC of Streptomycin
FIC of Rifampicin
G
FIC of Trifluoperazine
FIC of Isoniazid
H
FIC of Thioridazine
FIC of Isoniazid
0.0
0.5
1.0
1.5
2.0
2.5

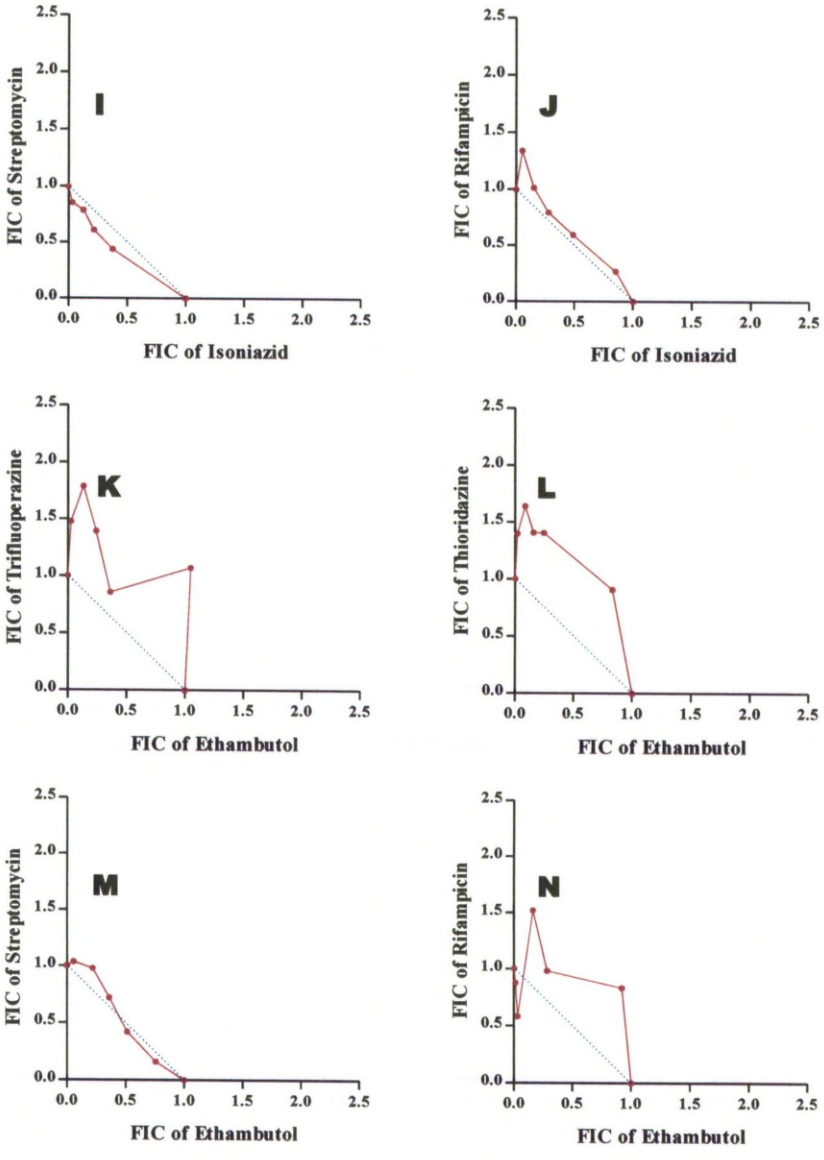

Fig. 3.28.: Typical isobolograms representing the interaction between trifluoperazine and thioridazine (A), streptomycin and trifluoperazine (B), streptomycin and thioridazine (C), rifampicin and trifluoperazine (D), rifampicin and thioridazine (E), rifampicin and streptomycin (F), isoniazid and trifluoperazine (G), isoniazid and thioridazine (H), isoniazid and streptomycin (I), isoniazid and rifampicin (J), ethambutol and trifluoperazine (K), ethambutol and thioridazine (L), ethambutol and streptomycin (M), ethambutol and rifampicin (N) and ethambutol and isoniazid (O).

3.3.5. Drug testing of various compounds against Mtb with variation in the length of exposure to the drug and in the aeration conditions

Fig. 3.29. to 3.57. and Tables 3.3. to 3.16. show the results of the drug susceptibility tests with variation of different conditions, including length of exposure to the drug (that varies between 7, 14 and 21 days) in aerobiosis. Data are also presented comparing the activity of the agents in cultures grown in aerobic and anaerobic conditions. The anaerobic assay had 7 days duration with severe hypoxia where Mtb was in contact with the drug followed by 7 days under normal aerobic conditions, to enable the detection of growth.

3.3.5.1. Streptomycin

Streptomycin, a first line anti-TB agent was effective against Mtb H37Rv in aerobiosis, with very low IC_{50} after 7 and 14 days exposure. The IC_{50} increased in the assay over 21 days (Fig. 3.29. and Table 3.3.) The inhibitory effect in the anaerobic assay was also low, with an IC_{50} of 0.10 μM (Fig. 3.30. and Table 3.3.).

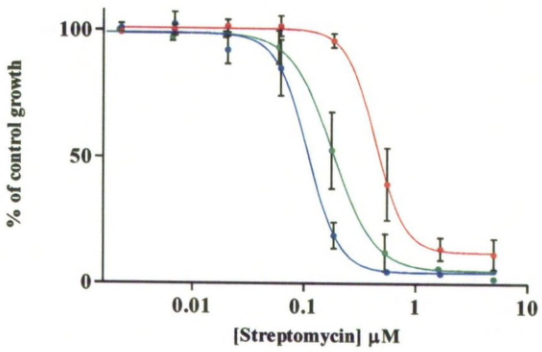

Fig. 3.29.: Curves of Mtb susceptibility to different concentrations of streptomycin. The exposure period of Mtb to the drug was 7 days (_, green line), 14 days (_, blue line) and 21 days (_, red line). The percentages of growth were estimated assuming that 100% growth occurred in the absence of the inhibitor.

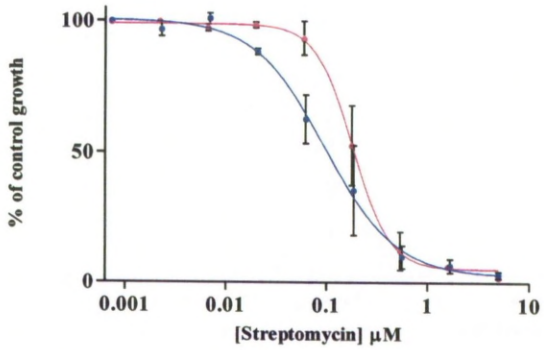

Fig. 3.30.: Curves of Mtb susceptibility to streptomycin. Cultures were grown under conditions of unlimited aeration (_, pink line) and under severe hypoxia (_, blue line).The percentages of growth were estimated assuming that 100% growth occurred in the absence of the inhibitor.

Table 3.3.: IC_{50} and IC_{90} values of streptomycin against Mtb strain H37Rv. The results are presented with the respective standard errors. n indicates the number of replicates.

Compound tested	Growth conditions	Exposure time	IC_{50} (µM)	SE (µM)	IC_{90} (µM)	SE (µM)	n
Streptomycin	Aerobiosis	7 days	**0.19**	0.020	**0.59**	0.146	4
	Aerobiosis	14 days	**0.11**	0.009	**0.25**	0.034	4
	Aerobiosis	21 days	**0.50**	0.051	**1.30**	0.314	3
	Hypoxia	14 days	**0.10**	0.017	**0.66**	0.232	4

3.3.5.2. Ethambutol

Ethambutol, another first line anti-TB drug was almost equally effective against Mtb H37Rv independent of the length of exposure to the drug (Fig. 3.31. and Table 3.4.) or the aeration conditions of the assay (Fig. 3.32. and Table 3.4.).

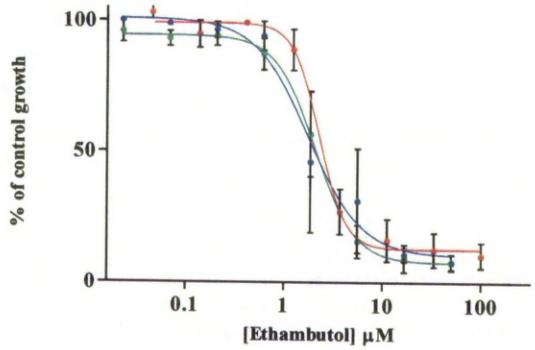

Fig. 3.31.: Curves of Mtb susceptibility to different concentrations of ethambutol. The exposure period of Mtb to the drug was 7 days (_, green line), 14 days (_, blue line) and 21 days (_, red line). The percentages of growth were estimated assuming that 100% growth occurred in the absence of the inhibitor.

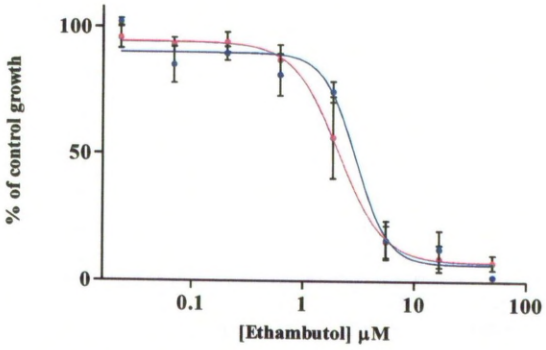

Fig. 3.32.: Curves of Mtb susceptibility to ethambutol. Cultures were grown under conditions of unlimited aeration (_, pink line) and under severe hypoxia (_, blue line).The percentages of growth were estimated assuming that 100% growth occurred in the absence of the inhibitor.

Table 3.4.: IC50 and IC90 values of ethambutol against Mtb strain H37Rv. The results are presented with the respective standard errors. n indicates the number of replicates.

Compound tested	Growth conditions	Exposure time	IC_{50} (µM)	SE (µM)	IC_{90} (µM)	SE (µM)	n
Ethambutol	Aerobiosis	7 days	**2.16**	0.330	**10.33**	3.564	6
	Aerobiosis	14 days	**2.37**	0.611	**14.78**	8.338	4
	Aerobiosis	21 days	**2.64**	0.317	**7.05**	1.663	4
	Hypoxia	14 days	**2.71**	0.380	**13.46**	4.107	6

3.3.5.3. Rifampicin

Rifampicin, the most effective anti-TB drug tested, had a stronger anti-TB effect in conditions of aerobiosis with 7 days exposure to the drug, decreasing its effect after 14 days duration of the assay and even more at 21 days (Fig. 3.33. and Table 3.5.). Rifampicin was less effective in the anaerobic assay (Fig. 3.34. and Table 3.5.).

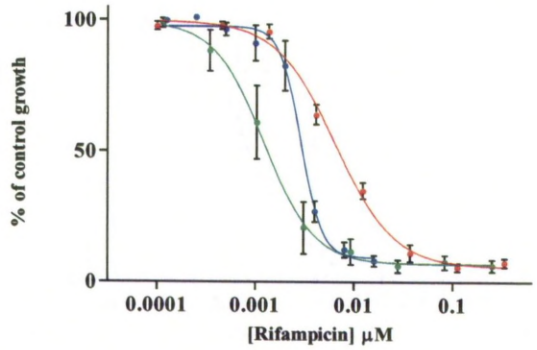

Fig. 3.33.: Curves of Mtb susceptibility to different concentrations of rifampicin. The exposure period of Mtb to the drug was 7 days (_, green line), 14 days (_, blue line) and 21 days (_, red line). The percentages of growth were estimated assuming that 100% growth occurred in the absence of the inhibitor.

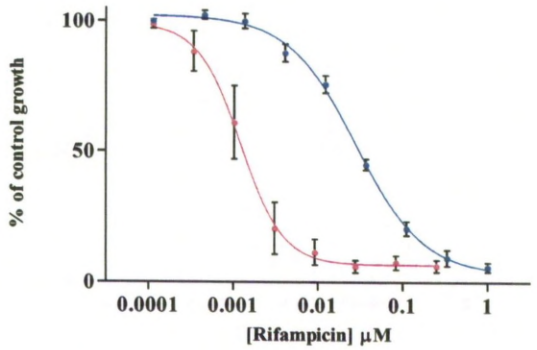

Fig. 3.34.: Curves of Mtb susceptibility to rifampicin. Cultures were grown under conditions of unlimited aeration (_, pink line) and under severe hypoxia (_, blue line).The percentages of growth were estimated assuming that 100% growth occurred in the absence of the inhibitor.

Table 3.5.: IC_{50} and IC_{90} values of rifampicin against Mtb strain H37Rv. The results are presented with the respective standard errors. n indicates the number of replicates.

Compound tested	Growth conditions	Exposure time	IC_{50} (μM)	SE (μM)	IC_{90} (μM)	SE (μM)	n
Rifampicin	Aerobiosis	7 days	1.38×10^{-3}	2.069×10^{-4}	6.70×10^{-3}	2.192×10^{-3}	7
	Aerobiosis	14 days	3.07×10^{-3}	1.771×10^{-4}	6.63×10^{-3}	8.000×10^{-4}	7
	Aerobiosis	21 days	7.40×10^{-3}	4.833×10^{-4}	4.17×10^{-2}	5.923×10^{-3}	6
	Hypoxia	14 days	3.25×10^{-2}	2.046×10^{-3}	2.55×10^{-1}	3.510×10^{-2}	7

3.3.5.4. Isoniazid

Isoniazid, another first line anti-TB drug, displayed a pattern of inhibition similar to rifampicin. This drug had a stronger anti-TB effect in aerobiosis with 7 days exposure to the drug, decreasing its effect after 14 days duration of the assay and even more at 21 days (Fig. 3.35. and Table 3.6.). Isoniazid was less effective in the anaerobic assay (Fig. 3.36. and Table 3.6.).

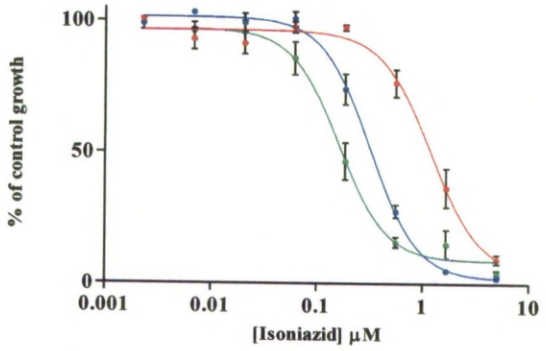

Fig. 3.35.: Curves of Mtb susceptibility to different concentrations of isoniazid. The exposure period of Mtb to the drug was 7 days (_, green line), 14 days (_, blue line) and 21 days (_, red line). The percentages of growth were estimated assuming that 100% growth occurred in the absence of the inhibitor.

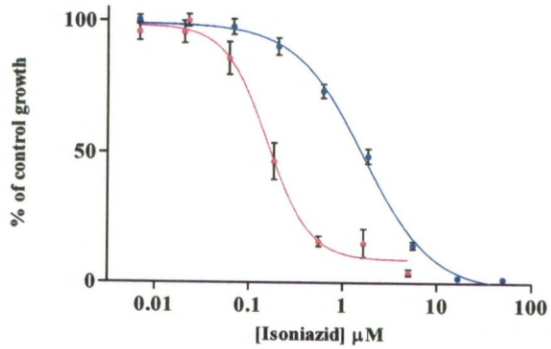

Fig. 3.36.: Curves of Mtb susceptibility to isoniazid. Cultures were grown under conditions of unlimited aeration (_ , pink line) and under severe hypoxia (_ , blue line).The percentages of growth were estimated assuming that 100% growth occurred in the absence of the inhibitor.

Table 3.6.: IC_{50} and IC_{90} values of isoniazid against Mtb strain H37Rv. The results are presented with the respective standard errors. n indicates the number of replicates.

Compound tested	Growth conditions	Exposure time	IC_{50} (µM)	SE (µM)	IC_{90} (µM)	SE (µM)	n
Isoniazid	Aerobiosis	7 days	**0.19**	0.019	**0.97**	0.213	7
	Aerobiosis	14 days	**0.34**	0.018	**1.061**	0.117	5
	Aerobiosis	21 days	**1.19**	0.098	**4.74**	0.852	5
	Hypoxia	14 days	**1.55**	0.080	**9.23**	1.042	5

3.3.5.5. Pyrazinamide

Pyrazinamide, the last first line anti-TB drug tested did not have an effect in either assay (Fig. 3.37. and Fig. 3.38.). The experiments were performed as a control but since no optimisation for the peculiarities of the action of this drug were done, no effect was expected.

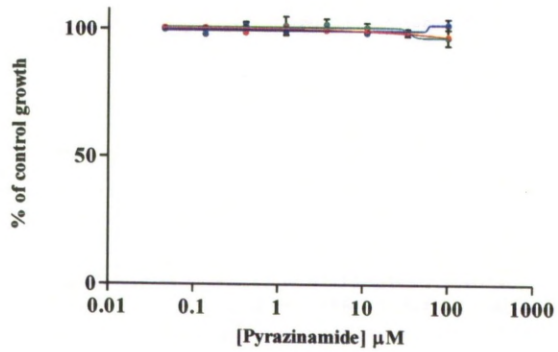

Fig. 3.37.: Curves of Mtb susceptibility to different concentrations of pyrazinamide. The exposure period of Mtb to the drug was 7 days (_, green line), 14 days (_, blue line) and 21 days (_, red line). The percentages of growth were estimated assuming that 100% growth occurred in the absence of the inhibitor.

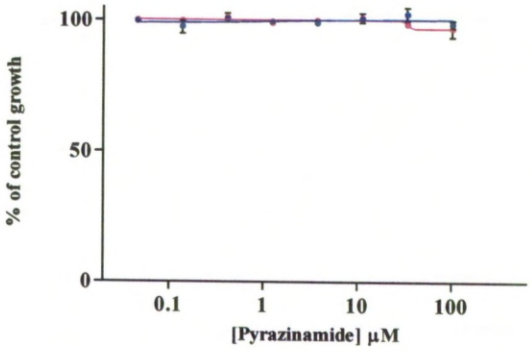

Fig. 3.38.: Curves of Mtb susceptibility to pyrazinamide. Cultures were grown under conditions of unlimited aeration (_, pink line) and under severe hypoxia (_, blue line).The percentages of growth were estimated assuming that 100% growth occurred in the absence of the inhibitor.

3.3.5.6. Metronidazole

Metronidazole was effective against anaerobic organisms, serving as a control for the growth conditions of the expeiments. It did not show significant inhibitory effect against aerobic Mtb (Fig. 3.39. and Table 3.7.).

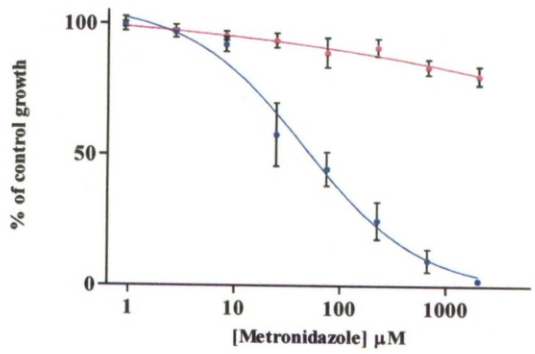

Fig. 3.39.: Curves of Mtb susceptibility to metronidazole. Cultures were grown under conditions of unlimited aeration (_, pink line) and under severe hypoxia (_, blue line).The percentages of growth were estimated assuming that 100% growth occurred in the absence of the inhibitor.

Table 3.7.: IC_{50} and IC_{90} values of metronidazole against Mtb strain H37Rv. The results are presented with the respective standard errors. n indicates the number of replicates.

Compound tested	Growth conditions	Exposure time	IC_{50} (µM)	SE (µM)	IC_{90} (µM)	SE (µM)	n
Metronidazole	Aerobiosis	7 days	**>2000**	-	**>2000**	-	5
	Hypoxia	14 days	**55.13**	8.856	**627.10**	225.900	4

3.3.5.7. Phenothiazine compounds

In the following graphs (Fig. 3.40. to Fig. 3.57.) the inhibitory effects of nine phenothiazine compounds are presented. All the phenothiazines tested had a higher inhibitory effect against anaerobic organisms, comparing with aerobic Mtb.

3.3.5.7.1. Thioridazine

Thioridazine was one of the more effective phenothiazines in aerobiosis and the most effective in anaerobiosis. This drug had an IC_{50} of 13.43 µM against Mtb in aerobiosis with 7 days exposure to the drug, decreasing its

effect after 14 days duration of the assay and even more at 21 days (Fig. 3.40. and Table 3.8.). Thioridazine had an IC_{50} of 3.64 μM against Mtb in anaerobiosis (Fig. 3.41. and Table 3.8.).

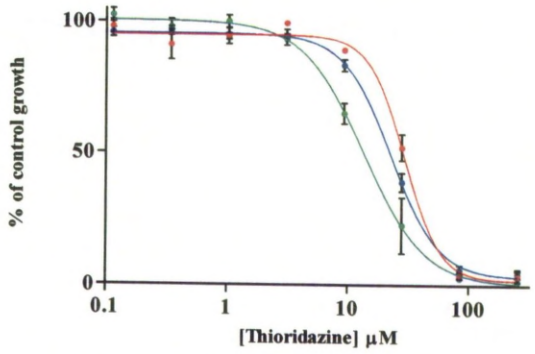

Fig. 3.40.: Curves of Mtb susceptibility to different concentrations of thioridazine. The exposure period of Mtb to the drug was 7 days (_, green line), 14 days (_, blue line) and 21 days (_, red line). The percentages of growth were estimated assuming that 100% growth occurred in the absence of the inhibitor.

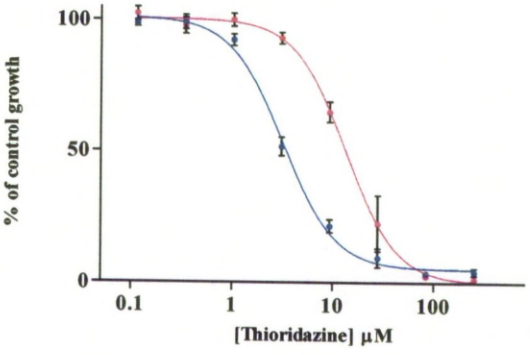

Fig. 3.41.: Curves of Mtb susceptibility to thioridazine. Cultures were grown under conditions of unlimited aeration (_, pink line) and under severe hypoxia (_, blue line).The percentages of growth were estimated assuming that 100% growth occurred in the absence of the inhibitor.

Table 3.8.: IC_{50} and IC_{90} values of thioridazine against Mtb strain H37Rv. The results are presented with the respective standard errors. n indicates the number of replicates.

Compound tested	Growth conditions	Exposure time	IC_{50} (μM)	SE (μM)	IC_{90} (μM)	SE (μM)	n
Thioridazine	Aerobiosis	7 days	**13.43**	1.078	**47.37**	8.245	5
	Aerobiosis	14 days	**21.67**	1.063	**72.84**	7.698	4
	Aerobiosis	21 days	**27.98**	1.662	**73.07**	11.15	4
	Hypoxia	14 days	**3.64**	0.231	**16.52**	2.420	4

3.3.5.7.2. Trifluoperazine

Trifluoperazine was the most effective phenothiazine in aerobiosis and one of the more effectives in anaerobiosis. This drug had a stronger inhibitory effect in the 7 days aerobic assay, followed by the 14 and 21 days assays (Fig. 3.42. and Table 3.9.). Trifluoperazine was much more effective under anaerobiosis (Fig. 3.43. and Table 3.9.).

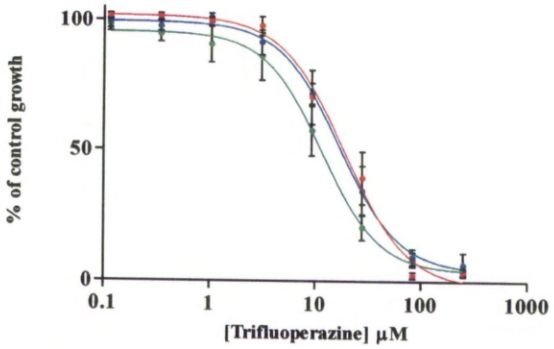

Fig. 3.42.: Curves of Mtb susceptibility to different concentrations of trifluoperazine. The exposure period of Mtb to the drug was 7 days (_ , green line), 14 days (_ , blue line) and 21 days (_ , red line). The percentages of growth were estimated assuming that 100% growth occurred in the absence of the inhibitor.

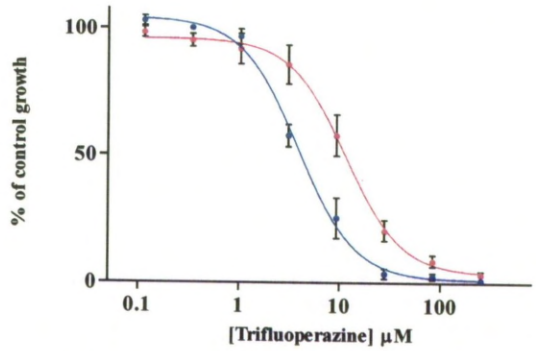

Fig. 3.43.: Curves of Mtb susceptibility to trifluoperazine. Cultures were grown under conditions of unlimited aeration (_, pink line) and under severe hypoxia (_, blue line).The percentages of growth were estimated assuming that 100% growth occurred in the absence of the inhibitor.

Table 3.9.: IC_{50} and IC_{90} values of trifluoperazine against Mtb strain H37Rv. The results are presented with the respective standard errors. n indicates the number of replicates.

Compound tested	Growth conditions	Exposure time	IC_{50} (µM)	SE (µM)	IC_{90} (µM)	SE (µM)	n
Trifluoperazine	Aerobiosis	7 days	**11.23**	1.208	**61.04**	14.430	7
	Aerobiosis	14 days	**17.77**	1.697	**85.28**	17.690	6
	Aerobiosis	21 days	**18.47**	1.993	**74.85**	17.370	6
	Hypoxia	14 days	**4.22**	0.306	**16.34**	2.592	6

3.3.5.7.3. Promazine

Promazine was one of the less effective phenothiazine tested. In aerobiosis it seemed to be more effective when the exposure time to the drug was 14 days, followed by the 7 and 21 days assays (Fig. 3.44. and Table 3.10.). Promazine was much more effective under anaerobiosis with an IC_{50} of 12.19 µM (Fig. 3.45. and Table 3.10.).

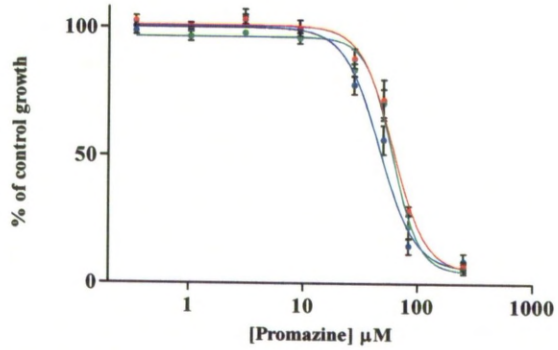

Fig. 3.44.: Curves of Mtb susceptibility to different concentrations of promazine. The exposure period of Mtb to the drug was 7 days (_, green line), 14 days (_, blue line) and 21 days (_, red line). The percentages of growth were estimated assuming that 100% growth occurred in the absence of the inhibitor.

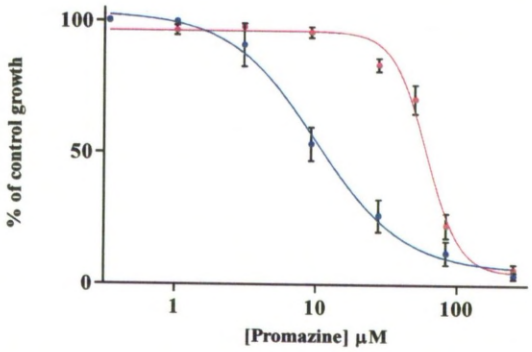

Fig. 3.45.: Curves of Mtb susceptibility to promazine. Cultures were grown under conditions of unlimited aeration (_, pink line) and under severe hypoxia (_, blue line).The percentages of growth were estimated assuming that 100% growth occurred in the absence of the inhibitor.

Table 3.10.: IC_{50} and IC_{90} values of promazine against Mtb strain H37Rv. The results are presented with the respective standard errors. n indicates the number of replicates.

Compound tested	Growth conditions	Exposure time	IC_{50} (µM)	SE (µM)	IC_{90} (µM)	SE (µM)	n
Promazine	Aerobiosis	7 days	**59.45**	2.331	**126.90**	11.820	4
	Aerobiosis	14 days	**48.99**	2.237	**115.70**	11.840	4
	Aerobiosis	21 days	**63.68**	2.375	**136.70**	12.420	4
	Hypoxia	14 days	**12.19**	1.315	**65.28**	15.390	4

3.3.5.7.4. Promethazine

Promethazine was one of the less effective phenothiazine tested. In aerobiosis it seemed to be more effective when the exposure time to the drug was 7 days, followed by the 14 days assay but its effect strongly decreases in the assay after 21 days (Fig. 3.46. and Table 3.11.). Promethazine was more effective under anaerobiosis with an IC_{50} of 21.02 μM (Fig. 3.47. and Table 3.11.).

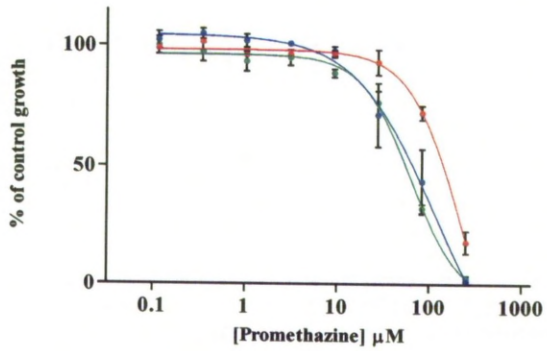

Fig. 3.46.: Curves of Mtb susceptibility to different concentrations of promethazine. The exposure period of Mtb to the drug was 7 days (_, green line), 14 days (_, blue line) and 21 days (_, red line). The percentages of growth were estimated assuming that 100% growth occurred in the absence of the inhibitor.

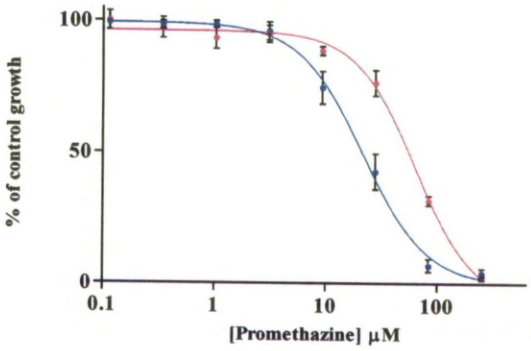

Fig. 3.47.: Curves of Mtb susceptibility to promethazine. Cultures were grown under conditions of unlimited aeration (_, pink line) and under severe hypoxia (_, blue line).The percentages of growth were estimated assuming that 100% growth occurred in the absence of the inhibitor.

Table 3.11.: IC_{50} and IC_{90} values of promethazine against Mtb strain H37Rv. The results are presented with the respective standard errors. n indicates the number of replicates.

Compound tested	Growth conditions	Exposure time	IC_{50} (µM)	SE (µM)	IC_{90} (µM)	SE (µM)	n
Promethazine	Aerobiosis	7 days	**52.16**	3.841	**194.90**	30.840	4
	Aerobiosis	14 days	**59.68**	8.282	**238.00**	72.590	4
	Aerobiosis	21 days	**126.80**	6.552	**351.10**	39.100	4
	Hypoxia	14 days	**21.02**	1.533	**91.16**	14.460	4

3.3.5.7.5. Phenothiazine

Phenothiazine was the least effective drug of the phenothiazine group tested. No significant effect that allowed the calculation of IC50 was obtained with the variation in the length of the experiment done under aerobiosis (Fig. 3.48. and Table 3.12.). Despite an apparent stronger effect against anaerobic Mtb bacilli, no IC_{50} could be calculated (Fig. 3.49. and Table 3.12.).

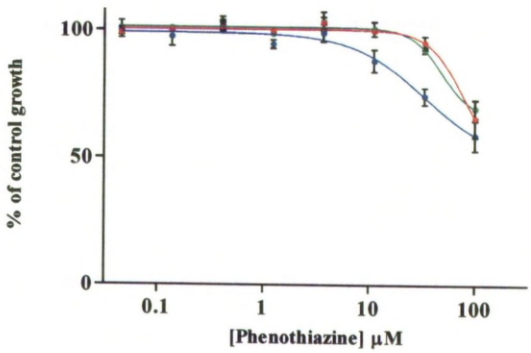

Fig. 3.48.: Curves of Mtb susceptibility to different concentrations of phenothiazine. The exposure period of Mtb to the drug was 7 days (_, green line), 14 days (_, blue line) and 21 days (_, red line). The percentages of growth were estimated assuming that 100% growth occurred in the absence of the inhibitor.

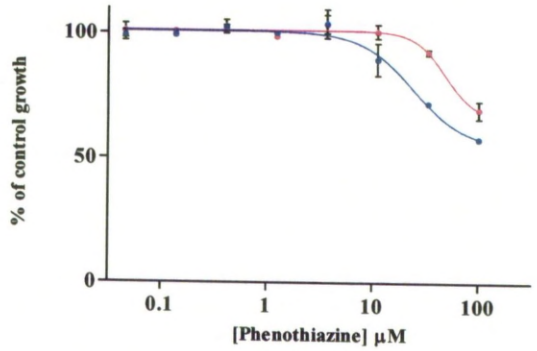

Fig. 3.49.: Curves of Mtb susceptibility to phenothiazine. Cultures were grown under conditions of unlimited aeration (_, pink line) and under severe hypoxia (_, blue line).The percentages of growth were estimated assuming that 100% growth occurred in the absence of the inhibitor.

Table 3.12.: IC_{50} and IC_{90} values of phenothiazine against Mtb strain H37Rv. The results are presented with the respective standard errors. n indicates the number of replicates.

Compound tested	Growth conditions	Exposure time	IC_{50} (µM)	SE (µM)	IC_{90} (µM)	SE (µM)	n
Phenothiazine	Aerobiosis	7 days	>100	-	>100	-	4
	Aerobiosis	14 days	>100	-	>100	-	3
	Aerobiosis	21 days	>100	-	>100	-	3
	Hypoxia	14 days	>100	-	>100	-	4

3.3.5.7.6. Perphenazine

Perphenazine in aerobiosis was more effective when the exposure time to the drug was 14 days, followed by the 7 and 21 days assays (Fig. 3.50. and Table 3.13.). Perphenazine was much more effective under anaerobiosis with an IC_{50} of 7.90 µM (Fig. 3.51. and Table 3.13.).

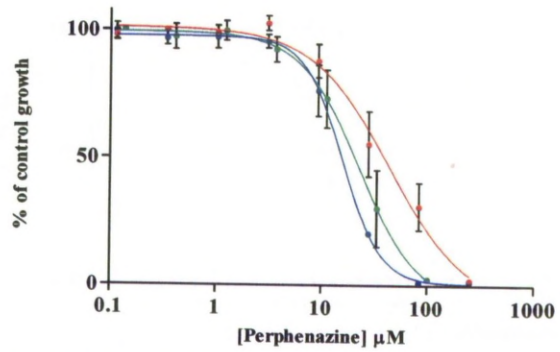

Fig. 3.50.: Curves of Mtb susceptibility to different concentrations of perphenazine. The exposure period of Mtb to the drug was 7 days (_, green line), 14 days (_, blue line) and 21 days (_, red line). The percentages of growth were estimated assuming that 100% growth occurred in the absence of the inhibitor.

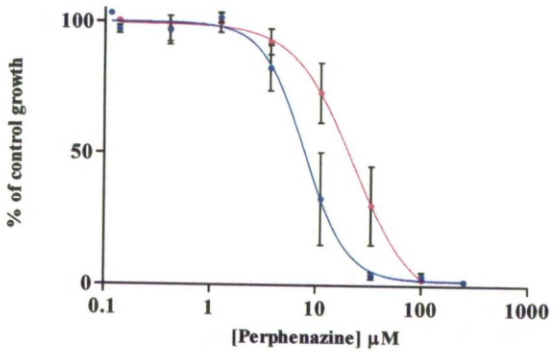

Fig. 3.51.: Curves of Mtb susceptibility to perphenazine. Cultures were grown under conditions of unlimited aeration (_, pink line) and under severe hypoxia (_, blue line).The percentages of growth were estimated assuming that 100% growth occurred in the absence of the inhibitor.

Table 3.13.: IC_{50} and IC_{90} values of perphenazine against Mtb strain H37Rv. The results are presented with the respective standard errors. n indicates the number of replicates.

Compound tested	Growth conditions	Exposure time	IC_{50} (µM)	SE (µM)	IC_{90} (µM)	SE (µM)	n
Perphenazine	Aerobiosis	7 days	**19.85**	2.453	**71.22**	18.540	4
	Aerobiosis	14 days	**15.35**	0.955	**40.49**	4.957	4
	Aerobiosis	21 days	**37.66**	4.588	**189.10**	51.060	4
	Hypoxia	14 days	**7.90**	0.909	**22.20**	5.135	4

3.3.5.7.7. Fluphenazine

Fluphenazine in aerobiosis was more effective when the exposure time to the drug was 14 days, followed by the 7 and 21 days assays (Fig. 3.52. and Table 3.14.). Fluphenazine was much more effective under anaerobiosis with one of the lower IC_{50} of the phenothiazines tested (Fig. 3.53. and Table 3.14.).

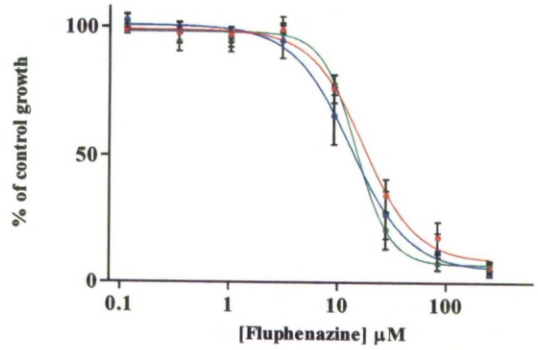

Fig. 3.52.: Curves of Mtb susceptibility to different concentrations of fluphenazine. The exposure period of Mtb to the drug was 7 days (_, green line), 14 days (_, blue line) and 21 days (_, red line). The percentages of growth were estimated assuming that 100% growth occurred in the absence of the inhibitor.

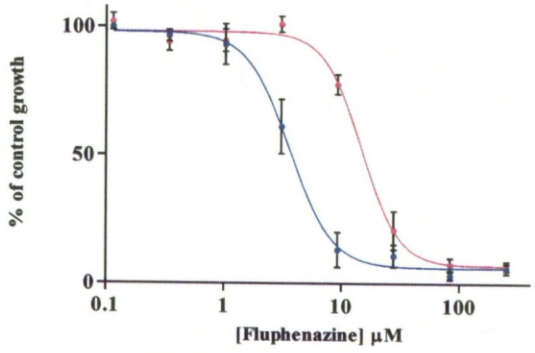

Fig. 3.53.: Curves of Mtb susceptibility to fluphenazine. Cultures were grown under conditions of unlimited aeration (_, pink line) and under severe hypoxia (_, blue line).The percentages of growth were estimated assuming that 100% growth occurred in the absence of the inhibitor.

Table 3.14.: IC_{50} and IC_{90} values of fluphenazine against Mtb strain H37Rv. The results are presented with the respective standard errors. n indicates the number of replicates.

Compound tested	Growth conditions	Exposure time	IC_{50} (μM)	SE (μM)	IC_{90} (μM)	SE (μM)	n
Fluphenazine	Aerobiosis	7 days	**15.99**	1.214	**42.04**	6.168	5
	Aerobiosis	14 days	**14.55**	1.692	**59.60**	14.98	5
	Aerobiosis	21 days	**20.46**	1.900	**98.79**	20000	4
	Hypoxia	14 days	**3.92**	0.414	**13.20**	3.303	4

3.3.5.7.8. Flupenthixol

Flupenthixol in aerobiosis was more effective when the exposure time to the drug was 14 days, with an IC_{50} of 10.61 μM followed by the 7 and 21 days assays (Fig. 3.54. and Table 3.15.). Flupenthixol was more effective under anaerobiosis with an IC_{50} of 10.45 μM (Fig. 3.55. and Table 3.15.), but this potency increase is not as significant as other phenothiazine compounds.

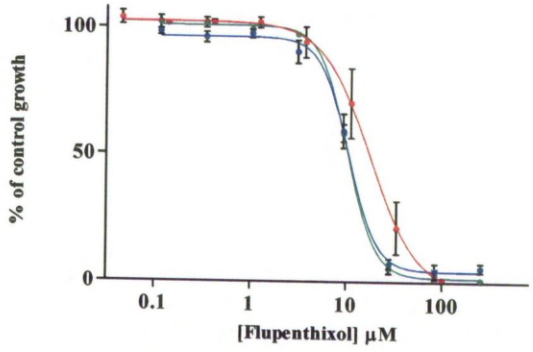

Fig. 3.54.: Curves of Mtb susceptibility to different concentrations of flupenthixol. The exposure period of Mtb to the drug was 7 days (_, green line), 14 days (_, blue line) and 21 days (_, red line). The percentages of growth were estimated assuming that 100% growth occurred in the absence of the inhibitor.

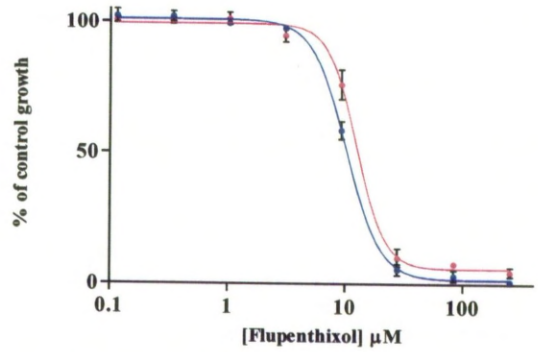

Fig. 3.55.: Curves of Mtb susceptibility to flupenthixol. Cultures were grown under conditions of unlimited aeration (_, pink line) and under severe hypoxia (_, blue line).The percentages of growth were estimated assuming that 100% growth occurred in the absence of the inhibitor.

Table 3.15.: IC_{50} and IC_{90} values of flupenthixol against Mtb strain H37Rv. The results are presented with the respective standard errors. n indicates the number of replicates.

Compound tested	Growth conditions	Exposure time	IC_{50} (µM)	SE (µM)	IC_{90} (µM)	SE (µM)	n
Flupenthixol	Aerobiosis	7 days	**13.64**	0.711	**29.35**	3.173	4
	Aerobiosis	14 days	**10.61**	0.620	**28.46**	4.141	4
	Aerobiosis	21 days	**17.19**	1.839	**51.89**	11.690	4
	Hypoxia	14 days	**10.45**	0.314	**22.41**	1.932	4

3.3.5.7.9. Chlorpromazine

Chlorpromazine in aerobiosis was more effective when the exposure time to the drug was 14 days, followed by the 7 and 21 days assays (Fig. 3.56. and Table 3.16.) however the IC_{50} values are all similar, especially considering the standard errors associated with the IC_{50} curve inference. Chlorpromazine was more effective under anaerobiosis similar to the other phenothiazines (Fig. 3.57. and Table 3.16.).

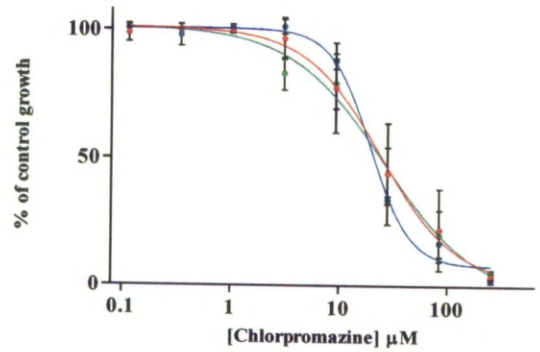

Fig. 3.56.: Curves of Mtb susceptibility to different concentrations of chlorpromazine. The exposure period of Mtb to the drug was 7 days (_, green line), 14 days (_, blue line) and 21 days (_, red line). The percentages of growth were estimated assuming that 100% growth occurred in the absence of the inhibitor.

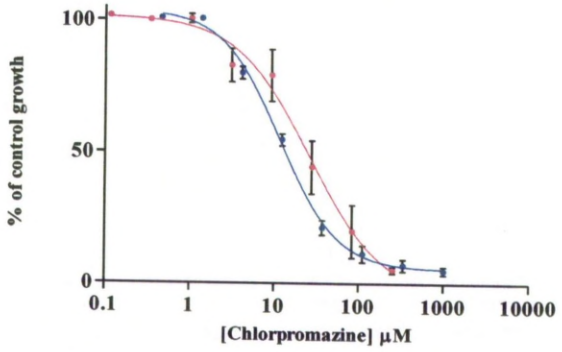

Fig. 3.57.: Curves of Mtb susceptibility to chlorpromazine. Cultures were grown under conditions of unlimited aeration (_, pink line) and under severe hypoxia (_, blue line).The percentages of growth were estimated assuming that 100% growth occurred in the absence of the inhibitor.

Table 3.16.: IC_{50} and IC_{90} values of chlorpromazine against Mtb strain H37Rv. The results are presented with the respective standard errors. n indicates the number of replicates.

Compound tested	Growth conditions	Exposure time	IC_{50} (µM)	SE (µM)	IC_{90} (µM)	SE (µM)	n
Chlorpromazine	Aerobiosis	7 days	**23.83**	3.554	**166.70**	55.200	4
	Aerobiosis	14 days	**22.11**	1.509	**69.59**	10.240	4
	Aerobiosis	21 days	**25.39**	5.722	**146.50**	72.870	4
	Hypoxia	14 days	**14.37**	0.975	**88.03**	13.030	4

3.3.6. Microscopy observation of Mtb grown under different aeration conditions

Microscopic images were obtained from Mtb cultures in order to identify any possible morphological differences between the cultures grown under no oxygen limitation (Fig. 3.58.A and Fig. 3.59.E) and those grown under severe hypoxia (Fig. 3.58.B and Fig. 3.59.A-D), using the Wayne model.

The anaerobic cultures (Fig. 3.58.B and Fig. 3.59.A-D) present a great amount of debris (blue arrow-heads) that results from cell death. The viable anaerobic bacteria appeared longer and with a thicker cell wall (pink arrow-heads). The aerobic Mtb (Fig. 3.58.A and Fig. 3.59.E, red arrow-heads) appeared as slender bacilli.

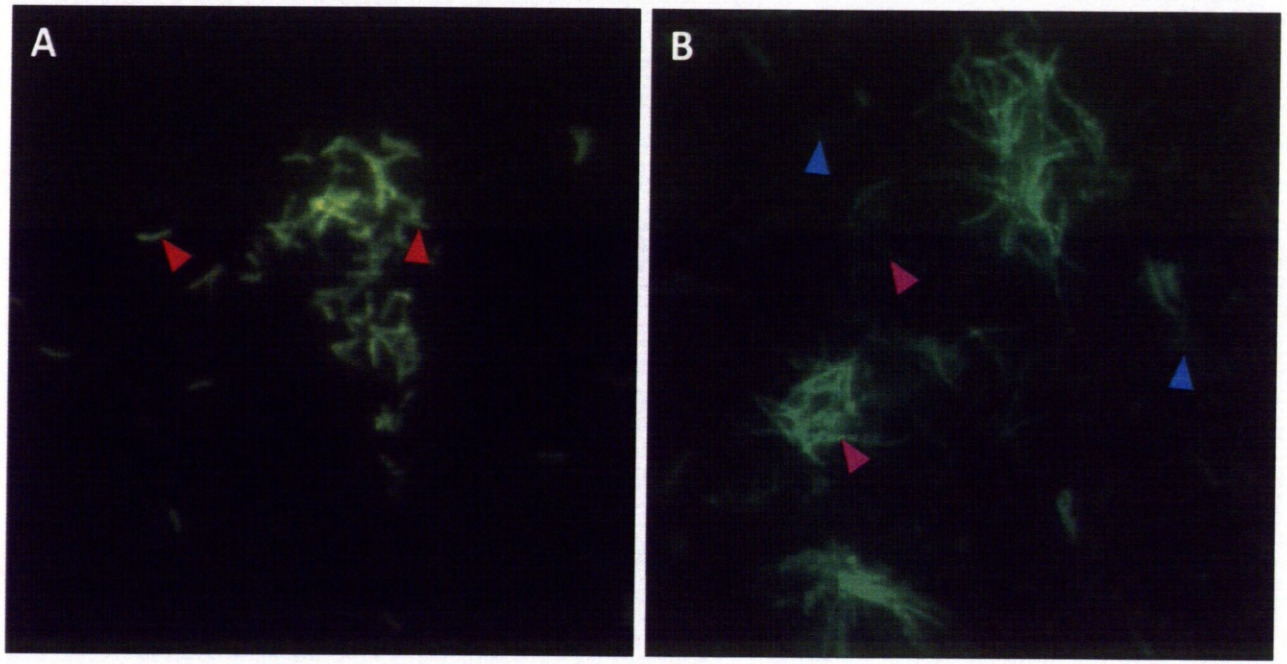

Fig. 3.58.: Fluorescence microscopy images of Mtb bacilli, strain H37Rv, stained using the Auramine Phenol method. The bacteria were grown *in vitro*, under conditions of unlimited oxygen supply (A) and grown under hypoxia conditions (B). (▶, red arrow-heads) show representative aerobic bacilli; (▶, pink arrow-heads) show representative anaerobic bacilli and (▶, blue arrow-heads) show cell debris. The images were viewed using 100x amplification.

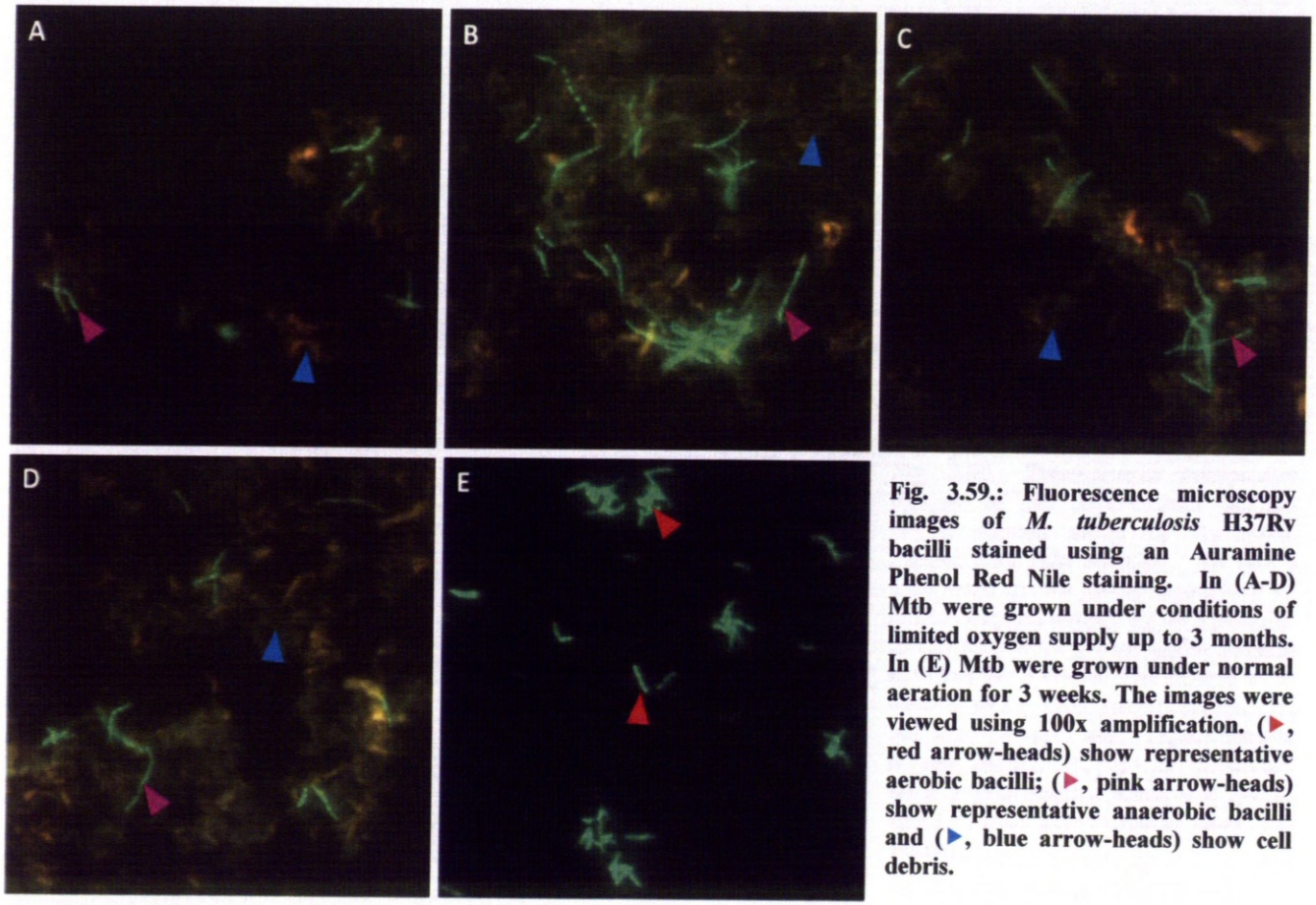

Fig. 3.59.: Fluorescence microscopy images of *M. tuberculosis* H37Rv bacilli stained using an Auramine Phenol Red Nile staining. In (A-D) Mtb were grown under conditions of limited oxygen supply up to 3 months. In (E) Mtb were grown under normal aeration for 3 weeks. The images were viewed using 100x amplification. (▶, red arrow-heads) show representative aerobic bacilli; (▶, pink arrow-heads) show representative anaerobic bacilli and (▶, blue arrow-heads) show cell debris.

3.4. Discussion

In this chapter the Wayne model of growth was optimised and an assay to test drug susceptibility of Mtb either in aerobic or anaerobic conditions was developed. Also, two of the more effective phenothiazines (thioridazine and trifluoperazine) were tested in combination with four of the current anti-TB compounds (ethambutol, isoniazid, rifampicin and streptomycin).

The purpose of the testing of streptomycin, ethambutol, isoniazid, pyrazinamide and rifampicin (DOTS drugs) was to use them as quality control of the method, a number of studies reported Mtb H37Rv drug susceptibility for these compounds, using different assays.

Table 3.17. provides an overview of some relevant literature data regarding the DOTS drugs. One striking feature is the heterogeneity of the indices used, which makes the comparison between studies extremely difficult or even impossible. Given this, any comparison between the results reported here and the literature will only be possible if an IC_{50} value was reported for the given compound. The only directly comparable value is isoniazid whose published IC_{50} value of less than 0.3 μM (Table 3.17.) is consistent with the 0.19 μM value reported here (Table 3.2.).

In this study a static model of drug testing was used. Mtb bacilli were submitted to a drug and the drug effect was measured at defined time points. One should point out that this way, bacterial growth is limited not only by the drug but also by nutrient limitation, space, aeration and accumulation of toxic metabolites in the culture (Vaddady et al. 2010).

Table 3.17.: Summary table of the indices obtained from different drug susceptibility tests in various studies from the literature.

Drug tested	On-growing broth/plate	Non-growing		References
		Wayne model/ Oxygen deprivation	Nutrient starvation	
Streptomycin	0.35 µg/ml (MIC)[b] < 0.625 µg/ml (MBC_{99})[c] 0.125 µg/ ml (MBC_{90})[e]	5 µg/ml (WCC_{90})[e] 1.2 µg/ml (MBC_{90})[f]	> 160 µg/ ml (MBC_{99})[c] > 100 µg/ml (LCC_{90})[e]	[a] (Hartkoorn et al. 2007) [b] (Collins and Franzblau 1997) [c] (Xie et al. 2005) [d] (Koul et al. 2008) [e] (Gengenbacher et al. 2010) [f] (Cho et al. 2007) [g](Delaine et al. 2010) [h](Torres et al. 2011)
Ethambutol	0.263 µg/ml (EC_{50})[a] 1.17 µg/ml (MIC)[b] 0.625 µg/ ml (MBC_{99})[c] 1.8 µg/ml (MBC_{90})[f]	> 128 µg/ml (MBC_{90})[f]	> 160 µg/ml (MBC_{99})[c]	
Rifampicin	0.00127 µg/ml (EC_{50})[a] 0.16 µg/ml (MIC)[b] < 0.625 µg/ ml (MBC_{99})[c] 0.03 µg/ ml (MBC_{90})[d] 0.01 µg/ ml (MBC_{90})[e]	0.5 µg/ml (WCC_{90})[d] 0.5 µg/ml (WCC_{90})[e] 1.8 µg/ml (MBC_{90})[f]	10 µg/ml (MBC_{99})[c] 25 µg/ml (LCC_{90})[e]	
Isoniazid	0.0572 µg/ml (EC_{50})[a] 0.031 µg/ml (MIC)[b] 0.25 µg/ml (MBC_{90})[d] 0.4 µg/ml (MBC_{90})[e] 0.21 µM (IC_{90})[g] < 0.3 µM (IC_{50})[h]	> 64 µg/ml (WCC_{90})[d] > 100 µg/ ml (WCC_{90})[e] > 128 µg/ml (MBC_{90})[f]	80 µg/ml (MBC_{99})[c] > 100 µg/ml (LCC_{90})[e]	

EC_{50}[a]: the concentration of the drug that will reduce Mtb viability by 50%; MIC[b]: the lowest concentration of the drug that will inhibit 99% of Mtb growth; MBC_{99}[c]: the lowest concentration of the drug that will kill 99% of the starting bacterial population; MBC_{90}[d,e,f]: Minimal concentration of drug that will inhibit 90% of the actively replicating bacilli; WCC_{90}[d,e]: Wayne cidal concentration, minimum concentration of drug that will inhibit 90% of the dormant bacilli; LCC_{90}[e]: Loebel cidal concentration, minimum concentration that will inhibit 90% of the growth of nutrient starved bacilli; IC_{90}[g]: 90% of the maximal inhibitory concentration; IC_{50}[h]: half maximal inhibitory concentration.

In aerobic conditions, DOTS drugs were effective. Rifampicin being the most effective of all the drugs tested. Pyrazinamide, a pro-drug that only works *in vivo* under acidic conditions (Zhang and Mitchison 2003), did not show any effect either in aerobiosis or in anaerobiosis. This drug was used only as control since no positive results were expected. The assay could have been modified but further optimisation would be needed since pyrazinamide acid requirements would compromise Mtb growth (See Fig. 3.5. for optimal pH for Mtb growth).

Bacilli were also exposed to the drug at different lengths of time: 7 days was the duration of the normal assay. The drug was added at day 0 and after 7, 14 and 21 days the growth was assessed (See Tables 3.3. to 3.6 and Tables 3.8 to 3.16.). Considering the DOTS compounds, the IC_{50} at day 7 and day 14 were very similar, and the IC_{50} greatly increased at day 21 except for ethambutol whose IC_{50}s remained nearly constant.

Isoniazid and streptomycin are reported to be rapid and concentration dependent bactericidal drugs (Turnidge 2003; Steenwinkel et al. 2010), so that hypothetically the drugs would act quickly on the first days of the assay, killing a great proportion of the population. It is known that in one population there are a certain number of individuals with phenotypic tolerance that will evade the action of these drugs (Balaban et al. 2004; Mitchison and Coates 2004), elevating the IC_{50}s, observable after 21 days, probably due to regrowth of sub-populations. Rifampicin according to Vaddady and colleagues is a concentration-dependent bactericidal drug (Vaddady et al. 2010) so the expected outcome is a similar pattern of IC_{50} to the one obtained for isoniazid and streptomycin, as was observed. Gangadharam and collaborators also obtained a decrease in the effect of both rifampicin and isoniazid after 6 days which they attributed to the development of drug-resistant mutants (Gangadharam et al. 1990). This could be a possible explanation for the increase of the IC_{50} values after

the initial 7 days of culture but it is more likely to be due to the existence of highly tolerant organisms during the initial 7 days.

Ethambutol's major role is to prevent emergence of resistance to other anti-mycobacterial drugs and its effect is mainly bacteriostatic, only inhibiting mycobacterial growth (Rastogi et al. 1996; Steenwinkel et al. 2010). However at high concentrations, ethambutol has also been pointed out as being bactericidal (Gangadharam et al. 1990; Bakker-Woudenberg et al. 2005). The IC_{50}s remained nearly constant along the 21 days, however with a small increase in the 21 days (Table 3.4.). One of the reasons why the effect of ethambutol seems constant throughout the 21 duration of the assay is the fact that ethambutol has a bacteriostatic action which led to the inhibition of the growth at a steady rate during the time of the experiment impairing the occurrence of an initial exponential phase of growth (Fig. 3.31.). Also, ethambutol has been pointed out as a time-dependent bactericidal drug whose effects increased with time of exposure (Bakker-Woudenberg et al. 2005).

Regarding the results of the DOTS drugs tested under severe hypoxia, rifampicin and isoniazid showed higher IC_{50} ($3.25\times10^{-2}\mu M$ and $1.55\mu M$ respectively) than those obtained under aerobic conditions ($1.38\times10^{-3}\mu M$ and $0.19\mu M$ respectively). Streptomycin and ethambutol, drugs that typically target growing organisms and that should present much higher concentrations needed to inhibit mycobacterial growth showed unexpected results. Streptomycin decreased its IC_{50} by almost half ($0.19\mu M$ in aerobiosis and $0.10\mu M$ in hypoxia) and ethambutol IC_{50} was similar to the one obtained in aerobiosis only slightly higher ($2.16\mu M$ in aerobiosis and $2.71\mu M$ in hypoxia).

The result obtained for ethambutol (Fig. 3.32.) is explained by the assay design, where after the period of exposure to the drug and due to the need for the recognition of growth, Mtb is transferred to aerobiosis and after 7

days the growth in the wells is assessed. The bacteriostatic effect of this drug will mainly happen in the aerobic growth, showing a value close to (but higher than) the one obtained in the aerobic assay, since the growth under anaerobiosis conditions is minimal. Ethambutol targets the biosynthesis of a polysaccharide of the mycobacterial cell wall (arabinogalactan) (Takayama and Kilburn 1989).

The result obtained for streptomycin is not theoretically expected since streptomycin is a bactericidal drug that targets protein synthesis (Zhang 2005) so a higher IC_{50} under anaerobic conditions was expected. However, streptomycin was previously reported to be either active (Li and Franzblau 1999; Cho et al. 2007) or inactive (Heifets et al. 2005) in the Wayne hypoxia model. The reasons for this are unknown.

A possible explanation may be the existence of sub-populations of bacteria still actively growing, along with the hypoxia adapted ones that showed sensitivity to metronidazole and more susceptibility to phenothiazines. Due to the possibility of existence of heterogeneous subpopulations with different metabolic rates, the IC_{50}s and even IC_{90}s may provide uncertain results specially when comparing the results between different assays.

In the studied case, the IC_{50} may correspond mainly to the inhibition of growing organisms and one could require a measure that considered a much larger percentage of inhibition in order to be certain that that measure is accounting for action in the slow- and non-growing organisms.

The phenothiazine data showed that they have different modes of action and that these drugs are much more effective under anaerobic conditions. The IC_{50} were still in a range unlikely to be able to be achieved *in vivo*, but they are a promising group of drugs that could be used as starting point for new drug development. There are several studies involving

phenothiazines but none until now performed chemical validation of this group. In this work, not only a couple of phenothiazines were proven to have an inhibitory effect against Mtb but the entire group (a wide range of phenothiazines picked carefully due to their chemical structures) was tested and important differences in terms of their particular behaviour were identified through the different drug susceptibility profiles (Fig. 3.28. and Fig. 3.40. to 3.55. and Tables 3.8. to 3.16.). Also a structure-activity study could be made of the different phenothiazines to establish the reasons for the differences in the observed inhibitory effects and thus determine the ideal scaffold compound for the synthesis of new anti-TB compounds.

The isobologram data showed additive effects for the combination of rifampicin and streptomycin with the two phenothiazines tested (Fig. 3.28.-B,-C,-D,-E). The combination of ethambutol and trifluoperazine (Fig. 3.28.-K) or thioridazine (Fig. 3.28.-L) showed a slight sub-additive effect. These results are not consistent with the studies by Amaral and colleagues that reported synergistic effects between phenothiazines and the current used anti-TB drugs (Amaral and Kristiansen 2000; Amaral et al. 2004). It is not possible to explain discrepancies between the data presented here and the work by Amaral and colleagues, however, considering the modes of actions for these compounds, the expected results would be a lack of synergism or antagonism with the respiratory chain inhibiting phenothiazines as reported here.

Trifluoperazine and thioridazine were shown to be significantly antagonistic with isoniazid (Fig. 3.28.-G,-H). This result is consistent with the mode of action of this drug and with the observation that mutations in *ndh* are seen in INH-resistant Mtb isolates (Viveiros and Amaral 2001). Isoniazid targets the enzyme InhA, a key enyme in the fatty acid biosynthesis pathway (Lei et al. 2000). However the inhibitory effect of isoniazid is only possible after the compound has formed an

adduct with NAD^+ catalysed by the catalase peroxidise KatG. This way the inhibitory effect of isoniazid will decrease with a higher ratio of intracellular $NADH/NAD^+$. Such a change in the ratio can be caused by mutation in *ndh*, where the mutations in this gene were revealed to cause isoniazid resistance in Mtb (Lee et al. 2001) and in *M. smegmatis* and *M. bovis* (Miesel et al. 1998; Vilchèze et al. 2005). NADH might compete with the isoniazid-NAD^+ adduct at the active site of InhA or, since NADH is a peroxidase substrate, might compete with the adduct formation (Miesel et al. 1998; Lee et al. 2001; Rawat et al. 2003; Argyrou et al. 2007). Phenothiazines are known to act by inhibiting type II NADH dehydrogenases mimicking the effect of the afore-mentioned mutations in *ndh* and leading to an increase in the intracellular $NADH/NAD^+$ ratios (Yano et al. 2006). This antagonism between isoniazid and phenothiazines is confirmed by the isobole data (Fig. 3.28.-G,-H). In terms of therapeutic use this suggests the contraindication of both isoniazid and a phenothiazine since this could result in a sub-optimal response.

Thioridazine and trifluoperazine combined (Fig. 3.28.-A) showed a synergistic effect, suggesting a complementary mode of action between these two phenothiazines with a similar mode of action. Jia and colleagues describe this as one particular case of synergism (Jia et al. 2009).

The metronidazole data (Fig. 3.39.) served as validation, showing that in this adaptation of the Wayne model, the cells survived in hypoxia. This drug showed no effect against Mtb grown under aerobic conditions but had a bactericidal effect against Mtb grown under severe hypoxia (Wayne and Sramek 1994).

The results obtained through microscopy confirmed that notable morphological differences are visible between aerobic grown Mtb and

Mtb grown under severe oxygen limitation (Gillespie et al. 1986). Mtb cells enlarged (Fig. 3.58.B and Fig. 3.59.A-D) and their cell walls thickened, as previously reported (Wayne and Sohaskey 2001), since when submitted to high levels of stress bacteria become more heterogeneous in morphology (Kolter et al. 1993).

There are still no standardised methods for Mtb drug susceptible tests. However suggestions and recommendations have been made in order to establish a comparable standard between laboratories (Mitchison 2005).

The choice of using IC_{50}s throughout this thesis was made since a comparison was meant to be established between the inhibitory effects of anti-TB compounds against the whole organism (values obtained in this chapter) and the inhibitory effects of these compounds using a kinetic enzymatic assay. The effect of phenothiazines against different enzymes of the Mtb ETC would ideally be made and a correlation would be obtained in terms of IC_{50}s comparisons. With this purpose, using a MIC or a MBC would not be as precise, since MIC and MBC rely on visual identification of growth and on a close (or wider) range in which the compounds are tested.

In conclusion, the work presented here further validates the respiratory chain of Mtb, and more specifically its type II NADH: menaquinone oxidoreductase as a viable target for development of anti-tubercular compounds. Phenothiazines should be evaluated as promising candidates for future TB treatments since they show activity against bacilli grown under different conditions.

Chapter 4. Cloning and expression of *Mycobacterium tuberculosis ndhA*

4.1. Introduction

The *ndhA* gene is a homologue of the *ndh* gene of Mtb that encodes a type II NADH: menaquinone oxidoreductase (Ndh-2). Instead of the 463 amino-acids of *ndh*, *ndhA* has 470 amino-acids and comparing their sequences, they have a similarity of 63%.

Ndh-2 is already a validated drug target against malaria (Biagini et al. 2006), it is non-proton pumping and it is insensitive to the drug rotenone, which inhibits the initial steps in the ETC (Melo et al. 2004; Teh et al. 2007). Ndh-2 is located in the inner part of the mycobacterial membrane and it catalyses the reaction: NADH + Menaquinone → NAD + Menaquinol (Fig. 4.1.).

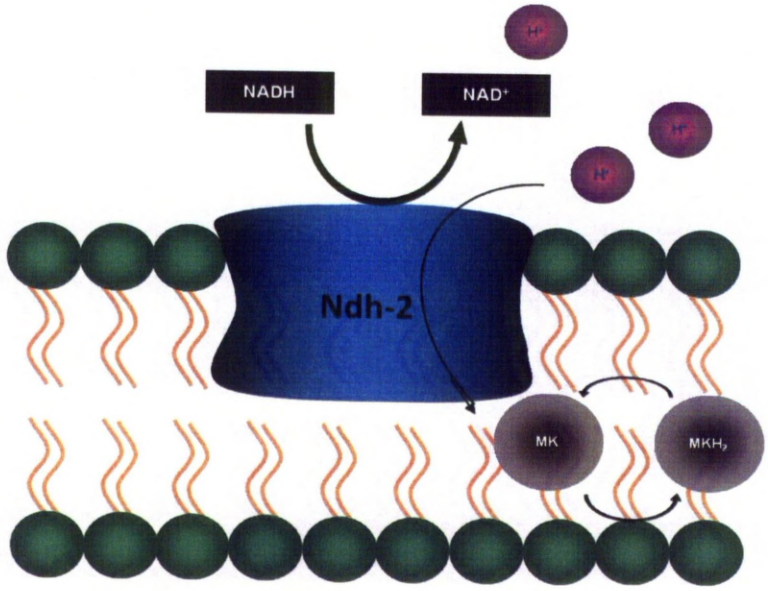

Fig. 4.1.: Scheme of the location of the enzyme Ndh-2 in the membrane of Mtb and representation of the reaction that it catalyses: NADH + MK (menaquinone) → NAD + MKH_2 (menaquinol).

Gene disruption of *ndh* is believed to be lethal to Mtb, but the inactivation of *ndhA* is non-lethal (Weinstein et al. 2005). Until recently, none of these genes featured in the list of essential genes for the growth of Mtb in aerobic, anaerobic or hypoxic conditions (Sassetti et al. 2003; Sassetti and Rubin 2003; Rustad et al. 2008). In 2011, Griffin and colleagues confirmed the essentiality of *ndh* for Mtb growth, this gene being the sole Mtb NADH dehydrogenase that could not tolerate insertional mutations (Griffin et al. 2011).

The *ndh* gene was studied in terms of functionality, essentiality and drug susceptibility (Weinstein et al. 2005; Teh et al. 2007), however, its homologue *ndhA* is poorly studied and it is often only mentioned in these studies focusing on *ndh* but not studied in detail.

4.2. Methods

4.2.1. Considerations regarding the molecular biology methods used throughout this thesis

This section gives a description of the molecular biology methods employed in order to clone the gene *ndhA* in a pUC19 vector using the sites *SphI* and *XbaI*. A detailed description of all the methods used can be found in (Sambrook and Russell 2001).

Initially, four inserts of the *ndhA* gene were prepared, however when the sequences were checked by automated sequencing after insertion in the cloning vector only one confirmed the presence of the gene. However for the methodological purpose the initial four planned inserts are described. It is uncertain why the other three planned inserts failed but for the purpose of the methodology only one was required to display the inserted gene so the work was carried out with this single one.

4.2.2. Chemicals, reagents, enzymes and buffers used

All restriction enzymes and respective buffers were from New England BioLabs, UK and they will be mentioned in the relevant sections , as well as all the other reagents.

4.2.3. Vectors

The vectors used during these studies were pET15b (5,708 bp) which contained the template *ndhA* gene, that was kindly supplied by Professor H. Rubin (School of Medicine, University of Pennsylvania, USA). The cloning vector, TOPO® plasmid vector pCR® 2.1-TOPO® and the expression vector, pUC19 vector (2,686 bp) were from Invitrogen™ (USA).

4.2.4. Glycerol stocks

Every time a new batch of cells was produced during these experiments, they were stored as glycerol stocks as a backup. 500 µl of cell suspension was added to 200 µl of 50% (v/v) glycerol in dH_2O and stored at -80°C.

4.2.5. Preparation of LB Media and plates

The nutrient media required for the growth of *E. coli* cells was prepared using a Luria-Bertani (LB) broth media powder, from Fisher (Fisher Scientific, UK). The media was prepared by adding 25 g of powder per 1 L of dH_2O. The solution was autoclaved for 15 minutes at 121°C and allowed to cool down to 45-50°C before the addition of antibiotics.

Sterile agar plates were prepared using a LB agar media powder (Sigma, USA), adding 37 g of powder per 1 L of dH_2O. The solution was autoclaved for 15 minutes at 121°C, allowed to cool down to 45-50°C before the addition of antibiotics. 20 ml of media was dispensed into each 9 cm diameter Petri dish.

4.2.6. Gel electrophoresis

All PCR amplifications and restriction enzyme digestions were verified using electrophoresis in agarose gel.

Samples were run in 1% agarose gels (0.5 g of agarose, 50 ml tris-borate-EDTA (TBE) buffer and 1.3 µl of ethidium bromide was added after the mixture cooled down to avoid aerosol formation).

A molecular weight ladder of 1Kb intervals, TrackIt™ 1Kb DNA ladder (Invitrogen™, USA) or Hyperladder I™ (Bioline, UK) were used to confirm the size of the fragments.

4.2.7. Determination of DNA concentration using a NanoDrop™

The concentration of DNA in the samples were determined using a NanoDrop™ 1000 (Thermo Fisher Scientific, USA) fitted with the software ND1000 v.3.7.1.

A volume of 1.5 µl of dH_2O was used to blank the instrument, followed by the measurement of an equivalent volume of the isolated DNA sample to test. A micropipette was used to deposit the samples onto the equipment without touching the probe.

After each measurement, the graph obtained was checked to confirm that the DNA peak was at 260 nm and in general, the ratio 260/280 nm should be between 1.8 and 2.0 to assure the purity of the sample.

4.2.8. Enzyme digestion of DNA template

In order to confirm that the template DNA was correctly inserted in the vector pET15b (5708 bp), two restriction analyses were used. The ApE-A Plasmid Editor v2.0.37 software (available at http://biologylabs.utah.edu/jorgensen/wayned/ape) was used to check the restriction map of the pET15b vector with and without the insert. All the sequences of the different vectors were obtained from the lab life website (http://www.lablife.org/vectordb). The map of the vector pET15b is shown in Fig. 4.2.

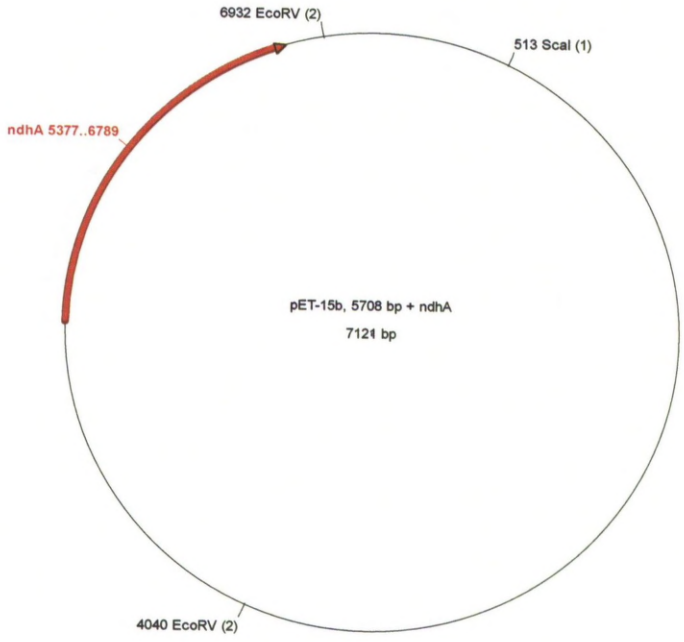

Fig. 4.2.: Restriction map of the pET-15b vector with the *ndhA* gene inserted using restriction enzymes *EcoRv* and *ScaI*. Position and length of the *ndhA* gene are indicated with the red arrow. Values in brackets indicate the number of restriction sites of an enzyme.

EcoRv would cut the vector in two positions (Fig 4.2.) which would produce two fragments, one with 4229 bp and another with 1479 bp if the gene is not inserted, and one with 2892 bp would be produced if the gene is inserted.

The second test was to use the enzyme *SacI* that cuts within pET15b vector once. This restriction would just open the vector resulting in a single fragment of 7112 bp.

The reactions were set up to a final volume of 30 µl according to Table 4.1.

Table 4.1.: Quantities of reagents necessary for the enzyme restriction reactions.

Reaction 1	Reaction 2
5 µl DNA template	5 µl DNA template
3 µl BSA (100µg/ml)	3 µl BSA (100µg/ml)
3 µl buffer 3	3 µl buffer 1
2 µl enzyme *EcoRv*	2 µl enzyme *SacI*
17 µl sterile dH_2O	17 µl sterile dH_2O

Both reaction vials were incubated at 37°C for 2 hours and loaded on the agarose gel (according to section 4.2.6.).

4.2.9. PCR

Polymerase chain reaction (PCR) allows the generation of millions of copies of a targeted region of DNA defined by two flanking primers. The reaction is performed by a heat-stable DNA polymerase with high fidelity, Platinum® *Pfx* (Invitrogen™, USA), by thermo-cycling (cycles of denaturation, primer annealing and DNA extension).

The reaction was prepared to a final volume of 50 µl, containing 2 µl of 10 mM deoxynucleoside triphosphates (dNTPs) mix (New England BioLabs, UK); 1 µl of 50 mM magnesium sulphate ($MgSO_4$); 5 µl of 10× *Pfx* amplification buffer; 1.5 µl of each primer to obtain a final concentration of 200 nM; 1 µl of DNA template (*ndhA* in pET15b); 5 µl of 10× PCR enhancer solution; 0.4 µl of Platinum® *Pfx* DNA polymerase and 34.6 µl of sterile dH_2O.

Four pairs of primers were used in these reactions and all of them share the same reverse primer.

Table 4.2.: Primers used in the PCR reactions.

Primer	Direction	Sequence	Reaction
ndhpFw	Forward	5'-GGGCATGCCCATCATCATCATCATCACAGC-3'	1
AJW22	Forward	5'- GGAGAACTAGTATGGGCAGCAGCC-3'	3
AJW27	Forward	5'-GGTGCCGCGCGGCACTAGTATGACGCTCTC-3'	4
AJW69	Forward	5'-GCGCGCATGCAATGACGCTCTCATCTGG-3'	2
AJW70	Reverse	5'-CGGCTCTAGACTAACCCGCTGCCTCTTGC-3'	1, 2, 3, 4

The annealing temperature was determined by the lowest melting temperature (Tm) of both primers that covered the optimum temperature for each primer. The extension time used was according to the size of the fragments to be replicated (typically 1 minute *per* Kb). PCR conditions are reported in Table. 4.3..

Forward primer ndhFw provides a polyhistidine-tag to the *ndhA* gene by annealing with the penta-polyhistidine located in the pET15b vector 33 bp upstream of the inserted *ndhA* gene.

Table 4.3.: Description of the PCR reaction conditions.

Initial denaturation step	94°C for 3 minutes	
25 cycles	94°C for 30 seconds	**Denaturation**
	56°C for 30 seconds	**Annealing**
	72°C for 90 seconds	**Extension**
Final extension step	72°C for 10 minutes	

The PCR product was run in an agarose gel (see section 4.2.6.) to confirm that the sizes of the fragments obtained matched the expected ones. Then the bands were cut under an UV-light transluminator and purified using a QIAquick® gel extraction kit (QIAGEN®, Germany).

4.2.10. A-tailing of PCR products

Platinum® *Pfx* leaves the PCR fragments with blunt ends. In order to successfully insert the PCR products into the TOPO® cloning vector (Invitrogen™, USA) that has single, overhanging 3' deoxythymidine (T) residues, the PCR product needs to have single deoxyadenosines (A) at their 3' ends. *Taq* polymerase acts as a terminal transferase, adding a single A to the end of the strands and thus improving the ligation process.

The A-tailing reaction consisted of the incubation of 15 µl of PCR product, 1 µl of *Taq* polymerase, 2 µl 10× *Taq* polymerase buffer and 2 µl of 10 mM dATPs (New England BioLabs, UK) for 15 minutes at 72°C.

4.2.11. Ligation using TOPO TA Cloning®

The ligations were performed using a TOPO® Cloning reaction. Briefly, 4 µl of PCR product were mixed with 1 µl of salt solution and 1 µl of a

TOPO® plasmid vector pCR® 2.1-TOPO® (Invitrogen™, USA). This mix was incubated for 45 minutes at room temperature.

4.2.12. Transformation of One Shot® TOP10 chemically competent *E. coli* cells

A vial of One Shot® TOP10 chemically competent *E. coli* cells (Invitrogen™, USA) was thawed on ice. The cell suspension was transformed with the addition of 6 µl of TOPO® cloning reaction, followed by an incubation on ice for 30 minutes.

The cells were heat-shocked in a water bath at 42°C for 45 seconds and transferred immediately to ice for 2 minutes. 200 µl of super optimal broth with glucose (SOC) medium were added to the vial at room temperature and shaken horizontally at 200 rpm for 1 hour. 40 µl of X-Gal (from a stock of 40 mg/ml in dimethylformamide (DMF) kept at 4°C in the dark) were added to the cells, before plating them in selective LB agar plates, containing 50 µg/ml ampicillin. The TOPO vector encodes a gene that confers ampicillin resistance, allowing only the cells with the plasmid to grow. The cells were allowed to grow overnight at 37°C.

The successful plasmid-containing cells appeared white due to the disruption of *lacZ* gene, and a consequential inability to express beta-galactosidase. Cells without the insert in the *lacZ* are able to express the gene that converts X-Gal (colourless) into a sugar that oxidises into a blue pigment resulting in the formation of blue colonies.

Isolated white colonies were picked and grown in 30 ml universals containing 5 ml LB broth supplemented with 50 µg/ml ampicillin for 6-8 hours at 37°C.

4.2.13. Mini prep of plasmid DNA

The cells from the white colonies were then harvested and their DNA purified using a QIAprep® Spin Miniprep Kit (QIAGEN®, Germany) according to the manufacturer's instructions. This procedure causes the lysis of the cells under alkaline conditions and the adsorption of DNA onto silica in high salt conditions.

4.2.14. Confirmation of recombinant-plasmid size by enzyme restriction analysis

In order to confirm that the plasmid was correctly inserted, restriction enzyme analysis was used. The ApE-A Plasmid Editor v2.0.37 software was used to obtain the expected restriction lengths of the fragments when digested with the enzymes *XmnI* and *PstI* (Fig. 4.3).

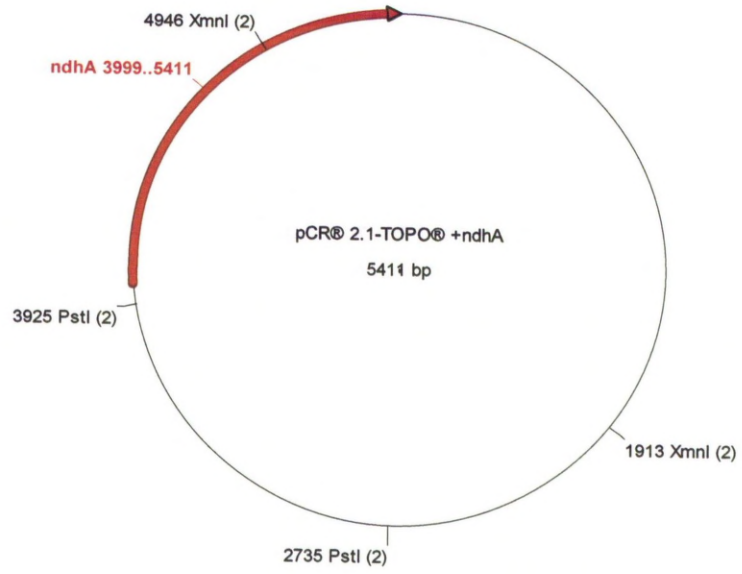

Fig. 4.3.: Restriction map of the pCR® 2.1-TOPO® vector with the *ndhA* gene inserted using restriction enzymes *XmnI* and *PstII*. Position and length of the *ndhA* gene are indicated with the red arrow. Values in brackets indicate the number of restriction sites of an enzyme.

The enzyme *XmnI* would have two recognition sites one within the TOPO vector and the second within the *ndhA* insert (Fig. 4.3.). This would create a fragment of 2221 bp that contains the end of the insert and a fragment of 3200 bp that would contain the beginning of the *ndhA* gene. If the insert was not present, *XmnI* would just open the vector and a single band corresponding to its length (3931 bp) would be obtained.

The enzyme *PstI* recognises two restriction sites within the TOPO vector (Fig. 4.3.). This would result in a fragment of 1190 bp that does not contain the insert and a second one of 4221 bp that would contain the insert. If the insert was not present this second fragment would be of 2741 bp.

The reactions were set up to a final volume of 30µl according to Table 4.4.

Table 4.4.: Quantities of reagents required for the enzyme restriction reactions.

Reaction 1	Reaction 2
12 µl sample	12 µl sample
3 µl BSA (100µg/ml)	3 µl BSA (100µg/ml)
3 µl buffer 4	3 µl buffer 3
2 µl enzyme *XmnI*	2 µl enzyme *PstI*
10 µl sterile dH_2O	10 µl sterile dH_2O

Both reaction vials were incubated at 37°C for 2 hours and separated on an agarose gel (according to section 4.2.6.).

After a positive confirmation by enzyme restriction analysis of the size of the fragments obtained, the samples were sequenced.

4.2.15. Capillary sequencing

DNA sequencing by capillary electrophoresis using the dideoxy chain termination technique was performed externally by Cogenics™ (Beckman Coulter Genomics, UK).

The DNA supplied to the sequencing company had a concentration that was always higher than 100 ng/µl.

The primers used for the sequencing reaction (Table 4.5.) were the universal primers for the TOPO vector M13 Forward and M13 Reverse while ndhAFwd and ndhARev were internal primers that anneal within the *ndhA* gene designed in the laboratory.

After retrieving the sequences from the company, they were aligned against the published reference sequence for the gene using ClustalW in the BioEdit software (Hall 1999), to confirm their presence in the clone.

Table 4.5.: Primers used to sequence the *ndhA* gene inserted in the TOPO vector.

Primer	Direction	Sequence
M13Fwd	Forward	5'-GTAAAACGACGGCCAG-3'
M13Rev	Reverse	5'-CAGGAAACAGCTATGAC-3'
ndhaFwd	Forward	5'-GCCGATGGGTCCAAAGCTG-3'
ndhaRev	Reverse	5'-GATGCCTTTGTAGTCGACCG-3'

4.2.16. *ndhA* cloning in a pUC19 vector

pUC19 vector and the *ndhA* TOPO clone were double digested with the restriction enzymes *SphI* and *XbaI*. The reactions were set up to a final volume of 50 µl according to Table 4.6. The restriction sites within the TOPO vector were set up in the primers of the initial PCR reactions (seeTable 4.2.) this way flanking the *ndhA* gene. Accordingly, both

pUC19 vector and *ndhA* clone extracted from the TOPO vector have cohesive extremities.

Table 4.6.: Quantities of reagents required for the enzyme restriction reactions.

Reaction 1 **pUC19 vector**	**Reaction 2** **TOPO *ndhA* clone**
4 µl buffer 2	4 µl buffer 2
4 µl BSA (100µg/ml)	4 µl BSA (100µg/ml)
3 µl enzyme *XbaI*	3 µl enzyme *XbaI*
3 µl enzyme *SphI*	3 µl enzyme *SphI*
36 µl pUC19	10 µl *ndhA* clone
-	26 µl sterile dH_2O

Both reaction vials were incubated at 37°C for 2 hours. A restriction map of the TOPO vector containing *ndhA* using enzymes *XbaI* and *SphI* was designed using the ApE-A Plasmid Editor v2.0.37 software (Fig. 4.4.).

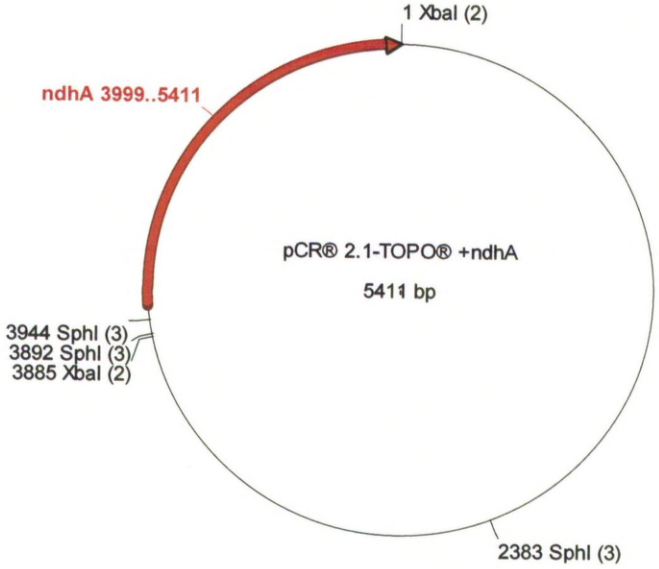

Fig. 4.4.: Restriction map of the pCR® 2.1-TOPO® vector with the *ndhA* gene inserted using restriction enzymes *XbaI* and *SphI*. Position and length of the *ndhA* gene are indicated with the red arrow. Values in brackets indicate the number of restriction sites of an enzyme.

pUC19 will generate a band of 2668 bp corresponding to virtually the original length of the vector (losing only 18 bp).

The double digestion of the TOPO vector (containing the *ndhA* gene) generates 5 fragments with sizes 2382, 1502, 1468, 52 and 7 bp. The 1468 bp fragment contains the *ndhA* gene and it is the one to transfer to the pUC19 vector.

To improve the likelihood of a successful ligation and to prevent the relegation of the plasmid, the 5'-phosphates were removed from pUC19. 3 µl of Antarctic phosphatase buffer and 1 µl of Antarctic phosphatase were added to the pUC19 digest, incubated for 30 minutes at 37°C and heat deactivated at 65°C for 10 minutes.

Two processes were used to isolate the DNA from the digests.

The *ndhA* clone digest was loaded in a low melting point 1.5% agarose gel (0.7 5g of AquaPor LE (National Diagnosis, UK) melted in 50 ml of TBE buffer. 1.3 µl of ethidium bromide was added to the gel when cooled down but before it solidified). The band corresponding to the cloned gene was cut from the gel under an UV-light transluminator and the DNA purified using a QIAquick® gel extraction kit (QIAGEN®, Germany). The DNA concentration was determined in a NanoDrop (see section 4.2.7.).

The pUC19 digest DNA was at a much lower concentration in the gel and a more efficient method of purification was used. It was purified using Agencourt AMPure beads (Beckman Coulter Genomics, UK) due to the higher efficiency of this method to recover amplicons than the procedure referred to above. 50 µl of the digested pUC19 product was mixed with 90 µl AMPure beads and placed in a Agencourt SPRIPlate Magnet plate (Beckman Coulter Genomics, UK). This results in the pUC19 DNA binding to the magnetic beads. After 10 minutes the supernatant, containing the contaminants is discarded and the pUC19 DNA and beads

are washed twice with 70% (v/v) ethanol in dH_2O. After being dried out, 50 µl of dH_2O was added, allowing the elution of DNA from the magnetic particles. The DNA was collected in a new tube and its concentration checked by a NanoDrop (see section 4.2.7.)

4.2.17. Ligation

To infer the ideal concentrations used in the ligation procedure, a "ligation calculator" was used, freely available at http://www.insilico.uni-duesseldorf.de/Lig_Input.html. According to the recommended quantities based on the size and concentration of fragments, 1 µl of T4 DNA Ligase and 1 µl of T4 DNA Ligase buffer (New England BioLabs, UK) were added to 2 µl of pUC19 DNA, 1.5 µl of *ndhA* clone and 4.5 µl of dH_2O. The reaction was incubated in the thermocycler at 25°C for 6 hours.

The ligations (10 µl) were transformed to One Shot® TOP10 chemically competent *E. coli* cells using the standard method. Briefly the DNA was directly incubated with the cells on ice for 30 minutes. Then the samples were heat-shocked at 42°C for 45 seconds and incubated with 200 µl of SOC medium for 1 hour at 37°C on a rotary shaking incubator.

200 µl of SOC medium was added to the vial and shaken horizontally at 200 rpm for 1 hour at room temperature. The sample was plated in selective LB agar plates, containing 50 µg/ml ampicillin, which is selective for the cells that incorporated the plasmid (that contains a gene conferring resistance to ampicillin).

The cells were allowed to grow overnight at 37°C.

Thereafter, isolated white colonies were picked (as explained in section 4.2.12.) and grown for 6-8 hours at 37°C, in 30 ml universals containing 5 ml LB broth supplemented with 50 µg/ml ampicillin.

DNA extraction was performed on the grown cells with CompactPrep plasmid maxi unit Kit (QIAGEN®, Germany), which is a fast spin column-based large-scale plasmid purification system.

4.2.18. Confirmation of clone size by enzyme restriction analysis

In order to confirm that the cloning process was successful, restriction enzyme analysis with enzymes *ScaI*, *EcoRI* and *PvuII* was used. A restriction map of the pUC19 vector incorporating the *ndhA* gene was designed with the ApE-A Plasmid Editor v2.0.37 software (Fig. 4.5.).

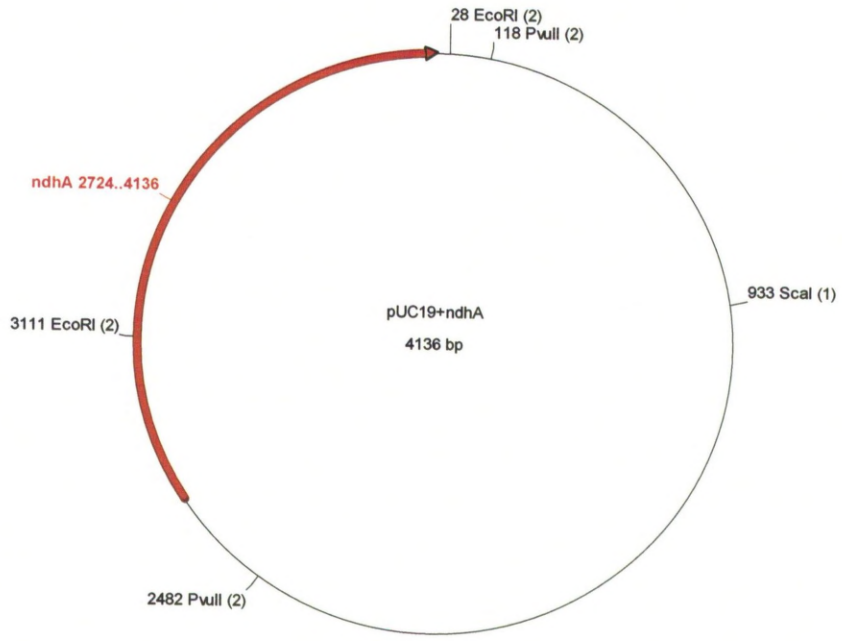

Fig. 4.5.: Restriction map of the pUC19 vector with the *ndhA* gene inserted using restriction enzymes *ScaI*, *EcoRI* and *PvuII*. Position and length of the *ndhA* gene are indicated with the red arrow. Values in brackets indicate the number of restriction sites of an enzyme.

The enzyme *ScaI* would create a single fragment of 4136 bp if *ndhA* is incorporated since it only cuts once within the vector. The enzyme *EcoRI*

cuts once within the vector and once within the insertion producing fragments of 1053 and 3083 bp. The enzyme *PvuII* recognizes two sites in the vector flanking the place of the insertion, creating fragments of 1772 and 2364 bp, the first containing the full *ndhA* sequence.

The reactions were set up to a final volume of 15 µl according to Table 4.7.

Table 4.7.: Quantities of reagents required for the enzyme restriction reactions.

Reaction 1	Reaction 2	Reaction 3
2 µl sample	2 µl sample	2 µl sample
1.5 µl *EcoRI* buffer	1.5 µl buffer 3	1.5 µl buffer 2
1 µl enzyme *EcoRI*	1 µl enzyme *ScaI*	1 µl enzyme *PvuII*
10.5 µl sterile dH_2O	10.5 µl sterile dH_2O	10.5 µl sterile dH_2O

Reaction vials were incubated at 37°C for 2 hours and loaded in an agarose gel (according to section 4.2.6.).

4.2.19. Preparation of ANN0222 *E. coli* competent cells using calcium chloride

ANN0222 cells are *E. coli* NADH dehydrogenase knockout strain (nuoB::nptI-sacRB, ndh::tet) with no associated NADH: quinone oxidoreductase (Fisher et al. 2009).

Cells from an ANN0222 cell stock were streaked onto a LB Agar plate supplemented with 30 µg/ml kanamycin and 12.5 µg/ml tetracycline and incubated overnight at 37°C. ANN0222 are kanamycin and tetracycline resistant. Single colonies were picked and grown in 5 ml LB broth (same antibiotic concentrations) until dense.

100 µl of cells were inoculated with 100 ml of LB supplemented with 30 µg/ml kanamycin and 12.5 µg/ml tetracycline and grown until OD_{600}= 0.4. The cells were poured into two ice cold 50 ml Falcon tubes and left on ice for 10 minutes. The suspensions were centrifuged at 4000 rpm at 4°C for 10 minutes and the supernatant discarded.

Treatment with calcium chloride makes the cell competent, enhancing the permeability of the cell membrane to allow the incorporation of the plasmid DNA. The cells were resuspended in 15 ml of ice cold solution of magnesium chloride ($MgCl_2$) at 80 mM and calcium chloride ($CaCl_2$) at 20 mM before being centrifuged at 4000 rpm at 4°C for 10 minutes and the supernatant discarded.

The cell pellet was resuspended in 2 ml of 100 mM ice cold $CaCl_2$. Then, 200 µl of glycerol was added to the cells, mixed gently, aliquoted into 20 cold eppendorfs and stored at -80°C, constituting a ready to use cell stock.

4.2.20. Transformation into ANN0222 competent *E. coli* cells

The cloned DNA was transformed to ANN0222 competent *E. coli* cells. The DNA was directly incubated with the cells on ice for 30 minutes, heat-shocked at 42°C for 90 seconds and incubated with 200 µl of SOC medium for 1 hour at 37°C on a rotary shaking incubator.

200 µl of SOC medium was added to the vial and shaken horizontally at 200 rpm for 1 hour at room temperature. The cells were then plated in selective LB agar plates, containing 100 µg/ml ampicillin, 30 µg/ml kanamycin and 12.5 µg/ml tetracycline. Ampicillin resistance is conferred by the incorporation of the pUC19 vector, ensuring that only the cells that incorporated the clone will grow.

The cells were allowed to grow overnight at 37°C. Isolated white colonies were picked and grown in 30 ml universals containing 5 ml LB broth supplemented with 100 μg/ml ampicillin, 30 μg/ml kanamycin and 12.5 μg/ml tetracycline. When dense, the 5 ml of cell suspension was transferred to 500 ml of broth supplemented with the same drugs.

The cells were induced at an OD_{600}= 0.4 with 1 mM IPTG (from a 1 M stock solution, diluted in dH_2O). If successful, *ndhA* would replace the gene *lacZ* of the lac operon and IPTG would switch on this inserted gene consequentially leading to the production of the protein of interest.

The cells were grown for a minimum of 32 hours before being harvested by centrifugation at 4000 rpm for 5 minutes at 4°C.

4.2.21. Preparation of membranes for kinetic studies

For the preparation of cell membranes, the transformed cells were harvested by centrifugation at 4000 *g* for 20 minutes. The supernatant was discarded and the resultant pellet resuspended in 50 mM potassium phosphate buffer pH 7.4 (50 ml of buffer was added for every 1 L of cell culture) and centrifuged at 4000 *g* for 20 minutes. Once again the supernatant was discarded and the pellet re-suspended in the same buffer (20 ml of buffer were added for every 1 L of cell culture). Cells were maintained on ice for 30 minutes following the addition of hen-egg lysozyme to a final concentration of 0.2 $mg \cdot ml^{-1}$.

A One Shot Constant (Constant Systems Ltd, UK) cell disruptor was used to break the cells. Cells were maintained on ice to avoid denaturation of proteins due to generation of heat and submitted to 1 shot at 20,000psi. An anti-foam cup was used in order to minimise foam produced during the process and 6 ml of cell culture was used per shot.

The suspension was centrifuged at 10,000 *g* for 30 minutes at 4°C before the supernatant was collected and centrifuged at 100,000 *g* for 1 hour, at 4°C. The resultant pellet was homogenized with a hand homogeniser in 2 ml of 50 mM potassium phosphate buffer, 2 mM ethylenediaminetetraacetic acid (EDTA) pH 7.4 containing 20% (v/v) glycerol. The isolated membrane preparation was stored at -80°C until required.

4.2.22. Preparation of the quinone electron acceptor and of the NADH stock solution

Decylubiquinone (dQ) and NADH are commercially available (Sigma, UK). To prepare dQ stock approximately 1mg was dissolved in 1ml of 96% ethanol. NADH stock was prepared by dissolving approximately 70mg in 1ml of 50nM potassium phosphate, 2mM EDTA (pH 7.5). The precise concentration of the dQ and NADH stocks were measured in a Cary-UV 4000 UV-VIS spectrophotometer (Varian, UK) using extinction coefficients of 8.1 and 6.22 $mM^{-1}cm^{-1}$ respectively.

4.2.23. Enzyme activity of isolated membranes

In order to confirm the enzyme activity of the prepared membrane fraction, steady-state activity of the *ndhA* encoded enzyme was measured spectrophotometrically at room temperature, in a Cary-UV 4000 UV-VIS spectrophotometer (Varian, UK), and quartz cuvette of pathlength 1 cm.

The total volume of the assay was 700 µl. The crude membrane (approximately $15\mu g.ml^{-1}$) was mixed with 50 mM potassium phosphate (pH 7.5), 2 mM EDTA, pH 7.4 containing 10 mM potassium cyanide (pH

7.5) and variable concentrations of NADH. Potassium cyanide was used to inhibit endogenous *E. coli* quinol oxidases. The reaction was initiated by the addition of 50 μM decylubiquinone (dQ), a synthetic analogue of ubiquinone and was monitored spectrophotometrically by following the absorbance changes at 283 nm (quinone reduction) and 340 nm (NADH oxidation) at room temperature, according to Fisher et al. 2009.

4.3. Results

4.3.1. Cloning and expression the Mtb *ndhA* gene

The restriction analyses confirmed that the provided template contained the *ndhA* gene (Fig. 4.6.).

The restriction analysis with *EcoRv* demonstrated that the enzyme cut the vector in two places, generating a fragment of 2883 bp that was present whether the gene was inserted or not, and a second fragment of 4229 bp that had the size of the remaining vector plus an insertion of the *ndhA* gene (Fig. 4.6., lane B).

In the second restriction analysis, *SacI* cuts only once producing a single band of the total vector plus gene, at 7112 bp (Fig. 4.6., lane C).

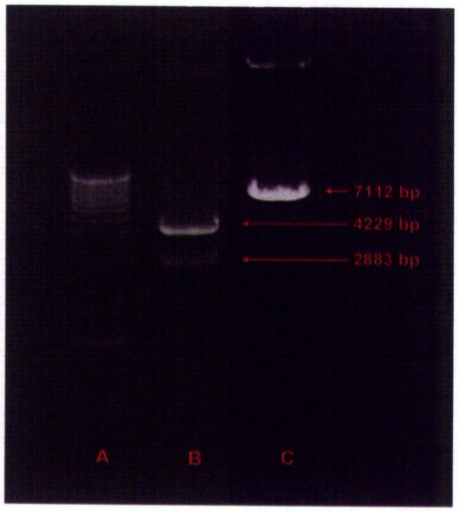

Fig. 4.6.: Electrophoretic gel showing the restriction analysis with *EcoRv* and *SacI* in the vector pET15b with the *ndhA* insertion. Lanes correspond to (A) TrackIt™ 1Kb DNA ladder, (B) *EcoRv* restriction and (C) *SacI* restriction.

Amplification of the *ndhA* gene from the pET15b vector using four pairs of primers (Table 4.2.) was confirmed by gel electrophoresis. As expected, all the pairs of primers produced a PCR fragment of about 1450 bp (Fig. 4.7., lanes B, C, D,E).

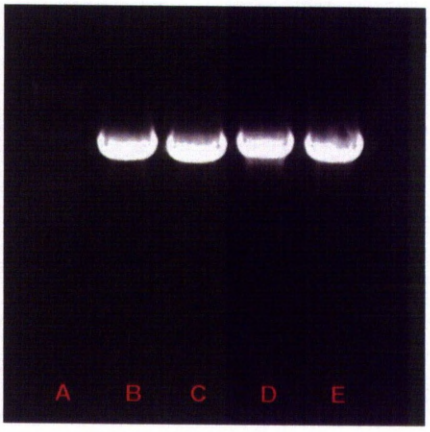

Fig. 4.7.: Electrophoretic gel displaying the four amplified products of the *ndhA* gene using the four pairs of primers described in the text. Lanes correspond to (A) TrackIt™ 1Kb DNA ladder, (B) PCR reaction 1, (C) PCR reaction 2, (D) PCR reaction 3 and (E) PCR reaction 4.

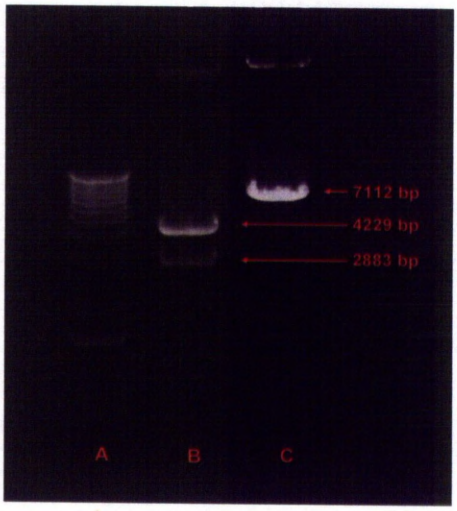

Fig. 4.6.: Electrophoretic gel showing the restriction analysis with *EcoRv* and *SacI* in the vector pET15b with the *ndhA* insertion. Lanes correspond to (A) TrackIt™ 1Kb DNA ladder, (B) *EcoRv* restriction and (C) *SacI* restriction.

Amplification of the *ndhA* gene from the pET15b vector using four pairs of primers (Table 4.2.) was confirmed by gel electrophoresis. As expected, all the pairs of primers produced a PCR fragment of about 1450 bp (Fig. 4.7., lanes B, C, D,E).

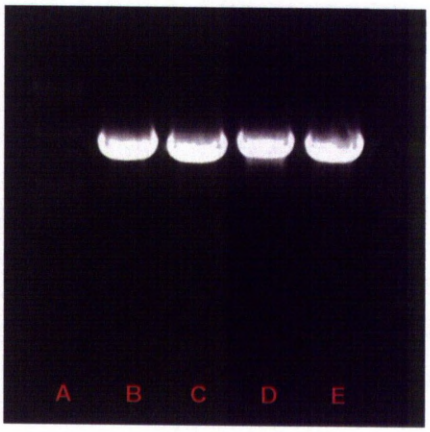

Fig. 4.7.: Electrophoretic gel displaying the four amplified products of the *ndhA* gene using the four pairs of primers described in the text. Lanes correspond to (A) TrackIt™ 1Kb DNA ladder, (B) PCR reaction 1, (C) PCR reaction 2, (D) PCR reaction 3 and (E) PCR reaction 4.

The restriction analyses with enzymes *XmnI* and *PstI* revealed that the *ndhA* gene was inserted in the TOPO vector.

The restriction with *XmnI* produced two fragments of 3200 and 2221 bp (Fig. 4.8., lane B). These two fragments were produced due to the presence of one restriction site in the TOPO vector and another one within the *ndhA* gene (Fig. 4.3.).

PstI recognizes two restriction sites within the TOPO vector and it generates a band of 1190 bp independent of the insertion being present or not (Fig. 4.8., lane C). The second band has 4221 bp which corresponds to the remaining TOPO vector with the inserted *ndhA* (Fig. 4.3.).

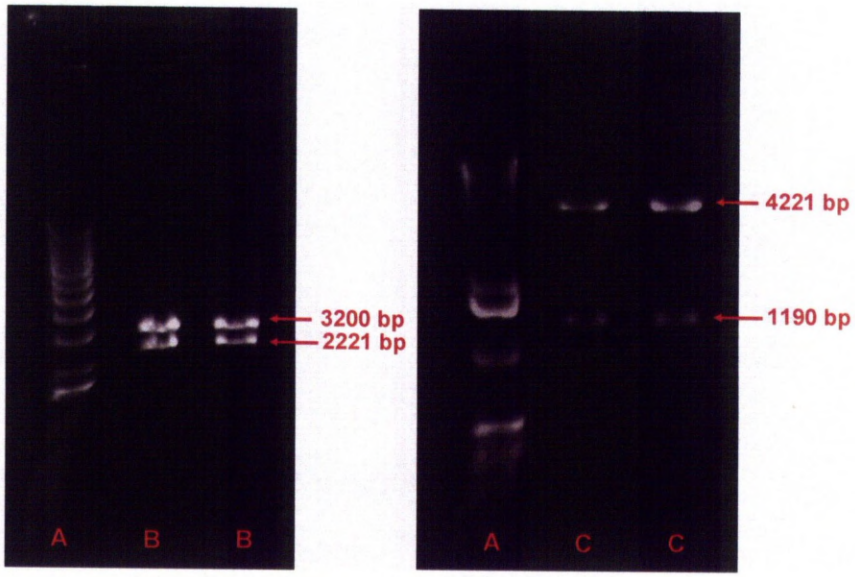

Fig. 4.8.: Electrophoretic gel showing the restriction analyses with *XmnI* (left) and *PstI* (right). The lanes correspond to (A) TrackIt™ 1Kb DNA ladder, (B) *XmnI* restriction in duplicate and (C) *PstI* restriction in duplicate.

After the restriction analyses with *XmnI* and *PstI,* the samples were sequenced to verify if the insertion had occurred and if the gene was inserted in the right direction. The sequencing was done with four

primers (Table 4.5.). The M13F and M13R are universal primers located in TOPO vector flanking the location of the insertion. The two other primers used were located within the *ndhA* gene to check the complete sequence of the gene.

The sequencing with M13F revealed the sequence of the TOPO vector followed by an insertion in the expected location of the sequence (Fig 4.9.). This insertion contains the ndhPFw primer, a small portion of the pET-15b that linked the polyhistidine to the *ndhA* sequence in that vector and the beginning of the *ndhA* sequence.

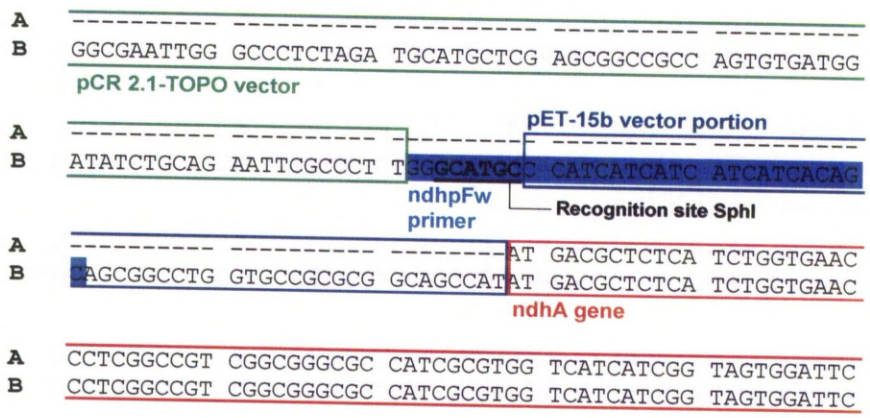

Fig. 4.9.: Alignment of the sequence of the pCR2.1-TOPO vector with the *ndhA* gene obtained with the universal M13F primer.

The sequencing using the M13R primer revealed the TOPO vector sequence following an insertion in the expected place (Fig. 4.10.). The inserted sequence corresponded to the AJW70 primer sequence the *ndhA* sequence that in this case overlaps with the primer sequence since this was designed partially on top of the termination of the gene.

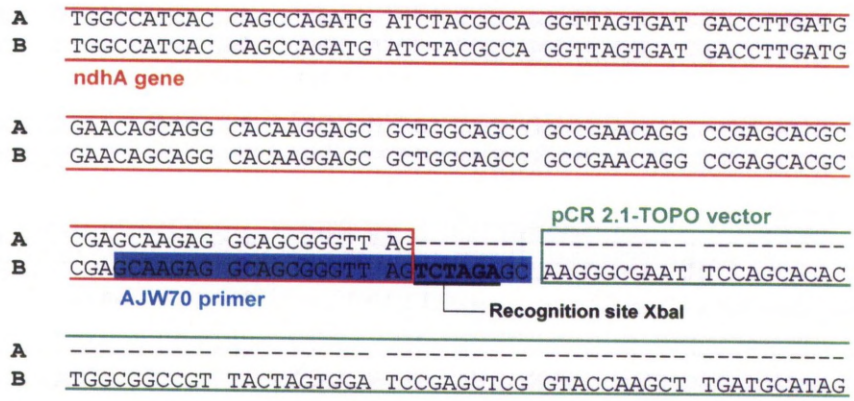

Fig. 4.10.: Alignment of the sequence of the pCR2.1-TOPO vector obtained with the universal M13R primer and the *ndhA* gene. Sequence shown is the reversed complement of the obtained sequence in order to show the 5'-3' direction of the *ndhA* gene.

The two internal primers, ndhpFw and AJW70, did not reveal any abnormality within the *ndhA* gene sequence.

The pUC19 vector and the TOPO vector with the inserted *ndhA* gene were double digested by the enzymes *XbaI* and *SphI*, whose recognition sites in the TOPO vector are shown in Fig. 4.9. and 4.10.. The restriction cleavages within the pUC19 vector resulting in only one band, of 2686 bp, of the entire vector in the gel (Fig. 4.11, lane B). A second band exists but since it is less than 20 bp, it would not appear in the electrophoretic gel.

In the case of the TOPO vector the restriction sites for these enzymes were introduced in the primers of the original amplification of the *ndhA* gene and so the sites are flanking the gene. A fragment of 1468 bp containing almost exclusively the gene was generated. A second fragment of 2382 bp was easily separated in the electrophoretic gel, however a third band of 1502 bp was also generated (see Fig. 4.4.). This band is proximal to the band of interest in the gel and it could also be extracted when the band of 1468 bp was taken from the gel (Fig. 4.11., lane C). The tips of this fragment were also generated through the restriction by

XbaI and *SphI* so the fragment could be incorporated into the pUC19 vector.

This is a flaw in the design of the experiment which could have been avoided, for example by the digestion of the TOPO vector/*ndhA* gene with a further restriction enzyme that would cut halfway the 1502 bp fragment (e.g. *PsiI*) leaving the 1468 bp band of interest alone in the gel or the gel should have run for longer using a high resolution agarose gel. This issue was just detected in the writing up of this thesis. However although it should decrease the efficiency of the designed experiment it should not make it unviable or the results discarded.

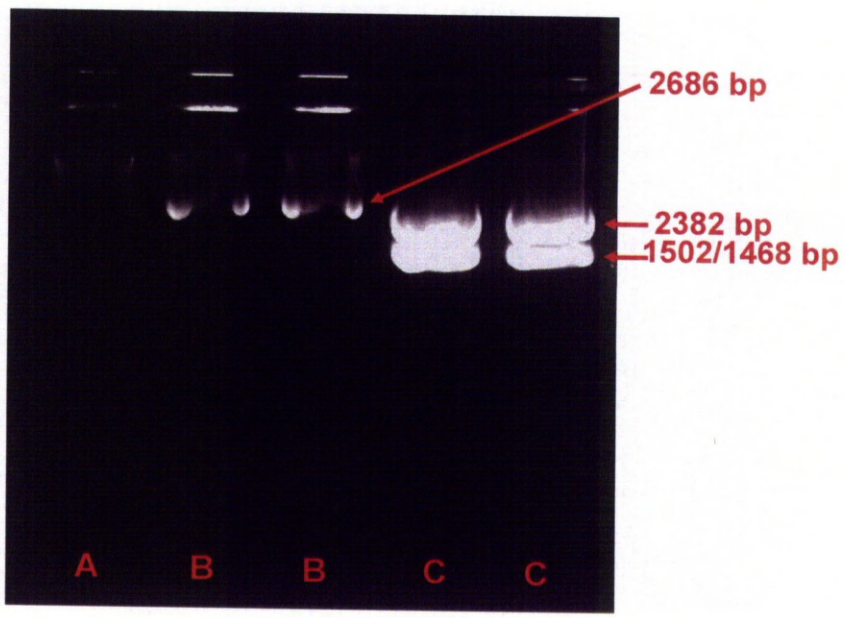

Fig. 4.11.: Electrophoretic gel of the restriction analyses with *XbaI* and *SphI*. The lanes correspond to (A) TrackIt™ 1Kb DNA ladder, (B) pUC vector and (C) *ndhA* gene incorporated in the TOPO vector.

The pUC19 with the insertion was checked by using three restriction enzymes, *ScaI*, *EcoRI* and *PvuII*. In order to interpret the gel electrophoresis results, a restriction map of the possible second type of insertion (part of the TOPO vector) was constructed (Fig. 4.12.), using the ApE-A Plasmid Editor v2.0.37 software.

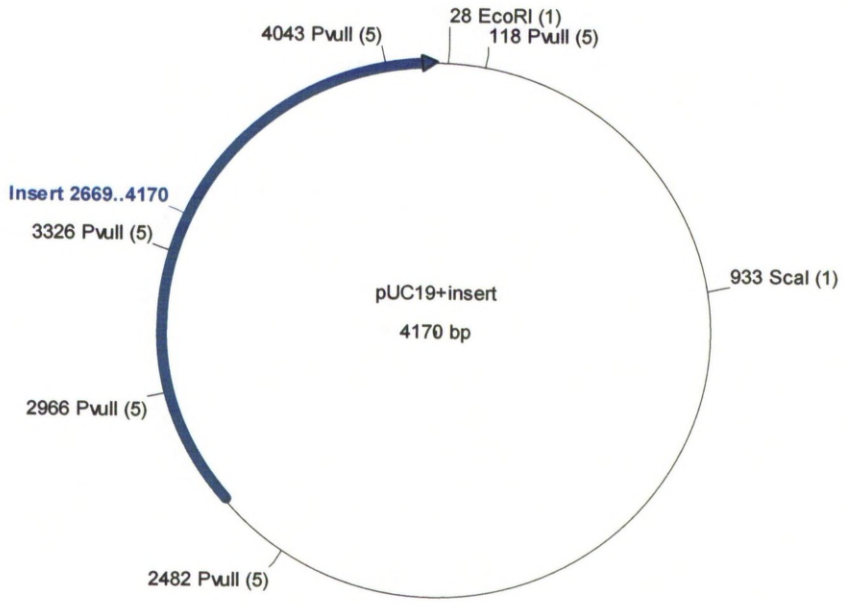

Fig. 4.12.: Restriction map of the pUC19 vector with the possible insert originated from the pCR2.1TOPO vector using restriction enzymes *ScaI*, *EcoRI* and *PvuII*. Position and length of the insert is indicated with the blue arrow. Values in brackets indicate the number of restriction sites of an enzyme.

The *ScaI* restriction analysis revealed the presence of an insertion since a band of more than 4000 bp was present (Fig 4.13., lane C). However this restriction does not distinguish between the *ndhA* gene and the other possible insert.

The *EcoRI* enzyme cuts twice, one within the *ndhA* gene and the other in the pUC19 vector (Fig. 4.5.) generating two bands. Gel electrophoresis revealed the presence of the *ndhA* insert in the pUC19 vector since two

bands were present, one of about 3000 bp and one of about 1000 bp (Fig. 4.13., lane B). However, in some cases the restriction with *EcoRI* showed both these two bands but also a band of the size of the overall vector, similar to the restriction with *ScaI* (Fig 4.13., lane D). This means that either the digestion was not complete or that some of the molecules in those samples contained an insert that does not present a restriction site for *EcoRI*. If the restriction was not complete, some of the pUC19 are circular and the migration rate is different from the one obtained with the *ScaI*. This suggests that some of the vectors just cut once with *EcoRI*, as expected for the abnormal insertion, considering that one of the bands had a molecular weight of the full vector with the inserted portion (Fig. 4.12.). In future work, the experiment will need to be designed so that this abnormal insert is not selected during the extraction of the *ndhA* band in the gel, by maximising the separation of the bands in the gel.

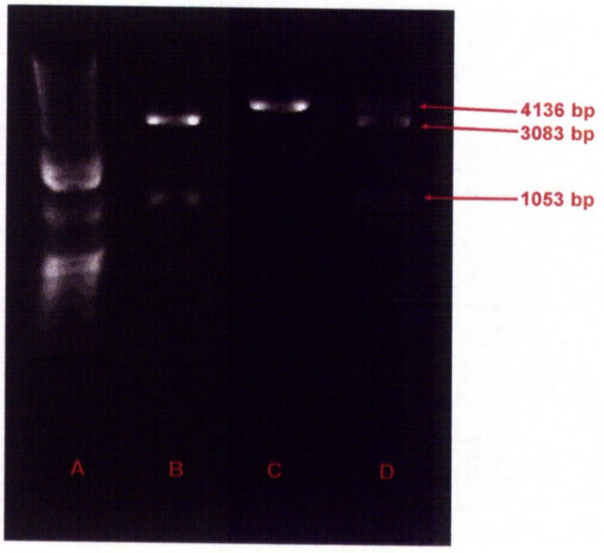

Fig. 4.13.: Electrophoretic gel of the restriction analyses of the recombinant pUC19 vector with *EcoRI* and *ScaI*. The lanes correspond to (A) TrackIt™ 1Kb DNA ladder, (B) and (D) restriction with *EcoRI* and (C) restriction with *ScaI*.

The restriction with enzyme *PvuII* revealed two bands of 1772 and 2364 bp, indicating that the *ndhA* gene was inserted in the pUC19 (Fig. 4.14., lanes B and C). However, the sample loaded in lane C displayed some extra bands that at the time of the experiment were interpreted as over-digestion by the restriction enzyme, since *PvuII* is known to exhibit star activity (non-specific cutting). Analysing the pUC19 vector with the abnormal insert, *PvuII* cuts in three places in that sequence (Fig. 4.12.). This restriction generates several fragments, one of 2634 bp but also, a greater number of smaller fragments with 717, 484, 360 and 245 bp (Fig. 4.14., lane C).

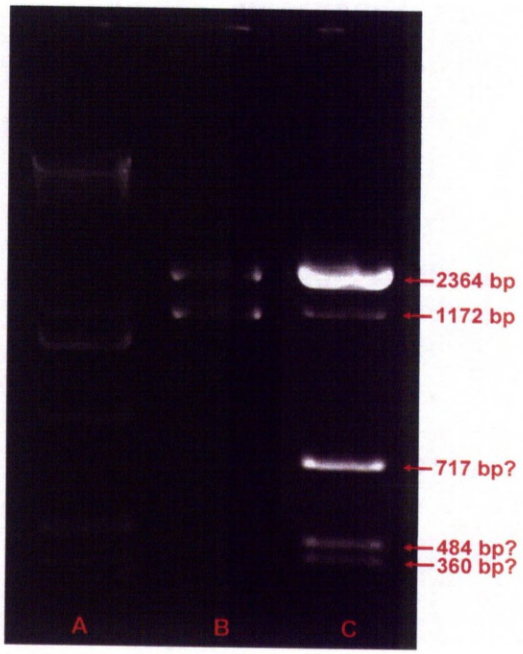

Fig. 4.14.: Electrophoretic gel of the restriction analyses of the recombinant pUC19 vector with *PvuII*. The lanes correspond to (A) Hyperladder I^{TM} DNA ladder and (B) and (C) restriction with *PvuII*.

Mainly visible on lane C (Fig. 4.14.) is a set of bands whose comparison with the ladder (Fig. 4.14., lane A) fits the expected pattern of the

insertion with a portion of the TOPO vector, the possible abnormal insertion mentioned above. The band with lower weight (245 bp) is missing in the gel because it might have just run out of the gel.

Overall it seems that it is quite probable that the abnormal insertion, corresponding to a portion of the TOPO vector, is being incorporated in some pUC19 vectors. Considering that the pattern observed in lane B (Fig. 4.14.) was the prevailing one, it is quite probable that there is a higher tendency for the *ndhA* insert to be incorporated. *ndhA* is slightly smaller than the other possible insert and the conditions in the "ligation calculator" were optimized for the *ndhA* gene which could have generated this preponderance.

4.3.2. Kinetic profile of the *ndhA* gene

After the transformation of the gene *ndhA* in the *E. coli* cells and its probable expression, the cells were disrupted and the enzyme activity of the resultant membranes was investigated spectrophotometrically by following the absorbance changes at 283 nm (quinone reduction) and 340 nm (NADH oxidation) that result upon the addition of decylubiquinone to the isolated membrane proteic complexes (See Section 4.2.23.). However upon analysis of the recombinant *ndhA*, no NADH: quinone reductase activity was measurable (Fig. 4.15.). Similar to its homologue Ndh-2, encoded by *ndh*, *ndhA* crude membranes should catalise the oxidation of NADH with concomitant reduction of quinone visible spectrophotometrically at 340 and 283 nm.

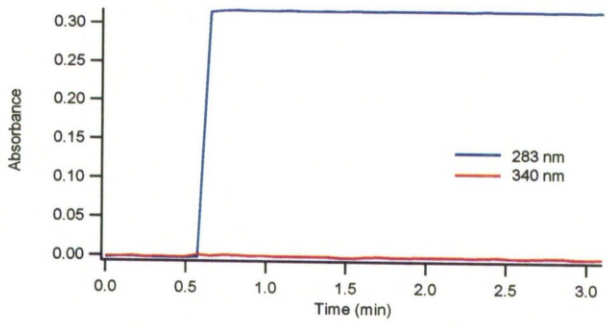

Fig. 4.15.: Graphical representation of the steady state kinetic data of *ndhA* encoded enzyme activity (NADH: menaquinone oxidoreductase). The data were monitored at 283 nm (quinone reduction, blue line) and 340 nm (NADH oxidation, red line) and it is evidence of the inexistence of enzyme activity. The reaction started with the addition of decylubiquinone at t= 35 seconds.

In order to confirm the validity of the assay, in parallel, using the same conditions, the activity of the enzyme encoded by *ndh* (*ndhA* analogue) was assessed using membranes with the *ndh* gene cloned (provided by Doctor Ashley Warman, from this laboratory and whose methodology is reported in (Fisher et al. 2009)). The activity of the enzyme encoded by the *ndh* gene was confirmed (Fig. 4.16.).

NADH dehydrogenase catalyses the reaction NADH + Q (quinone) → NAD + KH_2 (quinol).

Absorbance changes at 283 nm measure quinone reduction and absorbance changes at 340 nm measure NADH oxidation. Before the addition of decylubiquinone, the changes in both absorbances were negligible. After the addition of decylubiquinone (noticible by the peak measured at 283nm), both absorbances (measured at 283 and 340nm) decreased (Fig. 4.16.). This indicates that quinone is reduced to quinol and NADH is being oxidised (according to the reaction above) and this is an indication of electron transport to an alternative acceptor, most probably oxygen.

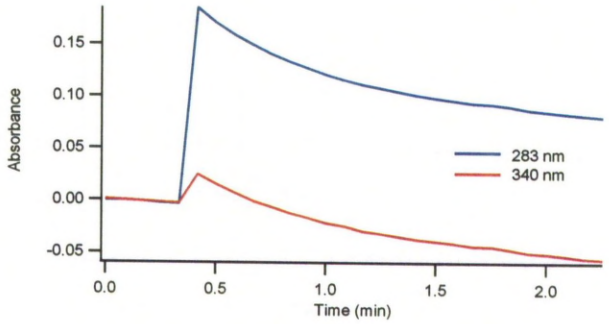

Fig. 4.16.: Graphical representation of the steady state kinetic data of *ndh* encoded enzyme activity (NADH: menaquinone oxidoreductase). The data were monitored at 283 nm (quinone reduction, blue line) and 340 nm (NADH oxidation, red line) and it is evidence of the enzyme activity. The reaction started with the addition of decylubiquinone at t= 20 seconds.

For the validation of an enzyme to be used in future drug assays, it would be important to do a characterisation of its kinetic parameters, K_m and v_{max}. Data would be analysed using the Michaelis-Menten equation in order to determine these values. V_{max} is the rate at which a substrate will be converted to a product once bound to the enzyme and the K_m is how effectively the enzyme would bind the substrate, hence affinity. If the assay was to be developed further, different substrates could have been tried (different analogues of quinone) and also different coenzymes (NADH/NADPH) before moving to drug screening.

4.4. Discussion

The objective of this chapter was to transform *E. coli* cells with their own *ndh* gene knocked out and express the Mtb *ndhA* gene.

ndh is an already identified Mtb drug target, whose expression was already studied (Weinstein et al. 2005; Teh et al. 2007). In this context, it is essential to know if this known *ndh* homologue is functional and if it shows susceptibility to the same drugs.

Bacteria have plasticity and this means that they can use different pathways to achieve the same outcome, in different scenarios, which can be difficult to assess in the lab. This factor creates doubt in studies focusing on the up-regulation and down-regulation of genes when submitting bacteria to different conditions. Similar issues arise with the notion of essentiality or non-essentiality since these concepts can easily shift depending on a great multitude of conditions. In the case of Mtb, plasticity is particularly important due to the fact that this organism is extremely successful, not only infecting and surviving inside the human host, but being able to persist in a latent state and re-emerge long after the initial infection.

The pET15b vector containing the *ndhA* gene, was inserted in a pCR® 2.1-TOPO®, which was followed by insertion of the gene into a pUC19 vector and the transformation of the *ndhA*-encoding plasmid into ANN0222 competent *E. coli* cells. The efficiency of intermediate steps was evaluated using restriction enzymes and direct sequencing in order to assure that the gene was always correctly cut and inserted. After expression of the gene in the ANNO0222 competent *E. coli* cells, the cells were disrupted, the membranes isolated and the activity of the enzymes checked. However, no enzyme activity was detected. A number of factors may be responsible for the lack of observable enzyme activity: one is the possibility that the *ndhA* gene is not a functional type II NADH: menaquinone oxidoreductase and the second is that some undetected irregularity in the protocol did not allow for the expression of the enzyme.

The observations are in conflict with published results reporting the *ndhA* gene expression and enzymatic activity (Weinstein et al. 2005). Also, the genes *ndh* and *ndhA* show a considerable degree of similarity and as shown in the next chapter, their rate of evolution indicates similar evolutionary constraints, probably indicating that both are equally

functional. Taking this into account, it seems unlikely that *ndhA* does not possess enzymatic activity. However the possibility that *ndhA* may be less favourably expressed and translated needs to be considered. *ndhA* could also be toxic to the host cell or may not fold correctly in the cell environment of the host *E. coli* cell.

Regarding the protocol irregularity, it has been recently noted in our laboratory (at a time after termination of my laboratory work) that expression of active recombinant protein is very much reliant on sustained drug pressure in order for the host *E. coli* cells to retain the gene-encoding plasmid. Indeed, it has been observed that expression of *ndh*, which has previously been seen to be highly active, can be lost if ampicillin concentrations fall. It has been seen that upon scale up from small (e.g. 10 ml) to large volumes (e.g. 500 ml) that failure to maintain the drug (in this case ampicillin) at a sufficiently high concentration over the longer growth period required for expression, the plasmid will be lost and no expression will occur (personal communication by Doctor Ashley Warman). This can be mitigated by the use of freshly prepared drug stocks and the mantainence of a high concentration of ampicillin (typically 100μg/ml) in all solid and liquid media. This recent observation may well account for the apparent lack of *ndhA* activity seen during my expression trials.

In summary, the *ndhA* gene was successfully isolated and cloned from Mtb and transfected into an *E. coli* expression system (suitable for high-throughput screening) (Fisher et al. 2009). The final scale-up and enrichment of recombinant *ndhA* was not possible, but it is envisaged that this is due to a technical problem which could not be resolved at the time that this study was conducted. Nevertheless this work represents a considerable step forward towards the characterisation of *ndhA* and provides a platform for further studies aimed at understanding the role of this protein in the ETC of Mtb.

Chapter 5. Phylogenetic analysis of type II NADH: menaquinone oxidoreductase in the Actinomycetales group

5.1. Introduction

Mtb possesses two types of NADH: menaquinone oxidoreductase, the type I encoded by 14 genes (*nuoABCDEFGHIJKLMN*) and type II with two known copies coded by the genes *ndh* and *ndhA*. These are single subunit enzymes and catalyze the first step in the respiratory chain, transferring electrons from NAD(P)H to the quinone pool (Kerscher 2000; Yagi and Matsuno-Yagi 2003).

Unlike type I NADH: menaquinone oxidoreductases, type II enzymes are believed to be essential for Mtb survival and they are the only NADH: menaquinone oxidoreductase used during hypoxia (Rao et al. 2001). Due to this fact and since no homologue exists in the human host this enzyme is a promising drug target.

There is very little biochemical information on the structure and function of type II NADH: menaquinone oxidoreductases since there are no crystal structures described. In addition, very little information exists on the evolution of this enzyme and its phylogenetics across species. In this Chapter, a molecular phylogenetics and bioinformatics study was undertaken to address some of the gaps in knowledge with respect to this enzyme.

Melo and collaborators phylogenetically grouped the type II NADH: menaquinone oxidoreductases into three groups, A, B and C, or more precisely two considering that group B is a sub-group of A, present in eukaryotic organisms (Melo et al. 2004). From the 61 prokaryotic species analysed in that study nearly 75% had type II NADH: menaquinone oxidoreductases and in about 15%, this was the only type of NADH: menaquinone oxidoreductase detected in the organism. In the prokaryotic organisms that contained type II NADH: menaquinone oxidoreductases nearly 90% of the analysed sequences belonged to group A, including in Mtb. The group C sequences were typical of hyperthermophilic prokaryotes and were quite divergent from the group A sequences (Melo et al. 2004).

Specifically this Chapter addresses:

- Detection of all of the type II NADH: menaquinone oxidoreductase homologues within the Actinomycetales groups and also hypothetical homologues.

- Phylogenetical characterisation of the different type II NADH: menaquinone oxidoreductase homologues to better understand the relationships between different Actinomycetales, including mycobacteria, in terms of *ndh* genes with the view of understanding their use as models for *ndh*-targeting drug susceptibility tests.

- Characterisation of *ndh* homologues in mycobacteria in terms of patterns of substitution to try to understand the evolutionary forces acting on them, specifically on the *ndhA* gene of Mtb.

5.2. Methods

5.2.1. Database

In the genome section of NCBI website (http://www.ncbi.nlm.nih.gov/genome/) a search was performed that aimed to detect all the available complete genomes of Actinomycetales. Only genomes that had an available complete draft with annotated genes were used in the following analyses. A total of 98 complete genomes of the Actinomycetales group were retrieved. Additionally, 11 genomes of Actinobacteria that are not from the Actinomycetales group were included for comparison. The latter ones correspond to one genome of each of the different genus in the NCBI database.

In order to locate probable *ndh* genes or its closest homologues (a set of protein sequences sharing a common ancestor) the proteomes of the previously indicated genomes were searched. These proteomes include predicted sequences using software tools and many have unknown functions. A pBLAST (basic local alignment search tool for proteins) search in NCBI using the *ndh* sequence of other organisms outside the Actinobacteria group was carried out. The software performs a search in the defined database of search (in this case each of the individual genomes) and retrieves sequences with similarities providing a statistically significant match helping to identify families of genes. It is important to use sequences outside the Actinobacteria group so that the significance of the sequences detected in the search can be compared in the same way for all the groups. For example, if a sequence of the *ndh* of *Mycobacterium tuberculosis* was used in the query, the obtained score could expectedly be higher for the genus *Mycobacterium*, lower for the sequences in the remaining Corynebacterineae group and even lower for the remaining Actinobacteria. More problematic would be the possibility that an organism acquired an *ndh* sequence from other bacteria outside

the Actinobacteria group by horizontal transmission. Using a standard significance obtained from analysing Actinobacteria, this sequence could be dismissed in the analysis.

The BLAST search was performed using several homologues of *ndh* to increase the confidence of the detection. The query sequences were the following:

- ZP_07101259 from the well-studied model organism *Escherichia coli* (Taxonomy: Bacteria/ Proteobacteria/ Gammaproteobacteria/ Enterobacteriales/ Enterobacteriaceae/ Escherichia) and NP_389111 of *Bacillus subtilis* subsp. subtilis str. 168 (Taxonomy: Bacteria/ Firmicutes/ Bacillales/ Bacillaceae/ Bacillus) were used as representatives of other Bacteria (non-Actinobacteria).
- Sequences NP_213539 and NP_214500 from the *Aquifex aeolicus* VF5 (Taxonomy: Bacteria/ Aquificae/ Aquificales/ Aquificaceae/ Aquifex) were included because they represented the further apart group C of type II NADH: menaquinone oxidoreductase as defined by (Melo et al. 2004). Some preliminary BLAST queries with the other sequences defined here presented low scores for these sequences.
- YP_001581346 of the Archaea *Nitrosopumilus maritimus* SCM1 (Taxonomy: Archaea/ Thaumarchaeota/ marine archaeal group 1/ Nitrosopumilales/ Nitrosopumilaceae/ Nitrosopumilus) in order to use a sequence probably further apart from the first two groups in relation to the Actinomycetales group;
- Sequences CAB52797 and CAB52796 from the plant *Solanum tuberosum* (Taxonomy: Eukaryota/ Viridiplantae/ Streptophyta/ Embryophyta/ Tracheophyta/ Spermatophyta/ Magnoliophyta/ eudicotyledons/ core eudicotyledons/ asterids/ lamiids/ Solanales/ Solanaceae/ Solanoideae/ Solaneae) were included in the query to

represent an even further apart organism from the Actinomycetales, a Eukaryotic organism.

BLAST searches with the query sequences above were performed in the annotated genome of the organisms that included in their proteomes both experimentally-defined and predicted proteins.

Sequences queries retrieved sequences with BLAST scores between 200 and 40. Results were compared between the retrieved sequences with the different queries and a criterion was stipulated to probabilistically define which sequences were *ndh* homologues.

Usually sequences that displayed scores higher than 50 in all the queries and usually more than 100 in one of them were hypothesized to be type II NADH dehydrogenases. Sequences that were not so clearly placed (scores lower than 50 in some of the queries) were further investigated by checking the functional motifs classified by NCBI usually by performing a BLAST search in the entire NCBI database and looking for the closest homologues to that sequence. The placement of a score of 50 as the line of investigation was not random. It is around that point that the BLAST search also indicates mainly ferredoxin reductases and nitrite reductases as possible homologues.

5.2.2. Alignment

Both annotated and hypothetical NADH dehydrogenases were aligned using the software "PROMALS3D multiple sequence and structure alignment server" (Pei et al. 2008). One of the advantages of this multiple alignment software is that it allows the input of secondary structures, taking into account secondary structure prediction as well as the primary

structure. The three-dimensional structure of type II-NADH menaquinone oxidoreductase in *E. coli* was used (Schmid and Gerloff 2004).

Additionally a few sequences outside the Actinobacteria were included in the alignment to better root the Actinobacteria sequences or to better place them in the overall tree (described in Melo et al. 2004) in the Phylogenetic reconstruction. These sequences corresponded to the sequences used in the queries for the BLAST described before as well as the sequences:

- AJ489504 from the Archaea *Acidianus ambivalens* that represents a further group C sequence as described previously (Melo et al. 2004). Another sequence (YP_919639- *ThpenH*) from Archaea *Thermofilum pendens* Hrk 5 was used to better phylogenetically establish group C.

- Apart from the sequence NP_389111 of *Bacillus subtilis* subsp. subtilis str. 168 that was used in the BLAST search, three further homologue sequences were present in this organism (NP_391090, ZP_03592999 and NP_391100).

- Sequence NP_279851 of Archaea *Halobacterium sp.* NRC-1 was included because it was in the root of the group A (Melo et al. 2004).

It is not feasible to show the multiple alignments of more than 300 proteins. Instead, the regions of major conservation of the protein using the WebLogos website (http://weblogo.berkeley.edu/logo.cgi) (Crooks et al. 2004) are shown. Logos are graphic representations of the conservation of a sequence. Alignments are represented by stacks of symbols (amino-acids in this case) whose height is higher or lower depending on how conserved the position is. Additionally within each stack two or more amino-acids can be present with relative height

indicating their frequency within that position (Schneider and Stephens 1990).

5.2.3. Phylogenetic reconstruction

The aligned sequences were run in MrBayes v3.2.1. This software estimates a phylogeny using Bayesian inference (Huelsenbeck and Ronquist 2001). MrBayes uses a Markov Chain Monte Carlo (MCMC) method algorithm. The software performs a number of iterations with the calculated data moving from one state to the other in each step of the chain. The algorithm uses the state of the chain after a large number of iterations to calculate a posterior probability distribution. The confidence in the calculated probability distribution will be higher, the larger the number of iterations. The number of iterations was set to 1,000,000 iterations (or generations in the terms used by the software) however this value can be extended if convergence of the data was not obtained, but this was not the case. The value indicating convergence in the run is the standard deviation of split frequencies. The authors suggest a value below 0.10 to indicate convergence, although the software was run until this value was below 0.05, for better confidence.

The obtained tree with posterior probability of each node in the tree was displayed using FigTree v1.3.1 (http://tree.bio.ed.ac.uk/software/figtree).

5.2.4. Calculation of Ka/Ks using maximum likelihood

Nucleotide sequences encoding proteins are limited by natural selection in the kind of mutations that can occur. In protein coding genes, mutations can be either non-synonymous or synonymous. Synonymous

mutations (Ks or dS) not changing the protein sequence are far more neutral than non-synonymous (Ka or dN) mutations (there are still issues involving codon-usage where one of the codons that code for the same amino acid is preferred in relation to another by the organism). Non-synonymous mutations will alter the protein sequence and the seriousness of mutations will depend on the region of sequence and the differences in properties between the original residue and the new amino acid. Some non-synonymous mutations can be neutral.

Given the outcomes described above, a sequence that is not functional or essential will allow a much more random number of non-synonymous mutations to occur at a much faster rate than in a gene that is functional and essential since natural selection will eliminate the organism where the mutation occurred if this mutation impaired its survival. However the number of mutations observed is dependent on the mutation rate that depends on the organism and region of the genome (Yang 2007). Synonymous mutations on the other hand accumulate almost neutrally and the number of synonymous mutations observed will also depend on the mutation rate. This way, synonymous mutations can be used to scale the number of non-synonymous mutations in the branches and allow comparison using a ratio of non-synonymous to synonymous mutation (Ka/Ks or dN/dS ratio) (Yang 2007). If this value is high when compared to other closely related homologous sequence, it could mean that the gene is accumulating a larger number of non-synonymous mutations than the other. This could mean either that it is possible evidence that the gene might not be essential and natural selection is allowing it to accumulate mutations randomly (Yang 2007). On the other hand, if that value is substantially higher than what would be obtained randomly, it could mean that a series of non-synonymous mutations were selected to persist during evolution and it could be a sign of positive selection. However, instances of positive selection are rare. A low value suggests that

mutations are probably occurring randomly in the gene but damaging non-synonymous mutations were continuously eliminated. For example the Ka/Ks average value per homologous genes between Human and Chimpanzee is 0.23 (Chimpanzee sequencing and analysis consortium 2005).

The software PAML 4 (Yang 2007) was used to calculate dS/dN ratios across clades of the *ndh* tree. This software uses maximum likelihood in the calculations and allows testing for significant differences across this ratio in the tree. Sub-trees of interest from the main tree were selected. One of these sub-trees was the sub-branch containing the Mtb *ndh* and *ndhA* genes to check for differences in their selective pressure.

5.3. Results

5.3.1. Retrieved sequences

A total of 299 sequences were retrieved using the BLAST queries described above. Almost all the retrieved sequences were classified as either "NADH dehydrogenases", "dehydrogenase"," oxidoreductase" and "FAD-dependent pyridine nucleotide-disulfide oxidoreductase". Some were just classified as "Hypothetical protein". All the retrieved sequences within the Actinomycetales group are displayed in Table 5.1.

NCBI also displays probable functional motifs in the description of the protein sequences. From the hypothetical 299 retrieved sequences within the Actinomycetales group 266 (89%) contained the multi-domain motif *ndh* (code: COG1252) defined as "NADH dehydrogenase, FAD-containing subunit: Energy production and conversion" (Marchler-Bauer et al. 2011). 33 (11%) contained the motif HcaD (code: COG0446)

defined as "Uncharacterized NAD(FAD)-dependent dehydrogenases: General function prediction only" (Marchler-Bauer et al. 2011).

As mentioned before a sequence representative of each genus within Actinobacteria outside the Actinomycetales group that is available in NCBI was incorporated for the phylogenetic analysis. The species were the following:

- *Acidimicrobium ferrooxidans* DSM 10331 retrieved sequences YP_003110137, YP_003108805, YP_003108722, YP_003110002) as hypothetical *ndh* homologues;
- *Bifidobacterium animalis* subsp. lactis DSM 10140 and *Gardnerella vaginalis* 409-05 are from the Actinobacteridae group but Bifidobacteriales subgroup did not have any type II NADH dehydrogenase detected;
- *Atopobium parvulum* DSM 20469, *Coriobacterium glomerans* PW2, *Cryptobacterium curtum* DSM 15641, *Eggerthella lenta* DSM 2243, *Olsenella uli* DSM 7084 and *Slackia heliotrinireducens* DSM 20476 from the Coriobacteridae group also did not display any retrievable sequence;
- *Rubrobacter xylanophilus* DSM 9941 from the Rubrobacteridae group displayed sequences YP_643995, YP_643877, YP,_643890 and YP_643877 and *Conexibacter woesei* DSM 14684 from that same group had the sequences YP_003394640 and YP_003396921 detected in the BLAST queries.

The number of the hypothetical *ndh* homologues is not similar across all the Actinomycetales (see Table 5.1.). One thing to take into account is that several bacteria evolved with reduction of the genome as is the case of *Mycobacterium leprae* (Gómez-Valero et al. 2007). It is expected that these smaller genomes will have a lower number of hypothetical *ndh* homologues. In order to obtain a clear picture of the relationship between

genome size of the different Actinomycetales and the number of hypothetical *ndh* homologues, a dispersion graph was drawn (Fig. 5.1.) and a linear regression was calculated.

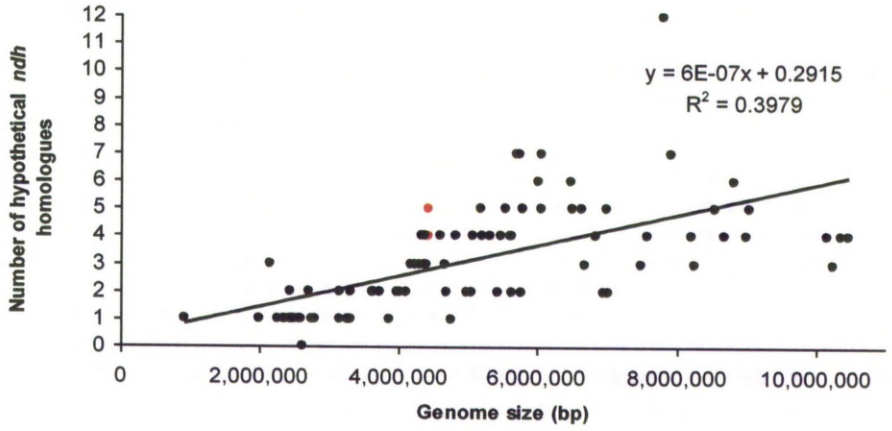

Fig. 5.1.: Relation between the sizes of the genome of the analysed Actinomycetales and the number of hypothetical type II NADH dehydrogenases detected. A regression curve was calculated in order to illustrate the general trend. Data points for the five Mtb strains are shown in red. The lower red dot refers to the overlapping of 4 of the Mtb strains.

The distance between the line and the observed number of hypothetical *ndh* homologues allows one to visualise the ones with the most abnormal number of sequences. A graph of the distance between observed and expected hypothetical number of *ndh* homologues is shown in Fig. 5.2. The expected number of hypothetical *ndh* genes was obtained from the correlation shown in Fig. 5.1. Values above the line (positive) indicate that those species have more hypothetical *ndh* homologues than it was expected from its genome size, and negative values indicate that the strain has lower number of hypothetical *ndh* homologue genes than it was expected from its genome size.

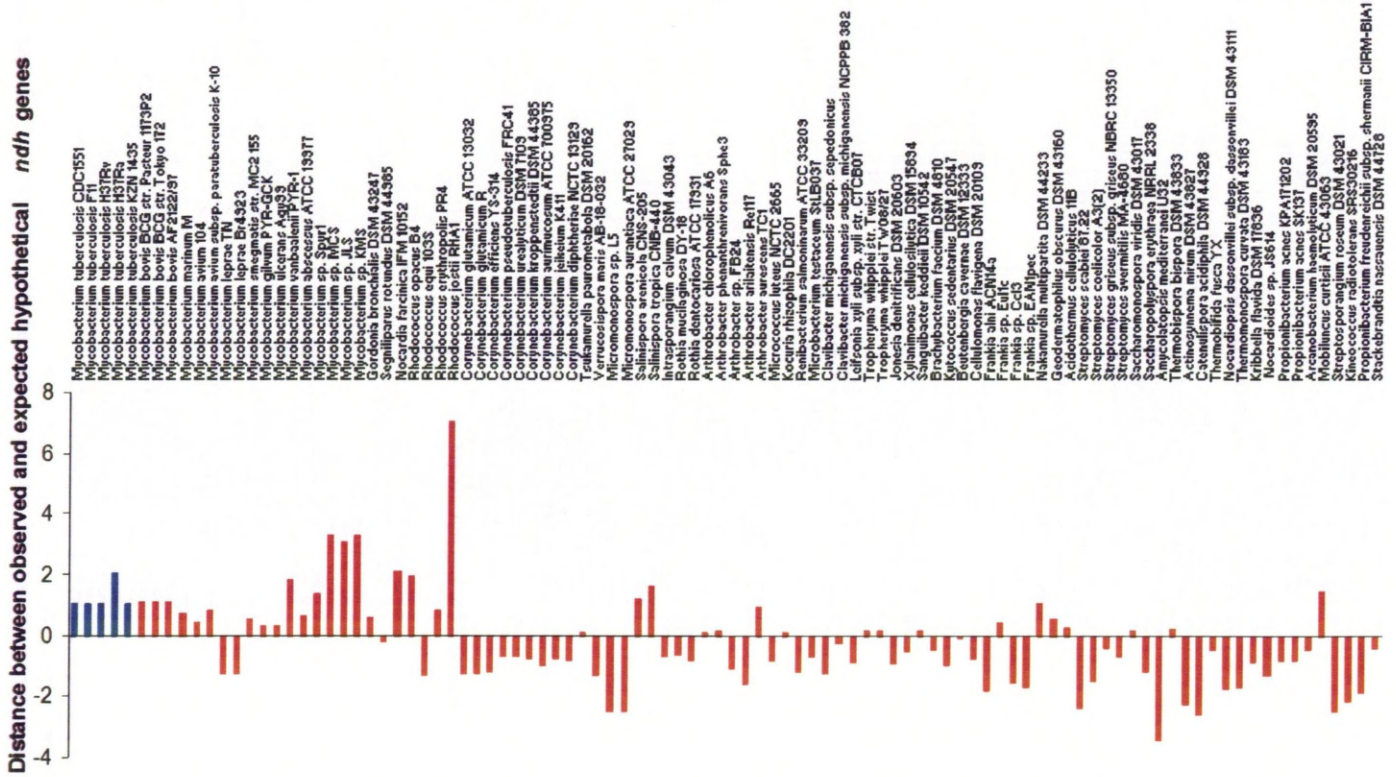

Fig. 5.2.: Differences between the number of observed hypothetical *ndh* genes and the expected value in the correlation with the genome size in the Actinomycetales data. Mtb strains are shown in blue.

Table 5.1.: Actinomycetales strains for which the complete genome is sequenced and annotated and the identified hypothetical type II NADH dehydrogenases. Individuals are further grouped into their taxonomical divisions with Actinomycetales. Genus and species are not indicated as sub-divisions since that information can be obtained from the full strain name. Code refers to 5 to 6 letter denomination of the strain in the phylogenetic analysis.

Group 1	Group 2	Strain	NCBI complete genome reference	Genome length (bp)	Code	Hypothetical Ndh-2 proteins
Corynebacterineae	Mycobacteriaceae	*Mycobacterium tuberculosis* CDC1551	NC_002755	4,403,837	MtbCD	NP_336359 (a), NP_334811 (b), NP_336319 (c), NP_334755 (d)
		Mycobacterium tuberculosis F11	NC_009565	4,424,435	MtbF11	YP_001287819 (a), YP_001286341 (b), YP_001287779 (c), YP_001286281 (d)
		Mycobacterium tuberculosis H37Rv	NC_000962	4,411,532	Mtb37v	NP_216370 (a), NP_214906 (b), NP_216328 (c), NP_214845 (d)
		Mycobacterium tuberculosis H37Ra	NC_009525	4,419,977	Mtb37a	YP_001283183 (a), YP_001283183 (b), ZP_02552610 (c), YP_001283141 (d), YP_001281620 (e)
		Mycobacterium tuberculosis KZN 1435	NC_012943	4,398,250	MtbKZ	YP_003032103 (a), YP_003030315 (b), YP_003032145 (c), YP_003030258 (d)
		Mycobacterium bovis BCG str. Pasteur 1173P2	NC_008769	4,374,522	MboPa	YP_977980 (a), YP_976527 (b), YP_977937 (c), YP_976468 (d)
		Mycobacterium bovis BCG str. Tokyo 172	NC_012207	4,371,711	MboTo	YP_002644928 (a), YP_002643463 (b), YP_002644885 (c), YP_002643405 8d)

		Mycobacterium bovis AF2122/97	NC_002945	4,345,492	MboAF	NP_855537 (a), NP_854061 (b), NP_855494 (c), NP_854002 (d)
		Mycobacterium marinum M	NC_010612	6,636,827	MMaM	YP_001849003 (a), YP_001851025 (b), YP_001852747 (c), YP_001850986 (d), YP_001851031 (e)
		Mycobacterium avium 104	NC_008595	5,475,491	Mav10	YP_882053 (a), YP_883899 (b), YP_883252 (c), YP_880382 (d)
		Mycobacterium avium subsp. paratuberculosis K-10	NC_002944	4,829,781	MavPK	NP_960495 (a), NP_962808 (b), NP_962199 (c), NP_959881 (d)
		Mycobacterium leprae TN	NC_002677	3,268,203	MleTN	NP_302374 (a)
		Mycobacterium leprae Br4923	NC_011896	3,268,071	MleBr	YP_002504004 (a)
		Mycobacterium smegmatis str. MC2 155	NC_008596	6,988,209	MsmM	YP_887924 (a), YP_887761 (b), YP_888708 (c), YP_891023 (d), YP_889682 (e)
		Mycobacterium gilvum PYR-GCK	NC_009338	5,619,607	MgiPY	YP_001134612 (a), YP_001134722 (b), YP_001133196 (c), YP_001132257 (d)
		Mycobacterium ulcerans Agy99	NC_008611	5,631,606	MulAg	YP_906748 (a), YP_908065 (b), YP_906785 (c), YP_906742 (d)
		Mycobacterium vanbaalenii PYR-1	NC_008726	6,491,865	MvaPY	YP_953886 (a), YP_953765 (b), YP_956125 (c), YP_955584 (d), YP_952659 (e), YP_954805 (f)
		Mycobacterium abscessus ATCC 19977	NC_010397	5,067,172	MabAT	YP_001703164 (a), YP_001701869 (b), YP_001704926 (c), YP_001705465 (d)

		Mycobacterium sp. Spyr1	NC_014814	5,547,747	MspSp	YP_004077145 (a), YP_004077259 (b), YP_004075845 (c), YP_004074535 (d), YP_004079565 (e)
		Mycobacterium sp. MCS	NC_008146	5,705,448	MspMC	YP_639964 (a), YP_640044 (b), YP_637884 (c), YP_641429 (d), YP_641431 (e), YP_642468 (f), YP_637532 (g)
		Mycobacterium sp. JLS	NC_009077	6,048,425	MspJL	YP_001071099 (a), YP_001071181 (b), YP_001069003 (c), YP_001072903 (d), YP_001072905 (e), YP_001073944 (f), YP_001068648 (g)
		Mycobacterium sp. KMS	NC_008705	5,737,227	MspKM	YP_938829 (a), YP_938909 (b), YP_936727 (c), YP_940335 (d), YP_940337 (e), YP_941376 (f), YP_936372 (g)
	Gordoniaceae	*Gordonia bronchialis* DSM 43247	NC_013441	5,208,602	GbrDS	YP_003273861 (a), YP_003273525 (b), YP_003275624 (c), YP_003274107 (d)
	Segniliparaceae	*Segniliparus rotundus* DSM 44985	NC_014168	3,157,527	SroDS	YP_003659063 (a), YP_003657611 (b)
	Nocardiaceae	*Nocardia farcinica* IFM 10152	NC_006361	6,021,225	NfaIF	YP_118753 (a), YP_120489 (b), YP_118634 (c), YP_121494 (d), YP_119535 (e),

		Rhodococcus opacus B4	NC_012522	7,913,450	RopB4	YP_002784235 (a), YP_002781616 (b), YP_002777716 (c), YP_002778266 (d), YP_002777428 (e), YP_002782825 (f), YP_002779888 (g)
		Rhodococcus equi 103S	NC_014659	5,043,170	Req10	YP_004005216 (a), YP_004007131 (b)
		Rhodococcus erythropolis PR4	NC_012490	6,516,310 7,804,765	RerPR	YP_002766558 (a), YP_002769033 (b), YP_002767889 (c), YP_002765779 (d), YP_345654 (e)
		Rhodococcus jostii RHA1	NC_008268	7,804,765	RjoRH	YP_704447 (a), YP_707178 (b), YP_707195 (c), YP_708044 (d), YP_700119 (e), YP_701340 (f), YP_705277 (g), YP_705502 (h), YP_707025 (i), YP_708113 (j), YP_708140 (k), YP_704495/YP_7044956 (l)
	Corynebacteriaceae	*Corynebacterium glutamicum* ATCC 13032	NC_006958	3,282,708	CglAT	NP_600682 (a)
		Corynebacterium glutamicum R	NC_009342	3,314,179	CgluR	YP_001138420 (a)
		Corynebacterium efficiens YS-314	NC_004369	3,147,090	CefYS	NP_738203 (a)
		Corynebacterium pseudotuberculosis FRC41	NC_014329	2,337,913	CpsFR	YP_003783415 (a)

		Corynebacterium urealyticum DSM 7109	NC_010545	2,369,219	CurDS	YP_001800457 (a)
		Corynebacterium kroppenstedtii DSM 44385	NC_012704	2,446,804	CkrDS	YP_002906176 (a)
		Corynebacterium aurimucosum ATCC 700975	NC_012590	2,790,189	CauAT	YP_002834822 (a)
		Corynebacterium jeikeium K411	NC_007164	2,462,499	CjeK4	YP_250696 (a)
		Corynebacterium diphtheriae NCTC 13129	NC_002935	2,488,635	CdiNC	NP_939574
	Tsukamurellaceae	*Tsukamurella paurometabola* DSM 20162	NC_014158	4,379,918	TpaDS	YP_003647256 (a), YP_003646293 (b), YP_003645098 (c)
Micromonosporineae	Micromonosporaceae	*Verrucosispora maris* AB-18-032	NC_015434	6,673,976	VmaAB	YP_004403570 (a), YP_004406390 (b), YP_004406809 (c)
		Micromonospora sp. L5	NC_014815	6,962,533	MspL5	YP_004080843 (a), YP_004085189 (b)
		Micromonospora aurantiaca ATCC 27029	NC_014391	7,025,559	MauAT	YP_003834048 (a), YP_003835929 (b)
		Salinispora arenicola CNS-205	NC_009953	5,786,361	SarCN	YP_001535757 (a), YP_001537121 (b), YP_001535195 (c), YP_001539363 (d), YP_001537708 (e)
		Salinispora tropica CNB-440	NC_009380	5,183,331	StrCN	YP_001157760 (a), YP_001158953 (b), YP_001157096 (c), YP_001158798 (d), YP_001158453 (e)

Micrococcineae	Intrasporangiaceae	*Intrasporangium calvum* DSM 43043	NC_014830	4,024,382	IcaDS	YP_004099666 (a), YP_004099509 (b)
	Micrococcaceae	*Rothia mucilaginosa* DY-18	NC_013715	2,264,603	RmuDY	YP_003363283 (a)
		Rothia dentocariosa ATCC 17931	NC_014643	2,506,025	RdeAT	YP_003984264 (a)
		Arthrobacter chlorophenolicus A6	NC_011886	4,395,537	AchA6	YP_002487305 (a), YP_002486923 (b), YP_002489092 (c)
		Arthrobacter phenanthrenivorans Sphe3	NC_015145	4,250,414	AphSp	YP_004242170 (a), YP_004240499 (b), YP_004242412 (c)
		Arthrobacter sp. FB24	NC_008541	4,698,945	AspFB	YP_830646 (a), YP_832713 (b)
		Arthrobacter arilaitensis Re117	NC_014550	3,859,257	AarRe	YP_003915938 (a)
		Arthrobacter aurescens TC1	NC_008711	4,597,686	AauTC	YP_946743 (a), YP_947052 (b), YP_950334 (c), YP_947749 (d)
		Micrococcus luteus NCTC 2665	NC_012803	2,501,097	MleNC	YP_002956596 (a)
		Kocuria rhizophila DC2201	NC_010617	2,697,540	KrhDC	YP_001855630 (a), YP_001856011 (b)
		Renibacterium salmoninarum ATCC 33209	NC_010168	3,155,250	RsaAT	YP_001623507 (a)
		Microbacterium testaceum StLB037	NC_015125	3,982,034	MteSt	YP_004225844 (a), YP_004225398 (b)
		Clavibacter michiganensis subsp. sepedonicus	NC_010407	3,258,645	Cmise	YP_001711109 (a)
		Clavibacter michiganensis subsp. michiganensis NCPPB 382	NC_009480	3,297,891	Cmimi	YP_001223004 (a), YP_001221127 (b)
		Leifsonia xyli subsp. xyli str. CTCB07	NC_006087	2,584,158	Lxyxy	YP_062580 (a)
	Unclassified	*Tropheryma whipplei* str. Twist	NC_004572	927,303	TwhTw	NP_787908 (a)
	Unclassified	*Tropheryma whipplei* TW08/27	NC_004551	925,938	TwhT0	NP_789711 (a)

	Jonesiaceae	*Jonesia denitrificans* DSM 20603	NC_013174	2,749,646	JdeDS	YP_003161865 (a)
	Promicromonosporace	*Xylanimonas cellulosilytica* DSM	NC_013530	3,742,776	XceDS	YP_003327248 (a), YP_003325724 (b)
	Sanguibacteraceae	*Sanguibacter keddieii* DSM 10542	NC_013521	4,253,413	SkeDS	YP_003313140 (a), YP_003313578 (b), YP_003314814 (c)
	Dermabacteraceae	*Brachybacterium faecium* DSM 4810	NC_013172	3,614,992	BfaDS	YP_003156102 (a), YP_003154779 (b)
	Dermacoccaceae	*Kytococcus sedentarius* DSM 20547	NC_013169	2,785,024	KseDS	YP_003149670 (a)
	Beutenbergiaceae	*Beutenbergia cavernae* DSM 12333	NC_012669	4,669,183	BcaDS	YP_002881052 (a), YP_002882152 (b), YP_002883530 (c)
	Cellulomonadaceae	*Cellulomonas flavigena* DSM 20109	NC_014151	4,123,179	CflDS	YP_003636024 (a), YP_003638568 (b)
Frankineae	Frankiaceae	*Frankia alni* ACN14a	NC_008278	7,497,934	FalAC	YP_711866 (a), YP_716365 (b), YP_714488 (c)
		Frankia sp. EuI1c	NC_014666	8,815,781	FspEu	YP_004019631 (a), YP_004014605 (b), YP_004016502 (c), YP_004014403 (d), YP_004016541 (e), YP_004014796 (f)
		Frankia sp. CcI3	NC_007777	5,433,628	GspCo	YP_480088 (a), YP_482997 (b)
		Frankia sp. EAN1pec	NC_009921	8,982,042	FspEA	YP_001509173 (a), YP_001508624 (b), YP_001506817 (c), YP_001507876 (d)
	Nakamurellaceae	*Nakamurella multipartita* DSM 44233	NC_013235	6,060,298	NmuDS	YP_003201686 (a), YP_003199801 (b), YP_003201220 (c), YP_003204224 (d), YP_003199769 (e)
	Geodermatophilaceae	*Geodermatophilus obscurus* DSM 43160	NC_013757	5,322,497	GceDS	YP_003410798 (a), YP_003409005 (b), YP_003408059 (c), YP_003408166 (d)
	Acidothermaceae	*Acidothermus cellulolyticus* 11B	NC_008578	2,443,540	Ace11	YP_873660 (a), YP_872282 (b)

Streptomycineae	Streptomycetaceae	*Streptomyces scabiei* 87.22	NC_013929	10,148,695	Ssc87	YP_003491021 (a), YP_003487438 (b), YP_003490507 (c), YP_003486171 (d)
		Streptomyces coelicolor A3(2)	NC_003888	8,667,507	ScoA3	NP_631162 (a), NP_733592 (b), NP_631374 (c), NP_624494 (d)
		Streptomyces griseus subsp. griseus NBRC 13350	NC_010572	8,545,929	Sgrgr	YP_001825955 (a), YP_001827833 (b), YP_001825418 (c), YP_001825084 (d), YP_001821751 (e)
		Streptomyces avermitilis MA-4680	NC_003155	9,025,608	SavMA	NP_824706 (a), NP_823068 (b), NP_821600 (c), NP_825286 (d), NP_821985 (e)
Pseudonocardineae	Pseudonocardiaceae	*Saccharomonospora viridis* DSM 43017	NC_013159	4,308,349	SviDS	YP_003132731 (a), YP_003135017 (b), YP_003133661 (c)
		Saccharopolyspora erythraea NRRL 2338	NC_009142	8,212,805	SerNR	YP_001103119 (a), YP_001103375 (b), YP_001103666 (c), YP_001105181 (d)
		Amycolatopsis mediterranei U32	NC_014318	10,236,715	AmeU3	YP_003767388 (a), YP_003770286 (b), YP_003768320 (c)
		Thermobispora bispora DSM 43833	NC_014165	4,189,976	TbiDS	YP_003652125 (a), YP_003653714 (b), YP_003653783 (c)
	Actinosynnemataceae	*Actinosynnema mirum* DSM 43827	NC_013093	8,248,144	AmiDS	YP_003098497 (a), YP_003099605 (b), YP_003103613 (c)
Catenulisporineae	Catenulisporaceae	*Catenulispora acidiphila* DSM 44928	NC_013131	10,467,782	CacDS	YP_003112856 (a), YP_003111408 (b), YP_003110948 (c), YP_003117794 (d)
Streptosporangineae	Nocardiopsaceae	*Thermobifida fusca* YX	NC_007333	3,642,249	TfuYX	YP_288493 (a), YP_289011 (b)

		Nocardiopsis dassonvillei subsp. dassonvillei DSM 43111	NC_014210	5,767,958	Ndada	YP_003678033 (a), YP_003681170 (b)
	Thermomonosporaceae	*Thermomonospora curvata* DSM	NC_013510	5,639,016	TcuDS	YP_003299295 (a), YP_003298665 (b)
	Nocardioidaceae	*Kribbella flavida* DSM 17836	NC_013729	7,579,488	KflJS	YP_003383495 (a), YP_003382990 (b), YP_003381730 (c), YP_003378991 (d)
		Nocardioides sp. JS614	NC_008699	4,985,871	NspJS	YP_925473 (a), YP_924225 (b)
Actinomycineae	Actinomycetaceae	*Arcanobacterium haemolyticum* DSM 20595	NC_014218	1,986,154	AhaDS	YP_003697502 (a)
		Mobiluncus curtisii ATCC 43063	NC_014246	2,146,480	McuAT	YP_003718315 (a), YP_003718312 (b), YP_003719267 (c)
Streptosporangineae	Streptosporangiaceae	*Streptosporangium roseum* DSM 43021	NC_013595	10,341,314	SroDS	YP_003338799 (a), YP_003343960 (b), YP_003340434 (c), YP_003340656 (d)
Kineosporiineae	Kineosporiaceae	*Kineococcus radiotolerans* SRS30216	NC_009664	4,761,183	KraSR	YP_001360750 (a)
Propionibacterineae	Propionibacteriaceae	*Propionibacterium freudenreichii* subsp. shermanii CIRM-BIA1	NC_014215	2,616,384	Pfrsh	-
		Propionibacterium acnes KPA171202	NC_006085	2,560,265	PacKA	YP_054868 (a)
		Propionibacterium acnes SK137	NC_014039	2,495,334	PacSK	YP_003580355 (a)
Glycomycineae	Glycomycetaceae	*Stackebrandtia nassauensis* DSM 44728	NC_013947	6,841,557	SnaDS	YP_003510388 (a), YP_003513083 (b), YP_003508890 (c), YP_003510872 (d)

The organism that presents the most abnormal number of possible *ndh* homologues in this study is *Rhodococcus jostii* RHA1 that was described as a catabolic powerhouse in an O_2-rich environment (McLeod et al. 2006), followed by the strains of *Mycobacterium sp.* However, not all the genes necessarily code NADH dehydrogenases or are functional. For example, the hypothetical proteins YP_704495 and YP_704496 of *Rhodococcus jostii* RHA1 (Table 5.1.) are a single typical *ndh* sequence that has been separated by a mutation generating a STOP codon halfway, possibly suggesting that it was not an essential copy. In this study, *Amycolatopsis mediterranei* U32 is the organism with the lowest number of *ndh* homologues considering its genome size , mainly because it presents one of the larger bacterial genomes sequenced so far (Zhao et al. 2010).

Mtb strains contained four hypothetical *ndh* homologues, not only the *ndh* and the *ndhA* genes, but also two other sequences that differ greatly from these but showed some significant degree of homology to the sequences used in the queries. Mtb strain H37Ra actually has two exact copies of the *ndh* gene according to the BLAST search (YP_001283183 and YP_001281620 in Table 5.1.), which could represent a very recent duplication, possibly even in its laboratory life since it is not present in the other four strains. *M. smegmatis* that is sometimes used as a model organism for the study of Mtb (Chapter 2) contained 5 hypothetical *ndh* homologues (Table 5.1. and Fig. 5.1.).

5.3.2. Alignment

The Logo (Crooks et al. 2004) representing the obtained alignment is shown in Fig. 5.3. It can be seen that some regions contained a much higher level of conserved residues partly corresponding to the multi-

domain motif *ndh* (code: COG1252) (Marchler-Bauer et al. 2011). The red and blue lines below each of the lines of the Logo correspond to the regions of the general alignment that contains the Mtb *ndh* and *ndhA* respectively.

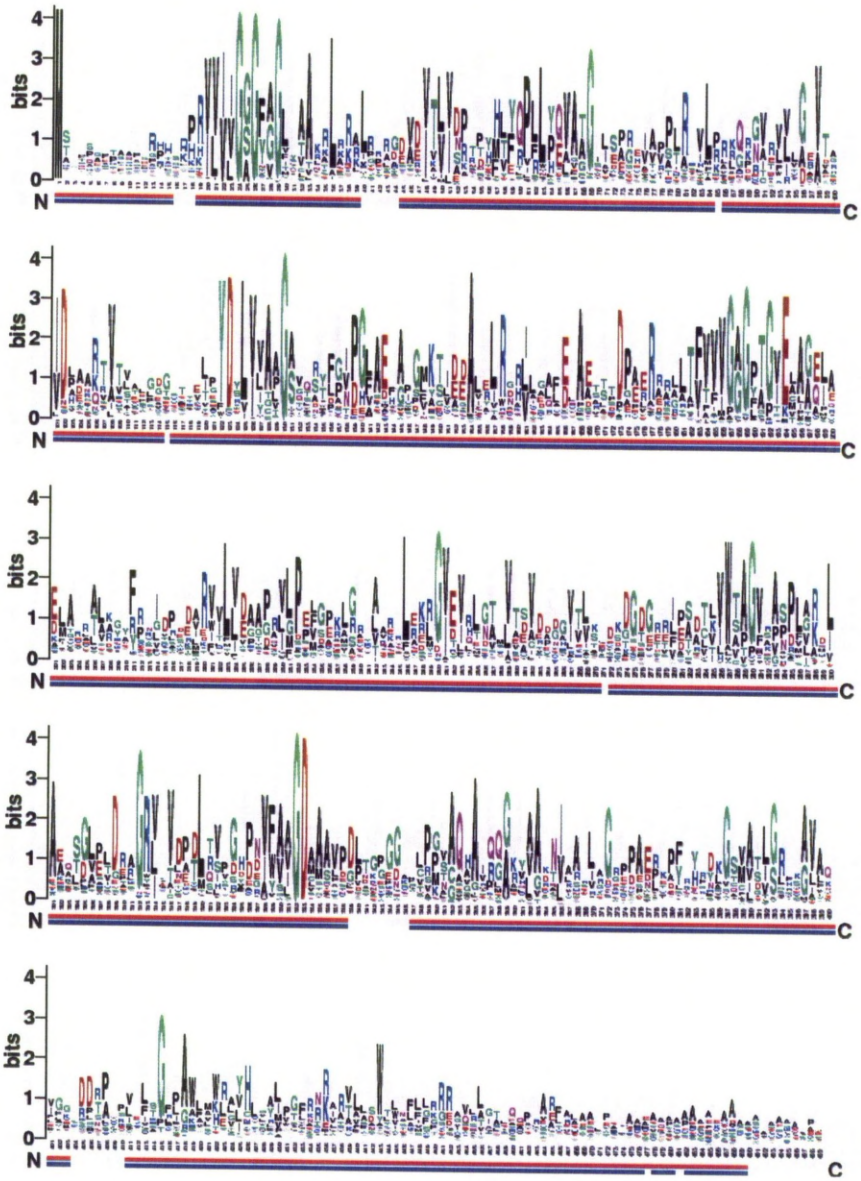

Fig. 5.3.: Logo of the alignment of proteins encoded by the different hypothetical *ndh* genes. Red and blue line below each section represented the common region with the *ndh* and *ndhA* protein products, respectively. Each lane represents 100 amino-acids of the overall alignment.

All the *ndh* proteins contain a motif GXGXXG for NAD(P)H binding. This is displayed in positions 24 to 29 of the alignment. A second one is present in most of the *ndh* protein sequences and is displayed in positions 187 to 192 of the alignment. Other highly conserved residues are observed in the alignment. The region of the alignment 120-130 presents a series of highly conserved amino-acids. Another important feature is the total conservation of the amino-acids Glycine-Aspartic Acid in positions 332-333 of the alignment (Fig. 5.3.).

5.3.3. Phylogenetic reconstruction

Phylogenetic reconstruction was performed using the part of the molecule that was alignable between all the available sequences. In order not to lose a portion of the sequence in the analysis a few sequences were excluded:

- NP_821985 (SavMAe) from *Streptomyces avermitilis* MA-4680 does not contain about 25 residues of the homologue sequence in the beginning of the alignment. A pBLAST search indicated that the most similar sequences in the alignment were YP_003340434 (SroDSc) from *Streptosporangium roseum* DSM 43021 and YP_956125 (MvaPyc) from *Mycobacterium vanbaalenii* PYR-1 and both contain this homologous region.

- YP_001507876 (FspEAd) from *Frankia sp.* EAN1pec is the smaller protein sequence in the alignment (299 residues). Although it shows homology to the remaining sequences in the beginning and end of the sequence, it lacks a great portion of the alignable region in the middle of the alignment (about 100 aa). A BLAST search indicates that it is more similar to the sequence

YP_003112856 (CacDSa) of *Catenulispora acidiphila* DSM 44928.

- YP_002765779 (RerPRd) from *Rhodococcus erythropolis* PR4 lacks about 50 residues of the homologous sequence. A BLAST search indicates that the sequence is similar to the sequence YP_001852747 (MmaMc) in *Mycobacterium marinum* M and sequence YP_908065 (MulAgb) of *Mycobacterium ulcerans* Agy99.

The obtained phylogenetic tree is displayed in two formats in Figs. 5.4. and 5.5. showing the two groups described by Melo et al. 2004 as well as two other possible sub-branches. Showing all the information in a single tree is difficult considering the number of stains involved, so in Fig. 5.4. the posterior distribution of each node was displayed and in Fig. 5.5. the code for each of the *ndh* homologues in the strains was shown. Also although Fig. 5.5. allows a clearer visualization of the phylogeny, Fig 5.4. shows a more traditional format. Fig. 5.6. displays the same tree format as in Fig. 5.5. but focusing on the taxonomy of the strains from which the *ndh* genes were extracted.

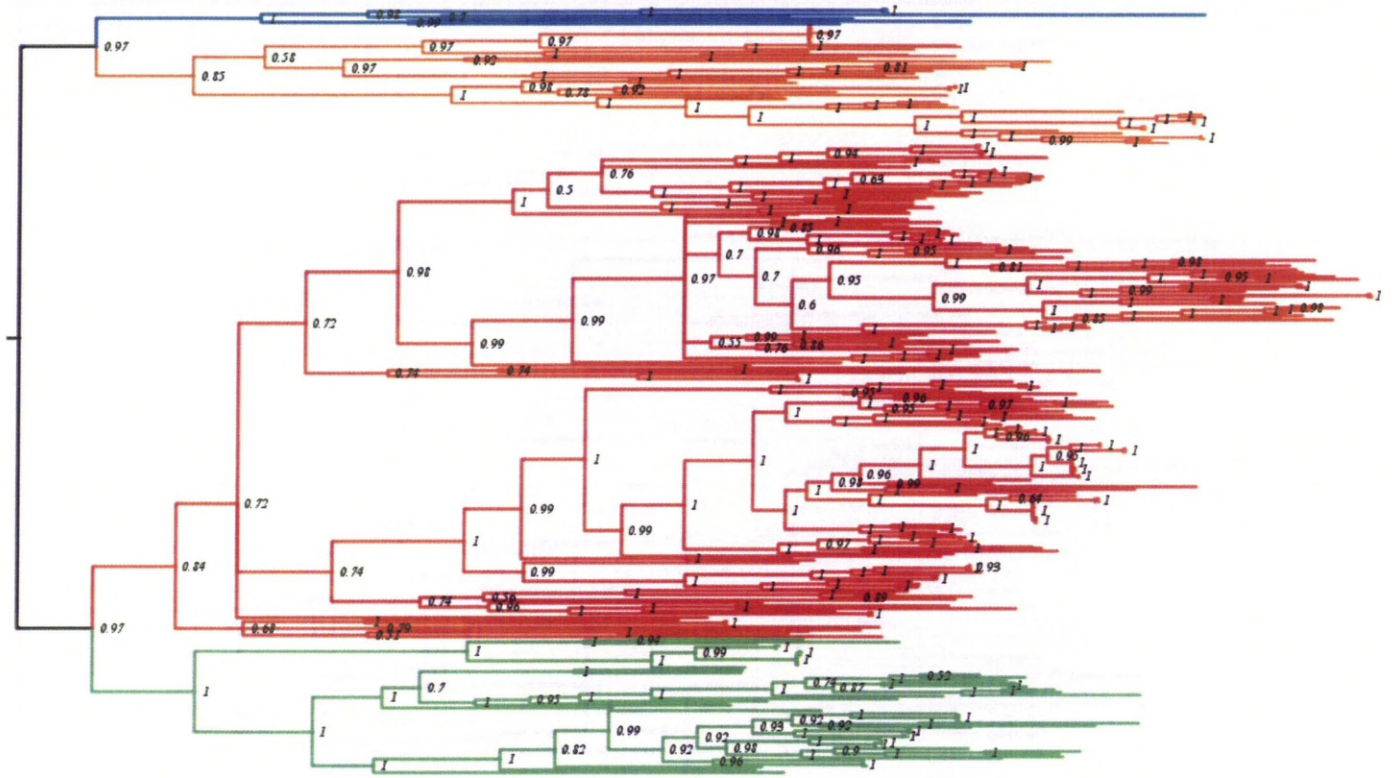

Fig. 5.4.: Phylogenetic tree of the hypothetical type II NADH dehydrogenase homologues in Actinomycetales. Red branch corresponds to group A as described by Melo and colleagues (Melo et al. 2004), Blue branch to group C and orange and green branches correspond to new possible sub-branches. Numbers in nodes correspond to the posterior probability of the nodes.

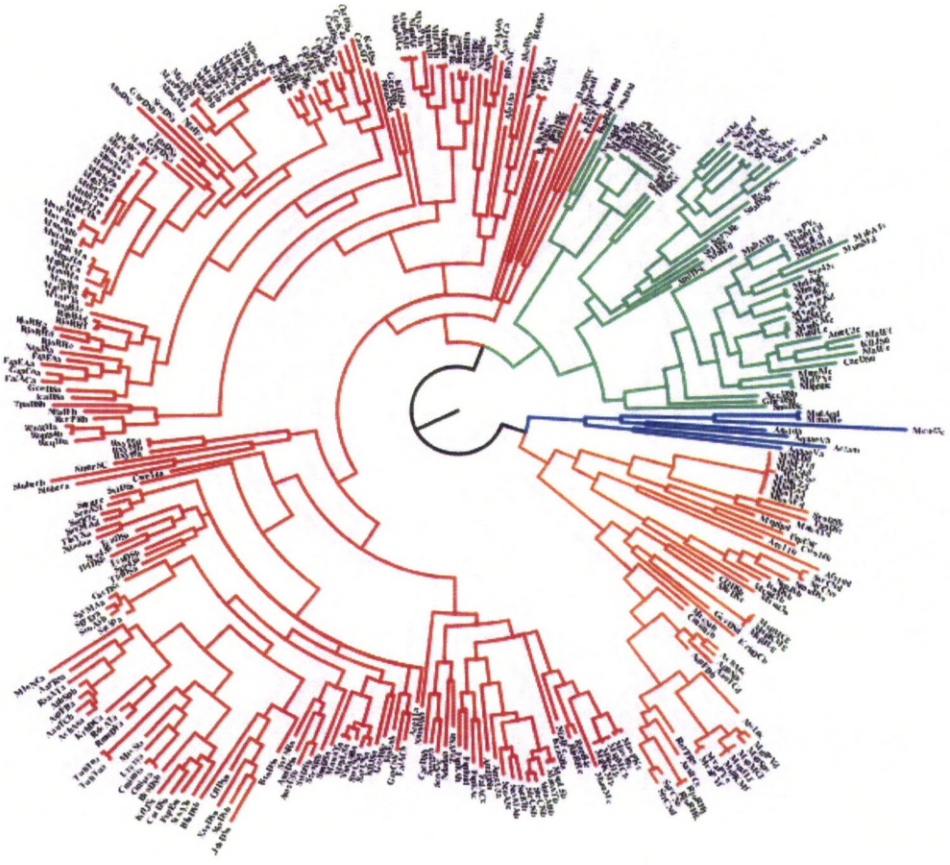

Fig. 5.5.: Phylogenetic tree of the hypothetical type II NADH dehydrogenase homologues in Actinomycetales. Red branch corresponds to group A described by Melo and colleagues (Melo et al. 2004), Blue branch to group C and orange and green branches correspond to new possible sub-branches. Codes of the proteins according to Table 5.1. are indicated in the tips of the branches.

The phylogenetic analysis divided the data into four main groups: one in red in Figs. 5.4 and 5.5 and by far the largest one corresponds to group A of Melo et al. 2004. Species in Actinomycetales mainly possess *ndh* homologues from group A. The group C defined by the authors is typical of hyper-thermophilic prokaryotes and only contains the first GXGXXG NAD(P)H binding motif. It is only present in 3 sequences in all the 299 hypothetical sequences (YP_003719267 of *Mobiluncus curtisii* ATCC 43063, YP_906742 of *Mycobacterium ulcerans* Agy99, YP_001851031 of *Mycobacterium marinum* M).

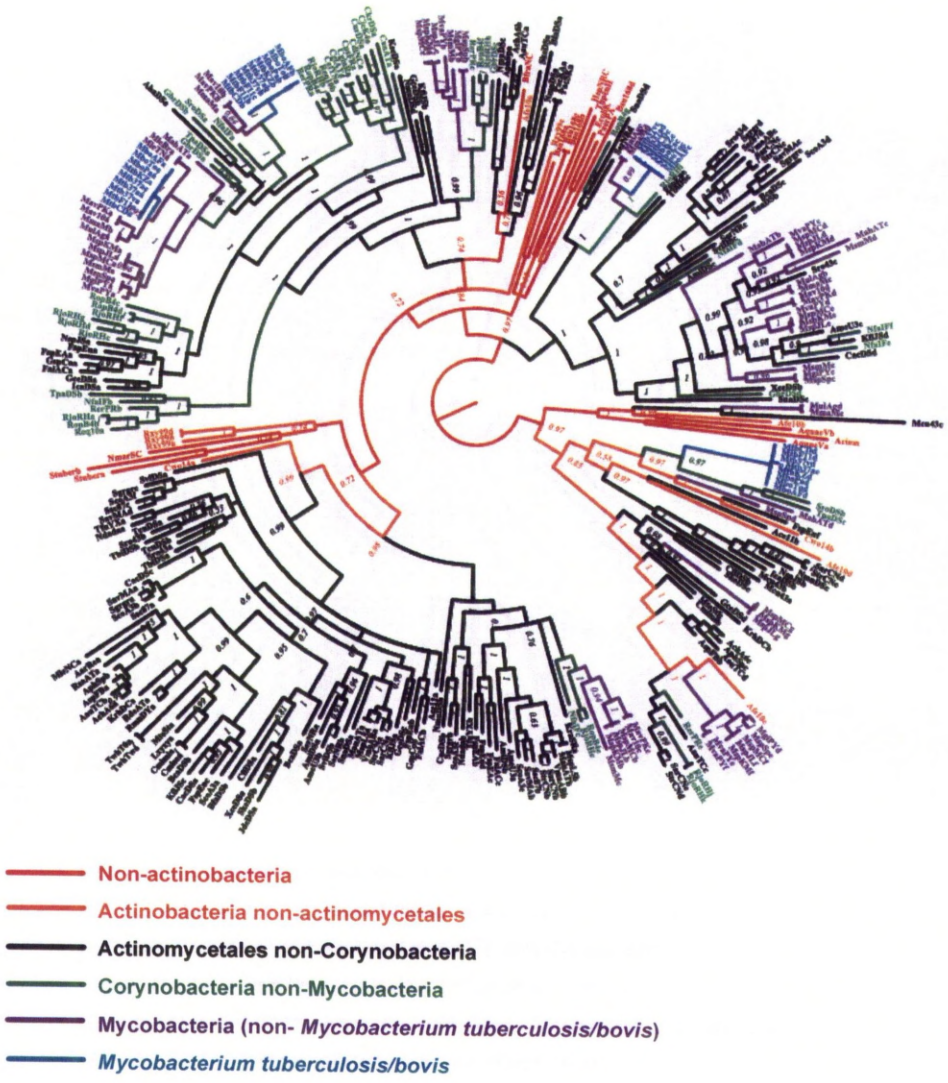

Fig. 5.6.: Phylogenetic tree of the hypothetical type II NADH dehydrogenase homologues in Actinomycetales. *Mycobacterium tuberculosis/bovis*, other mycobacteria, other corynebacteria, Actinomycetales non-corynebacteria, remaining Actinobacteria and other organisms are indicated in the tree in different colours.

5.3.4. Group D

In relation to the tree by Melo et al. 2004, two other groups show up as sister groups to A and C. For the purpose of making things easier throughout the results and discussion the sister group to group C is labelled as group D (in orange in Fig. 5.5 and 5.6). This group contains an intertwining of genes or predicted genes that either contain the motif COG1252 "NADH dehydrogenase, FAD-containing subunit: Energy production and conversion" (Marchler-Bauer et al. 2011) or the retrieved genes with the motif COG0446: "Uncharacterized NAD(FAD)-dependent dehydrogenases: General function prediction only" (Marchler-Bauer et al. 2011). This shows that sequences with the motifs COG1252 and COG0446 are indistinguishable when analysed evolutionarily.

Most of the *Mycobacterium* sp. strains possess two possible homologues within this group and corynebacteria (including mycobacteria) are not well represented here. *Mycobacterium tuberculosis/bovis* however possess a hypothetical homologue (Fig. 5.6.). None of the mycobacteria or corynebacteria strains that showed proximity in group A (see below) present a similar copy of this homologue. It could mean that the other mycobacteria lost the gene during evolution or that the gene was acquired by the common ancestor of the Mtb complex. The analysis of Becq and colleagues actually indicated that this is a probable *Mycobacterium tuberculosis* complex-specific genomic island acquired by horizontal transfer (Becq et al. 2007).

5.3.4. Group E

The most common group A presented a sister group in the analysis that is labelled as group E (in green in Fig. 5.4. and 5.5.). Contrarily to the new hypothetical group D described previously almost all the mycobacteria have a homologue in this clade with nearly all of them clustering together. However Mtb has a homologue quite divergent from the ones presented in the other mycobacteria, with the exception of *Mycobacterium marinum* and *Mycobacterium ulcerans* that present two homologues in this group E. One clusters with the gene from the remaining mycobacteria and another closely related with the homologue present in Mtb.

5.3.5. Group A

This group defined by Melo et al. 2004 is the most common one and it is found in almost all Prokaryotic and in some Eukaryotic organisms.

Apart from a couple of exceptions, all the sequences outside of the Actinomycetales that were placed in the analysis in order to contextualize the Actinomycetales sequences (described in section 5.2.2) present a more basal position in the tree (sequences in red and orange in Fig. 5.6. and 5.7.). The Actinomycetales mostly cluster together (Fig. 5.7). The Actinomycetales variation further divides into two well-defined major subclades (group A and B in Fig. 5.7). One, group A in Fig. 5.7. mainly contains Actinomycetales that are not corynebacteria (more than 90% of the sequences of the sequences in this sub-group) while the other (group B) mainly contains corynebacteria (around 86% of the sequences), suggesting that the separation between corynebacteria and the other Actinomycetales might represent the first or one of the first major evolutionary splits within the Actinomycetales group. Caution should be

exercised about general inferences regarding separation of groups since this corresponds to the analysis of a type of gene and not the overall genome of the strains.

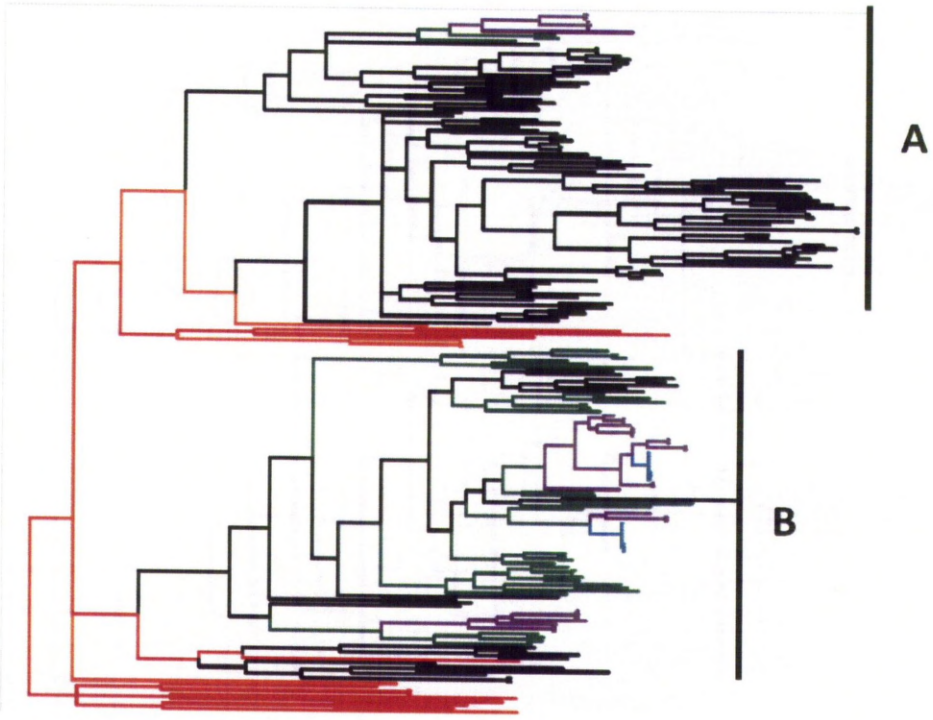

Fig. 5.7.: Phylogenetic tree of the group A (Melo et al 2004) of type II NADH dehydrogenase in Actinomycetales. *Mycobacterium tuberculosis/bovis* specifically, other mycobacteria, other corynebacteria, Actinomycetales non-corynebacteria, remaining Actinobacteria and other organisms are indicated in the tree and the colour code is the same as in the tree in Fig. 5.6. from which this sub-tree is an extracted part. Two groups are indicated (A and B) representing the two groups that contain Actinomycetales.

The analysis also shows mycobacteria almost confined to specific sub-clades. The largest one of these contains the *ndh* gene of Mtb. This gene is evolutionarily closer to its equivalent in *M. avium*, *M. marinum* and *M. ulcerans* followed by *M. leprae*. The *ndh* gene of *M. smegmatis* and other mycobacteria are contained in this clade but evolutionarily more distant than the previous ones. A second clade represented by homologues in mycobacteria contains the Mtb *ndhA* gene. *M. avium* and *M. marinum*

also possess close homologues to the Mtb *ndhA*. This is the only instance in the tree where the *M. marinum* gene is not closely accompanied by an equivalent in *M. ulcerans*. It happens in the other four analysed genes of *M. marinum* suggesting that most probably it was recently lost from its genome. *M. leprae* does not contain a corresponding copy but genome reduction is the rule in the evolution of this species (Gómez-Valero et al. 2007). These species (Mtb, *M. avium, M. leprae, M. ulcerans, M. marinum*) appear together in the common *ndh* homologue and although they use different hosts they are all pathogenic to some extent, suggesting that this *ndh* clade might represent an evolutionary clade where acquisition of pathogenicity occurred.

ndhA is a closely related copy of the common *ndh*. Phylogenetically it is closer to the regular *ndh* gene of all mycobacteria suggesting it was the result of a gene copy in an ancestor. The fact that it is not present in all mycobacteria is most probably due to gene loss during their evolution. The fact that some corynebacteria (and even one Actinomycetales non-corynebacteria) also appear intertwined in the mycobacteria *ndh/ndhA* clade (Fig. 5.6 and 5.7) might suggest that this duplication actually occurred in an ancestor corynebacteria, but their presence in the *ndh/ndhA* clade might be caused by horizontal transfer, incorrect taxonomy of the species or erroneous phylogenetic reconstruction (although the overall clade has a probability of 100% in the analysis (Fig. 5.5 and 5.6)). Horizontal gene transfer in bacteria is known to be a common process involving plasmid exchange and this occurs even between evolutionary distinct strains (Barlow 2009).

The *M. smegmatis* used as a model organism for Mtb studies (Chapter 2) showed 5 hypothetical *ndh* homologues (Table 5.1) and usually evolutionarily very distant from the Mtb clades (the *ndh* homologue described in this section is the closest relative) (Fig 5.5 and 5.6), again suggesting that it is a bad model organism when dealing with ETC.

5.3.6. Similarities between the 4 hypothetical *ndh* homologues in Mtb

After performing the search with the queries, four hypothetical *ndh* homologues arose in Mtb. Two were the known *ndh* and *ndhA*, while two others are unidentified genes with predicted function only. In the UniProt database (http://www.uniprot.org/) they are both classified as "FAD-dependent pyridine nucleotide-disulphide oxidoreductase" (IPR013027) and "Pyridine nucleotide-disulphide oxidoreductase, FAD/NAD(P)-binding domain" (IPR023753), similar to the *ndh* and *ndhA* genes. The overall similarities of the 4 *ndh* Mtb homologueswere checked to see if they were in the range of the observed in other type II NADH: menaquinone oxidoreductase genes, when compared with the known *E. coli* gene and also with a sequence from group C, *Acidianus ambivalens*. The percentage of identity of the different type II NADH: menaquinone oxidoreductase described by Melo et al 2004 when compared with the *E. coli* homologue varied between 12 and 54% (Melo et al. 2004). The four hypothetical *ndh* homologues in Mtb had percentage of identities in relation to *E. coli* varying between 15 and 24% (Table 5.2.). *ndh* and *ndhA* have the highest percentage of similarity to *E. coli* since they are from group A, followed by the *ndh* homologue from the clade E that it was presented as a sister clade of group A in the phylogenetic analysis (Fig. 5.4 and 5.5). The *ndh* homologue in clade D, a sister clade of clade C in the phylogeny (Fig. 5.4 and 5.5), had a level of similarity comparable to the representative of group C included (*A. ambivalens*). The level of similarity supports the obtained phylogeny and indicates that the levels of similarity are within the perceived for an *ndh* homologue.

Table 5.2.: Percentage of identity between the *ndh* gene of *E. coli*, *A. ambivalens* and the four hypothetical *ndh* homologues of Mtb (*ndh*, *ndhA*, *ndh-E* and *ndh-D*).

	E. coli	*ndh*	*ndhA*	*ndh-E*	*ndh-D*	*A. ambivalens*
E. coli	100	24	24	19	15	15
ndh		100	63	20	18	10
ndhA			100	19	16	16
ndh-E				100	21	16
ndh-D					100	20
A. ambivalens						100

A protein distance matrix (ProtDist) that takes into account the distance between the different amino-acids in a position was also calculated using the Bioedit Software (Hall 1999). The results are displayed in Table 5.3.

Table 5.3.: Protein distances between the *ndh* gene of *E. coli*, *A. ambivalens* and the four hypothetical *ndh* homologues of Mtb (*ndh*, *ndhA*, *ndh-E* and *ndh-D*).

	E. coli	*ndh*	*ndhA*	*ndh-E*	*ndh-D*	*A. ambivalens*
E. coli	0.0000	2.7820	2.7366	3.4730	3.9874	4.3692
ndh		0.0000	0.7940	3.3216	3.8134	4.5462
ndhA			0.0000	3.2657	3.9119	4.7834
ndh-E				0.0000	3.8402	4.0378
ndh-D					0.0000	3.3614
A. ambivalens						0.0000

The results are very similar to the ones obtained with the percentage of similarity. *ndh* and *ndhA* of Mtb are more similar to the *ndh* of *E. coli* followed by *ndh-E*. *ndh-D* appears more similar to the *ndh* of Mtb and *E. coli* genes than the group C sequence included (*A. ambivalens*).

5.3.7. Rates of non-synonymous *vs.* synonymous mutations

As mentioned in the methodology the Ka/Ks ratio or dN/dS ratio allows one to detect selection on genes. The basic idea is that a low non-synonymous to synonymous ratio would mean that purifying selection is acting on the genes eliminating many of the new originated non-synonymous mutations. A higher ratio could either mean that the gene is under positive selection or that the purifying selection is relaxed or inexistent, a scenario that could happen if the gene is not necessary or it is an unused copy.Usually a dN/dS ratio of one or close to that value is usually considered a signal of relaxed negative selection probably indicating that the gene is non-functional.

Running the entire tree in a Maximum Likelihood analysis, including the alternative analysis required, would take several months for each of the analyses. For that reason a few representative branches of interest were selected. These include the branches where Mtb *ndh* hypothetical homologues are present. Also a major branch that contains the only copy of *ndh* homologues in some of the Actinomycetales studied and that are undoubtedly *ndh* homologues (Group A) was included as a control to obtain an independent dN/dS ratio.

The selected clades are indicated in Fig. 5.8. The green section is part of the group A and contains the *ndh/ndhA* clade of Mtb (portion A of Fig. 5.7). The red section is another part of group A that does not contain mycobacteria representatives (portion B of Fig. 5.7). The yellow section corresponds to group E. The blue section corresponds to the part of group D that contains Mtb representatives.

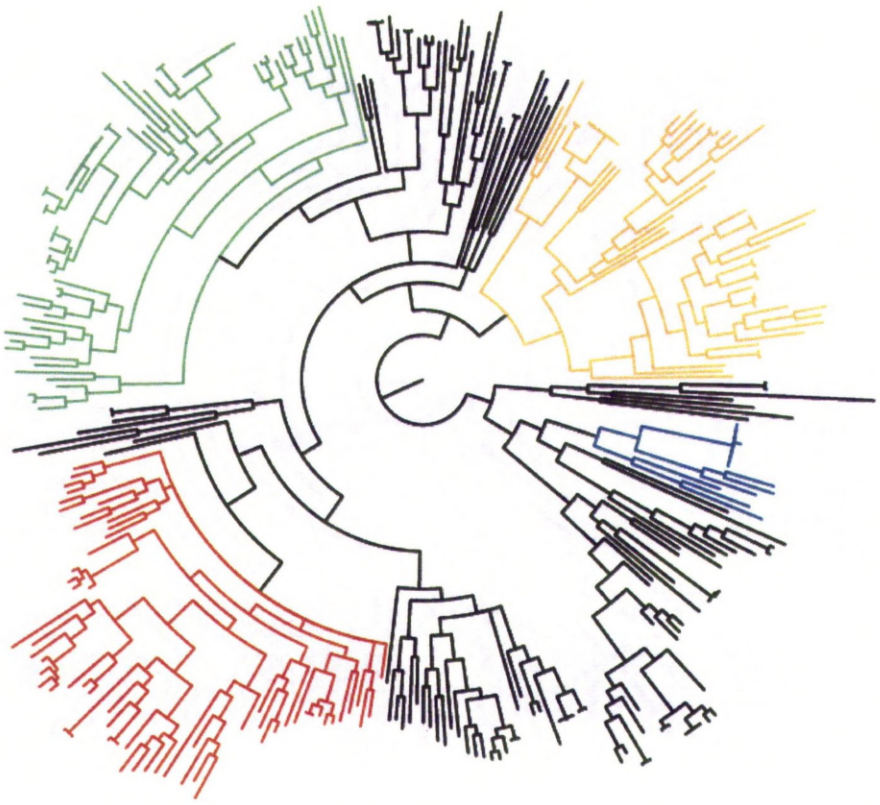

Fig. 5.8.: Phylogenetic tree of hypothetical *ndh* homologues in Actinomycetales indicating groups used in the dN/dS analysis in red (Group A control), green (Group A – *ndh* and *ndhA*), orange (group E) and blue (Group D). Branches in black represent groups sequences not used in the dN/dS analysis.

The results for the dN/dS ratio of the four sub-trees are shown on Table 5.4.. Except for the case of the control the Mtb homologue branches were investigated to check if they had a different behaviour from the remaining sub-tree (for example recent relaxation of selection meaning higher dN/dS). This was done by stipulating that the branch with the Mtb homologue has a different dN/dS ratio from the remaining tree. The software also allows a comparison between this analysis and the analysis considering a single dN/dS ratio using a test named likelihood ratio test (Felsenstein 1981) that provides a p-value of significance (Table 5.4).

This indicates if the Mtb branch in each analysis is significantly different from the remaining tree.

Table 5.4.: dN/dS ratios for four separate sub-trees. Trees with Mtb homologues were also run stipulating two ratios. A likelihood ratio test (LRT) was used to calculate significance values between both analyses.

	Single dN/dS ratio	Two dN/dS ratios		
Clade	**Overall tree**	**Mtb branch**	**Remaining tree**	**LRT p-value**
Group A Control	0.05995	-	-	-
Group A *ndh*	0.06463	0.04512	0.06580	0.077
Group A *ndhA*		0.06819	0.06455	0.853
Group D	0.02188	0.05885	0.02153	0.597
Group E	0.07877	0.06263	0.08054	0.124

Most of the dN/dS estimates indicate a value around 0.06. Group D presents overall dN/dS ratio of just above 0.02 and group E presents a value close to 0.08. These differences are probably caused by chance. Overall the values are very similar and all very far from 1. Values between 0.02 and 0.08 indicate a strong effect of purifying selection which just acts on genes whose alteration would decrease the probability of survival of the organism. It can be seen that all the 4 individual branches of possible *ndh* homologues have even more similar dN/dS ratios (0.04512 to 0.06819), suggesting that the four genes are under similar levels of selective pressure. Also the dN/dS ratio in the Mtb branches was never significantly different from the one in the remaining sub-clades.

In order to provide evidence that the methodology would be efficient in detecting non-functional genes it was tested in a gene that has been suggested to be a pseudogene. One such case is the adenylyl cyclase gene that is only present in some of the tuberculosis complex strains. It is

thought to be a pseudogene in Mtb but actually functional in other *Mycobacterium* species, namely *M. avium* (Shenoy et al. 2005). A sub-set of sequences of this clade were extracted from mycobacteria from NCBI (YP_001133357, YP_001852602, YP_904378, EGO37700, YP_880496, YP_641253, NP_215636, NP_854807, ZP_06798993 and YP_004744585) and submitted the sequences to the same methodology described previously (reconstruction with MrBayes and calculations in PAML of dN/dS ratios). The overall dN/dS ratio of the tree was 0.10343. When calculating the ratio in the Mtb branch against the remaining tree the value was of 0.69314 against 0.05096 with the comparison of the analyses yielding a significant difference (LTR $p=4.213 \times 10^{-14}$). The value for the remaining tree was clearly in the range of what was obtained for the hypothetical *ndh* homologues sub-trees but the value for the Mtb branch was about 10 times higher suggesting that the Mtb branch was accumulating 10 times more non-synonymous mutations than the average analysed mycobacteria genes suggesting lower selective pressure in Mtb. Considering that the gene is thought to be functional in *M. avium* the individual dN/dS ratio for that branch was calculated and it yielded the value of 0.04920 in line with the possible *ndh* homologues.

5.4. Discussion

While in eukaryotic organisms, specially animals, where horizontal transfer does not occur and the history of the genes can provide a good approximation to the history of the species, in bacteria a given strain can easily acquire the gene of another relatively distant species and it will appear phylogenetically proximal when studying that gene (Philippe and Douady 2003). Horizontal transfer is known in Mtb genomes (Becq et al. 2007) and even eukaryotic genes might have been incorporated in the Mtb genome (Gamieldien et al. 2002). Recombination between strains has also been hypothesized as a force in shaping the Mtb genome (Liu

and Gutacker 2006). However some possible cases are obtained from the evolutionary history of the genes. In this work an extensive search of all possible *ndh* homologues within the available complete genome of Actinomycetales as well as on other Actinobacteria was carried out in order to establish an evolutionary history of the genes in this group. Melo and collaborators performed an evolutionary analysis in a wide group of bacteria that contained only three Actinomycetales (Melo et al. 2004). At least one *ndh* homologue is present in most of the Actinomycetales species. Here a phylogenetic analysis using Bayesian analysis in MrBayes was carried out. This is a character-based method where the phylogeny obtained is based on a pattern of shared amino-acid changes that is shared between a given group. In the case of distance-based methods like the neighbour-joining one used by Melo and collaborators (Melo et al. 2004) phylogenies are based on a matrix of genetic distances where evolutionary relationships could be totally mixed due to different mutation rates of the different species or region of the genome. The two main groups described by (Melo et al. 2004), group A (containing B) and C are well defined considering the long distance between the two, but for more detailed and well-defined relationships between sequences within a group, a more powerful phylogenetic analysis is required like the one employed here. Almost all the Actinomycetales had an *ndh* homologue from group A. One interesting point is that there is a possible split between the corynebacteria group (that includes mycobacteria) and the remaining Actinomycetales (Fig. 5.6 and 5.7). There are exceptions in the phylogeny for the described group relationships that may be due to the occurrence of horizontal transfer, erroneous phylogenetic reconstruction and taxonomic misclassification. Hence studies of evolutionary relationships between organisms should be performed in overall genomes or at least a set of genes, and not on a single gene or family of genes. Within the clade containing mainly corynebacteria two *ndh* of Mtb exist, the *ndh* and the *ndhA* genes (group B in Fig. 5.7). These homologues are

closely related but the phylogeny suggests that the duplication occurred probably in an ancestor corynebacteria or an early mycobacteria. Most probably the *ndhA* gene was lost in most mycobacteria species during evolution. This homologue was kept in the Mtb complex, in *M. marinum* and *M. avium* (Fig. 5.7). In terms of the *ndh* gene the species closer to the Mtb complex were *M. avium, M. leprae, M. ulcerans* and *M. marinum* which also have pathogenic potential in different organisms. This homologue is present in all mycobacteria and its phylogeny might provide the best approximation to the relationship between mycobacteria. In this sense this branch could represent a group where some level of pathogenicity was acquired. This most probably does not reflect any relationship between *ndh* and virulence, since no report of such association was detected in the literature (Triccas and Gicquel 2000; Smith 2003). Incidentally one of the genes that codes one of the subunits of type I NADH: menaquinone oxidoreductase, *nuoG*, has been suggested to be a virulence gene (Velmurugan et al. 2007).

The search queries also retrieved two types of proteins with unknown but predicted functions (Table 5.1). Both types show predicted oxidoreductase activity and both possess the NAD binding motif. In databases (like UniProt) they are classified in the same groups as other *ndh* homologues. These two abnormal clades are present in Mtb. One was labelled as group D. This homologue in Mtb was present in the list of non-essential genes in the study of (Sassetti et al. 2003), however it showed up-regulation after 24-hours starvation (Betts et al. 2002) and at high temperatures (Stewart et al. 2002).This not only shows that this gene is expressed (and not only a predicted gene) but also that might be important in stress conditions. The group E homologue is also most probably expressed since its product was identified in the cell membrane fraction of Mtb H37Rv (Mawuenyega et al. 2005). It is possible that these proteins could act as type II NADH: menaquinone oxidoreductases.

Considering that *ndh* is targeted in drugs against TB it is important to characterize these proteins. They could act as alternative NADH dehydrogenases not susceptible to the same drugs, as suggested for *ndhA* in chapter 4. Data presented here showed that one of the hypothetical *ndh* homologues in Mtb was more closely related with group A of (Melo et al. 2004) while the second was more closely related with group C, and the latter one was possibly obtained by horizontal transfer (Fig.5.6). Melo and collaborators (Melo et al. 2004) did not consider these sequences although they used an Mtb genome in the analysis. Percentages of similarity and calculated protein distances showed that their similarity was within the range of the overall diversity of type II NADH: menaquinone oxidoreductases as in that paper, supporting the fact that they belonged to this group of enzymes. This is not conclusive and they might just be enzymes with similarities but with different functions. Further research is necessary to unravel these possibilities.

Independently of the actual function of the hypothetical *ndh* homologues, they presented a very low ratio of non-synonymous mutations when compared with synonymous mutations during their evolution (Table 5.4). Ratio of non-synonymous to synonymous was used to detect probable pseudogenes in the Human Genome (Torrents et al. 2003). Also dN/dS ratio has been used to compare essential against non-essential genes in bacteria showing that the firsts had a lower rate of change (Jordan et al. 2002). This is the first characterization of dN/dS ratios in mycobacteria genes. The ratio should be close to 1 when mutations are happening randomly or when there is a positive selection elevating the number of non-synonymous mutations. A low dN/dS ratio indicates that the gene has been under purifying selection (Yang 2007), indicating that a selective force has been acting against changes in the proteins. This observed conservation just makes sense if the gene has a function and if its impairment decreases or prevents the survival of the organism (Jordan

et al. 2002). This could easily be the definition of an essential gene. However the four Mtb genes studied here are in the list of non-essential genes in the study of Sasseti and colleagues (Sassetti et al. 2003), which is contradictory in many ways. One must take into account that these essentiality studies test the necessity of a gene under a given condition of growth or a limited set of conditions. They do not take into account the plasticity of a bacterial genome in adapting to different conditions or the changing conditions that bacteria will be under during its evolution. For example one gene might not be even expressed under ideal conditions but it could be expressed in an extreme condition such as starvation and in such a case, that gene may play an important role for the survival of the bacteria in that scenario. In a population of a given bacteria there will be variation in their genome and if some of that variation includes a harmful mutation in that gene, in ideal conditions where that gene is not essential that mutation is harmless. In case of environmental changes into an extreme condition where that gene is activated, natural selection will eliminate the individuals in that population carrying the mutation, making the gene essential in that situation. This way the essentiality in evolutionary terms is measured in a sequence of conditions taking place during thousands and millions of years, where environment and natural selection shaped the genome of the bacteria and where genes were conserved because of both continuous and episodic conditions.

Comparing for example the reduced genome of *M. leprae* to hypothesize which genes are essential in the genome of Mtb can also be misleading because both genomes evolved in separate ways and they adapted to different life cycles, conditions and inevitably acquired different requirements. Genes that are not considered essential in these essentiality studies could play a role in survival in the host or even under the action of drugs. This research confined to essential genes can be misdirected. Russell and colleagues also point out that knockout studies and search for

essential genes is a paradigm in drug discovery that should change since researchers do not consider the full range of interactions between pathways and gene products that occur for the survival of Mtb in the different microenvironments of the host (Russell et al. 2010).

The application of the analytical methodology described here (phylogenetic reconstruction with calculation of rates of change in different clusters) in the genes of the entire genome of Mtb can provide a pattern of genes whose evolution suggests that they have been conserved during evolution. These patterns could be contrasted with results from studies of predicted essentiality, for example those in knockout studies, in order to see how they compare. Such a study would require powerful bioinformatics' tools. The patterns of conservation within groups might be a useful tool in detecting novel drug targets for therapeutic interventions.

Chapter 6. General discussion

In the course of this work, different methodologies in the study of *Mycobacterium tuberculosis* were undertaken for the first time in the laboratories of the School of Tropical Medicine in Liverpool.

TB is currently one of the deadliest diseases worldwide and probably one of the most distributed infections worldwide (WHO 2009). There are studies revealing the existence of a large number of Mtb carriers, latently infected and potentially able to create new episodes of disease and infection (WHO 2011). International efforts are now in place in order to develop alternative and more efficient anti-TBtreatments.

The first approach to the study of Mtb (Chapter 2) was using the non-pathogenic *Mycobacterium smegmatis*. It was hoped that the use of a non-pathogenic organism instead of the highly pathogenic Mtb would facilitate the use of all the resources of the lab instead of being contained in the category 3 environment which poses limitations on the full use of lab resources. Given this, the first objective that was proposed in this thesis was the validation of *M. smegmatis* as a model for Mtb.

This validation was successful in terms of the biochemical characterization by spectral analyses of the ETC of *M. smegmatis*, since it was possible to correlate the spectrum profile with growth conditions and this enabled further drug testing using this approach. This spectrophotometric approach was difficult to implement with Mtb in LSTM due to technical limitations (the lack of a gamma-radiation device to kill Mtb or of ultra-centrifuges and a cell disruptor machine inside the containment level III lab in order to prepare the Mtb crude membranes). Using *M. smegmatis* allowed the implementation of microbiology techniques that were later needed for the Mtb studies. However, the use

of this model was abandoned due to the fact that previously reported differences between Mtb and *M. smegmatis* were found during the experiments. The more obvious ones were in terms of patterns of growth, endurance against stressful conditions and resistance to antimicrobial drugs, since the drug susceptibility profile obtained testing DOTS agents pointed to high tolerance of these drugs, especially ethambutol and isoniazid (Chapter 2). *M. smegmatis* ETC has significant differences in relation to the ETC of Mtb and this invalidates its use as an Mtb model in its susceptibility to drugs targeting the ETC, such as the phenothiazines, since the phylogenetic study also suggests that there are significant differences in terms of the *ndh* homologues (Chapter 5).

In Chapter 3, drug susceptibility tests were evaluated in Mtb and were successful in terms of the possibility of using the Wayne model to screen new compounds, using a colorimetric assay. Drug susceptibility was also tested comparing drug effects using anaerobic and aerobic organisms and using different lengths of exposure to the drugs. All DOTS agents tested were active against Mtb in the aerobic assays however with the exception of ethambutol they all showed a decrease in efficiency over time. The results obtained suggested the existence of different subpopulations of bacteria, with different drug tolerance, consistent with the suggestion that under stress, bacteria populations will become more heterogeneous (Kolter et al. 1993). In terms of the efficiency of DOTS against hypoxic organisms, there is a significant decrease in efficacy, apart from streptomycin, something that was previously reported (Li and Franzblau 1999).

The purpose of chemical validation of the phenothiazines group as potential anti-TB drugs was achieved.

The results obtained with the phenothiazines serve to confirm the potential utility of these drugs as new candidates for anti-TB treatment

due to their effect against TB, highly accentuated against TB grown under severe hypoxia. This shows that phenothiazines have potential against growing TB but a greater potential against hypoxia-adapted organisms, and definitely phenothiazine compounds should be used as promising scaffold compounds for the synthesis of even more effective drugs but especially less harmful to the host. They could be useful in targeting specific sub-populations of hypoxic Mtb bacilli identified in *in vivo* Mtb infections. Although one contra-indication of the use of phenothiazines in anti-TB therapy is the possible antagonistic effect with one of the first line anti-TB agents, isoniazid. Despite the reported synergistic effect of phenothiazines with DOTS compounds (Amaral and Kristiansen 2000; Amaral et al. 2004), no synergism was found in this study using isobolographic analysis of drug combination between two of the most effective phenothiazines (thioridazine and trifluoperazine) and DOTS.

ndh is a recognized anti-TB drug target, phenothiazines being one of its specific inhibitors (Weinstein et al. 2005). In this context the objective of Chapter 4 was to determine if its homologue *ndhA* is a viable alternative type II NADH: menaquinone oxidoreductase and also if it shows susceptibility to the same drugs, namely phenothiazines, as *ndh*. The study of *ndhA* would allow further insight into the ETC of Mtb. A successful attempt was made, in terms of cloning this gene to modified *E. coli* expression cells, but no activity was detected (Chapter 4). This result is dubious, since this was achieved by another group (Weinstein et al. 2005). Some protocol irregularities (the inexistence of sustained drug pressure in order for the host cell to retain the gene-encoding plasmid or a possible abnormal insert) would need to be corrected in order to achieve a reliable conclusion.

Chapter 5 attempted to further characterize the ETC of Mtb in terms of the type II NADH: menaquinone dehydrogenase enzymes. There is a lack

of phylogenetic studies focused in Mtb and the only study focusing on these enzymes (Melo et al. 2004) is well cited but is probably out of date. Also, a more detailed exploration of the Mtb genome and other mycobacteria and Actinomycetales genomes was made (Chapter 5) in order to detect potential *ndh* homologues and to infer an evolutionary history was made. In Mtb not only the *ndh* and the *ndhA* gene were detected but also two other genes with potential NADH reductase activity, deserving further investigation. The existence of these homologues could be important in terms of drug development targeted at *ndhA* in Chapter 4.

In terms of *ndh* and *ndhA*, phylogenetically they share a recent common ancestor, their presence meaning that at some point in the past, a duplication of an ancestral gene occurred, most probably in an organism from which all mycobacteria descend. More importantly, both *ndh* and *ndhA* genes, as well as the two hypothetical homologues show similar rates of changing. This suggests that they have been under strict purifying selection, meaning that they should have been functional and important genes during the evolution of the organism.

6.1. Critical assessment of the study

This work, namely the drug testing was initially done with *M. smegmatis*. As mentioned before this proved to be an unsuitable model for Mtb. However even the use of Mtb has its limitation and drawbacks. The extracellular model of study was not completely representative of a normal infectious Mtb population so it cannot be expected that it completely behaves like one. The static model of drug susceptibility test that was used is also not an ideal model of study. If possible, a chemostat culture could be maintained, with constant monitoring and continuous maintenance of the Mtb cultures in the desired conditions. IC_{50}, the

measure of drug susceptibility used, is considered more exact and it is the standard measure employed in enzymatic kinetic studies. One of the objectives of this and future work is to allow the comparison between the results reported here (Chapter 3) and further studies regarding enzymes of the Mtb ETC. So the studies were optimized to calculate IC_{50}s but considering published work and the exponential nature of bacterial growth, this index should have ideally be complemented with indices measuring a more extreme rate of inhibition, for example the 99% minimal bactericidal concentration (MBC_{99}). Regarding the expression of *ndhA* in *E. coli* cells, some faults were already detected and outlined in Chapter 4.

6.2. Future work

The results obtained throughout this thesis led to a number of findings that demand further investigation.

Regarding phenothiazines, different drug susceptibility tests should be performed in order to further understand their mode of action and effectiveness. The use of whole blood assays, establishing an infection model in macrophages and monitoring the phagocytic process under high content imaging, would led to a more clear approximation of the behaviour of Mtb to the human infection scenario.

Due to the limitations of the drug assays performed throughout this thesis and in light of the new developments, more informative tests could be performed. Bioluminescence assays are very useful for screening drug susceptibility of mycobacteria either extracellularly or inside macrophages. Andreu and colleagues proposed a simple and rapid 96-well microplate assay where using auto-luminescent bacteria facilitates the determination of growth and inhibition kinetics (Andreu et al. 2012).

Targeted knockout techniques could be used in order to study the function of proteins in Mtb, namely for all the electron transport chain proteins, testing their functionality and importance. Particularly interesting would be to look at the other ETC components in terms of drug targets, such as cytochrome *bd*, the alternative branch used when the bacilli are submitted to anaerobic conditions.

In the last few years, metabolomics emerged as a powerful approach that allows an insight into the molecular processes that are the result of all cellular activity (Villas-Bôas et al. 2005). This approach uses a great variety of analytical procedures in order to analyse all small weight molecules in the cell, which directly offers a view of the processes that occurred. It is much more informative than looking at the genome and proteome. Metabolomics can be used to clearly assess the mode of action of a given drug as pointed out previously (Carvalho et al. 2010; Olivier and Loots 2011) and it would be a desirable approach in future studies.

In terms of evolutionary studies, it may be helpful to consider the complete range of genes that constitute the ETC of Mtb and probably even considering the complete genome of Mtb and related species. This work would require the designing of new bioinformatic tools.

References

Abate, G., A. Aseffa, A. Selassie, S. Goshu, B. Fekade, D. WoldeMeskal and H. Miörner (2004). "Direct colorimetric assay for rapid detection of rifampin-resistant *Mycobacterium tuberculosis*." Journal of Clinical Microbiology **42**(2): 871-873.

Abate, G., R. N. Mshana and H. Miörner (1998). "Evaluation of a colorimetric assay based on 3-(4,5-dimethylthiazol-2-yl)-2,5-diphenyl tetrazolium bromide (MTT) for rapid detection of rifampicin resistance in *Mycobacterium tuberculosis*." The International Journal of Tuberculosis and Lung Disease **2**(12): 1011-1016.

Achkar, J. M. and E. R. Jenny-Avital (2011). "Incipient and subclinical tuberculosis: defining early disease states in the context of host immune response." Journal of Infectious Diseases **204**: S1179-S1186.

Altaf, M., C. H. Miller, D. S. Bellows and R. O'Toole (2010). "Evaluation of the *Mycobacterium smegmatis* and BCG models for the discovery of *Mycobacterium tuberculosis* inhibitors." Tuberculosis **90** 333-337.

Amaral, L., M. J. Boeree, S. H. Gillespie, Z. F. Udwadia and D. v. Soolingene (2010). "Thioridazine cures extensively drug-resistant tuberculosis (XDR-TB) and the need for global trials is now!" International Journal of Antimicrobial Agents **35**: 524-526.

Amaral, L. and J. E. Kristiansen (2000). "Phenothiazines: an alternative to conventional therapy for the initial management of suspected multidrug resistant tuberculosis. A call for studies." International Journal of Antimicrobial Agents **14**: 173-176.

Amaral, L., J. E. Kristiansen, L. S. Abebe and W. Millett (1996). "Inhibition of the respiration of multi-drug resistant clinical isolates of *Mycobacterium tuberculosis* by thioridazine: potential use for initial therapy of freshly diagnosed tuberculosis." Journal of Antimicrobial Chemotherapy **38**: 1049-1053.

Amaral, L., J. E. Kristiansen, M. Viveiros and J. Atouguia (2001). "Activity of phenothiazines against antibiotic-resistant *Mycobacterium tuberculosis*: a review supporting further studies that may elucidate the potential use of thioridazine as anti-tuberculosis therapy." Journal of Antimicrobial Chemotherapy **47**: 505-511.

Amaral, L., M. Martins and M. Viveiros (2007). "Enhanced killing of intracellular multidrug-resistant *Mycobacterium tuberculosis* by compounds that affect the activity of efflux pumps." Journal of Antimicrobial Chemotherapy **59**: 1237–1246.

Amaral, L., M. Martins, M. Viveiros, J. Molnar and J. E. Kristiansen (2008). "Promising therapy of XDR-TB/MDR-TB with thioridazine an inhibitor of bacterial efflux pumps." Current Drug Targets **9**(9): 816-819.

Amaral, L., M. Viveiros and J. Molnar (2004). "Antimicrobial activity of phenothiazines." In Vivo **18**: 725-732.

Ananthan, S., E. R. Faaleolea, R. C. Goldman, J. V. Hobrath, C. D. Kwong, B. E. Laughon, J. A. Maddry, A. Mehta, L. Rasmussen, R. C. Reynolds, J. A. Secrist III, N. Shindo, D. N. Showe, M. I. Sosa, W. J. Suling and E. L. White (2009). "High-throughput screening for inhibitors of *Mycobacterium tuberculosis* H37Rv." Tuberculosis **89**: 334-353.

Andreu, N., T. Fletcher, N. Krishnan, S. Wiles and B. D. Robertson (2012). "Rapid measurement of antituberculosis drug activity *in vitro* and in macrophages using bioluminescence." Journal of Antimicrobial Chemotherapy **67**(2): 404-414.

Andries, K., P. Verhasselt, J. Guillemont, H. W. H. Göhlmann, J.-M. Neefs, H. Winkler, J. V. Gestel, P. Timmerman, M. Zhu, E. Lee, P. Williams, D. Chaffoy, E. Huitric, S. Hoffner, E. Cambau, C. Truffot-Pernot, N. Lounis and V. Jarlier (2005). "A diarylquinoline drug active on the ATP synthase of *Mycobacterium tuberculosis*." Science **307**(5707): 223-227.

Angeby, K. A., L. Klintz and S. E. Hoffner (2002). "Rapid and inexpensive drug susceptibility testing of *Mycobacterium tuberculosis* with a nitrate reductase assay." Journal of Clinical Microbiology **40**(2): 553-555.

Anuchin, A. M., A. L. Mulyukin, N. E. Suzina, V. I. Duda, G. I. El-Registan and A. S. Kaprelyants (2009). "Dormant forms of *Mycobacterium smegmatis* with distinct morphology." Microbiology **155**: 1071-1079.

Argyrou, A., M. W. Vetting and J. S. Blanchard (2007). "New insight into the mechanism of action and resistance to isoniazid: Interaction of *Mycobacterium tuberculosis* enoyl-ACP reductase with INH-NADP." Journal of the American Chemical Society **129**: 9582-9583.

Bakker-Woudenberg, I. A. J. M., W. v. Vianen, D. v. Soolingen, H. A. Verbrugh and M. A. v. Agtmael (2005). "Antimycobacterial agents differ with respect to their bacteriostatic versus bactericidal activities in relation to time of exposure, mycobacterial growth phase, and their use in combination." Antimicrobial Agents and Chemotherapy **49**(6): 2387-2398.

Balaban, N. Q., J. Merrin, R. Chait, L. Kowalik and S. Leibler (2004). "Bacterial persistence as a phenotypic switch." Science **305**(5690): 1622-1625.

Barlow, M. (2009). "What antimicrobial resistance has taught us about horizontal gene transfer." Methods in Molecular Biology **532**: 397-411.

Barry III, C. E. (2001). "*Mycobacterium smegmatis*: an absurd model for tuberculosis?" TRENDS in Microbiology **9**(10): 473-474.

Barry III, C. E. and J. S. Blanchard (2010). "The chemical biology of new drugs in the development for tuberculosis." Current Opinion in Microbiology **14**: 456-466.

Bartek, I. L., R. Rutherford, V. Gruppo, R. A. Morton, R. P. Morris, M. R. Klein, K. C. Visconti, G. J. Ryan, G. K. Schoolnik, A. Lenaerts and M. I. Voskuil (2009). "The DosR regulon of *M. tuberculosis* and antibacterial tolerance." Tuberculosis **89**: 310-316.

Bate, A. B., J. H. Kalin, E. M. Fooksman, E. L. Amorose, C. M. Price, H. M. Williams, M. J. Rodig, M. O. Mitchell, S. H. Cho, Y. Wang and S. G. Franzblau (2007). "Synthesis and antitubercular activity of quaternized promazine and promethazine derivatives." Bioorganic & Medicinal Chemistry Letters **17**: 1346-1348.

Bayer, R. and D. Wilkinson (1995). "Directly observed therapy for tuberculosis: history of an idea." Lancet **345**: 1545-1548.

Becq, J., M. C. Gutierrez, V. Rosas-Magallanes, J. Rauzier, B. Gicquel, O. Neyrolles and P. Deschavanne (2007). "Contribution of horizontally acquired genomic islands to the evolution of the tubercle bacilli." Molecular Biology and Evolution **34**(8): 1861-1871.

Bentley, R. and R. Meganathan (1982). "Biosynthesis of vitamin K (menaquinone) in bacteria." Microbiology **46**(3): 241-280.

Bentrup, K. H. and D. G. Russell (2001). "Mycobacterial persistence: adaptation to a changing environment." TRENDS in Microbiology **9**: 597-605.

Berenbaum, M. C. (1978). "A method for testing for synergy with any number of agents." Journal of Infectious Diseases **137**(2): 122-130.

Berney, M. and G. M. Cook (2010). "Unique flexibility in energy metabolism allows mycobacteria to combat starvation and hypoxia." PLoS One **5**(1): e8614.

Betts, J. C., P. T. Lukey, L. C. Robb, R. A. McAdam and K. Duncan (2002). "Evaluation of a nutrient starvation model of *Mycobacterium tuberculosis* persistence by gene and protein expression profiling." Molecular Microbiology **43**(3): 717-731.

Biagini, G. A., P. Viriyavejakul, P. O'Neill, P. G. bray and S. A. Ward (2006). "Functional characterization and target validation of alternative complex I of *Plasmodium falciparum* mitochondria." Antimicrobial Agents and Chemotherapy **50**(5): 1841-1851.

Bloch, K. (1977). "Control mechanisms for fatty acid synthesis in *Mycobacterium smegmatis*." Advances in Enzymology and Related Areas of Molecular Biology **45**: 1-84.

Boon, C. and T. Dick (2002). "*Mycobacterium bovis* BCG response regulator essential for hypoxic dormancy." Journal of Bacteriology **184**(24): 6760-6767.

Boon, C., R. Li, R. Qi and T. Dick (2001). "Proteins of *Mycobacterium bovis* BCG induced in the Wayne dormancy model." Journal of Bacteriology **183**(8): 2672-2676.

Boshoff, H. I. and C. E. Barry III (2005). "A low-carb diet for a high-octane pathogen." Nature Medicine **11**(6): 599-600.

Boshoff, H. I., V. Mizrahi and C. E. Barry III (2002). "Effects of pyrazinamide on fatty acid synthesis by whole mycobacterial cells and purified fatty acid synthase I." Journal of Bacteriology **184**(8): 2167-2172.

Boshoff, H. I. M. and C. E. Barry III (2005). "Tuberculosis- metabolism and respiration in the absence of growth." Nature Reviews in Microbiology **3**: 70-80.

Boshoff, H. I. M., T. G. Myers, B. R. Copp, M. R. McNeil, M. A. Wilson and C. E. B. III (2004). "The transcriptional responses of *Mycobacterium tuberculosis* to inhibitors of metabolism: Novel insights into drug mechanisms of action." Journal of Biological Chemistry **279**(38): 40174-40184.

Bott, M. and A. Niebisch (2003). "The respiratory chain of *Corynebacterium glutamicum*." Journal of Biotechnology **104**: 129-153.

Brandt, L., J. F. Cunha, O. A. Weinreich, B. Chilima, P. Hirsch, R. Appelberg and P. Andersen (2002). "Failure of the *Mycobacterium bovis* BCG vaccine: some species of environmental mycobacteria block multiplication of BCG and induction of protective immunity to tuberculosis." Infection and Immunity **70**: 672-678.

Brandt, U. (2006). "Energy converting NADH: quinone oxidoreductase (complex I)." Annual Review of Biochemistry **75**: 69-92.

Brandt, U. and B. Trumpower (1994). "The protonmotive Q cycle in mitochondria and bacteria." Critical Reviews in Biochemistry and Molecular Biology **29**(3): 165-197.

Brewer, T. F. (2000). "Preventing tuberculosis with Bacillus Calmette-Guèrin vaccine: a meta-analysis of the literature." Clinical Infectious Diseases **31**: S64-S67.

Butcher, P. D. (2004). "Microarrays for *Mycobacterium tuberculosis*." Tuberculosis **84**(131-137).

Canetti, G., S. Froman, J. Grosset, P. Hauduroy, M. Langerova, H. T. Mahler, G. Meissner, D. A. Mitchison and L. Sula (1963). "Mycobacteria: Laboratory methods for testing drug sensitivity and resistance." Bulletin of the World Health Organization **29**: 565-578.

Carvalho, L. P. S. d., S. M. Fischer, J. Marrero, C. Nathan, S. Ehrt and K. Y. Rhee (2010). "Metabolomics of *Mycobacterium tuberculosis* reveals compartmentalized co-catabolism of carbon substrates." Chemistry & Biology **17**: 1122-1131.

Castañón-Arreola, M. and Y. López-Vidal (2004). "A second-generation anti TB vaccine is long overdue." Annals of Clinical Microbiology and Antimicrobials **3**: 10.

Chao, M. C. and E. J. Rubin (2010). "Letting sleeping *dos* lie: does dormancy play a role in Tuberculosis?" Annual Review of Microbiology **64**: 293-311.

Chimpanzee sequencing and analysis consortium, T. (2005). "Initial sequence of the chimpanzee genome and comparison with the human genome." Nature **437**(7055): 69-87.

Cho, S. H., S. Warit, B. Wan, C. H. Hwang, G. F. Pauli and S. G. Franzblau (2007). "Low-oxygen-recovery assay for high-throughput screening of compounds against nonreplicating *Mycobacterium tuberculosis*." Antimicrobial Agents and Chemotherapy **51**(4): 1380-1385.

Coates, A. R. M. and Y. Hu (2008). "Targeting non-multiplying organisms as a way to develop novel antimicrobials." TRENDS in Pharmacological Sciences **29**(3): 143-150.

Cole, S. T. and P. M. Alzari (2007). "Towards new tuberculosis drugs." Biochemical Society Transactions **35**(5): 1321-1324.

Cole, S. T., R. Brosch, J. Parkhill, T. Garnier, C. Churcher, D. Harris, S. V. Gordon, K. Eiglmeier, S. Gas, C.E. Barry, F. Tekaia, K. Badcock, D. Basham, D. Brown, T. Chillingworth, R. Connor, R. Davies, K. Devlin, T. Feltwell, S. Gentles, N. Hamlin, S. Holroyd, T. Hornsby, K. Jagles, A. Krogh, J. McLean, S. Moule, L. Murphy, K. Oliver, J. Osborne, M. A. Quail, M. A. Rajandream, J. Rogers, S. Rutter, K. Seeger, J. Skelton, R. Squares, S. Squares, J. E. Sulston, K. Taylor, S. Whitehead and B. G. Barrell (1998). "Deciphering the Biology of *Mycobacterium tuberculosis* from the complete genome sequence." Nature **393**: 537-544.

Collins, L. and S. G. Franzblau (1997). "Microplate alamar blue assay versus BACTEC 460 system for high-throughput screening of compounds against *Mycobacterium tuberculosis* and *Mycobacterium avium*." Antimicrobial Agents and Chemotherapy **41**(5): 1004-1009.

Cosma, C. L., D. R. Sherman and L. Ramakrishnan (2003). "The secret lives of the pathogenic mycobacteria." Annual Review of Microbiology **57**: 641-676.

Cox, R. A. and G. M. Cook (2007). "Growth regulation in the mycobacterial cell." Current Molecular Medicine 7: 231-246.

Crofts, A. R. (2004). "The cytochrome bc1 complex: function in the context of structure." Annual Review in Physiology **66**: 689-733.

Crooks, G. E., G. Hon, J. M. Chandonia and S. E. Brenner (2004). "WebLogo: A sequence logo generator." Genome Research **14**: 1188-1190.

David, H. L. (1970). "Probability distribution of drug-resistant mutants in unselected populations of *Mycobacterium tuberculosis*." Applied Microbiology **20**(5): 810-814.

Deb, C., C.-M. Lee, V. S. Dubey, J. Daniel, B. Abomoelak, T. D. Sirakova, S. Pawar, L. Rogers and P. E. Kolattukudy (2009). "A novel *in vitro* multiple-stress dormancy model for *Mycobacterium tuberculosis* generates a lipid-loaded, drug-tolerant, dormant pathogen." PLoS One **4**(6): e6077.

Debouck, C. and P. N. Goodfellow (1999). "DNA microarrays in drug discovery and development." Nature Genetics **21**: 48-50.

Delaine, T., V. Bernardes-Génisson, A. Quémard, P. Constant, B. Meunier and J. Bernadou (2010). "Development of isoniazid-NAD truncated adducts embedding a lipophilic fragment as potential bi-substrate *InhA* inhibitors and antimycobacterial agents." European Journal of Medicinal Chemistry **45**: 4554-4561.

DeMaio, J., Y. Zhang, C. Ko, D. B. Young and W. R. Bishai (1996). "A stationary-phase stress-response sigma factor from *Mycobacterium tuberculosis*." Proceedings of the National Academy of Sciences **93**: 2790-2794.

Dheda, K., S. K. Schwander, B. Zhu, R. N. v. Zyl-Smit and Y. Zhang (2010). "The immunology of tuberculosis: from bench to bedside." Respirology **15**(3): 433-450.

Dhillon, J., B. W. Allen, Y. M. Hu, A. R. Coates and D. A. Mitchison (1998). "Metronidazole has no antibacterial effect in Cornell model murine tuberculosis." The International Journal of Tuberculosis and Lung Disease **2**: 736-742.

Díaz-Infantes, M. S., M. J. Ruiz-Serrano, L. Martínez-Sánchez, A. Ortega and E. Bouza (2000). "Evaluation of the MB/BacT *Mycobacterium* detection system for susceptibility testing of *Mycobacterium tuberculosis*." Journal of Clinical Microbiology **38**(5): 1988-1989.

Dick, T. (2001). "Dormant tubercle bacilli: The key to more effective TB chemotherapy?" Journal of Antimicrobial Chemotherapy **47**: 117-118.

Dick, T., B. H. Lee and B. Murugasu-Oei (1998). "Oxygen depletion induced dormancy in *Mycobacterium smegmatis*." FEMS Microbiology Letters **163**: 159-164.

Domenech, P., C. E. Barry III and S. T. Cole (2001). "*Mycobacterium tuberculosis* in the post-genomic age." Current Opinion in Microbiology **4**: 28-34.

Dormans, J., M. Burger, D. Aguilar, R. Hernandez-Pando, K. Kremer, P. Roholl, S. M. Arend and D. V. Soolingen (2004). "Correlation of virulence, lung pathology, bacterial load and delayed type hypersensitivity responses after infection with different *Mycobacterium tuberculosis* genotypes in a BALB/c mouse model." Clinical and Experimental Immunology **137**: 460-468.

Dutta, N. K., S. Mehra and D. Kaushal (2010). "A *Mycobacterium tuberculosis* sigma factor network responds to cell-envelope damage by the promising anti-mycobacterial thioridazine." PLoS One **5**(4): e10069.

Dye, C. and K. Floyd (2006). Tuberculosis. Disease Control Priorities in Developing Countries. New York, Oxford University Press: 289-312.

Ehlers, S. (2009). "Lazy, dynamic or minimally recrudescent? On the elusive nature and location of the *Mycobacterium* responsible for latent tuberculosis " Infection **37**(2): 87-95.

Farrand, S. K. and H. W. Taber (1974). "Changes in menaquinone concentration during growth and early sporulation in *Bacillus subtillis*." Journal of Bacteriology **117**(1): 324-326.

Fauvart, M., V. N. d. Groote and J. Michiels (2011). "Role of persister cells in chronic infections: clinical relevance and perspectives on anti-persister therapies." Journal of Medical Microbiology **60**: 699-709.

Felsenstein, J. (1981). "Evolutionary trees from DNA sequences: a maximum likelihood approach " Journal of Molecular Evolution **17**(6): 368-376.

Fisher, N., A. J. Warman, S. A. Ward and G. A. Biagini (2009). "Type II NADH: quinone oxidoreductases of *Plasmodium falciparum* and *Mycobacterium tuberculosis*: kinetic and high-throughput assays." Methods in Enzymology **456**: 303-320.

Fleischmann, R. D., D. Alland, J. A. Eisen, L. Carpenter, O. White, J. Peterson, R. DeBoy, R. Dodson, M. Gwinjn, D. Haft, E. Hickey, J. F. Kolonay, W. C. Nelson, L. A. Umayam, M. Ermolaeva, S. L. Salberg, A. Delcher, T. Utterback, J. Weidman, H. Khouri, J. Gill, A. Mikula, W. Bishai, W. R. J. Jr., J. C. Venter and C. M. Fraser (2002). "Whole-genome comparison of *Mycobacterium tuberculosis* clinical and laboratory strains." Journal of Bacteriology **184**(19): 5479-5490.

Franzblau, S. G., R. S. Witzig, J. C. McLaughlin, P. Torres, G. Madico, A. Hernandez, M. T. Degnan, M. B. Cook, V. K. Quenzer, R. M. Ferguson and R. H. Gilman (1998). "Rapid, low-technology MIC determination with clinical *Mycobacterium tuberculosis* isolates by using the microplate alamar blue assay." Journal of Clinical Microbiology **36**(2): 362-366.

Gamieldien, J., A. Ptitsyn and W. Hide (2002). "Eukaryotic genes in *Mycobacterium tuberculosis* could have a role in pathogenesis and immunomodulation." TRENDS in Genetics **18**(1): 5-8.

Gangadharam, P. R. J., P. F. Pratt, V. K. Perumal and M. D. Iseman (1990). "The effects of exposure time, drug concentration, and temperature on the activity of ethambutol versus *Mycobacterium tuberculosis*." American Journal of Respiratory and Critical Care Medicine **141**(6): 1478-1482.

Gengenbacher, M., S. P. S. Rao, K. Pethe and T. Dick (2010). "Nutrient-starved, non-replicating *Mycobacterium tuberculosis* requires respiration, ATP synthase and isocitrate lyase for maintenance of ATP homeostasis and viability." Microbiology **156**: 81-87.

Gill, W. P., N. S. Harik, M. R. Whiddon, R. P. Liao, J. E. Mittler and D. R. Sherman (2009). "A replication clock for *Mycobacterium tuberculosis*." Nature Medicine **15**(2): 211-214.

Gillespie, J., L. L. Barton and E. W. Rypka (1986). "Phenotypic changes in mycobacteria grown in oxygen-limited conditions." Journal of Medical Microbiology **21**: 251-255.

Gillespie, S. H. (2002). "Evolution of drug resistance in *Mycobacterium tuberculosis*: clinical and molecular perspective." Antimicrobial Agents and Chemotherapy **46**(2): 267-274.

Glickman, M. S. and W. R. Jacobs Jr. (2001). "Microbial pathogenesis of *Mycobacterium tuberculosis*: dawn of a discipline." Cell **104**: 477-485.

Gómez-Valero, L., E. P. C. Rocha, A. Latorre and F. J. Silva (2007). "Reconstructing the ancestor of *Mycobacterium leprae*: The dynamics of gene loss and genome reduction " Genome Research **17**(1178-1185).

Gomez, J. E. and J. D. McKinney (2004). "*M. tuberculosis* persistence, latency, and drug tolerance." Tuberculosis **84**(1-2): 29-44.

Granich, R., C. Akolo, C. Gunneberg, H. Getahun, P. Williams and B. Williams (2010). "Prevention of tuberculosis in people living with HIV." Clinical Infectious Diseases **50**: S215-S222.

Gray, G. R., M. Y. Wong and S. J. Danielson (1982). "The major mycolic acids of *Mycobacterium smegmatis*." Progress in Lipid Research **21**(2): 91-107.

Griffin, J. E., J. D. Gawronski, M. A. DeJesus, T. R. Ioerger, B. J. Akerley and C. M. Sassetti (2011). "High-resolution phenotypic profiling defines genes essential for mycobacterial growth and cholesterol catabolism." PLoS Pathogens **7**(9): e1002251.

Gupta, A., A. Kaul, A. G. Tsolaki, U. Kishore and S. Bhakta (2012). "*Mycobacterium tuberculosis*: Immune evasion, latency and reactivation." Immunology **217**(3): 363-374.

Hall, T. A. (1999). "BioEdit: a user-friendly biological sequence alignment editor and analysis program for Windows 95/98/NT." Nucleic Acids Symposyum Series **41**: 95-98.

Hampshire, T., S. Soneji, J. Bacon, B. W. James, J. Hinds, K. Laing, R. A. Stabler, P. D. Marsh and P. D. Butcher (2004). "Stationary phase gene expression of *Mycobacterium tuberculosis* following a progressive nutrient depletion: a model for persistent organisms?" Tuberculosis **84**: 228-238.

Handbook of anti-tuberculosis agents, T. (2008). "Ethambutol." Tuberculosis **88**(102-105).

Handbook of anti-tuberculosis agents, T. (2008). "Isoniazid." Tuberculosis **88**(112-116).

Handbook of anti-tuberculosis agents, T. (2008). "Pyrazinamide." Tuberculosis **88**(141-144).

Handbook of anti-tuberculosis agents, T. (2008). "Streptomycin." Tuberculosis **88**(162-163).

Handbook of anti-tuberculosis agents, T. (2008). "Thioridazine." Tuberculosis **88**(164-167).

Hartkoorn, R. C., B. Chandler, A. Owen, S. A. Ward, S. B. Squire, D. J. Black and S. H. Khoo (2007). "Differential drug susceptibility of intracellular and extracellular tuberculosis, and the impact of P-glycoprotein." Tuberculosis **87**: 248-255.

Heifets, L., J. Simon and V. Pham (2005). "Capreomycin is active against non-replicating *M. tuberculosis*." Annals of Clinical Microbiology and Antimicrobials **4**: 6.

Hiratsuka, T., K. Furihata, J. Ishikawa, H. Yamashita, N. Itoh, H. Seto and T. Dairi (2008). "An alternative menaquinone biosynthetic pathway operating in microorganisms." Science **321**: 1670-1673.

Hoff, D. R., G. J. Ryan, E. R. Driver, C. C. Ssemakulu, M. A. D. Groote, R. J. Basaraba and A. J. Lenaerts (2011). "Location of intra- and extracellular *M. tuberculosis* populations in lungs of mice and guinea pigs during disease progression and after drug treatment." PLoS One **6**(3): e17550.

Horsburgh Jr., C. R. (1996). "Epidemiology of disease caused by nontuberculous mycobacteria." Seminars in respiratory infections **11**(4): 244-251.

Hosler, J. P., S. Ferguson-Miller and D. A. Mills (2006). "Energy transduction: proton transfer through the respiratory complexes." Annual Review of Biochemistry **75**: 165-187.

Huelsenbeck, J. and F. Ronquist (2001). "MrBayes: Bayesian inference of phylogenetic trees." Bioinformatics **17**(8): 754-755.

Hurdle, J. G., A. J. O'Neill, I. Chopra and R. E. Lee (2011). "Targeting bacterial membrane function: an underexploited mechanism for treating persistent infections." Nature Reviews in Microbiology **9**: 62-75.

Hutter, B. and T. Dick (1998). "Increased alanine dehydrogenase activity during dormancy in *Mycobacterium smegmatis*." FEMS Microbiology Letters **167**: 7-11.

Inglese, J., R. L. Johnson, A. Simeonov, M. Xia, W. Zheng, C. P. Austin and D. S. Auld (2007). "High-throughput screening assays for the identification of chemical probes." Nature Chemical Biology **3**(8): 466-479.

Inglese, J., C. E. Shamu and P. K. Guy (2007). "Reporting data from high-throughput screening of small-molecule libraries." Nature Chemical Biology **3**(8): 438-441.

Islam, M. S., J. P. Richards and A. K. Ojha (2012). "Targeting drug tolerance in mycobacteria: a perspective from mycobacterial biofilms." Expert Review of Anti-infective Therapy **10**(9): 1055-1066.

Jia, J., F. Zhu, X. Ma, Z. W. Cao, Y. X. Li and Y. Z. Chen (2009). "Mechanisms of drug combinations: interaction and network perspectives." Nature Reviews in Drug Discovery **8**: 111-128.

Johnson, R., E. M. Streicher, G. E. Louw, R. M. Warren, P. D. v. Helden and T. C. Victor (2006). "Drug resistance in *Mycobacterium tuberculosis*." Current Issues in Molecular Biology **8**: 97-112.

Johnston, J. C., N. C. Shahidi, M. Sadatsafavi and J. M. Fitzgerald (2009). "Treatment outcomes of multidrug-resistant tuberculosis: a systematic review and meta-analysis." PLoS One **4**(9): e6914.

Jordan, I., I. B. Rogozin, Y. I. Wolf and E. V. Koonin (2002). "Essential genes are more evolutionarily conserved than are nonessential genes in bacteria." Genome Research **12**(6): 962-968.

Kana, B. D., E. E. Machowski, N. Schechter, J.-S. Teh, H. Rubin and V. Mizrahi (2009). Electron transport and respiration in mycobacteria. *Mycobacterium*: genomics and molecular biology T. Parish and A. Brown. Norfolk, UK, Caister Academic Press: 35-64.

Kana, B. D., E. A. Weinstein, D. Avarbock, S. S. Dawes, H. Rubin and V. Mizrahi (2001). "Characterization of the *cydAB*-encoded cytochrome *bd* oxidase from *Mycobacterium smegmatis*." Journal of Bacteriology **183**(24): 7076-7086.

Kendall, S. L., F. Movahedzadeh, S. C. G. Rison, L. Wernisch, T. Parish, K. Duncan, J. C. Betts and N. G. Stoker (2004). "The *Mycobacterium tuberculosis dosRS* two component system is induced by multiple stresses." Tuberculosis **84**: 247-255.

Kerscher, S., S. Dröse, V. Zickermann and U. Brandt (2007). "The three families of respiratory NADH dehydrogenases." Results and Problems in Cell Differentiation **45**(222).

Kerscher, S. J. (2000). "Diversity and origin of alternative NADH:ubiquinone oxidoreductases." Biochimica et Biophysica Acta **1459**: 274-283.

Kharatmal, S., S. S. Jhamb and P. P. Singh (2009). "Evaluation of BACTEC 460 TB system for rapid *in vitro* screening of drugs against latent state *Mycobacterium tuberculosis* H37Rv under hypoxia conditions." Journal of Microbiological Methods **78**: 161-164.

Klinkenberg, L. G., L. A. Sutherland, W. R. Bishai and P. C. Karakousis (2008). "Metronidazole lacks activity against *Mycobacterium tuberculosis* in an *in vivo* hypoxic granuloma model of latency." The Journal of Infectious Diseases **198**: 275-283.

Kolter, R., D. A. Siegele and A. Tormo (1993). "The stationary phase of the bacterial life cycle." Annual Review of Microbiology **47**: 855-874.

Koul, A., N. Dendouga, K. Vergauwen, B. Molenberghs, L. Vranckx, R. Willebrords, Z. Ristic, H. Lill, I. Dorange, J. Guillemont, D. Bald and K. Andries (2007). "Diarylquinolines target subunit c of mycobacterial ATP synthase." Nature Chemical Biology **3**(6): 323-324.

Koul, A., L. Vranckx, N. Dendouga, W. Balemans, I. V. Wyngaert, K. Vergauwen, H. W. H. Göhlmann, R. Willebrords, A. Poncelet, J. Guillemont, D. Bald and K. Andries (2008). "Diarylquinolines are bactericidal for dormant mycobacteria as a result of disturbed ATP homeostasis." Journal of Biological Chemistry **283**(37): 25273-25280.

Kumar, A., J. C. Toledo, R. P. Patel, J. R. Lancaster Jr. and A. J. C. Steyn (2007). "*Mycobacterium tuberculosis* DosS is a redox sensor and DosT is a hypoxia sensor." Proceedings of the National Academy of Sciences **104**(28): 11568-11573.

Lee, A. S. G., A. S. M. Teo and S.-Y. Wong (2001). "Novel mutations in *ndh* in isoniazid-resistant *Mycobacterium tuberculosis* isolates." Antimicrobial Agents and Chemotherapy **45**(7): 2157-2159.

Lei, B. F., C.-J. Wei and S.-C. Tu (2000). "Action mechanism of antitubercular isoniazid: Activation by *Mycobacterium tuberculosis* KatG, isolation, and characterization of InhA inhibitor." Journal of Biological Chemistry **275**: 2520-2526.

Lemus, D., E. Montoro, M. Echemendía, A. Martin, F. Portaels and J. C. Palomino (2006). "Nitrate reductase assay for detection of drug resistance in *Mycobacterium tuberculosis*: simple and inexpensive method for low-resource laboratories." Journal of Medical Microbiology **55**: 861-863.

Leonard, B., J. Coronel, M. Siedner, L. Grandjean, L. Caviedes, P. Navarro, R. H. Gilman and D. A. J. Moore (2008). "Inter- and intra-assay reproducibility of microplate alamar blue assay results for isoniaid, rifampicin, ethambutol, streptomycin, ciprofloxacin, and capreomycin drug susceptibility testing of *Mycobacterium tuberculosis*." Journal of Clinical Microbiology **46**(10): 3526-3529.

Leung, A. N. (1999). "Pulmoary tuberculosis: the essentials." Radiology **210**: 307-322.

Li, Y. and S. G. Franzblau (1999). "Microplate assay for testing bactericidal activity of compounds against nongrowing *Mycobacterium tuberculosis*." Interscience Conference on Antimicrobial Agents and Chemotherapy **863**: 814.

Lim, A., M. Eleuterio, B. Hutter, B. Murugasu-Oei and T. Dick (1999). "Oxygen depletion-induced dormancy in *Mycobacterium bovis* BCG." Journal of Bacteriology **181**(7): 2252-2256.

Lin, P. L., M. Rodgers, L. Smith, M. Bigbee, A. Myers, C. Bigbee, I. Chiosea, S. V. Capuano, C. Fuhrman, E. Klein and J. L. Flynn (2009). "Quantitative comparison of active and latent tuberculosis in the Cynomolgus macaque model." Infection and Immunity 77(10): 4631-4642.

Liu, X. and M. M. Gutacker (2006). "Evidence for recombination in *Mycobacterium tuberculosis*." Journal of Bacteriology **188**(23): 8269-8177.

Loebel, R. O., E. Shorr and H. B. Richardson (1933). "The infuence of foodstuffs upon the respiratory metabolism and growth of human tubercle bacilli." Journal of Bacteriology **26**(2): 139-166.

Madrid, P. B., W. E. Polgar, L. Toll and M. J. Tanga (2007). "Synthesis and antitubercular activity of phenothiazines with reduced binding to dopamine and serotonin receptors." Bioorganic & Medicinal Chemistry Letters **17**: 3014-3017.

Magombedze, G. and N. Mulder (2012). "A mathematical representation of the development of *Mycobacterium tuberculosis* active, latent and dormant stages." Journal of Theoretical Biology **292**: 44-59.

Malone, L., A. Schurr, H. Lindh, D. McKenzie, J. S. Kiser and J. H. Williams (1952). "The effect of pyrazinamide (aldinamide) on experimental tuberculosis in mice." The American Review of Respiratory Diseases **65**(5): 511-518.

Mao, J., Y. Wang, B. Wan, A. P. Kozikowski and S. G. Franzblau (2007). "Design, synthesis, and pharmacological evaluation of mefloquine-based ligands as novel antituberculosis agents." ChemMedChem **2**: 1624-1630.

Marchler-Bauer, A., S. Lu, J. B. Anderson, F. Chitsaz, M. K. Derbyshire, C. DeWeese-Scott, J. H. Fong, L. Y. Geer, R. C. Geer, N. R. Gonzales, M. Gwadz, D. I. Hurwitz, J. D. Jackson, Z. Ke, C. J. Lanczycki, F. Lu, G. H. Marchler, M. Mullokandov, M. V. Omelchenko, C. L. Robertson, J. S. Song, N. Thanki, R. A. Yamashita, D. Zhang, N. Zhang, C. Zheng and S. H. Bryant (2011). "CDD: a Conserved Domain Database for the functional annotation of proteins." Nucleic Acids Research **39**: 225-229.

Martins, M., Z. Schelz, A. Martins, J. Molnar, G. Hajös, Z. Riedl, M. Viveiros, I. Yalcin, E. Aki-Sener and L. Amaral (2007). "*In vitro* and *ex vivo* activity of thioridazine derivatives against *Mycobacterium tuberculosis*." International Journal of Antimicrobial Agents **29**: 338-340.

Matsoso, L. G., B. D. Kana, P. K. Crellin, D. J. Lea-Smith, A. Pelosi, D. Powell, S. S. Dawes, H. Rubin, R. L. Coppel and V. Mizrahi (2005). "Function of the cytochrome bc_1-aa_3 branch of the respiratory network in mycobacteria and network adaptation occurring in response to its disruption." Journal of Bacteriology **187**(18): 6300-6308.

Mawuenyega, K. G., C. V. Forst, K. M. Dobos, J. T. Belisle, J. Chen, E. M. Bradbury, A. R. Bradbury and X. Chen (2005). "*Mycobacterium tuberculosis* functional network analysis by global subcellular protein profiling." Molecular Biology of the Cell **16**(1): 396-404.

McCune, R. M. and R. Tompsett (1956). "Fate of *Mycobacterium tuberculosis* in mouse tissues as determined by the microbial enumeration technique. I. The persistence of drug-susceptible tubercle bacilli in the tissues despite prolonged antimicrobial therapy." Journal of Experimental Medicine **104**: 737-762.

McCune, R. M., R. Tompsett and W. McDermott (1956). "The fate of *Mycobacterium tuberculosis* in mouse tissues as determined by the microbial enumeration technique. II. The conversion of tuberculous infection to the latent state by administration of pyrazinamide and a companion drug." Journal of Experimental Medicine **104**: 763-802.

McFarland, J. (1907). "The nephelometer: an instrument for estimating the number of bacteria in suspensions used for calculating the opsonic index and for vaccines." The Journal of the American Medical Association **49**(14): 1176-1178.

McKinney, J. D., K. H. z. Bentrup, E. J. Muñoz-Elías, A. Miczak, B. Chen, W.-T. Chan, D. Swenson, J. C. Sacchettinik, J. W. R. Jacobs and D. G. Russell (2000). "Persistence of *Mycobacterium tuberculosis* in macrophages and mice requires the glyoxylate shunt enzyme isocitrate lyase." Nature **406**: 735-738.

McLeod, M. P., R. L. Warren, W. W. Hsiao, N. Araki, M. Myhre, C. Fernandes, D. Miyazawa, W. Wong, A. L. Lillquist, D. Wang, M. Dosanjh, H. Hara, A.

Petrescu, R. D. Morin, G. Yang, J. M. Stott, J. E. Schein, H. Shin, D. Smailus, A. S. Siddiqui, M. A. Marra, S. J. Jones, R. Holt, F. S. Brinkman, K. Miyauchi, M. Fukuda, J. E. Davies, W. W. Mohn and L. D. Eltis (2006). "The complete genome of *Rhodococcus sp.* RHA1 provides insights into a catabolic powerhouse." Proceedings of the National Academy of Sciences **103**(42): 15582-15587.

Mdluli, K., R. A. Slayden, Y. Zhu, S. Ramaswamy, X. Pan, D. Mead, D. D. Crane, J. M. Musser and C. E. Barry III (1998). "Inhibition of a Mycobacterium tuberculosis b-Ketoacyl ACP synthase by Isoniazid." Science **280**: 1607-1610.

Megehee, J. A., J. P. Hosler and M. D. Lundrigan (2006). "Evidence for a cytochrome *bcc-aa*$_3$ interaction in the respiratory chain of *Mycobacterium smegmatis* " Microbiology **152**: 823-829.

Megehee, J. A. and M. D. Lundrigan (2007). "Temporal expression of *Mycobacterium smegmatis* respiratory terminal oxidases." Canadian Journal of Microbiology **53**: 459-463.

Melo, A. M. P., T. M. Bandeiras and M. Teixeira (2004). "New insights into type II NAD(P)H: quinone oxidoreductases." Microbiology and Molecular Biology Reviews **68**(4): 603-616.

Menzies, D., A. Benedetti, A. Paydar, I. Martin, S. Royce, M. Pai, A. Vernon, C. Lienhardt and W. Burman (2009). "Effect of duration and intermittency of rifampin on tuberculosis treatment outcomes: a systematic review and meta-analysis." PLoS Medicine **6**(9): e1000146.

Michel, J.-B., P. J. Yeh, R. Chait, R. C. Moellering Jr. and R. Kishony (2008). "Drug interactions modulate the potential for evolution of resistance." Proceedings of the National Academy of Sciences **105**(39): 14918-14923.

Miesel, L., T. R. Weisbrod, J. A. Marcinkeviciene, R. Bittman and W. R. J. Jr. (1998). "NADH dehydrogenase defects confer isoniazid resistance and conditional lethality in *Mycobacterium smegmatis*." Journal of Bacteriology **180**(9): 2459-2467.

Miller, C. H., S. Nisa, S. Dempsey, C. Jack and R. O'Toole (2009). "Modifying culture conditions in chemical library screening identifies alternative inhibitors of mycobacteria." Antimicrobial Agents and Chemotherapy **53**(12): 5279-5283.

Mitchison, D. A. (2005). "Drug resistance in tuberculosis." European Respiratory Journal **25**(2): 376-379.

Mitchison, D. A. and R. M. Coates (2004). "Predictive *in vitro* models of the sterilizing sctivity of anti-tuberculosis drugs." Current Pharmaceutical Design **10**: 3285-3295.

Mossman, T. (1983). "Rapid colorimetric assay for cellular growth and survival: application to proliferation and cytotoxicity assays." Journal of Immunology Methods **65**: 55-63.

Mueller, D. H., L. Mwenge, M. Muyoyeta, M. W. Muvwimi, R. Tembwe, R. McNerney, P. Godfrey-Faussett and H. M. Ayles (2008). "Costs and cost-effectiveness of tuberculosis cultures using solid and liquid media in a developing country." The International Journal of Tuberculosis and Lung Disease **12**(10): 1196-1202.

Mukherjee, J. S., M. L. Rich, A. R. Socci, J. K. Joseph, F. A. Virú, S. S. Shin, J. J. Furin, M. C. Becerra, D. J. Barry, J. Y. Kim, J. Bayona, P. Farmer, M. C. S. Fawzi and K. J. Seung (2004). "Programmes and principles in treatment of multidrug-resistant tuberculosis." Lancet **363**(9407): 474-481.

Muñoz-Elías, E. J. and J. D. McKinney (2005). "*Mycobacterium tuberculosis* isocitrate lyases 1 and 2 are jointly required for *in vivo* growth and virulence." Nature Medicine **11**(6): 638-644.

Murphy, D. J. and J. R. Brown (2007). "Identification of gene targets against dormant phase *Mycobacterium tuberculosis* infections." BMC Infectious Diseases **7**: 84.

Muttucumaru, D. G. N., G. Roberts, J. Hinds, R. A. Stabler and T. Parish (2004). "Gene expression profile of *Mycobacterium tuberculosis* in a non-replicating state." Tuberculosis **84**: 239-246.

Nantapong, N., A. Otofuji, C. T. Migita, O. Adachi, H. Toyama and K. Matsushita (2005). "Electron transfer ability from NADH to menaquinone and from NADPH to oxygen of type II NADH dehydrogenase of *Corynebacterium glutamicum*." Bioscience Biotechnology and Biochemistry **69**(1): 149-159.

Nguyen, L. and J. Pieters (2009). "Mycobacterial subversion of chemotherapeutic reagents and host defense tactics: challenges in tuberculosis drug development." Annual Review of Pharmacology and Toxicology **49**: 427-453.

Niebisch, A. and M. Bott (2003). "Purification of a cytochrome bc_1-aa_3 supercomplex with quinol oxidase activity from *Corynebacterium glutamicum*." Journal of Biological Chemistry **278**(6): 4339-4346.

Niederweis, M. (2008). "Nutrient acquisition by mycobacteria." Microbiology **154**: 679-692.

Niederweis, M., O. Danilchanka, J. Huff, C. Hoffmann and H. Engelhardt (2010). "Mycobacterial outer membranes: in search of proteins." Trends in Microbiology **18**(3): 109-116.

O'Brien, J., I. Wilson, T. Orton and F. Pognan (2000). "Investigation of the Alamar Blue (resazurin) fluorescent dye for the assessment of mammalian cell cytotoxicity." European Journal of Biochemistry **267**(17): 5421-5426.

Olivier, I. and D. T. Loots (2011). "An overview of tuberculosis treatments and diagnostics. What role could metabolomics play?" Journal of Cell and Tissue Research **11**(1): 2655-2671.

Palomino, J. C. and F. Portaels (1999). "Simple procedure for drug susceptibility testing of *Mycobacterium tuberculosis* using a commercial colorimetic assay." European Journal of Clinical Microbiology & Infectious Diseases **18**(5): 380-383.

Parida, S. K. and S. H. Kaufmann (2010). "Novel tuberculosis vaccines on the horizon." Current Opinion in Immunology **22**(3): 374-384.

Parish, T. and N. G. Stoker, Eds. (2001). *Mycobacterium tuberculosis* protocols. Methods in Molecular Medicine. New Jersey, USA, Humana Press Inc.

Park, H.-D., K. M. Guinn, M. I. Harrell, R. Liao, M. I. Voskuil, M. Tompa, G. K. Schoolnik and D. R. Sherman (2003). "Rv3133c/*dosR* is a transcription factor that mediates the hypoxic response of *Mycobacterium tuberculosis*." Molecular Microbiology **48**(3): 833-843.

Parrish, N. M., J. D. Dick and W. R. Bishai (1998). "Mechanisms of latency in *Mycobacterium tuberculosis*." TRENDS in Microbiology **6**(3): 107-112.

Parsons, L. M., M. Salfinger, A. Clobridge, J. Dormandy, L. Mirabello, V. L. Polletta, A. Sanic, O. Sinyavskiy, S. C. Larsen, J. Driscoll, G. Zickas and H. W. Taber (2005). "Phenotypic and molecular characterization of *Mycobacterium tuberculosis* isolates resistant to both isoniazid and ethambutol." Antimicrobial Agents and Chemotherapy **49**(6): 2218-2225.

Pei, J., B.-H. Kim and N. V. Grishin (2008). "PROMALS3D: a tool for multiple protein sequence and structure alignments." Nucleic Acids Research **36**(7): 2295-2300.

Peyron, P., J. Vaubourgeix, Y. Poquet, F. Levillain, C. Botanch, F. Bardou, M. Daffé, J.-F. Emile, B. Marchou, P.-J. Cardona, C. d. Chastellier and F. Altare (2008). "Foamy macrophages from tuberculous patients' granulomas constitute a nutrient-rich reservoir for *M. tuberculosis* persistence." PLoS Pathogens **4**(11): e1000204.

Philippe, H. and C. J. Douady (2003). "Horizontal gene transfer and phylogenetics." Current Opinion in Microbiology **6**(5): 498-505.

Piersimoni, C., A. Olivieri, L. Benacchio and C. Scarparo (2006). "Current Perspectives on Drug Susceptibility Testing of Mycobacterium tuberculosis Complex: the

Automated Nonradiometric Systems." Journal of Clinical Microbiology **44**(1): 20-28.

Piersimoni, C., C. Scarparo, A. Callegaro, C. P. Tosi, D. Nista, S. Bornigia, M. Scagnelli, A. Rigon, G. Ruggiero and A. Goglio (2001). "Comparison of MB/BacT ALERT 3D system with radiometric BACTEC system and Löwenstein-Jensen medium for recovery and identification of mycobacteria from clinical specimens: a multicenter study." Journal of Clinical Microbiology **39**(2): 651-657.

Puissegur, M. P., C. Botanch, J. L. Duteyrat, G. Delsol, C. Caratero and F. Altare (2004). "An in vitro dual model of mycobacterial granulomas to investigate the molecular interactions between mycobacteria and human host cells." Cell Microbiology **6**(5): 423-433.

Rao, M., T. L. Streur, F. E. Aldwell and G. M. Cook (2001). "Intracellular pH regulation by *Mycobacterium smegmatis* and *Mycobacterium bovis* BCG." Microbiology **147**: 1017-1024.

Rastogi, N., V. Labrousse and K. S. Goh (1996). "*In vitro* activities of fourteen antimicrobial agents against drug susceptible and resistant clinical isolates of *Mycobacterium tuberculosis* and comparative intracellular activities against the virulent H37Rv strain in human macrophages." Current Microbiology **33**: 167-175.

Ratnakar, P. and P. S. Murthy (1992). "Antitubercular activity of trifluoperazine, a calmodulin antagonist." FEMS Microbiology Letters **97**(1-2): 73-76.

Rawat, R. A., A. Whitty and P. J. Tonge (2003). "The isoniazid-NAD adduct is a slow, tight-binding inhibitor of InhA, the *Mycobacterium tuberculosis* enoyl reductase: Adduct affinity and drug resistance." Proceedings of the National Academy of Sciences of the United States of America **100**: 13881-13886.

Reed, M. B., S. Gagneux, K. DeRiemer, P. M. Small and C. E. Barry III (2007). "The W-Beijing lineage of *Mycobacterium tuberculosis* overproduces triglycerides and has the DosR dormancy regulon constitutively upregulated." Journal of Bacteriology **189**(7): 2583-2589.

Rifat, D., W. R. Bishai and P. C. KaraKousis (2009). "Phosphate depletion: a novel trigger for *Mycobacterium tuberculosis* persistence." The Journal of Infectious Diseases **200**: 1126-1135.

Rivers, E. C. and R. L. Mancera (2008). "New anti-tuberculosis drugs in clinical trials with novel mechanisms of action." Drug Discovery Today **13**: 1090-1098.

Roberts, D. M., B. P. Liao, G. Wisedchaisri, W. G. J. Hol and D. R. Sherman (2004). "Two sensor kinases contribute to the hypoxic response of *Mycobacterium tuberculosis*." Journal of Biological Chemistry **279**(22): 23082-23087.

Roberts, G. D., N. L. Goodman, L. Heifets, H. W. Larsh, T. H. Lindner, J. K. McClatchy, M. R. McGinnis, S. H. Siddiqi and P. Wright (1983). "Evaluation of the BACTEC radiometric method for recovery of mycobacteria and drug sensibility testing of *Mycobacterium tuberculosis* from acid-fast smear-positive specimens." Journal of Clinical Microbiology **18**(3): 689-696.

Roehm, K.-H. (2001). Electron carriers: proteins and cofactors in oxidative phosphorylation. Encyclopedia of Life Sciences. L. John Wiley & Sons.

Russell, D. G. (2001). "*Mycobacterium tuberculosis*: here today, and here tomorrow." Nature Reviews in Molecular Cell Biology **2**: 569-577.

Russell, D. G., C. E. Barry III and J. L. Flynn (2010). "Tuberculosis: what we don't know can, and does, hurt us." Science **328**(5980): 852-856.

Rustad, T. R., M. I. Harrell, R. Liao and D. R. Sherman (2008). "The enduring hypoxic response of *Mycobacterium tuberculosis*." PLoS One **3**(1): e1502.

Rustad, T. R., A. M. Sherrid, K. J. Minch and D. R. Sherman (2009). "Hypoxia: a window into *Mycobacterium tuberculosis* latency." Cellular Microbiology **11**(8): 1151-1159.

Sacchettini, J. C., E. J. Rubin and J. S. Freundlich (2008). "Drugs versus bugs: in pursuit of the persistent predator *Mycobacterium tuberculosis*." Nature Reviews in Microbiology **6**(41-52).

Saleh, A., J. Friesen, S. Baumeister, U. Gross and W. Bohne (2007). "Growth inhibition of *Toxoplasma gondii* and *Plasmodium falciparum* by nanomolar concentrations of 1-Hydroxy-2-Dodecyl-4(1H)Quinolone, a high-affinity inhibitor of alternative (Type II) NADH dehydrogenases." Antimicrobial Agents and Chemotherapy **51**(4): 1217-1222.

Salfinger, M. and L. B. Heifets (1988). "Determination of pyrazinamide MICs for *Mycobacterium tuberculosis* at different pHs by the radiometric method." Antimicrobial Agents and Chemotherapy **32**: 1002-1004.

Sambrook, J. and D. W. Russell (2001). Molecular cloning: a laboratory manual. Cold Spring Harbor, New York, Cold Spring Harbor Laboratory Press

Sassetti, C. M., D. H. Boyd and E. J. Rubin (2003). "Genes required for mycobacterial growth defined by high density mutagenesis." Molecular Microbiology **48**(1): 77-84.

Sassetti, C. M. and E. J. Rubin (2003). "Genetic requirements for mycobacterial survival during infection." Proceedings of the National Academy of Sciences **100**(22): 12989-12994.

Scanga, C. A., V. P. Mohan, H. Joseph, K. Yu, J. Chan and J. L. Flynn (1999). "Reactivation of latent tuberculosis: variations on the Cornell murine model." Infection and Immunity **67**(9): 4531-4538.

Schmid, R. and D. L. Gerloff (2004). "Functional properties of the alternative NADH: ubiquinone oxidoreductase from *E. coli* through comparative 3-D modelling." FEBS Letters **578**: 163-168.

Schnappinger, D., S. Ehrt, M. I. Voskuil, Y. Liu, J. A. Mangan, I. M. Monahan, G. Dolganov, B. Efron, P. D. Butcher, C. Nathan and G. K. Schoolnik (2003). "Transcriptional Adaptation of Mycobacterium tuberculosis within Macrophages: Insights into the Phagosomal Environment." Journal of Experimental Medicine **198**(5): 693-704.

Schneider, T. D. and R. M. Stephens (1990). "Sequence Logos: A New Way to Display Consensus Sequences." Nucleic Acids Research **18**( ): 6097-6100.

Sharbati-Tehrani, S., J. Stephan, G. Holland, B. Appel, M. Niederweis and A. Lewin (2005). "Porins limit the intracellular persistence of *Mycobacterium smegmatis*." Microbiology **151**(7): 2403-2410.

Sharma, S. K. and A. Mohan (2006). "Multidrug-resistant tuberculosis: a menace that threatens to destabilize tuberculosis control." CHEST **130**: 162-272.

Sharma, S. K. and A. Mohan (2006). "Multidrug-resistant tuberculosis: a menace that threatens to destabilize tuberculosis control." CHEST **130**: 261-272.

Shenoy, A. R., A. Srinivas, M. Mahalingam and S. S. Visweswariah (2005). "An adenylyl cyclase pseudogene in *Mycobacterium tuberculosis* has a functional ortholog in *Mycobacterium avium*." Biochimie **87**(6): 557-563.

Sherman, D. R., M. Voskuil, D. Schnappinger, R. Liao, M. I. Harrell and G. K. Schoolnik (2001). "Regulation of the *Mycobacterium tuberculosis* hypoxic response gene encoding α-crystallin." Proceedings of the National Academy of Sciences **98**(13): 7534-7539.

Shi, L., C. D. Sohaskey, B. D. Kana, S. Dawes, R. J. North, V. Mizrahi and M. L. Gennaro (2005). "Changes in energy metabolism of *Mycobacterium tuberculosis* in mouse lung and under *in vitro* conditions affecting aerobic respiration." Proceedings of the National Academy of Sciences **102**(43): 15629-15634.

Simons, S. O. and D. v. Soolingen (2011). "Drug susceptibility testing for optimizing tuberculosis treatment." Current Pharmaceutical Design **17**(27): 2863-2874.

Smeulders, M. J., J. Keer, R. A. Speight and H. D. Williams (1999). "Adaptation of *Mycobacterium smegmatis* to stationary phase." Journal of Bacteriology **181**(1): 270-283.

Smith, I. (2003). "*Mycobacterium tuberculosis* pathogenesis and molecular determinants of virulence." Clinical Microbiology Reviews **16**(3): 463-496.

Sohaskey, C. D. (2005). "Regulation of nitrate reductase activity in *Mycobacterium tuberculosis* by oxygen and nitric oxide." Microbiology **151**: 3803-3810.

Sohaskey, C. D. (2008). "Nitrate enhances the survival of Mycobacterium tuberculosis during inhibition of respiration." Journal of Bacteriology **190**(8): 2981–2986.

Soolingen, D. v., R. Hernandez-Pando, H. Orozco, D. Aguilar, C. Magis-Escurra, L. Amaral, J. v. Ingen and M. J. Boeree (2010). "The antipsychotic thioridazine shows promising therapeutic activity in a mouse model of multidrug-resistant tuberculosis." PLoS One **5**(9): e12640.

Sreevatsan, S., K. E. Stockbauer, X. Pan, B. N. Kreiswirth, S. L. Moghazeh, W. R. Jacobs, A. Telenti and J. M. Musser (1997). "Ethambutol resistance in *Mycobacterium tuberculosis*: critical role of *emB* mutations." Antimicrobial Agents and Chemotherapy **41**(8): 1677-1681.

Srivastava, I. K., H. Rottenberg and A. B. Vaidya (1997). "Atovaquone, a broad spectrum antiparasitic drug, collapses mitochondrial membrane potential in a malarial parasite." Journal of Biological Chemistry **272**(7): 3961-3966.

Steenwinkel, J. E. M. d., G. J. Knegt, M. T. t. Kate, A. v. Belkum, H. A. Verbrugh, K. Kremer, D. v. Soolingen and I. A. J. M. Bakker-Woudenberg (2010). "Time-kill kinetics of anti-tuberculosis drugs, and emergence of resistance, in relation to metabolic activity of *Mycobacterium tuberculosis*." Journal of Antimicrobial Chemotherapy **65**(12): 2582-2589.

Stewart, G. R., L. Wernisch, R. Stabler, J. A. Mangan, J. Hinds, K. G. Laing, D. B. Young and P. D. Butcher (2002). "Dissection of the heat-shock response in *Mycobacterium tuberculosis* using mutants and microarrays." Microbiology **148**: 3129-3138.

Stouthamer, A. H., F. C. Boogerd and H. W. v. Verseveld (1982). "The bioenergetics of denitrification." Antonie van Leeuwenhoek **48**(6): 545-553.

Takayama, K. and J. O. Kilburn (1989). "Inhibition of synthesis of arabinogalactan by ethambutol in *Mycobacterium smegmatis*." Antimicrobial Agents and Chemotherapy **33**: 1493-1499.

Takeda, S., H. Maeda, M. Hayakawa, N. Sawabata and R. Maekura (2005). "Current surgical intervention for pulmonary tuberculosis." The Annals of Thoracic Surgery **79**: 959-963.

Tallarida, R. J. (2006). "An overview of drug combination analysis with isobolograms." The Journal of Pharmacology and Experimental Therapeutics **319**(1): 1-7.

Teh, J. S., T. Yano and H. Rubin (2007). "Type II NADH: menaquinone oxidoreductase of *Mycobacterium tuberculosis*." Infectious Disorders - Drug Targets **7**: 169-181.

Thanacoody, H. K. R. (2007). "Thioridazine: resurrection as an antimicrobial agent?" British Journal of Clinical Pharmacology **64**(5): 566-574.

Thomas, J. P., C. O. Baughn, R. G. Wilkinson and R. G. Shepherd (1961). "A new synthetic compound with antituberculous activity in mice: ethambutol (dextro-2,2'-(ethylenediimino)-di-l-butanol)." The American Review of Respiratory Diseases **83**: 891-893.

Thompson, J. E. (1978). "How safe is isoniazid?" The Medical Journal of Australia **1**(3): 165-169.

Tian, J., R. Bryk, M. Itoh, M. Suematsu and C. Nathan (2005). "Variant tricarboxylic acid cycle in Mycobacterium tuberculosis: identification of alpha-ketoglutarate decarboxylase." Proceedings of the National Academy of Sciences of the United States of America **102**(30): 10670-10675.

Titgemeyer, F., J. Amon, S. Parche, M. Mahfoud, J. Bail, M. Schlicht, N. Rehm, D. Hillmann, J. Stephan, B. Walter, A. Burkovski and M. Niederweis (2007). "A genomic view of sugar transport in *Mycobacterium smegmatis* and *Mycobacterium tuberculosis*." Journal of Bacteriology **189**(16): 5903-5915.

Torrents, D., M. Suyama, E. Zdobnov and P. Bork (2003). "A genome-wide survey of human pseudogenes." Genome Research **13**(12): 2559-2567.

Torres, E., E. Moreno, S. Ancizu, C. Barea, S. Galiano, I. Aldana, A. Monge and S. Pérez-Silanes (2011). "New 1,4-di-N-oxide-quinoxaline-2-ylmethylene isonicotinic acid hydrazide derivatives as anti-Mycobacterium tuberculosis agents" Bioorganic & Medicinal Chemistry Letters **21**: 3699–3703.

Tran, S. L. and G. M. Cook (2005). "The F_1F_0-ATP synthase of *Mycobacterium smegmatis* is essential for growth." Journal of Bacteriology **187**(14): 5023-5028.

Triccas, J. A. and B. Gicquel (2000). "Life on the inside: probing *Mycobacterium tuberculosis* gene expression during infection." Immunology and Cell Biology **78**: 311-317.

Truglio, J. J., K. Theis, Y. Feng, R. Gajda, C. Machutta, P. J. Tonge and C. Kisker (2003). "Crystal structure of *Mycobacterium tuberculosis MenB,* a key enzyme in vitamin K_2 biosynthesis." Journal of Biological Chemistry **278**(43): 42352-42360.

Turnidge, J. (2003). "Pharmacodynamics and dosing of aminoglycosides." Infectious Disease Clinics of North America **17**: 503-528.

Ulrichs, T. and S. H. E. Kaufmann (2006). "New insights into the function of granulomas in human tuberculosis." Journal of Pathology **208**: 261-269.

Vaddady, P. K., R. E. Lee and B. Meibohm (2010). "*In vitro* pharmacokinetic/pharmacodynamic models in anti-infective drug development: focus on TB." Future Medical Chemistry **2**(8): 1355-1369.

Velmurugan, K., B. Chen, J. L. Miller, S. Azogue, S. Gurses, T. Hsu, M. Glickman, W. R. J. Jr., S. A. Porcelli and V. Briken (2007). "*Mycobacterium tuberculosis nuoG* is a virulence gene that inhibits apoptosis of infected host cells." PLoS Pathogens **3**(7): e110.

Vergne, I., J. Chua, S. B. Singh and V. Deretic (2004). "Cell biology of *Mycobacterium tuberculosis* phagosome." Annual Review of Cell and Developmental Biology **20**: 367-394.

Verver, S., R. M. Warren, N. Beyers, M. Richardson, G. D. Spuy, M. W. Borgdorff, D. A. Enarson, M. A. Behr and P. D. v. Helden (2005). "Rate of reinfection tuberculosis after successful treatment is higher than rate of new tuberculosis." American Journal of Respiratory and Critical Care Medicine **171**(VOL 171): 1430-1435.

Via, L. E., P. L. Lin, S. M. Ray, J. Carrillo, S. S. Allen, S. Y. Eum, K. Taylor, E. Klein, U. Manjunatha, J. Gonzales, E. G. Lee, S. K. Park, J. A. Raleigh, S. N. Cho, D. N. McMurray, J. L. Flynn and C. E. Barry III (2008). "Tuberculous granulomas are hypoxic in guinea pigs, rabbits, and nonhuman primates." Infection and Immunity **76**(6): 2333-2340.

Vilchèze, C., T. R. Weisbrod, B. Chen, L. Kremer, M. H. Hazbón, F. Wang, D. Alland, J. C. Sacchettini and W. R. Jacobs Jr. (2005). "Altered $NADH/NAD^+$ ratio mediates coresistance to isoniazid and ethionamide in mycobacteria." Antimicrobial Agents and Chemotherapy **49**(2): 708-720.

Villas-Bôas, S. G., S. Mas, M. Åkesson, J. Smedsgaard and J. Nielsen (2005). "Mass spectrometry in metabolome analysis." Mass Spectrometry Reviews **24**: 613-646.

Viveiros, M. and L. Amaral (2001). "Enhancement of antibiotic activity against poly-drug resistant *Mycobacterium tuberculosis* by phenothiazines." International Journal of Antimicrobial Agents **17**: 225-228.

Voskuil, M. I., K. C. Visconti and G. K. Schoolnik (2004). "*Mycobacterium tuberculosis* gene expression during adaptation to stationary phase and low-oxygen dormancy." Tuberculosis **84**: 218-227.

Voskuil, M. I., D. Schnappinger, K. C. Visconti, M. I. Harrell, G. M. Dolganov, D. R. Sherman and G. K. Schoolnik (2003). "Inhibition of respiration by nitric oxide induces a *Mycobacterium tuberculosis* dormancy program." Journal of Experimental Medicine **198**(5): 705-713.

Vrij, W. d., B. van den Burg and W. N. Konings (1987). "Spectral and potentiometric analysis of cytochromes from Bacillus subtilis." European Journal of Biochemistry **166**(3): 589-595.

Waagmeester, A., J. Thompson and J.-M. Reyrat (2005). "Identifying sigma factors in *Mycobacterium smegmatis* by comparative genomic analysis." TRENDS in Microbiology **13**(11): 505-509.

Wade, M. M. and Y. Zhang (2004). "Anaerobic incubation conditions enhance pyrazinamide activity against *Mycobacterium tuberculosis*." Journal of Medical Microbiology **53**: 769-773.

Wallace Jr., R. J., D. R. Nash, L. C. Steele and V. Steingrube (1986). "Susceptibility testing of slowly growing mycobacteria by a microdilution MIC method with 7H9 broth." Journal of Clinical Microbiology **24**(6): 976-981.

Walters, S. B. and B. A. Hanna (1996). "Testing of susceptibility of *Mycobacterium tuberculosis* to isoniazid and rifampin by Mycobacterium growth indicator tube method." Journal of Clinical Microbiology **34**(6): 1565-1567.

Watanabe, S., M. Zimmermann, M. B. Goodwin, U. Sauer, C. E. B. 3rd and H. I. Boshoff (2011). "Fumarate reductase activity maintains an energized membrane in anaerobic *Mycobacterium tuberculosis*." PLoS Pathogens 7(10): e1002287.

Wayne, L. G. (1994). "Dormancy of *Mycobacterium tuberculosis* and latency of disease." European Journal of Clinical Microbiology & Infectious Diseases **13**(11): 908-914.

Wayne, L. G. and C. D. S. . (2001). "Nonreplicating persistence of *Mycobacterium tuberculosis*." Annual Review of Microbiology **55**: 139-163.

Wayne, L. G. and L. G. Hayes (1996). "An in vitro model for sequential study of shiftdown of Mycobacterium tuberculosis through two stages of nonreplicating persistence." Infection and Immunity **64**(6): 2062-2069.

Wayne, L. G. and C. D. Sohaskey (2001). "Nonreplicating persistence of *Mycobacterium tuberculosis*." Annual Review of Microbiology **55**: 139-163.

Wayne, L. G. and F. A. Sramek (1994). "Metronidazole is bactericidal to dormant cells of *Mycobacterium tuberculosis*." Antimicrobial Agents and Chemotherapy **38**(9): 2054-2058.

Weinstein, E. A., T. Yano, L.-S. Li, D. Avarbock, A. Avarbock, D. Helm, A. A. McColm, K. Duncan, J. T. Lonsdale and H. Rubin (2005). "Inhibitors of type II NADH:menaquinone oxidoreductase represent a class of antitubercular drugs." Proceedings of the National Academy of Sciences **102**(12).

WHO (2009). Global tuberculosis control : epidemiology, strategy, financing : WHO report 2009. Geneva, Switzerland.

WHO (2010). Multidrug and extensively drug-resistant TB (M/XDR-TB): 2010 global report on surveillance and response. Geneva, Switzerland.

WHO (2011). Guidelines for the programmatic management of drug-resistant tuberculosis. Geneva, Switzerland.

WHO (2011). Tuberculosis control: WHO report 2011. Geneva, Switzerland.

Xie, Z., N. Siddiqi and E. J. Rubin (2005). "Differential antibiotic susceptibilities of starved *Mycobacterium tuberculosis* isolates." Antimicrobial Agents and Chemotherapy **49**: 4778-4780.

Yagi, T. and A. Matsuno-Yagi (2003). "The proton-translocating NADH-quinone oxidoreductase in the respiratory chain: the secret unlocked." Biochemistry **42**: 2266-2274.

Yagi, T., B. B. Seo, S. D. Bernardo, E. Nakamaru-Ogiso, M. C. Kao and A. Matsuno-Yagi (2001). "NADH dehydrogenases: from basic science to biomedicine." Journal of Bioenergetics and Biomembranes **33**(3): 233-242.

Yajko, D. M., J. J. Madej, M. V. Lancaster, C. A. Sanders, V. L. Cawthon, B. Gee, A. Babst and A. K. Hadley (1995). "Colorimetric method for determining MICs of antimicrobial agents for *Mycobacterium tuberculosis*." Journal of Clinical Microbiology **33**(9): 2324-2327.

Yang, Z. (2007). "PAML 4: a program package for phylogenetic analysis by maximum likelihood." Molecular Biology and Evolution **24**: 1586-1591.

Yang, Z., M. Rosenthal, N. A. Rosenberg, S. Talarico, L. Zhang, C. Marrs, V. Ø. Thomsen, T. Lillebaek and A. B. Andersen (2011). "How dormant is *Mycobacterium tuberculosis* during latency? A study integrating genomics and molecular epidemiology." Infection, Genetics and Evolution **11**(5): 1164-1167.

Yano, T., L. Lin-Sheng, E. Weinstein, J.-S. Teh and H. Rubin (2006). "Steady-state kinetics and inhibitory action of antitubercular phenothiazines on *Mycobacterium tuberculosis* Type-II NADH-menaquinone oxidoreductase (NDH-2)." Journal of Biological Chemistry **281**(17): 11456-11463.

Young, L. S. (2009). "Reconsidering some approved antimicrobial agents for tuberculosis." Antimicrobial Agents and Chemotherapy **53**(11): 4577-4579.

Yuan, Y., D. D. Crane and C. E. Barry III (1996). "Stationary phase-associated protein expression in *Mycobacterium tuberculosis*: Function of the mycobacterial alpha-crystallin homolog." Journal of Bacteriology **178**: 4484-4492.

Zamora, L. L. and M. T. Pérez-Gracia (2012). "Using digital photography to implement the McFarland method." Journal of the Royal Society **9**(73): 1892-1897.

Zhang, Y. (2004). "Persistent and dormant tubercle bacilli and latent tuberculosis." Frontiers in Bioscience **9**: 1136-1156.

Zhang, Y. (2005). "The magic bullets and tuberculosis drug targets." Annual Review of Pharmacology and Toxicology **45**: 529-564.

Zhang, Y. and D. Mitchison (2003). "The curious characteristics of pyrazinamide: a review." The International Journal of Tuberculosis and Lung Disease 7(1): 6-21.

Zhang, Y. and W. W. Yew (2009). "Mechanisms of drug resistance in *Mycobacterium tuberculosis*." The International Journal of Tuberculosis and Lung Disease **13**(11): 1320-1330.

Zhao, W., Y. Zhong, H. Yuan, J. Wang, H. Zheng, Y. Wang, X. Cen, F. Xu, J. Bai, X. Han, G. Lu, Y. Zhu, Z. Shao, H. Yan, C. Li, N. Peng, Z. Zhang, Y. Zhang, W. Lin, Y. Fan, Z. Qin, Y. Hu, B. Zhu, S. Wang, X. Ding and G. P. Zhao (2010). "Complete genome sequence of the rifamycin SV-producing *Amycolatopsis mediterranei* U32 revealed its genetic characteristics in phylogeny and metabolism." Cell Research **20**(10): 1096-1108.

Zimic, M., P. Fuentes, R. H. Gilman, A. H. Gutiérrez, D. Kierwan and P. Sheen (2012). "Pyrazinoic acid efflux rate in *Mycobacterium tuberculosis* is a better proxy of pyrazinamide resistance." Tuberculosis **92**(1): 84-91.

Zumla, A., R. Atun, M. Maeurer, P. Mwaba, Z. Ma, J. O'Grady, M. Bates, K. Dheda, M. Hoelscher and J. Grange (2011). "Scientific dogmas, paradoxes and mysteries of latent *Mycobacterium tuberculosis* infection." Tropical Medicine and International Health **16**(1): 79-83.